

Development of stimulus-responsive
materials with improved performance
characteristics for application as flow
controllers in microfluidic platforms

PhD Thesis

Bartosz Ziółkowski
MSc Eng

Supervisor:
Prof. Dermot Diamond

Dublin City University
School of Chemistry



August 2013

Declaration

I hereby certify that this material, which I now submit for assessment on the programme of study leading to the award of doctor of philosophy is entirely my own work, and that I have exercised reasonable care to ensure that the work is original, and does not to the best of my knowledge breach any law of copyright, and has not been taken from the work of others save and to the extent that such work has been cited and acknowledged within the text of my work.

Signed: _____ ID No.: 59110341 Date: 3.07.2013

This thesis includes 4 original papers published in peer reviewed journals and 2 unpublished manuscripts. The main theme of the thesis is the investigation and development of novel stimulus responsive soft gels suitable for applications as flow controllers in microfluidic sensors. Most of the work was done in collaboration with colleagues from my group or through collaborations with other universities. My contribution to the papers presented in this thesis is outlined below:

Thesis chapter	Publication title	Publication status	Nature and extent of candidate's contribution
2	Integrating stimulus responsive materials and microfluidics – The key to next generation chemical sensors	Published <i>Journal of Intelligent Material Systems and Structures</i> , Sept. 27, 2012 DOI: 10.1177/1045389X12459591	Co-author with Monika Czugała, literature review, review and proof reading
3	Mechanical properties and U.V. curing behaviour of Poly(<i>N</i> -isopropylacrylamide) in phosphonium based ionic liquids.	Published <i>Macromolecular Chemistry and Physics</i> , 2013 . 214(7): p. 787-796. DOI: 10.1002/macp.201200616	Manuscript author, synthesis, experimental design, experimental work and data analysis (Rheology, Differential Scanning Calorimetry)
4	Magnetic ionogels (MIGs) based on iron oxide nanoparticles, poly(<i>N</i> -isopropylacrylamide), and the ionic liquid trihexyl-tetradecyl phosphonium dicyanamide	Published <i>European Journal of Inorganic Chemistry</i> , 2012. 2012 (32): p. 5245-5251. DOI: 10.1002/ejic.201200597	Manuscript author, synthesis, experimental design, experimental work (Rheology, Dynamic Light Scattering) and data analysis (Electron Dispersive X-ray,, Differential Scanning Calorimetry)
5	Self-protonating spiropyran-co-NIPAM-co-acrylic acid hydrogel photoactuators	Published <i>Soft Matter</i> 2013 , 9, 8754-8760. DOI: 10.1039/C3SM51386F	Manuscript author, synthesis of starting materials, experimental design and data analysis
6	Porous and self-protonating spiropyran-based NIPAM gels with fast reswelling kinetics	In preparation	Manuscript author, synthesis of starting materials, experimental design and data analysis
7	Thermoresponsive poly ionic liquid gels	Submitted Chemical Communications 31 st July 2013	Manuscript author, key ideas, synthesis, characterisation and data analysis

Candidate's signature

Date

Supervisor's signature

Date

Bartosz Ziółkowski

Dermot Diamond

List of outputs:

Peer reviewed papers:

1. Bartosz Ziółkowski, Monika Czugafa, Dermot Diamond, “Integrating stimulus responsive materials and microfluidics: The key to next-generation chemical sensors”, *Journal of Intelligent Material Systems and Structures*, Published online 27 September **2012**. DOI: 10.1177/1045389X12459591.
2. Bartosz Ziółkowski, Zeliha Ates, Simon Gallagher, Robert Byrne, Andreas Heise, Kevin J Fraser and Dermot Diamond, "Mechanical properties and U.V. curing behaviour of Poly(*N*-isopropylacrylamide) in phosphonium based ionic liquids", *Macromolecular Chemistry and Physics*, **2013**. 214(7): p. 787-796. DOI: 10.1002/macp.201200616
3. Bartosz Ziółkowski, Katrin Bleek, Brendan Twamley, Kevin J. Fraser, Robert Byrne, Dermot Diamond, Andreas Taubert, “Magnetic Ionogels (MagIGs) Based on Iron Oxide Nanoparticles, Poly(*N*-isopropylacrylamide), and the Ionic Liquid Trihexyl(tetradecyl)phosphonium Dicyanamide”, *European Journal of Inorganic Chemistry*, 2012. **2012**(32): p. 5245-5251. DOI: 10.1002/ejic.201200597
4. Bartosz. Ziółkowski, Larisa Florea, Janick Theobald, Fernando Benito-Lopez and Dermot Diamond, “Self-protonating spiropyran-co-NIPAM-co-acrylic acid hydrogel photoactuators”, *Soft Matter*, **2013**, 9, 8754-8760., DOI: 10.1039/C3SM51386F
5. Bartosz. Ziółkowski, Larisa Florea, Janick Theobald, Fernando Benito-Lopez and Dermot Diamond, “Porous and self-protonating spiropyran-based NIPAM gels with fast reswelling kinetics”, in preparation
6. Bartosz Ziółkowski and Dermot Diamond, “Thermoresponsive poly ionic liquid gels”, *Chemical Communications*, submitted 31st July 2013

Patents:

1. Bartosz Ziółkowski, Larisa Florea, Janick Theobald and Dermot Diamond, “Self-protonating spiropyran-co-NIPAM-co-acrylic acid hydrogel photoactuators”, Patent filed: 24 July 2013, United Kingdom 1313220.4

Grants:

1. DFG (German Research Council) Research Intensification Grant (TA571/9-1) July-September 2011.

Invited oral presentations:

1. Bartosz Ziółkowski, Kevin J Fraser, Robert Byrne, Katrin Bleek, Andreas Taubert and Dermot Diamond, "Magnetic ionogels for fluid handling in microfluidic devices" EuroMat2011 Montpellier, France 12-15 September 2011
2. Bartosz Ziółkowski, Kevin J Fraser, Robert Byrne, Katrin Bleek, Andreas Taubert and Dermot Diamond; “Magnetic ionogels for fluid handling in microfluidic devices” CIMTEC 2012 Montecatini Terme, Italy 10-14 June 2012
3. Bartosz Ziółkowski and Dermot Diamond, Photo-responsive hydrogel based on phosphonium poly-ionic liquid, COIL 5, 5th International Congress on Ionic Liquids (COIL-5), Vilamoura, Algarve, Portugal 21-25 April 2013
4. Bartosz Ziółkowski and Dermot Diamond “Novel, stimuli-responsive materials for fluid handling in microfluidic sensor platforms” ATWARM International Conference 2013, Dublin, Ireland 14-16 May 2013

Conference posters:

1. Bartosz Ziólkowski, King Tong Lau and Dermot Diamond "Spectral barcode label for fighting illegal waste dumps", EPA National Research Conference 2010, 23 June 2010, Croke Park Conference Centre, Dublin, Ireland
2. Bartosz Ziólkowski, King Tong Lau and Dermot Diamond "Spectral barcode label for fighting illegal waste dumps", EMRS 2010 Spring Meeting, 07-11 June 2010, Strasbourg, France.
3. Bartosz Ziólkowski, Kevin J Fraser, Robert Byrne, Katrin Bleek, Andreas Taubert and Dermot Diamond, "Magnetic ionogels for fluid handling in microfluidic devices" EuroMat2011 Montpellier, France 12-15 September 2011
4. Bartosz Ziólkowski, Kevin J Fraser, Robert Byrne, Fernando Benito-Lopez and Dermot Diamond, "Next generation autonomous analytical platforms for remote environmental monitoring" Marie Curie Researchers Symposium, SCIENCE – Passion, Mission, Responsibilities, Polish Presidency of the EU Council 25-27 September 2011, Warsaw, Poland
5. Bartosz Ziólkowski and Dermot Diamond, "Magnetic ionogels for fluid handling in microfluidic devices", CIMTEC 2012 4th International Conference Smart Materials Structures Systems, 10-14 June 2012, Montecatini Terme, Italy.
6. Bartosz Ziólkowski, Kevin J. Fraser, Robert Byrne, Fernando Benito-Lopez and Dermot Diamond "Stimuli responsive materials for sensors & actuators", 2nd International Symposium on Functional Nanomaterials 2012, 6-7th September, Dublin City University, Dublin, Ireland.
7. Stephane Louisia, Bartosz Ziólkowski, Michele Zanoni and Dermot Diamond "Synthesis and characterisation of photo-responsive hydrogels", 2nd International Symposium on Functional Nanomaterials 2012, 6-7th September, Dublin City University, Dublin, Ireland.
8. Bartosz Ziólkowski and Dermot Diamond, Photo-responsive hydrogel based on phosphonium poly-ionic liquid, COIL 5, 5th International Congress on Ionic Liquids (COIL-5), Vilamoura, Algarve, Portugal 21-25 April 2013
9. Kevin J Fraser, Andrew Kavanagh Bartosz Ziólkowski, Simon Gallagher and Dermot Diamond, Physical and mechanical properties of Phosphonium based poly(ionic liquids), COIL 5, 5th International Congress on Ionic Liquids (COIL-5), Vilamoura, Algarve, Portugal 21-25 April 2013

Acknowledgements

I would like to thank Professor Dermot Diamond for giving me the opportunity to work in his group. Even though I started as a “troublemaker” with far too many idealistic expectations he trusted me and allowed to wonder freely in the scientific world. Now after 4 years I understand his wisdom that a doctorate is not only about the research but also about character building. I sincerely appreciate his teachings and I will surely carry the experience I gained into my future life.

I thank all the scientific mentors that I had the opportunity to work with. Kevin J. Fraser , Robert Byrne, Fernando Benito-Lopez, Claudio Zuliani, Andreas Taubert, Andreas Heise, Dermot Brougham, Garrett McGuinness, Steve Goodyer. I have learnt something valuable and interdisciplinary from all of you. Big thanks to all the crew in N205 Cormac, Damien, Dylan, Tom, John, Fiachra, Stephen, Eoghan for all the engineering support. You were always there to lead the lost chemist through the dark forests of circuitry and mechanical devices.

“We do not have problems – we have challenges”. To all the people that marked their presence in SG03 later SG04 and SG07. Larisa, Michele, Vincenzo, Monika, Simon and Simon, Giusy, Deirdre, Andy, Stephane, Jannick. Thank you for all the hours of laughter at the fumehood or in the kitchen. I appreciate that I developed as much in the latter as in the former. I would not be where I am now without you.

I cannot forget about all the ATWARM Fellows and coordinators. We had great times during our biannual meetings and summer schools. Thanks to Carlo, Giacomo, Francesco, Ciprian, Cecilia, Zahra, Alessandra, Yoan, Daragh, Yolanda, Svetlana, Feng, Saioa, Beatrice, Vasilios, Ciaran and Patricia.

I thank my mother, father and my brother. For supporting me all the way. For the countless hours on skype and for the constant assurance of having a place on earth to come home to. You know that all this is was possible because of what you have taught me.

Thank you Ania for being a personal medic and healer of both body and soul and for motivating me to be a better person every day during my stay abroad. Thank you for forcing me to see other cities than Dublin and Poznań. Now we can finally have our argument who is “the real” doctor.

Podziękowania

Dziękuję profesorowi Dermotowi Diamondowi za możliwość pracy w swojej grupie badawczej. Mimo, że zaczynałem jako „troublemaker” z wieloma wyidealizowanymi oczekiwaniami, obdarzony zostałem pełnym zaufaniem i swobodą w eksploracji świata naukowego. Dziś po czterech latach rozumiem jego słowa, że doktorat to nie tylko rozwój naukowy ale również formowanie osobowości. Doceniam tę naukę i zabieram ją w moją przyszłą drogę.

Dziękuję wszystkim naukowym mentorom, z którymi miałem okazję współpracować Kevin J. Fraser, Robert Byrne, Fernando Benito-Lopez, Claudio Zuliani, Andreas Taubert, Andreas Heise, Dermot Brougham, Garrett McGuinness, Steve Goodyer. Zdobylem wiele wartościowych i interdyscyplinarnych umiejętności dzięki wam. Podziękowania dla całej załogi z N205 Cormac, Damien, Dylan, Tom, John, Fiachra, Stephen, Eoghan za wsparcie w dziedzinie szeroko pojętej inżynierii. Zawsze chętnie prowadziliście mnie - zagubionego chemika, przez ciemny gąszcz obwodów i urządzeń elektrycznych.

„U nas nie ma problemów – są tylko wyzwania”. Dziękuję wszystkim, którzy zaznaczyli swoją obecność w SG03 potem SG04 i SG07 Larisa, Michele, Vincenzo, Monika, Simon i Simon, Giusy, Deirdre, Andy, Stephane, Jannick. Dziękuję za wszystkie godziny śmiechu przy dygestorium i w kuchni. Doceniam to, że dzięki Wam rozwinąłem swoje umiejętności w obu obszarach. Nie byłbym teraz tym kim jestem bez Was.

Nie mogę zapomnieć o koleżankach, kolegach i koordynatorach programu ATWARM. Dzięki Carlo, Giacomo, Francesco, Ciprian, Cecilia, Zahra, Alessandra, Yoan, Daragh, Yolanda, Svetlana, Feng, Saioa, Beatrice, Vasilios, Ciaran and Patricia za mile spędzony czas na naszych spotkaniach i szkołach letnich.

Dziękuję Mamie, Tacie i Bratu. Za wsparcie przez cały czas mojego pobytu za granicą. Za niezliczone godziny na skype i za niezachwiany komfort, że mam miejsce na ziemi gdzie mogę wrócić. Wszystko to co osiągnąłem było możliwe dzięki temu czego mnie nauczyliście.

Dziękuję Ani za bycie osobistym lekarzem ciała i duszy. Za motywację do stawania się lepszym człowiekiem przez ten cały czas pobytu za granicą. Dzięki Tobie zwiedziłem coś więcej poza Dublinem i Poznaniem. Teraz w końcu możemy się pospieszać kto jest „prawdziwym” doktorem.

Table of contents

Abstract	1
Chapter 1: Introduction	5
1.1 Stimulus responsive materials.....	6
1.1.1 Temperature responsive materials	7
1.1.2 Magnetic responsive materials.....	8
1.1.3 Light responsive materials	10
1.2 Ionic liquids.....	13
1.3 Ionogels	13
1.3.1 Stimulus responsive ionogels.....	14
1.4 References:.....	15
Chapter 2: Integrating stimulus responsive materials and microfluidics – The key to next generation chemical sensors	20
2.1 Introduction	23
2.2 Polymer actuator valves in microfluidic systems.....	24
2.2.1 Magnetically actuated valves	25
2.2.2 Pneumatic valves.....	26
2.2.3 Electrothermal valves.....	26
2.2.4 Soft polymer valves.....	27
2.3 Micropumps in fluidic systems	30
2.4 Photoswitchable polymer actuators.....	31
2.4.1 IR-responsive materials.....	32
2.4.2 Spiropyran-based photocontrolled soft actuators.....	33
2.4.3 Azobenzene based polymeric actuators	40
2.5 Conclusions	41
2.6 References:.....	42
Chapter 3: Mechanical properties and U.V. curing behaviour of Poly(<i>N</i>-isopropylacrylamide) in phosphonium based ionic liquids	46
3.1 Introduction	48
3.2 Experimental	50
3.2.1 Materials.....	50
3.2.2 Sample preparation.....	50
3.2.3 Rheometry	51
3.2.4 Gel Permeation Chromatography (GPC):	52
3.2.5 Thermal Analysis:	53
3.2.6 Heat of Polymerisation.....	53
3.3 Results and Discussion.....	54
3.3.1 Linear pNIPAM	54
3.3.2 Crosslinked polymers:.....	57
3.4 Conclusion	62
3.5 References:.....	63

Chapter 4: Magnetic ionogels (MIGs) based on iron oxide nanoparticles, poly(N-isopropylacrylamide), and the ionic liquid trihexyl-tetradecyl phosphonium dicyanamide	67
4.1 Introduction.....	69
4.2 Experimental.....	70
4.2.1 Materials.....	70
4.2.2 Fe ₃ O ₄ synthesis.....	71
4.2.3 Silane coating of the Fe ₃ O ₄ nanoparticles.....	71
4.2.4 Preparation of magnetic pNIPAM ionogels.....	72
4.2.5 FT-IR spectroscopy.....	73
4.2.6 Dynamic light scattering (DLS).....	73
4.2.7 Electron Microscopy.....	73
4.2.8 Mechanical testing.....	73
4.3 Results.....	74
4.4 Discussion.....	78
4.5 Conclusions.....	79
4.6 References.....	80
Chapter 5: Self-protonating spiropyran-co-NIPAM-co-acrylic acid hydrogel photoactuators	84
5.1 Introduction.....	86
5.2 Experimental.....	88
5.2.1 Materials.....	88
5.2.2 Gel preparation.....	88
5.2.3 Gel shrinking measurements.....	89
5.2.4 UV-Vis Spectroscopy.....	90
5.3 Results and discussion.....	90
5.3.1 Influence of AA content on gels with 1 % BSP.....	93
5.3.2 Influence of BSP content on gels.....	94
5.3.3 Gel photoactuation stability studies.....	96
5.3.4 Mechanism of gel protonation/deprotonation.....	98
5.4 Conclusions.....	100
5.5 References.....	100
Chapter 6: Porous and self-protonating spiropyran-based NIPAM gels with fast reswelling kinetics	103
6.1 Introduction.....	104
6.2 Experimental.....	105
6.2.1 Materials.....	105
6.2.2 Gel preparation.....	105
6.2.3 Gel shrinking measurements.....	106
6.2.4 SEM.....	106
6.2.5 Rheology.....	107
6.2.6 UV-Vis spectroscopy.....	107
6.3 Results and Discussion.....	107
6.3.1 Porous poly(NIPAM)-co-BSP-A-co-AA gels.....	107
6.3.2 Mechanical stability of the gels.....	108
6.3.3 Light induced shrinking and reswelling of the gels.....	109
6.4 Conclusions.....	111

6.5	References:	111
Chapter 7: Thermoresponsive poly ionic liquid gels		113
7.1	Communication	115
7.2	References:	120
Chapter 8: Thesis summary and future outlook		122
8.1	Thesis summary	123
8.2	Future outlook	125
8.3	References:	132
Appendix A: Mechanical properties and U.V. curing behaviour of Poly(N-isopropylacrylamide) in phosphonium based ionic liquids.....		125
Appendix B: Self-protonating spiropyran- <i>co</i> -NIPAM- <i>co</i> -acrylic acid hydrogels as reversible photoactuators		133
Appendix C: Porous and self-protonating spiropyran-based NIPAM gels with fast reswelling kinetics.....		137
Appendix D: Thermoresponsive poly ionic liquid gels		139

Abstract

This thesis investigates the synthesis and performance of various stimuli-responsive materials with the aim of obtaining a suitable material for flow control in microfluidic platforms. Therefore, at first a literature review is carried out to choose a material for investigation as well as to determine the limitations of current materials so that potential areas where improvements can be made are defined. The materials chosen are mainly based on thermo-responsive polymer *N*-isopropylacrylamide. Hence, in the beginning the polymerisation of this polymer is investigated in various phosphonium-based ionic liquids to afford novel ionogels with tuneable viscoelastic properties that can serve as robust platforms for incorporation of stimulus-responsive entities. Later these ionogels are demonstrated as a novel and suitable platform for incorporating functionalised magnetic particles to obtain a magneto-responsive, soft ionogel. Photo-responsive gels are obtained by incorporation of spiropyran molecule into the polymer matrix. Improvements to the existing formulations are made by incorporation poly-acid in the polymer chains which allows the material to be actuated without additional chemicals. Moreover, the speed of actuation is improved by engineering a porous microstructure of the gels. Finally, as a future outlook, recently discovered, thermo-responsive poly-ionic liquids are investigated as potential substrates for novel stimulus responsive poly-ionic liquid gels. All these materials have been investigated from the perspective of incorporation into microfluidic devices as soft polymeric valves.

Aim of this work – chapters overview

There is no doubt that stimulus responsive materials have diverse application potential. This work focuses on the development of stimulus responsive materials for valves in microfluidic sensors. It is known that fluid handling and the related energy consumption in sensor platforms are the dominant cost factors. The inherent robustness, low cost and low energy consumption of the stimulus responsive materials make them ideal for autonomous sensor platforms that could form networks of smart sensors in the future.

The ultimate goal in this field would be to synthesise a material that can actuate repeatedly at high rate resulting in fast swelling/shrinking/bending of the material. In addition, the material should be comprised of components that do not contaminate the sample (e.g. by leaching). Obviously the material has to be also mechanically robust to withstand the expansion/contraction cycles demanded by valve structures. The following sections explore these issues and examine the characteristics of a selection of responsive actuator gels.

Chapter 1

In the first chapter a general introduction to the concept of stimulus responsive materials is given. Thermal, electric, photonic and magnetic types of stimuli are introduced along with their mechanism of actuation.

Chapter 2

Chapter 2 is a published literature review on polymeric soft actuators that have been utilised as microfluidic flow controllers (valves, pumps). A comparison of different valve designs is given together with their crucial parameters such as power drain, response speed and pressure resistance. Materials with various modes of stimulation are presented with emphasis on photoresponsive materials. Main drawbacks of current microfluidic actuators and valves are highlighted. In the case of the more robust pneumatic and electrothermal/electromagnetic valves the issue is high power consumption. On the other hand for the soft polymer photoresponsive valves that require low power light sources the actuation times are slow and there are problems with reversibility and leaching.

Chapter 3

Recent reports on ionogels show a growing interest of scientists to form these materials in situ for various purposes. ILs can possess properties much different from the conventional solvents

used for forming hydrogels. Therefore in Chapter 3 photopolymerisation of NIPAM in a range of phosphonium based ILs is studied. As mentioned in Chapter 2 these ILs can have a significant effect on the performance of spiropyran-based photoactuators. Chapter 3 investigates how changing the anion in trihexyl-tetradecyl phosphonium ILs series influences the rate of NIPAM polymerisation, the mechanical properties of the ionogels and their temperature responsiveness. The results from this work can be a valuable guide for choosing an appropriate IL for the desired application.

Chapter 4

Magnetic soft actuators, as described in Chapter 1, are either obtained by mixing magnetic particles in a polymer matrix, copolymerising them with a hydrogel or by the use of a magnetic ionic liquid to form a magnetic ionogel. Chapter 4 demonstrates how all these advantages can be combined in one material. Magnetic particles having high magnetic response are coated with polymerisation-active groups and incorporated in a poly(NIPAM) gel containing a phosphonium based IL (chosen based on findings from Chapter 3). This results in a magnetic ionogel where the magnetic particles are covalently bound to the polymer matrix and do not leach. Moreover the ionic liquid and the particles used improve the mechanical stability of the gel. Lastly, this material can not only be moved by the use of gradient magnetic fields but also could be shrunk by oscillating magnetic fields that generate local heating (polyNIPAM's thermoresponsive property).

Chapter 5

As highlighted in Chapter 2 current spiropyran-based photoresponsive gels require soaking in milimolar HCl to activate the photosensitive molecule in the gel. This constitutes a serious drawback in potential real life applications of this material. Therefore, in Chapter 5 acrylic acid is incorporated into the standard spiropyran/NIPAM hydrogel to provide an internalised source of protons allowing the gel to be actuated immediately after swelling in water without the need to soak it in HCl. Also because of this internal source of protons the gel can be actuated repeatedly demonstrating the first fully reversible photoresponsive spiropyran/NIPAM gel. The effect of spiropyran and acrylic acid content on the actuation performance is studied together with the resistance towards drying and multiple washings with water. As demonstrated the gels show excellent resistance and are capable of photoactuation after 2 months of storage in water.

Chapter 6

The HCl soaking issue of the spiropyran-based photoresponsive gels has been solved in Chapter 5. However these gels still showed slow reswelling speeds that could limit the operation of these materials as microfluidic valves. Chapter 6 investigates the improvements that can occur when pores are induced in the gels. Light induced shrinking and reswelling is studied and compared between the porous and non-porous gels. The results suggest that in the porous gels the reswelling kinetics is no longer determined by the speed of water diffusion but by the spiropyran isomerisation kinetics. We believe that through these combinations of improvements, the way is now open to exploit these materials more broadly for control of liquid movement through their use as a photoresponsive soft actuator valve in microfluidic manifolds.

Chapter 7

Recently novel monomeric thermoresponsive ionic liquids have been discovered. Since these ILs have been polymerised and shown to behave similarly to poly(NIPAM) this chapter investigates the possibility to synthesise crosslinked thermoresponsive polyIL gels from these novel materials. Thermal characterisation is given together with an overview of the gels appearance, behaviour under stimuli and its deviations from standard thermoresponsive gels. Potential applications are also briefly discussed.

Future work

Given the rapid development in the field of stimulus responsive materials, polymers and ILs, new concepts arise every day. This final chapter discusses the remaining limitations of the presented materials and potential routes for further research in the field and beyond.

Chapter 1: Introduction

Chapter overview

New generations of chemical sensors require both innovative (evolutionary) engineering concepts and (revolutionary) breakthroughs in fundamental materials chemistry, such as the emergence of new types of stimuli responsive materials. Intensive research in those fields in recent years have brought interesting new concepts and designs for microfluidic flow control and sample handling that integrate high quality engineering with new materials. The following two chapters review the recent developments in the fascinating area of stimulus responsive materials science, with particular emphasis on photoswitchable soft actuators. Some examples of their incorporation into fluidic devices are also presented in Chapter 2.

1.1 Stimulus responsive materials

Stimulus responsive materials are synthetic materials that possess the ability to change their shape, size, colour, stiffness and many other properties on demand after a given stimulus is provided. [1, 2] These materials are often composed of polymers in a form of organic/inorganic gels. A gel is an interconnected network of molecules that reaches across the borders of the considered volume space. The free volume between the polymolecular structures is filled with a separate phase. This can be a gas or a solid but most often it is a liquid. If water fills the gel it is termed hydrogel.

Polymeric gels have been attracting considerable research attention due to their vast application possibilities in material science[3, 4], sensors[5], actuators[6, 7] and particularly stimulus responsive materials.[1, 8, 9] To possess the property of stimulus responsiveness materials must include an entity that behaves differently in the presence/absence of a stimulus. This entity might be a functional group on the backbone of the gel network or a separate component added together with the gel-filling phase.

Therefore, polymeric gels are a useful platform for incorporating stimulus responsive entities and thereby generating stimulus responsive gels.[1, 8, 10] Important applications for stimulus responsive gels (often termed smart materials) include drug delivery,[5, 10] sensing,[11] and microfluidics.[12-15] They can then be actuated by stimuli induced changes in temperature,[1, 16] pH,[17, 18] light,[19, 20] or electric[21]/magnetic fields.[22-24]

1.1.1 Temperature responsive materials

One of the most popular examples of thermally responsive polymers is poly(*N*-isopropylacrylamide) or pNIPAM. It is often used for gel manufacturing and in biomedical applications.[10] At the base of thermo-responsiveness of this polymer is the so called lower critical solution temperature or LCST. Below this temperature the chains are hydrated with water and the polymer is swollen. Above this temperature the hydrogen bonds between solvent and the polymer are broken due to the thermal motion and the chains become hydrophobic. This results in the coiling up of the chains and shrinking of the gel (Figure 1-1).

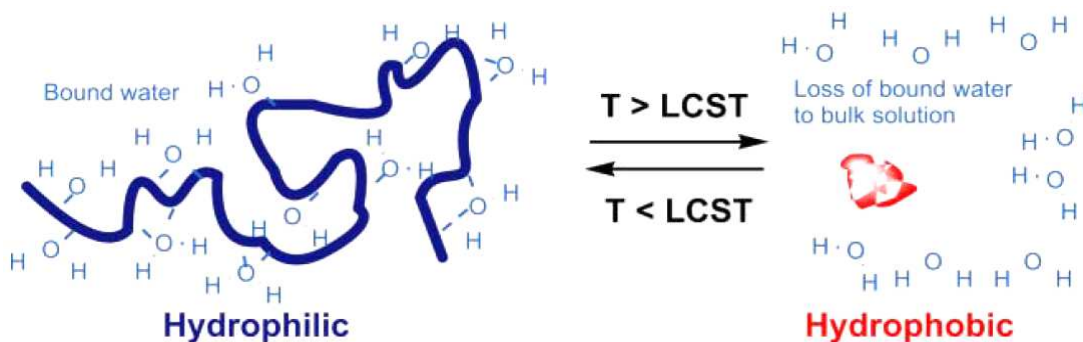


Figure 1-1. Schematic of ‘smart’ polymer response with temperature.[10]

This behaviour is common for other polymers containing H-bonding sites for water molecules. These are: *N,N*-diethylacrylamide, poly(*N*-vinylcaprolactam), poly(ethylene oxide), poly(propylene oxide) and copolymers of the latter two. The LCST in copolymers of PEO and PPO can be tuned by varying the amounts of the respective monomers in the polymer chain.[10] Similar LCST tuning is observed for pNIPAM if it is copolymerised with hydrophobic or hydrophilic monomers.[16]

Sun[25] *et al.* studied the volume transition of PNIPAM with 2 dimensional IR spectroscopy. The paper gives a thorough assignment of the IR peaks to the bonds present in the gel. It was discovered that the heat induced shrinking of the gel is a multistep or a smooth process while the cooling induced swelling exhibits two distinct steps. Authors managed to determine the order in which the polymer groups associate or disassociate first. It was proposed that the shrinking was induced by hydrogen bonds switching from the bonds between the amide group and solvent water to intermolecular hydrogen bonds. Water was expelled in this process. However, in the cooling-swelling process water molecules diffused initially between the polymer chains and then the hydrogen bonds rearranged from intermolecular to solvent-chain in nature. The general schematic of the mechanism is given in Figure 1-2.

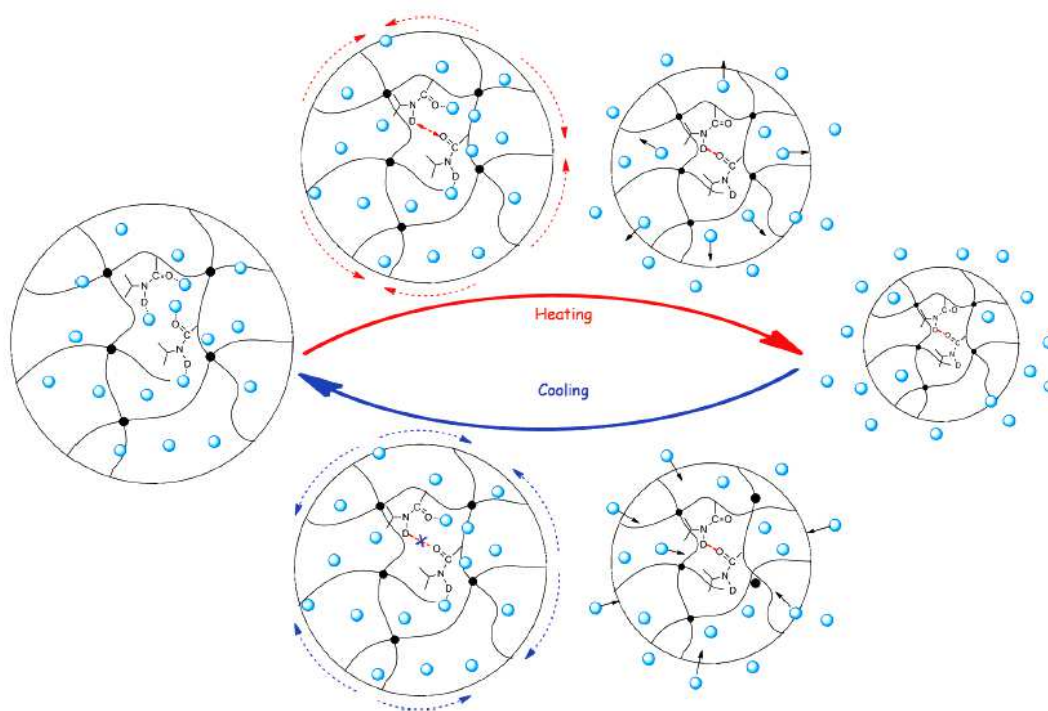


Figure 1-2. Proposed chain collapse and revival thermodynamic mechanism of PNIPAM hydrogel according to 2D cos analysis. Dashed arrows represent the chain collapse and revival directions along the backbone of PNIPAM hydrogel networks[25].

1.1.2 Magnetic responsive materials

If one introduces magnetic material into the gel pores the material becomes a magnetic-responsive gel. Detailed discussion about the different types of magnetism and their impact on the actuation performance is beyond the scope of this work. Therefore, the materials presented in this paragraph are described as magnetic without the differentiation of ferromagnetic to paramagnetic etc.

The magnetic material can be incorporated into the gel in different forms and ways. The magnetic susceptible component can be a liquid as reported by Xie *et al.*[26] These gels were based on PMMA and magnetic ionic liquid 1-butyl-3-methylimidazolium tetrachloroferrate (III) or [Bmim][FeCl₄]. Unfortunately, the magnetic susceptibility of this material was limited to the susceptibility of the Fe (III) ion (0.01-0.001 emu/g)[26] which is significantly lower than magnetite (Fe₃O₄) or metallic iron (8-140 emu/g).[27] Therefore, preferred strategies are to use magnetic particles based on magnetite, metallic iron or other metals with high magnetic susceptibility. Fuhrer *et al.*[23] used metallic cobalt nanoparticles coated with polymerisable groups to covalently link the particles to the gel network. In this way, a structurally stable gel was formed with magnetic particles as crosslinker. The gel responded strongly to magnetic fields at 60 % wt of particles (Figure 1-3).

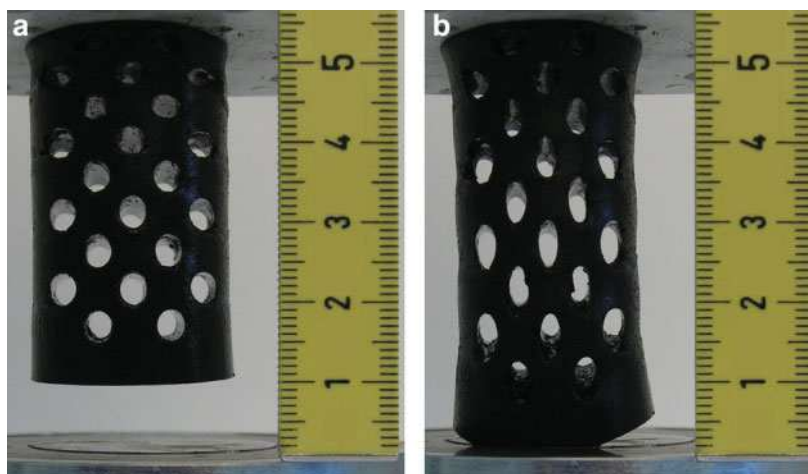


Figure 1-3. Elongation of a magnetic hydrogel (60 wt% vinyl functionalized cobalt nanoparticles) sticking to a permanent magnet (top) before (a) and after (b) switching on an additional electromagnetic field through a solenoid (bottom).

Another option, that is more often used due to its simplicity, is utilising organosilicon functionalised polymerisable magnetite particles.[28] The material was cured by means of 2 photon polymerization. The shapes manufactured were: a spring and a turbine (Figure 1-4).

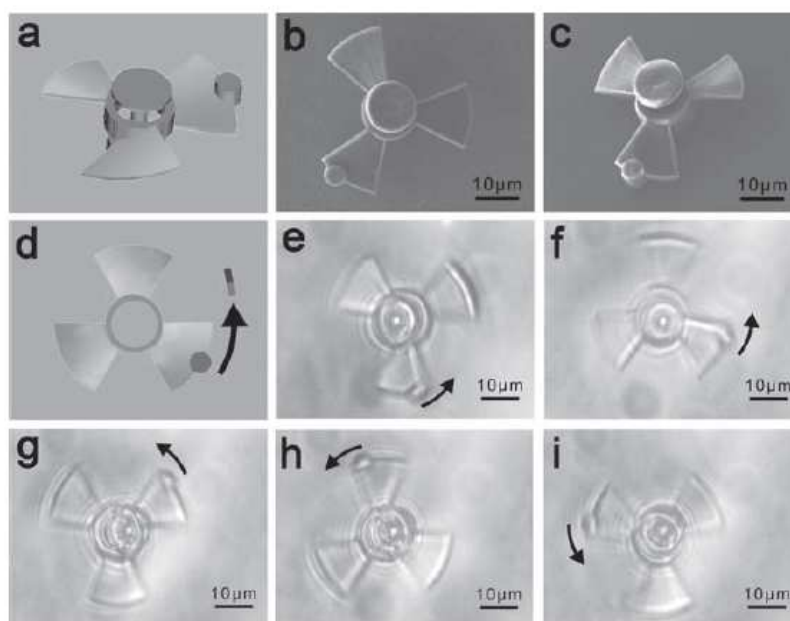


Figure 1-4. The microturbine actuated by magnetic field [28]

Both shapes were shown to move under magnetic field stimulation with just 2% magnetite concentration in the polymeric resin. The magnetite particles were prepared by the standard Massart method[29] and then modified by silane coupling chemistry. The surface was functionalized with methacrylic groups by means of 3-(trimethoxysilyl)propyl methacrylate. This molecule hydrolyses in an aqueous environment to form 3-(trihydroxysilyl)propyl methacrylate and its hydroxyl groups condensate with the OH groups present on the surface of the magnetite particles.[30] Magnetic particles with such surface polymerisable functional

groups could easily be reacted with other monomers to obtain materials with different properties.

Another example of magnetic-responsive gel incorporating polymerisable organosilicon magnetic particles was published by Wang *et al.*[31] In this work (3-mercaptopropyl) trimethoxysilane coating works as a chain transfer agent causing the gel network to grow from the surface of the particles. An even simpler example demonstrated by Caykara *et al.*[32] uses the standard pNIPAM crosslinked hydrogel. The gel was soaked in a 2:1 molar mixture of FeCl₃ and FeCl₂. When this gel was immersed in a base the Massart type reaction took place inside the gel pores resulting in a gel filled with magnetic particles. This gel was also shown to respond strongly to magnetic fields.

Alternatively, magnetic particles can also be used indirectly to provide stimuli to the material. One of the approaches is adopted from hyperthermia treatment. It is known that magnetic particles, when placed in an oscillating magnetic field, absorb the field energy and radiate it in the form of heat. This is due to the relaxation mechanisms of the magnetic moments and domains. The generated heat can be used to locally kill cancer cells.[33] However, in a thermoresponsive gel the local heat emitted triggers the magnetically induced LCST transition. This type of stimuli setup was used by Satarkar *et al.*[22] to produce a microfluidic valve that opened with applied alternating magnetic field. The disadvantage of these solutions is that the generation of magnetic field requires considerable power which at present is typically provided by a mains 220V power supply unit.[24] This makes it difficult to scale down such devices for autonomous, outdoor applications.

1.1.3 Light responsive materials

Light responsive materials are very attractive due to the non-invasive nature of light and availability of diverse light sources as stimuli. Two major groups of photoswitchable compounds have dominated research into these materials - spiropyrans and azobenzenes. In spiropyrans the carbon-oxygen bond is reversibly broken when light with a specific wavelength is absorbed. In azobenzenes an isomerisation takes place upon light absorption in which the energetically lower trans-isomer switches to cis-orientation.[34, 35] A detailed description of spiropyran-based soft actuators their performance and improvements published recently is contained in the literature review in Chapter 2. However, historically spiropyran-modified polymers were first discovered to exhibit photo-induced viscosity changes. For instance, the viscosity of solutions of poly(methylmethacrylate-co-1,3,3-trimethylindolino-6'-nitro-

8'(methacryloxy)methyl]spiropyrans) was reported to decrease by 17% with light irradiation at $\lambda > 310$ nm.[36] This was ascribed to the polar side groups of the methacrylate solvating the opened polar merocyanine form of the photochrome co-monomer. This effect decreased as the solvent polarity increased and disappeared in dichloromethane. The optimum concentration of the photochrome co-monomer in the polymer was of about 20 mol %.

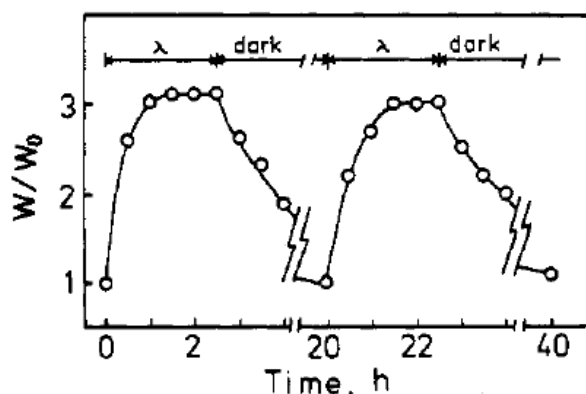


Figure 1-5. Photostimulated dilation and contraction of poly(acrylamide) gel having pendant triphenylmethane leucohydroxide groups (3.7 mol %) with light of wavelength longer than 270 nm at 25 °C. Initial pH of external water phase was 6.6. W, is the weight of the gel before photoirradiation.[37]

Irie[37] et. al. investigated diphenyl(4-vinylphenyl)-methane leucohydroxide or diphenyl(4-vinylphenyl)-methane leucocyanide[38] monomers copolymerised with acrylamide. These gels showed a photo-induced swelling in water, but once again the swelling was not directly linked with the colouration of the photochrome component. It was demonstrated that the disassociation of the photochrome produced ions in the gel (Figure 1-5) and the gel swelled because the appearance of these ions created an osmotic gradient, leading to increased water uptake. The optimum concentration of the chromophore was found to be 2 mol%. Higher chromophore concentrations decreased the degree of swelling as the increasing amount of hydrophobic co-monomer in the backbone made the whole system more hydrophobic and less capable of water uptake.

Regarding the copolymers bearing azobenzene derivative pendant groups, interesting work has been published by Zhao *et al.* [39] The change in azobenzene conformation can have dramatic effects on the surrounding environment.[34] The copolymer in (Figure 1-6) was shown to exhibit light dependent LCST behaviour. However, in contrast to the spiropyran modified pNIPAM, azobenzene modified pNIPAM, increased the LCST by ~ 5 °C after UV light irradiation and decreased the LCST with white light exposure. It is interesting that a reverse phenomenon is observed for poly(*N,N'*-dimethylacrylamide) modified with azobenzene. In this case the polymer's LCST dropped by an impressive value of 10 °C after UV-Vis irradiation (Figure 1-6).

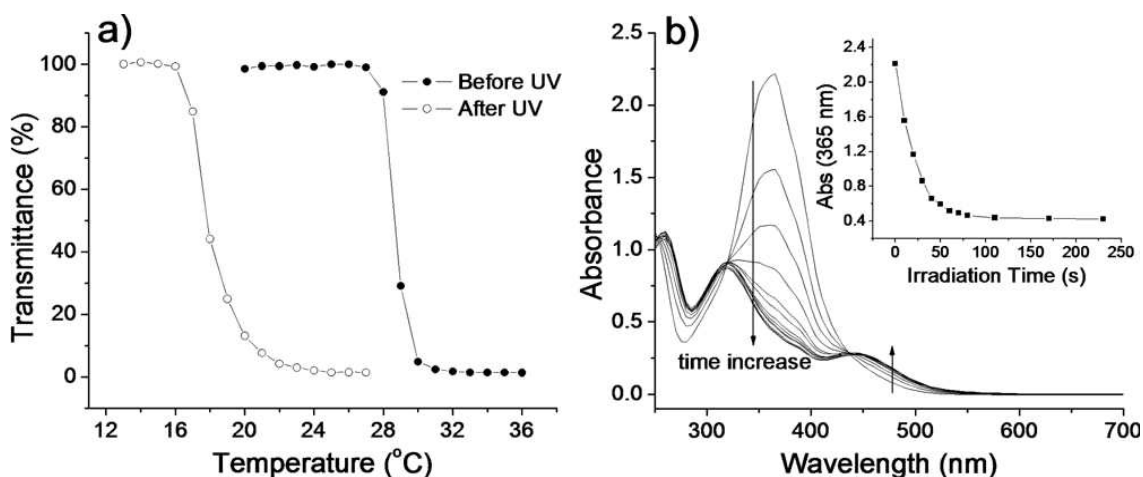


Figure 1-6. Transmittance versus temperature for aqueous solutions (poly(dimethylacrylamide) concentration: 2 mg mL) before and after UV light-induced photoisomerization of pendant azobenzene groups, as well as absorption spectra upon UV irradiation inducing the photoisomerization (solutions diluted to 0.1–0.2 mg mL), with the inset showing the change in absorbance of trans azobenzenes[39]

An excellent review by Beharry *et al.*[34] discusses different derivatives of azobenzenes, the mechanisms governing the rate of their isomerisation and their applications in biomolecules. Depending on the substituents on the benzene rings of azobenzenes the thermal relaxation times can be tuned from hours to milliseconds. The isomerisation of azobenzene results in a change of distance between the ends of the molecule. This was exploited in proteins where conformational changes allowed switching the activity of the protein “on” and “off”. More recently, Ueki *et al.* demonstrated that azobenzenes, in addition to inducing volume changes in gels containing 1-ethyl-3-methylimidazolium bis(trifluoromethanesulfonyl) amide, appear to be able to “lock” the gel structure in one of the states Figure 1-7.

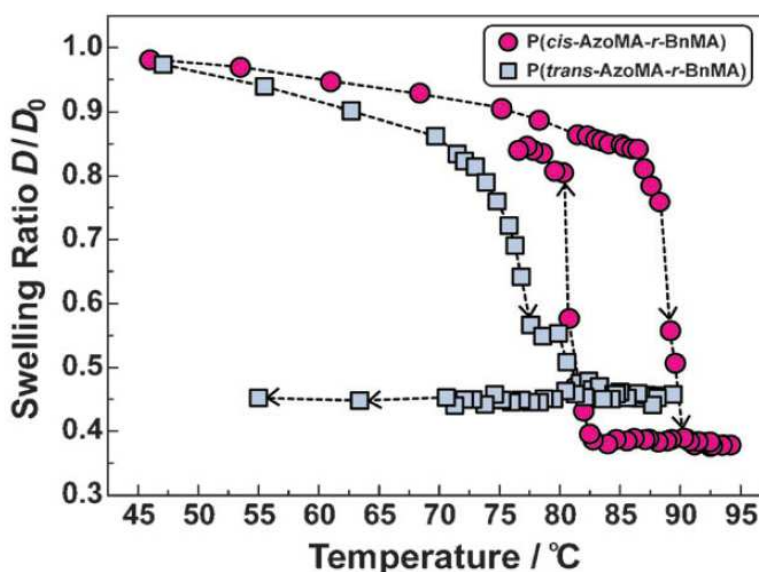


Figure 1-7. Shrinking of the thermoresponsive gel copolymerised with azobenzenes. “Locking” of the shrunken state in the trans form – no reswelling occurs.[35]

The azobenzene photoisomerisation effect was greatly enhanced by Broer *et al.* through incorporation of azobenzenes in liquid crystal structures.[40, 41] This work is described in more detail in Chapter 2.

1.2 Ionic liquids

Ionic liquids (ILs) are mainly organic compounds (although inorganic components are also known) consisting entirely of ions. Historically, ILs are defined as ionic salts having a melting point below 100 °C, even though this artificial border between ILs and salts with melting points slightly above 100 °C has recently largely been abandoned by researchers active in the field. A sub-class of ILs known as room temperature ionic liquids (RTILs) that is, ILs with melting points below ca. 25 °C, has attracted special interest. These ILs have many useful properties such as electronic and ionic conductivity, rather high thermal stability, negligible vapour pressure, and in some cases, high solvation power. This last property enables ILs to dissolve substances eg. monomers (NIPAM) and crosslinkers (N,N'-methylenebis acrylamide) that are difficult to dissolve in conventional molecular solvents.[42] Because it is possible to combine numerous anions and cations, the number of potential anion-cation combinations available reputedly equates to one trillion (10^{12}) different ILs each having different properties originating in from both the cation and anion.[43-45] ILs are currently attracting considerable attention as potentially benign solvents for many areas of chemistry, as well as various electrochemical devices[46-53], including rechargeable lithium cells,[54, 55] solar cells,[56-58] actuators[59-61] and double layer capacitors (DLCs).[62-64] Ionic liquids based on tetraalkylphosphonium cations exhibit greater thermal stability than their tetraalkylammonium based counterparts[65] and a range of phosphonium salts are commercially available in large quantities.[66] Reports of the utility of ionic liquids prepared from phosphonium cations with anions such as hexafluorophosphate ($[PF_6]^-$), tetrafluoroborate ($[BF_4]^-$) and bis(trifluoromethanesulfonimide) ($[NTf_2]^-$) have appeared in the literature and new ILs are being reported every month.[67]

1.3 Ionogels

As RTILs are liquid at ambient conditions, they have been explored for the use in functional hybrid materials termed ion-gels or ionogels.[68-70] Currently for applications in materials science, there is growing interest in “ionogels”, i.e. polymers with ILs integrated such that they

retain their specific properties within the polymer/gel environment. An excellent review by Le Bideau et. al.[70] discusses ionogels as a new class of hybrid materials, in which the properties of the IL are hybridized with those of various components, which may be organic (low molecular weight gelator[71], bio-polymer), inorganic (e.g. carbon nanotubes, silica[72] etc.) or hybrid organic–inorganic (e.g. polymer and inorganic fillers)[73]. An ionogel has properties arising from both the polymeric network stabilizing the ionogel and the functionalities of the contained IL. [2, 42, 74, 75] They exhibit a wide range of interesting properties, and can be soft or hard materials, with high resistance to drying and cracking due to their very low vapour pressure. This renders ionogels attractive for application in soft actuators as conventional materials often show rapid degradation of performance due to loss of solvent by evaporation.[68, 76] Properties such as their very low vapour pressure over a wide temperature range render ionogels superior to standard hydro- or organo-gels without imparting the properties of the polymeric matrix material.[68] Understandably therefore, in recent years there has been an explosion of research in ionogels, which is reflected in several review papers. [2, 69, 77, 78]

1.3.1 Stimulus responsive ionogels

A stimulus responsive polymeric network formed with an IL as the liquid component, rather than a conventional molecular solvent, can be termed a “stimulus responsive ionogel”. Several examples of this class of material based on different modes of actuation have been reported recently. Magnetic ionogels have been prepared by Xie et al.[26] by filling a poly(methyl-methacrylate) network with a magnetic IL 1-butyl-3-methylimidazolium tetrachloroferrate (III) or [Bmim][FeCl₄]. A different approach to prepare magnetic ionogels with magnetic particles copolymerised into the polymer structure is presented in Chapter 4. Photoresponsive ionogels have also been synthesised by Benito-Lopez et al.[76]. In this example, a spiropyran comonomer provides the pNIPAM network with photo actuating properties. The gel incorporates ILs based on trihexyl-tetradecyl-phosphonium cation.

Ionogels containing pendant azobenzene and based on poly(benzylmethacrylate) and imidazolium IL [C2mim][NTf₂] were reported by Ueki *et al.* [35] These materials shrank and expanded when exposed to light due to the well-known cis/trans-azobenzene photo-induced switching behaviour. The actuation appeared to be related to the presence of LCST behaviour in the ionogel polymer (Figure 1-8).

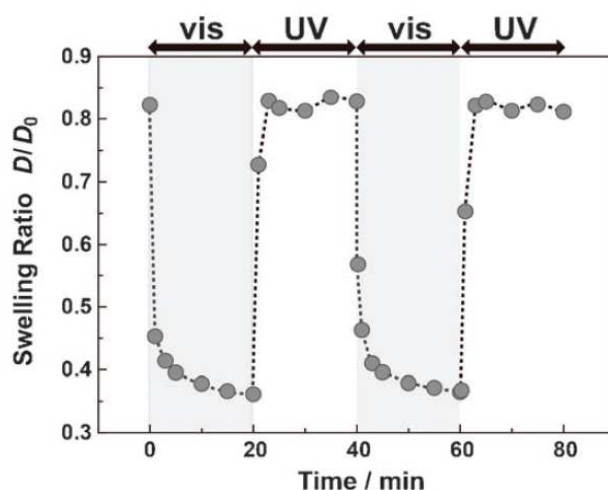


Figure 1-8. Photoinduced volume phase transition of poly(azobenzenemethacrylate-co-benzenemethacrylate) gel in $[C_2mim][NTf_2]$ at 83 °C. The plots show a change in swelling ratios under visible light (437 nm) irradiation and UV light (366 nm) irradiation.[35]

1.4 References:

1. Ahn, S.-k.; Kasi, R. M.; Kim, S.-C.; Sharma, N.; Zhou, Y., Stimuli-responsive polymer gels. *Soft Matter* **2008**, *4*, 1151-1157.
2. Kavanagh, A.; Byrne, R.; Diamond, D.; Fraser, K. J., Stimuli Responsive Ionogels for Sensing Applications—An Overview. *Membranes* **2012**, *2*, 16-39.
3. Messing, R.; Schmidt, A. M., Perspectives for the mechanical manipulation of hybrid hydrogels. *Polymer Chemistry* **2011**, *2*, 18-32.
4. Motornov, M.; Roiter, Y.; Tokarev, I.; Minko, S., Stimuli-responsive nanoparticles, nanogels and capsules for integrated multifunctional intelligent systems. *Progress in Polymer Science* **2010**, *35*, 174-211.
5. Pasparakis, G.; Vamvakaki, M., Multiresponsive polymers: nano-sized assemblies, stimuli-sensitive gels and smart surfaces. *Polymer Chemistry* **2011**, *2*, 1234-1248.
6. Suzuki, H., Stimulus-responsive Gels: Promising Materials for the Construction of Micro Actuators and Sensors. *Journal of Intelligent Material Systems and Structures* **2006**, *17*, 1091-1097.
7. Maeda, S.; Hara, Y.; Yoshida, R.; Hashimoto, S., Active Polymer Gel Actuators. *International Journal of Molecular Sciences* **2010**, *11*, 52-66.
8. Liu, F.; Urban, M. W., Recent advances and challenges in designing stimuli-responsive polymers. *Progress in Polymer Science* **2010**, *35*, 3-23.
9. Imran, A. B.; Seki, T.; Takeoka, Y., Recent advances in hydrogels in terms of fast stimuli responsiveness and superior mechanical performance. *Polymer Journal* **2010**, *42*, 839-851.
10. Alarcon, C. d. I. H.; Pennadam, S.; Alexander, C., Stimuli responsive polymers for biomedical applications. *Chemical Society Reviews* **2005**, *34*, 276-285.
11. Byrne, R.; Benito-Lopez, F.; Diamond, D., Materials science and the sensor revolution. *Materials Today* **2010**, *13*, 9-16.

12. Agarwal, A. K.; Dong, L.; Beebe, D. J.; Jiang, H., Autonomously-triggered microfluidic cooling using thermo-responsive hydrogels. *Lab on a Chip* **2007**, *7*, 310-315.
13. Fahrni, F.; Prins, M. W. J.; van Ijzendoorn, L. J., Micro-fluidic actuation using magnetic artificial cilia. *Lab on a Chip* **2009**, *9*, 3413-3421.
14. Hou, C.; Zhang, Q.; Wang, H.; Li, Y., Functionalization of PNIPAAm microgels using magnetic graphene and their application in microreactors as switch materials. *Journal of Materials Chemistry* **2011**, *21*, 10512-10517.
15. Ramírez-García, S.; Baeza, M.; O'Toole, M.; Wu, Y.; Lalor, J.; Wallace, G. G.; Diamond, D., Towards the development of a fully integrated polymeric microfluidic platform for environmental analysis. *Talanta* **2008**, *77*, 463-467.
16. Schild, H. G., Poly (n-isopropylacrylamide) - experiment, theory and application. . *Progress in Polymer Science* **1992**, *17*, 163-249.
17. Philippova, O. E.; Hourdet, D.; Audebert, R.; Khokhlov, A. R., pH-Responsive Gels of Hydrophobically Modified Poly(acrylic acid). *Macromolecules* **1997**, *30*, 8278-8285.
18. Beebe, D. J.; Moore, J. S.; Bauer, J. M.; Yu, Q.; Liu, R. H.; Devadoss, C.; Jo, B.-H., Functional hydrogel structures for autonomous flow control inside microfluidic channels. *Nature* **2000**, *404*, 588-590.
19. Techawanitchai, P.; Ebara, M.; Idota, N.; Asoh, T.-A.; Kikuchi, A.; Aoyagi, T., Photo-switchable control of pH-responsive actuators via pH jump reaction. *Soft Matter* **2012**, *8*.
20. Satoh, T.; Sumaru, K.; Takagi, T.; Kanamori, T., Fast-reversible light-driven hydrogels consisting of spirobenzopyran-functionalized poly(N-isopropylacrylamide). *Soft Matter* **2011**, *7*, 8030-8034.
21. O'Grady, M. L.; Kuo, P.-I.; Parker, K. K., Optimization of Electroactive Hydrogel Actuators. *ACS Applied Materials & Interfaces* **2009**, *2*, 343-346.
22. Satarkar, N. S.; Zhang, W.; Eitel, R. E.; Hilt, J. Z., Magnetic hydrogel nanocomposites as remote controlled microfluidic valves. *Lab on a Chip* **2009**, *9*, 1773-1779.
23. Fuhrer, R.; Athanassiou, E. K.; Luechinger, N. A.; Stark, W. J., Crosslinking Metal Nanoparticles into the Polymer Backbone of Hydrogels Enables Preparation of Soft, Magnetic Field-Driven Actuators with Muscle-Like Flexibility. *Small* **2009**, *5*, 383-388.
24. Ghosh, S.; Yang, C.; Cai, T.; Hu, Z. B.; Neogi, A., Oscillating magnetic field-actuated microvalves for micro- and nanofluidics. *Journal of Physics D-Applied Physics* **2009**, *42*.
25. Sun, S.; Hu, J.; Tang, H.; Wu, P., Chain Collapse and Revival Thermodynamics of Poly(N-isopropylacrylamide) Hydrogel. *The Journal of Physical Chemistry B* **2010**, *114*, 9761-9770.
26. Xie, Z.-L.; Jelicic, A.; Wang, F.-P.; Rabu, P.; Friedrich, A.; Beuermann, S.; Taubert, A., Transparent, flexible, and paramagnetic ionogels based on PMMA and the iron-based ionic liquid 1-butyl-3-methylimidazolium tetrachloroferrate(iii) [Bmim][FeCl₄]. *Journal of Materials Chemistry* **2010**, *20*, 9543-9549.
27. Burke, N. A. D.; Stöver, H. D. H.; Dawson, F. P., Magnetic Nanocomposites: Preparation and Characterization of Polymer-Coated Iron Nanoparticles. *Chemistry of Materials* **2002**, *14*, 4752-4761.
28. Xia, H.; Wang, J. A.; Tian, Y.; Chen, Q. D.; Du, X. B.; Zhang, Y. L.; He, Y.; Sun, H. B., Ferrofluids for Fabrication of Remotely Controllable Micro-Nanomachines by Two-Photon Polymerization. *Advanced Materials* **2010**, *22*, 3204.
29. Massart, R., Preparation of aqueous magnetic liquids in alkaline and acidic media. . *Ieee Transactions on Magnetics* **1981**, *17*, 1247-1248.

30. Posthumus, W.; Magusin, P.; Brokken-Zijp, J. C. M.; Tinnemans, A. H. A.; van der Linde, R., Surface modification of oxidic nanoparticles using 3-methacryloxypropyltrimethoxysilane. *Journal of Colloid and Interface Science* **2004**, *269*, 109-116.
31. Wang, S.; Zhou, Y.; Guan, W.; Ding, B., One-step copolymerization modified magnetic nanoparticles via surface chain transfer free radical polymerization. *Applied Surface Science* **2008**, *254*, 5170-5174.
32. Caykara, T.; Yoruk, D.; Demirci, S., Preparation and Characterization of Poly(N-tert-butylacrylamide-co-acrylamide) Ferrogel. *Journal of Applied Polymer Science* **2009**, *112*, 800-804.
33. Jordan, A.; Wust, P.; Fahling, H.; John, W.; Hinz, A.; Felix, R., Inductive heating of ferrimagnetic particles and magnetic fluids - physical evaluation of their potential for hyperthermia. *International Journal of Hyperthermia* **1993**, *9*, 51-68.
34. Beharry, A. A.; Woolley, G. A., Azobenzene photoswitches for biomolecules. *Chemical Society Reviews* **2011**, *40*, 4422-4437.
35. Ueki, T.; Yamaguchi, A.; Watanabe, M., Unlocking of interlocked heteropolymer gel by light: photoinduced volume phase transition in an ionic liquid from a metastable state to an equilibrium phase. *Chemical Communications* **2012**, *48*, 5133-5135.
36. Irie, M.; Menju, A.; Hayashi, K., Photoresponsive Polymers. Reversible Solution Viscosity Change of Poly(methyl methacrylate) Having Spirobenzopyran Side Groups. *Macromolecules* **1979**, *12*, 1176-1180.
37. Irie, M.; Kunwathakun, D., Photoresponsive polymers. 8. Reversible photostimulated dilation of polyacrylamide gels having triphenylmethane leuco derivatives. *Macromolecules* **1986**, *19*, 2476-2480.
38. Herz, M. L., Photochemical ionization of the triarylmethane leuconitriles. *Journal of the American Chemical Society* **1975**, *97*, 6777-6785.
39. Zhao, Y.; Tremblay, L.; Zhao, Y., Doubly photoresponsive and water-soluble block copolymers: Synthesis and thermosensitivity. *Journal of Polymer Science Part A: Polymer Chemistry* **2010**, *48*, 4055-4066.
40. van Oosten, C. L.; Bastiaansen, C. W. M.; Broer, D. J., Printed artificial cilia from liquid-crystal network actuators modularly driven by light. *Nature Materials* **2009**, *8*, 677-682.
41. van Oosten, C. L.; Corbett, D.; Davies, D.; Warner, M.; Bastiaansen, C. W. M.; Broer, D. J., Bending Dynamics and Directionality Reversal in Liquid Crystal Network Photoactuators. *Macromolecules* **2008**, *41*, 8592-8596.
42. Fraser, K. J.; MacFarlane, D. R., Phosphonium-Based Ionic Liquids: An Overview. *Australian Journal of Chemistry* **2009**, *62*, 309-321.
43. Rogers, R. D.; Seddon, K. R., *Ionic Liquids as Green Solvents: Progress and Prospects*. American Chemical Society: 2003; Vol. 125, p 15684.
44. Wasserscheid, P.; Keim, W., Ionic liquids - new "solutions" for transition metal catalysis. *Angewandte Chemie, International Edition* **2000**, *39*, 3772-3789.
45. Welton, T., Room-Temperature Ionic Liquids. Solvents for Synthesis and Catalysis. *Chemical Reviews (Washington, D. C.)* **1999**, *99*, 2071-2083.
46. Bansal, D.; Cassel, F.; Croce, F.; Hendrickson, M.; Plichta, E.; Salomon, M., Conductivities and Transport Properties of Gelled Electrolytes with and without an Ionic Liquid for Li and Li-Ion Batteries. *Journal of Physical Chemistry B* **2005**, *109*, 4492-4496.

47. Frackowiak, E.; Lota, G.; Pernak, J., Room-temperature phosphonium ionic liquids for supercapacitor application. *Applied Physics Letters* **2005**, *86*, 164104/164101-164104/164103.
48. Lee, J. S.; Bae, J. Y.; Lee, H.; Quan, N. D.; Kim, H. S.; Kim, H., Ionic liquids as electrolytes for Li ion batteries. *Journal of Industrial and Engineering Chemistry (Seoul, Republic of Korea)* **2004**, *10*, 1086-1089.
49. Lu, W.; Norris, I. D.; Mattes, B. R., Electrochemical Actuator Devices Based on Polyaniline Yarns and Ionic Liquid Electrolytes. *Australian Journal of Chemistry* **2005**, *58*, 263-269.
50. MacFarlane, D. R.; Forsyth, M., Plastic crystal electrolyte materials: new perspectives on solid state ionics. *Advanced Materials* **2001**, *13*, 957-966.
51. Marwanta, E.; Mizumo, T.; Nakamura, N.; Ohno, H., Improved ionic conductivity of nitrile rubber/ionic liquid composites. *Polymer* **2005**, *46*, 3795-3800.
52. Pernak, J.; Stefaniak, F.; Weglewski, J., Phosphonium acesulfamate based ionic liquids. *European Journal of Organic Chemistry* **2005**, 650-652.
53. Wassercheid, P.; Welton, T., *Ionic liquids in synthesis*. Wiley-VCH: 2003.
54. Webber, A.; Blomgren, G. E., *Ionic liquids for lithium ion and related batteries*. 2002; p 185-232.
55. Sakaebe, H.; Matsumoto, H., N-Methyl-N-propylpiperidinium bis(trifluoromethanesulfonyl)imide (PP13-TFSI) - novel electrolyte base for Li battery. *Electrochemistry Communications* **2003**, *5*, 594-598.
56. Papageorgiou, N.; Athanassov, Y.; Armand, M.; Bonhote, P.; Pettersson, H.; Azam, A.; Graetzel, M., The performance and stability of ambient temperature molten salts for solar cell applications. *Journal of the Electrochemical Society* **1996**, *143*, 3099-3108.
57. Wang, P.; Zakeeruddin, S. M.; Exnar, I.; Graetzel, M., High efficiency dye-sensitized nanocrystalline solar cells based on ionic liquid polymer gel electrolyte. *Chemical Communications (Cambridge, United Kingdom)* **2002**, 2972-2973.
58. Wang, P.; Zakeeruddin, S. M.; Graetzel, M.; Kantlehner, W.; Mezger, J.; Stoyanov, E. V.; Scherr, O., Novel room temperature ionic liquids of hexaalkyl substituted guanidinium salts for dye-sensitized solar cells. *Applied Physics A: Materials Science & Processing* **2004**, *A79*, 73-77.
59. Lu, W.; Fadeev, A. G.; Qi, B.; Smela, E.; Mattes, B. R.; Ding, J.; Spinks, G. M.; Mazurkiewicz, J.; Zhou, D.; Wallace, G. G.; MacFarlane, D. R.; Forsyth, S. A.; Forsyth, M., Use of ionic liquids for p-conjugated polymer electrochemical devices. *Science (Washington, DC, United States)* **2002**, *297*, 983-987.
60. Ding, J.; Zhou, D.; Spinks, G.; Wallace, G.; Forsyth, S.; Forsyth, M.; MacFarlane, D., Use of Ionic Liquids as Electrolytes in Electromechanical Actuator Systems Based on Inherently Conducting Polymers. *Chemistry of Materials* **2003**, *15*, 2392-2398.
61. Zhou, D.; Spinks, G. M.; Wallace, G. G.; Tiyaiboonthaiya, C.; MacFarlane, D. R.; Forsyth, M.; Sun, J., Solid state actuators based on polypyrrole and polymer-in-ionic liquid electrolytes. *Electrochimica Acta* **2003**, *48*, 2355-2359.
62. Nanjundiah, C.; McDevitt, S. F.; Koch, V. R., Differential capacitance measurements in solvent-free ionic liquids at Hg and C interfaces. *Journal of the Electrochemical Society* **1997**, *144*, 3392-3397.
63. McEwen, A. B.; McDevitt, S. F.; Koch, V. R., Nonaqueous electrolytes for electrochemical capacitors: imidazolium cations and inorganic fluorides with organic carbonates. *Journal of the Electrochemical Society* **1997**, *144*, L84-L86.

64. McEwen, A. B.; Ngo, E. L.; LeCompte, K.; Goldman, J. L., Electrochemical properties of imidazolium salt electrolytes for electrochemical capacitor applications. *Journal of the Electrochemical Society* **1999**, *146*, 1687-1695.
65. Wooster, T. J.; Johanson, K. M.; Fraser, K. J.; MacFarlane, D. R.; Scott, J. L., Thermal degradation of cyano containing ionic liquids. *Green Chemistry* **2006**, *8*, 691-696.
66. Bradaric, C. J.; Downard, A.; Kennedy, C.; Robertson, A. J.; Zhou, Y., Industrial preparation of phosphonium ionic liquids. *Green Chemistry* **2003**, *5*, 143-152.
67. Ramnial, T.; Ino, D. D.; Clyburne, J. A. C., Phosphonium ionic liquids as reaction media for strong bases. *Chemical Communications (Cambridge, United Kingdom)* **2005**, 325-327.
68. Ueki, T.; Watanabe, M., Macromolecules in Ionic Liquids: Progress, Challenges, and Opportunities. *Macromolecules* **2008**, *41*, 3739-3749.
69. Néouze, M.-A.; Bideau, J. L.; Gaveau, P.; Bellayer, S.; Vioux, A., Ionogels, New Materials Arising from the Confinement of Ionic Liquids within Silica-Derived Networks. *Chemistry of Materials* **2006**, *18*, 3931-3936.
70. Le Bideau, J.; Viau, L.; Vioux, A., Ionogels, ionic liquid based hybrid materials. *Chemical Society Reviews* **2011**, *40*, 907-925.
71. Mohmeyer, N.; Kuang, D.; Wang, P.; Schmidt, H.-W.; Zakeeruddin, S. M.; Gratzel, M., An efficient organogelator for ionic liquids to prepare stable quasi-solid-state dye-sensitized solar cells. *Journal of Materials Chemistry* **2006**, *16*, 2978-2983.
72. Viau, L.; Tourne-Peteilh, C.; Devoisselle, J.-M.; Vioux, A., Ionogels as drug delivery system: one-step sol-gel synthesis using imidazolium ibuprofenate ionic liquid. *Chemical Communications* **2010**, *46*, 228-230.
73. Gayet, F.; Viau, L.; Leroux, F.; Mabile, F. d. r.; Monge, S.; Robin, J.-J.; Vioux, A., Unique Combination of Mechanical Strength, Thermal Stability, and High Ion Conduction in PMMA–Silica Nanocomposites Containing High Loadings of Ionic Liquid. *Chemistry of Materials* **2009**, *21*, 5575-5577.
74. Susan, M. A. B. H.; Kaneko, T.; Noda, A.; Watanabe, M., Ion Gels Prepared by in Situ Radical Polymerization of Vinyl Monomers in an Ionic Liquid and Their Characterization as Polymer Electrolytes. *Journal of the American Chemical Society* **2005**, *127*, 4976-4983.
75. Pernak, J.; Goc, I.; Mirska, I., Anti-microbial activities of protic ionic liquids with lactate anion. *Green Chemistry* **2004**, *6*, 323-329.
76. Benito-Lopez, F.; Byrne, R.; Raduta, A. M.; Vrana, N. E.; McGuinness, G.; Diamond, D., Ionogel-based light-actuated valves for controlling liquid flow in micro-fluidic manifolds. *Lab on a Chip* **2010**, *10*, 195-201.
77. Vioux, A.; Viau, L.; Volland, S.; Le Bideau, J., Use of ionic liquids in sol-gel; ionogels and applications. *Comptes Rendus de l' Academie des Sciences Serie IIc:Chemie* **2009**, *13*, 242-255.
78. Le Bideau, J.; Viau, L.; Vioux, A., Ionogels, ionic liquid based hybrid materials. *Chemical Society Reviews* **2011**.

Chapter 2:

Integrating stimulus responsive materials and microfluidics – The key to next generation chemical sensors

Bartosz Ziółkowski, Monika Czugała and Dermot Diamond

CLARITY Centre for Sensor Web Technologies, National Centre for Sensor Research, Dublin City University, Dublin 9, Ireland

Published online before print: *Journal of Intelligent Material Systems and Structures*, September 27, 2012

DOI: 10.1177/1045389X12459591

Abstract

New generations of chemical sensors require both innovative (evolutionary) engineering concepts and (revolutionary) breakthroughs in fundamental materials chemistry, such as the emergence of new types of stimuli responsive materials. Intensive research in those fields in recent years have brought interesting new concepts and designs for microfluidic flow control and sample handling that integrate high quality engineering with new materials. In this paper we review recent developments in this fascinating area of science, with particular emphasis on photoswitchable soft actuators and their incorporation into fluidic devices that are increasingly biomimetic in nature.

Keywords: stimuli responsive materials, microfluidics, flow handling

2.1 Introduction

In a utopian future, water quality will be monitored through large numbers of densely deployed sensors that are capable of detecting key quality parameters with exquisite selectivity and sensitivity, and of functioning reliably in an autonomous manner for long periods of time (years). The information generated by these sensor networks will be analysed and filtered, and key events flagged in real time to key stakeholders (agency enforcement officers, water treatment specialists, and the general public). However, in reality, issues like biofouling and surface degradation mean that sensor characteristics change rapidly in real samples, and consequently, chemical sensors must be regularly recalibrated to ensure the information they send is reliable. This results in complex and very costly devices that must integrate fluidics, standards, and waste storage, as well as sampling and analytical procedures. Consequently, monitoring programmes are dominated by manual grab sampling at a relatively small number of locations, with a frequency often restricted to 3 or 4 times per year. Scale up in terms of sampling frequency and number of locations is dictated by cost, and therefore the key to significant movement towards the utopian vision is to drive down the cost base of environmental monitoring.

Analysis of the component cost base of autonomous analysers we have built (Gen1¹ and Gen2), together with a speculated cost analysis of a future platform based on fully integrated polymer actuator valves and pumps are presented in Figure 2-1. These show clearly for Gen1 and Gen 2, that the single greatest contribution to the cost base is the fluidic handling category. In the first generation (Gen1) design, this amounted to over 80% of the total cost of ca. €2,000, and while this dropped in the second generation design through good engineering and careful choice of components, it was still almost 2/3 of the total component cost of ca. €180. These are accurate figures based on platforms that we are currently making. We have also made a ‘concept’ integrated analyser with integrated polymer actuator pumps and estimate the total cost to be in the region of €20-50 per unit, of which we estimate ca. 50% is costs related to fluid handling components. The figures here are more speculative, but there is no doubt that if the fluid handling components could be fully integrated into the fluidic system, for example using highly automated in-situ photopolymerisation of the key liquid handling components, the unit cost would be considerably lower. Furthermore, if the control stimulus for valve actuation/fluidic control does not require physical contact (e.g. light, heat, magnetism..) then manufacturing would be further simplified, as the fluid handling layer could be produced as an entirely stand-alone unit. Therefore in this contribution, we will review strategies for making and integrating

¹ These are 1st and 2nd Generation versions of fluidic based colorimetric chemical analysers targeting analytes such as phosphate, nitrate, pH, COD etc.

polymer actuators in microfluidic systems, and speculate on how the field may progress over the coming years.

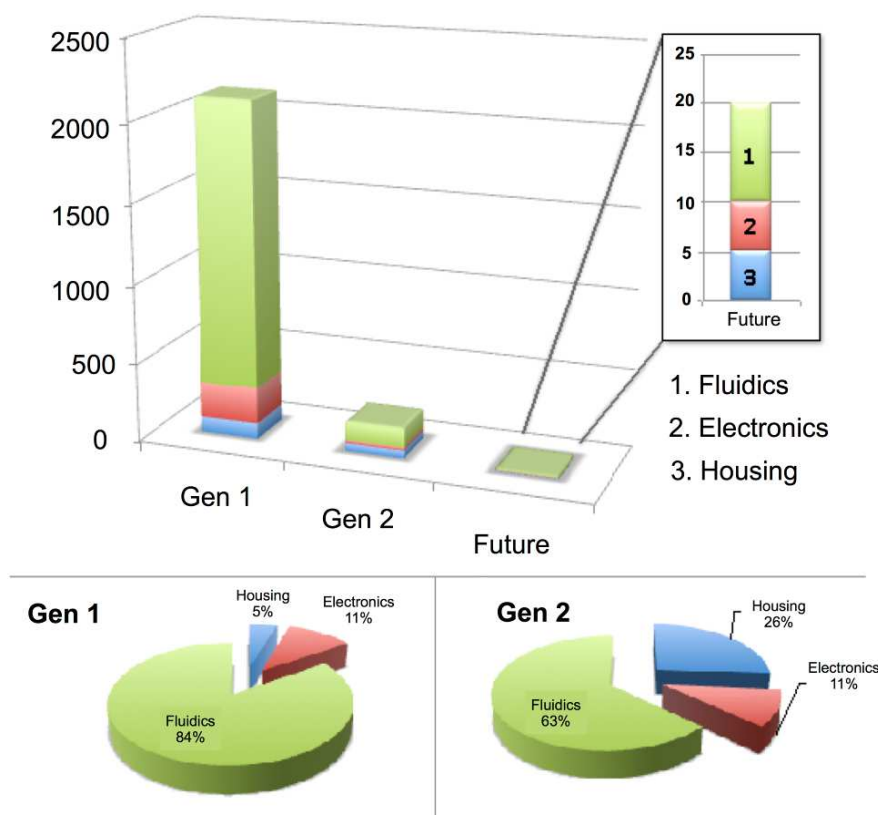


Figure 2-1. Analysis of component costs (€) for first generation (Gen1), second generation (Gen2) and future 'concept' analyser. Total component cost by category (top) drops from ca. €2,000, to under €200, to ca. €20 per unit, respectively.

2.2 Polymer actuator valves in microfluidic systems

Valves are one of the most important components within microfluidic systems, since they provide directional control of flow and facilitate essential actions, such as sample/standard selection and addition of reagents. Some key requirements of an ideal microvalve are;

- Zero flow resistance in the open position;
- Zero leakage in the closed position;
- Infinite tolerance to high pressure in the closed position;
- Instant response to switching between the open and closed positions
- Simple routes to fabrication and integration in-situ within the microfluidic system
- Prepared from readily available and processable materials.

Many different types of microvalves have been demonstrated, and while none of these can be described as totally satisfactory, they do present significant advances in the realisation of some of these ideal characteristics.[1] In most conventional systems a diaphragm is coupled to an actuator, powered from an external source, which deflects the diaphragm via a magnetic field, high voltage or heating.

2.2.1 Magnetically actuated valves

Flow regulation in microfluidic devices by magnetic forces has many advantages, such as capability of generating large angular displacement as well as possibility of using very strong magnetic force to drive actuation. Satarkar and co-workers developed the nanocomposite hydrogel valve, in which magnetic nanoparticles were dispersed in temperature-responsive *N*-isopropylacrylamide (NIPAAm) polymer matrix[2] (Figure 2-2). The swelling and collapse of the hydrogel nanocomposite can be remotely controlled by application of an alternating magnetic field (AMF) at a frequency 293 kHz. The disadvantage of this hydrogel microvalve is that its response as reported is sluggish, but this can be improved by moving to smaller valve dimensions, as gel processes are typically diffusion driven, and smaller feature sizes reduce the diffusion pathlength. Similar oscillating magnetic field actuated valves were prepared by Ghosh *et al.*[3]

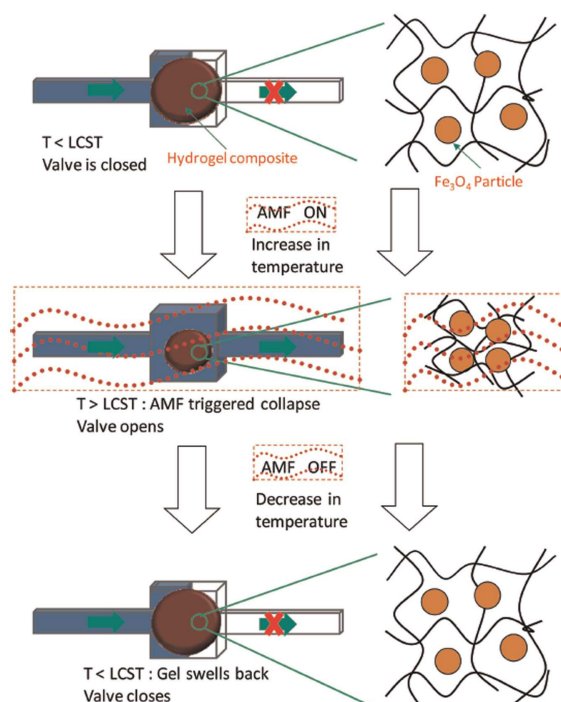


Figure 2-2. Scheme presenting the hydrogel nanocomposite valves performance with an AMF. The application of the AMF results in the collapse of the hydrogel, leading to the opening of the valve. Source: Reproduced from Satarkar *et al.* (2009) by permission of The Royal Society of Chemistry. AMF: alternating magnetic field; LCST: lower critical solution temperature.

2.2.2 Pneumatic valves

Pneumatic microvalves represent another type of fluid handling, however, they require external laboratory infrastructure – gas cylinders, computers, ground electricity, for their operation which makes it difficult to incorporate them into autonomous monitoring instruments. The development of PMMA/PDMS pneumatic valves and pumps for disposable microfluidics was reported by Zhang *et. al.*[4]. Pneumatic microstructures were fabricated by sandwiching a PDMS membrane between PMMA fluidic channel and manifold wafers, as in Figure 2-3. Valve control was obtained by applying pressure on the pneumatic layer sited in a displacement chamber using a computer regulated solenoid. Apart from providing fluid pressure up to 15.4 mL/s at 60 kPa, the valve seals reliably against forward fluid pressures as high as 60 kPa. A PMMA diaphragm pump was presented based by connecting three valves in series. Simultaneously, the fluid flow rate could be accurately controlled from nL to mL per second, simply by changing the valve actuation time, the displacement chamber volume, and the applied pressure. Go and Shoji presented a three-dimensional in-plane hemisphere PDMS microvalve without dead volume and leakage flow.[5] A closing time of 0.1 s and an opening time of 0.5 s were obtained by applying a pneumatic pressure of 10 kPa to the PDMS membrane. Even though a faster response for closing was possible, it took a longer time to release the membrane for opening.

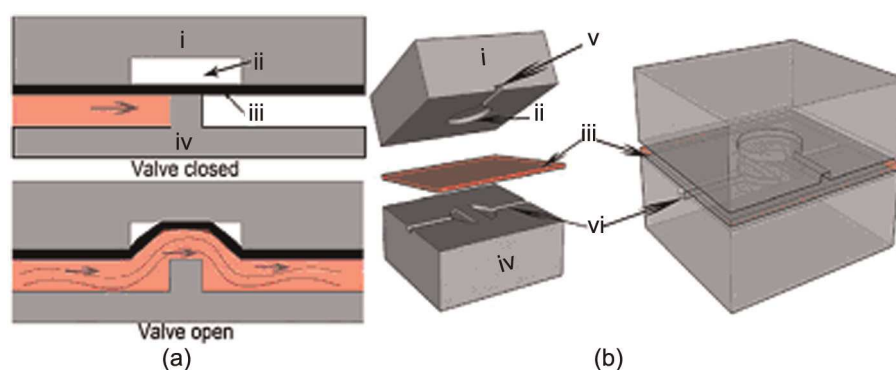


Figure 2-3. (a) Cross-sectional views of a three-layer monolithic PMMA/PDMS membrane valve and (b) exploded and assembled illustrations of a single PMMA/PDMS membrane valve. (i) PMMA pneumatic wafer, (ii) displacement chamber, (iii) PDMS membrane, (iv) PMMA fluidic wafer, (v) pneumatic channel and (vi) fluidic channel. Source: Reproduced from Zhang *et al.* (2009) by permission of The Royal Society of Chemistry. PMMA: poly(methyl methacrylate); PDMS: polydimethylsiloxane.

2.2.3 Electrothermal valves

In contrast to many other technologies, electrothermally actuated phase change microvalves developed by Kaigala *et. al.* can be readily scalable to smaller dimensions, allowing the fabrication of a portable and inexpensive genetic analysis platform.[6] This easily integrated,

reusable microvalve technology that can be easily incorporated within standard lab on a chip (LOC) technologies is based on the polyethylene glycol polymer (PEG) that exhibits a large volumetric change between its solid and liquid phases. The volumetric expansion, thermally controlled by applying thin film resistive elements that are patterned with standard microfabrication techniques, switches a flexible PDMS membrane between opened or closed state between two discontinuous channels (Figure 2-4). The switching time for opening/closing, was on the order of minutes, and the microvalve was reported to be leakage-free to a pressure of 30 psi at a temperature of 50 °C in the PEG reservoir. Selvaganapathy *et al.* realized normally open electrothermally actuated inline microvalve for liquid regulation[7]. The actuation mechanism was based on a thermally activated phase change in the Paraffin layer resulting in a high volumetric expansion. The microvalve was surface micromachined on top of preformed flexible microfluidic channels using a low temperature fabrication process. As the Paraffin was heated beyond its melting point using the microheaters underneath them, it undergoes a volume expansion, which deflects the flexible diaphragm of the piston, closing the microchannel beneath it. Actuation was achieved at power as low as 35 mW with the response times of 15 ms. Similar valves opened by melting a polymer with heat provided from a laser were demonstrated by Garcia-Cordero *et al.*[8] These valves were fully integrated into a microfluidic platform and are characterised by very low cost. The disadvantage is that they can be used only once.

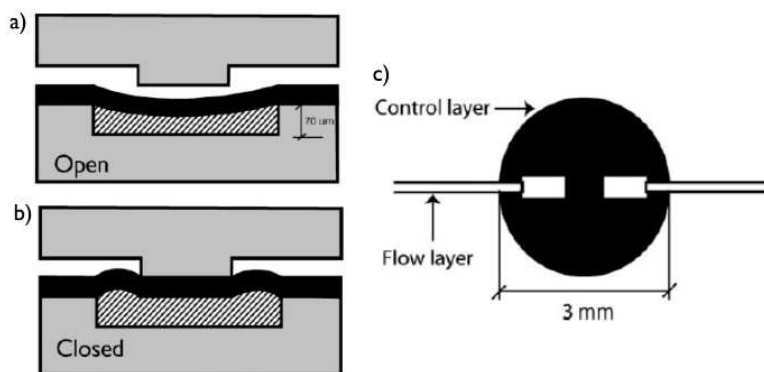


Figure 2-4. (a and b) Cross-sectional and (c) top views of the microvalve structure. The features in the control layer are 70 mm deep while those in the fluidic layer are 90 mm deep. (a) Open state of valve and (b) closed state of valve. Source: Reproduced from Kaigala *et al.* (2008) by permission of The Royal Society of Chemistry.

2.2.4 Soft polymer valves

Most conventional microvalves coupled to piezoelectric, thermopneumatic, electrostatic or electromagnetic actuators require high power consumption, which is highly unfavourable for autonomously deployed instruments. Soft polymer actuators offer an alternative approach that is more biomimetic in nature, and in principle can require relatively low energy for actuation. For example, hydrogels swell and contract significantly due to water movement into/out of the

gel. These volume changes are associated with phase transition behaviour triggered by small alterations of certain external stimuli. These materials can respond to a variety of external stimuli, such as pH, temperature, or light. Among these hydrogels, pH responsive materials have been the focus of particular attention. By converting chemical energy into mechanical work, pH sensitive hydrogels can exhibit both sensing and actuating functions simultaneously. For example, for the pH-sensitive hydrogel poly(2-hydroxyethyl methylacrylate-co-acrylic acid) or poly(HEMA-co-AA), the movement of water is initiated by the ionization of the polymer backbone[9]. Beebe *et. al.* reported a channel with two strips of poly(HEMA-co-AA) deposited along the walls using the laminar flow characteristics to enable polymer precursors to be restricted only to the channel wall region (Figure 2-5)[10]. Under conditions of high pH, swelling of the hydrogel structures occurred and blocked the channel. As the pH in the sensing channel was changed from 11 to 2, the hydrogel contracted to open the flow in the adjacent channel. Although swelling and shrinkage of the hydrogel in response to pH change are reversible and repeatable, reopening of the channel from the closed state (at which point the hydrogel is fully expanded) may limit the use of this design in some applications. In general it is found that the dynamics of reswelling in hydrogels are much slower than contraction, due to the inherent asymmetry of diffusion in these materials.[11, 12]

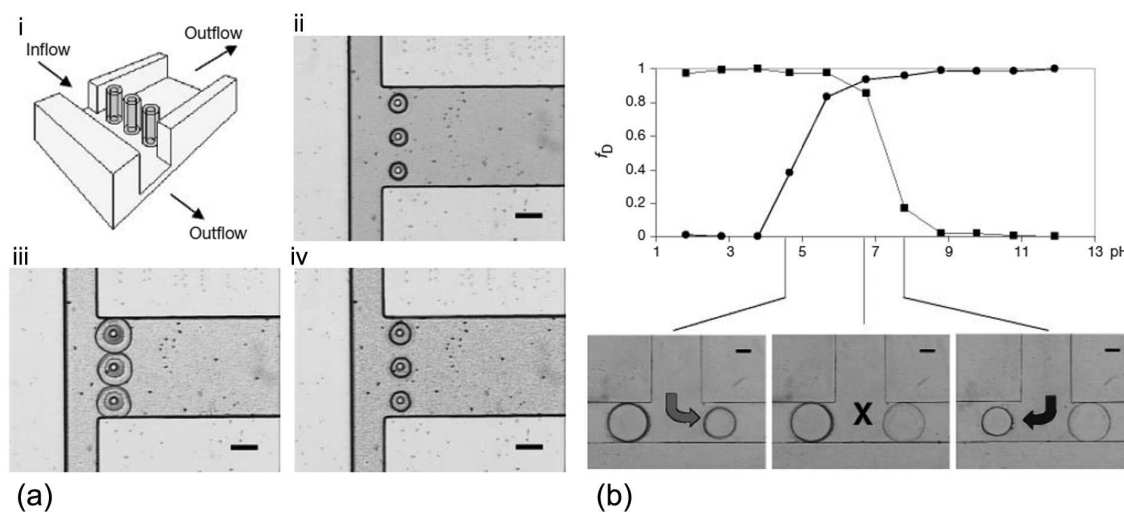


Figure 2-5 (a) Prefabricated posts in a microchannel serve as supports for hydrogel films, improving stability during volume changes: (i) a diagram of the hydrogel films around the posts, (ii) the actual device after polymerisation of the hydrogel, (iii) the hydrogel films block the side channel branch in their expanded state and (iv) the contracted hydrogels allow fluid to flow down the side branch. (b) The volume response of two different hydrogels with respect to the pH of the surrounding fluid. Top, the fractional change in diameter (f_D) of the hydrogels with respect to pH. Bottom, images showing a device that directs a fluid stream on the basis of its pH. The hydrogel gating the right branch (circles) expands in base and contracts in acid. The hydrogel gating the left branch (squares) behaves in the opposite manner (expands in acid and contracts in base). The fluid enters from the centre channel at a rate of 0.05 mL min⁻¹. At a pH of 7.8, the flow is directed down the left branch. At a pH of 4.7, the flow is directed down the right branch. Both hydrogels expand to shut off the flow when the pH is changed to 6.7. Scale bars, 300 μ m. Source: Reprinted with permission from Beebe *et al.* (2000). Copyright 2000 Nature.

Since diffusion is the rate-limiting factor governing the swelling process of hydrogels, the response time can be improved by reducing the size of hydrogel microstructures. In order to fabricate stable hydrogel actuators with fast response times, hydrogel films were photopolymerized using a photomask around prefabricated posts (Figure 2-5a) [10]. At pH 11, the films expanded, closing the channel, whereas flushing the channel with solution at pH 2 resulted in the valves opening, with response time of 12 s. Based on the valve mechanism described above, a pH-dependent flow sorter was also demonstrated (Figure 2-5b)[10]. The entrance to each branch of ‘T’ channel was gated with hydrogel microstructure that expanded in one branch of the channels at high pH and contracts in low pH, whereas a hydrogel of different composition in another branch exhibited an inverse behaviour. In this way, the microfluidic device directed the flow to the appropriate branch, depending on the pH of the solution.

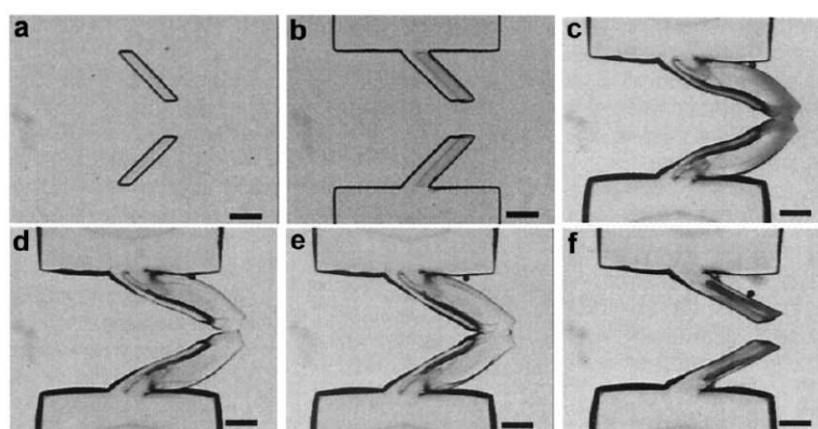


Figure 2-6. Fabrication and operation of a biomimetic valve based on a bistrrip hydrogel. (a) Bistrrip hydrogel is patterned by simultaneous photopolymerisation. (b) The anchor of the valve is formed using a non-responsive hydrogel. (c) When exposed to basic solution, the bistrrip hydrogels expand and curve to form a normally closed valve. (d) The bistrrip valve is pushed open to allow the flow in one direction (from left to right). (e) The flow is restricted in the opposite direction. (f) When exposed to acidic solutions, the valve is deactivated, returning to the permanently open state. Scale bars represent 500 μm . Source: Reproduced from Yu *et al.* (2001). Copyright American Institute of Physics

Yu *et al.* [13] presented a biomimetic bistrrip valve capable of directional flow control in response to changes in the local fluid environment[14]. The valve structure is similar to the venous valve, consisting of a pair of pH sensitive poly(HEMA-co-AA) hydrogel strips overlapped by the pair of pH-insensitive strips (Figure 2-6). When exposed to high pH, dissimilar expansion to adjacent hydrogel strips caused the valve to bend during swelling, thus forming a normally closed check valve allowing only forward flow of pressure above the threshold value. If low pH solution enters the channel, the pH sensitive strips shrink, allowing both forward and backward flow. In comparison to traditional microfluidic valves where actuation occurs very rapidly, here the activation and deactivation times are quite slow, at 6 and 3 minutes respectively. However, this slow operating valve can be successfully applied in drug delivery and bioassay devices, where timescales for events can be of the order of hours.

However, in order to handle biological cells and proteins, manipulation of fluids with neutral pH is desired. In order to minimize the complexity of fully polymeric integrated fluidic circuits (IFC), all electronically controllable components should ideally be made with one type of hydrogel. This can be achieved with poly(*N*-isopropylacrylamide) (PNIPAAm), one of the best-known temperature-sensitive multifunctional hydrogels. At a temperature above the lower critical solution temperature (LCST) of 32 °C PNIPAAm chains undergo rapid and reversible entropy driven phase transition from extended hydrated coils to collapsed hydrophobic globules that precipitate in water.[15, 16] The temperature-sensitive PNIPAAm hydrogel, which is typically controlled by electronic heating elements, has been used widely for fabrication of not only the standard elements of liquid handling, such as microvalves [17-19] and micropumps [20], but also specific active components such as chemostat valves and chemical sensors [21].

Although robust valves with fast response to external stimuli and successful performance of repeated “open-close” cycles have been reported, their transition temperature (slightly above 30 °C causes shrinkage and valve opening) is too low for some applications, such as on-chip PCR, for which the valves must remain closed at much higher temperatures. Frechet *et. al.* realized thermally actuated valves by crosslinking NIPAAm with *N*-ethylacrylamide (NEAAm), for which the LCST can be adjusted within a wide temperature range to meet the specific requirements of some applications[22]. In order to avoid valve displacement during operation, the microchannels were vinylized to enable covalent attachment of the photopolymerized gels. As a result, a 5 mm long poly(NIPAAm-co-NEAAm) (1:1 molar ratio) valve holds pressure up to 18 MPa without noticeable dislocation, leakage or structural damage in closed mode. Although the authors demonstrated the versatility of the valve and its ability to perform well under conditions typical of numerous microfluidic processes, displaying actuation times in the range of 1-4 s, there is still the need for thermoelectrical elements to implement temperature control. What is more, application of heat induced phase transition is not suitable for samples containing heat sensitive materials, such as protein and cells.

2.3 Micropumps in fluidic systems

In contrary to widely researched and tested microvalves, there is not much interest in hydrogel-based electronically controllable micropumps. Richter *et. al.*[20] presented diffusion micropump (Figure 2-7a), which peristaltic operation provides a continuous and relatively homogeneous pumping. The flow rate obtained for this device is $2.8 \pm 0.35 \mu\text{l min}^{-1}$, with the maximum flow rate of pumping stroke determined by the shrinking kinetics of the hydrogel. This process is strongly dependent on the heating power of the heating meanders in addition to the properties of the elastic PDMS membrane. The higher the pressure of the membrane

(directly proportional to its increasing thickness), the faster actuator shrinks. On the other hand, the increase of membrane thickness significantly influences the reload time of the pump and decreases the maximum swelling volume of hydrogel.

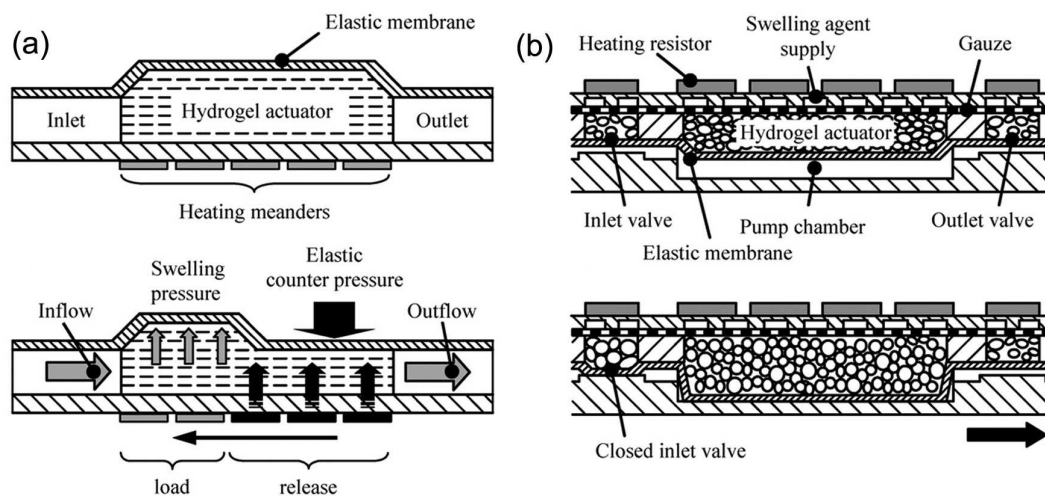


Figure 2-7. (a) Schematic set-up and operating principle of diffusion micropump and (b) displacement micropump. Source: Reproduced from Richter *et al.* (2009) by permission of The Royal Society of Chemistry.

However, this kind of micropump is unsuitable for some applications. For example, some solvents can destroy the hydrogel structure, particles cannot pass the actuation chamber, since the monolithic PNIPAAm actuator is placed directly in the pump chamber, or the pumping pressure can be not sufficient enough. Another pump described by this group based on displacement (Figure 2-7b), provides higher performance (flow rate of 4.5 ul min^{-1} and a back pressure of 1.28 kPa) based on a hydrogel actuator separated from the process medium by a movable membrane. Inexpensive design, simple control and soft lithographic fabrication makes these hydrogel pumps a significant advance towards the realisation of disposable microfluidic components.

2.4 Photoswitchable polymer actuators

In recent years, the range of applications for lab-on-a-chip systems has significantly increased due to several promising aspects, such as smaller sample and reagent volume consumption and less wastage produced, which is cost-effective and environmental friendly. Since it is possible to place many microfluidic architectures in a relatively small area, it enables complex sample processing operations with rapid analysis times to be performed, due to the large increase in the surface area to volume ratio associated with reduction in dimensions. Because of the numerous advantages offered by the microscaled channels, the concept of microfluidic “lab on a chip” has triggered significant effort in development of materials and their employment in miniaturized

devices. In particular, switchable materials offer intriguing possibilities and the potential to integrate sophisticated functions in a simple overall design. Because of their relative ease of fabrication and simple control, stimuli responsive materials integrated with microfluidic manifolds could significantly advance the development of fully integrated microfluidic systems.

Smart engineering of analytical fluidic devices can generate improvements up to a limit, beyond which new, robust and smart materials are needed for further progress.[23] One of the most attractive strategies to implement fluid manipulation on integrated microfluidic platforms is light irradiation, which allows not only for non-contact operation but also independent and remote manipulation of multiple fluids. Photoresponsive polymer materials have been studied by many research groups, and many polymers and polymer gels functionalized with azobenzene [24-26], leukochromophore [23, 24], and spirobenzopyran [25, 26] have been examined. Valves can be controlled with IR[27], blue [28, 29] or white [30, 31] light.

2.4.1 IR-responsive materials

The performance of microvalves based on the volumetric change due to infrared (IR) light illumination was reported by Lo *et al.*[27] They presented an IR-light responsive hydrogel based on thermo-responsive pNIPAAm hydrogels incorporating glycidyl methacrylate functionalized graphene-oxide (GO-GMA). The valve operates in two states – closed, adopted when the IR source is turned off, and opened, adopted when the IR source is turned on, due to absorbance of the IR light by the GO-GMA sheets, which triggers the hydrogel to contract, allowing for fluidic flow. The performance of the hydrogel microvalve is shown in Figure 2-8. When the infrared light is switched off, the heat is dissipated to the surrounding environment, and the hydrogel absorbs water, expanding its volume and blocking the microchannel again.

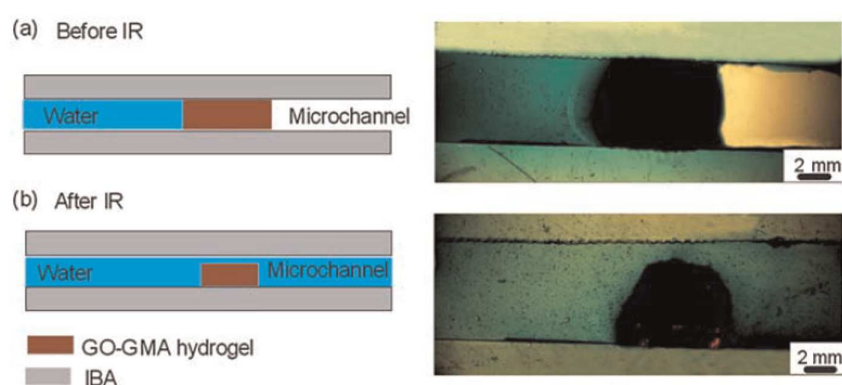


Figure 2-8. A microvalve made of GO-GMA IR-responsive hydrogel. Top views of the microvalve are on the left. Respective images taken under a microscope are on the right. (a) GO-GMA hydrogel microvalve before actuated by IR irradiation (OFF state) and (b) after exposure to IR light (ON state). Source: Reproduced from Lo *et al.* (2011) by permission of The Royal Society of Chemistry. IR: infrared; GO-GMA: glycidyl methacrylate functionalised graphene-oxide.

2.4.2 Spiropyran-based photocontrolled soft actuators.

One of the first reports of a spiropyran monomer copolymerised with vinyl monomers to obtain a photoresponsive polymer was published by Smets[32] *et. al.* in 1978. The author synthesised a crosslinker consisting of two connected spiropyran molecules each having one vinyl group attached. They showed that the spiropyran-crosslinked poly-bisphenol-A-pimelate or polyethyleneglycol tere/isophthalate rubbers contracted as the sample is irradiated with light, and the spiropyran opened into a merocyanine form. Furthermore, they showed that the opening of the spiropyran and consequential colour change was not directly linked with the polymer contraction. Figure 2-9 shows that when the samples are exposed to light in the range $290 \text{ nm} < \lambda < 400 \text{ nm}$ the polymer does not contract significantly, but colouration appears. Illuminating the sample with the light above 472 nm wavelength produces a rapid contraction reaching a maximum when the light wavelength matches the merocyanine absorption wavelength.

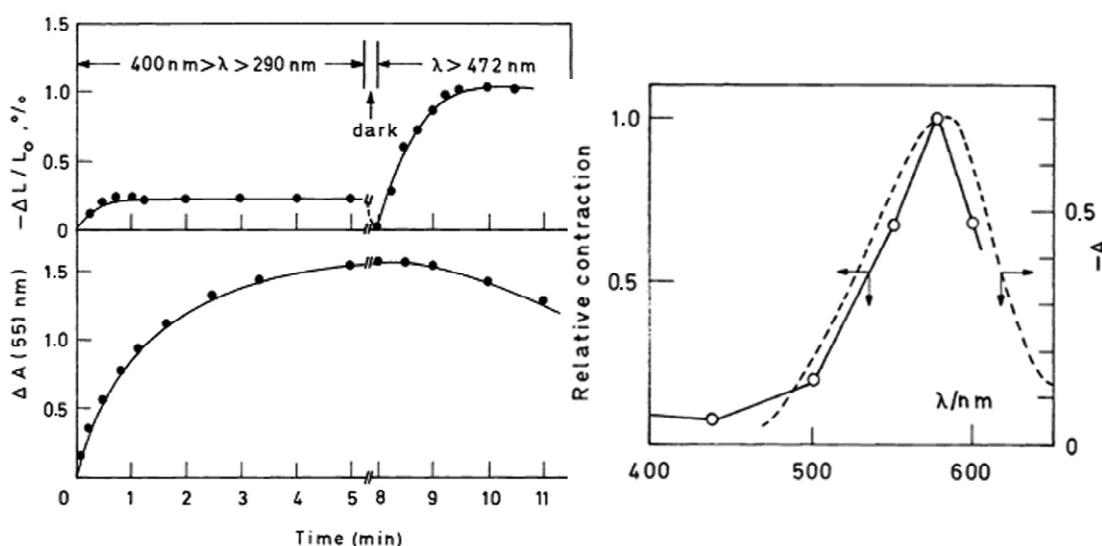


Figure 2-9. Left: Colouration/contraction of spiropyran cross-linked rubbers under UV and visible light illumination. Right: Contraction (—) and absorption (...) spectra of photochromic rubbers. Source: Reprinted from Smets *et al.* (1978). Copyright 1978 IUPAC. UV: ultraviolet.

Therefore, the authors claimed that[32]:

- The irradiation wavelength dependence of the contraction corresponds closely with the absorption spectrum of the merocyanine.
- The rates of ring opening/closure in the spiropyran \leftrightarrow merocyanine equilibrium do not control the rates of dilatation/contraction. The contribution of ring opening/closure is of secondary importance, except for the initial formation of the merocyanine.
- The isomerisation between different open merocyanine forms forces conformation changes in the neighbouring polymer units and this results in shrinkage

Another report from the same group claimed that the viscosity of solutions of poly(methylmethacrylate-co-1,3,3-trimethylindolino-6'-nitro-8'(methacryloxy)methyl]spiropyrans) can also be altered with light irradiation $\lambda > 310$ nm.[33] This is ascribed to the polar neighbouring methacrylate groups solvating the polar merocyanine form of the photochrome co-monomer. This effect decreases as the solvent polarity is increased and disappears in dichloromethane.

In more recent work, on spiropyran (1 mol %) copolymers of pNIPAM, by Sumaru[34] *et al* presented an actuation mechanism based on the lower critical solubility temperature (LCST) of poly(*N*-isopropylacrylamide)[16] and the fact that it changes depending on the chromophore state. Figure 2-10 shows the copolymer used in this study, and the effect of switching. When the copolymer is immersed in an acidic (0.26 mM HCl) solution the spiropyran part of the polymer changes to the open merocyanine form, and becomes protonated. When this polymer is irradiated with light at 422 nm, which matches the absorbance of the protonated merocyanine form, the polymer chains collapse and the proton is released. A correlated change in both absorbance at 422 nm and ionic conductivity is observed.

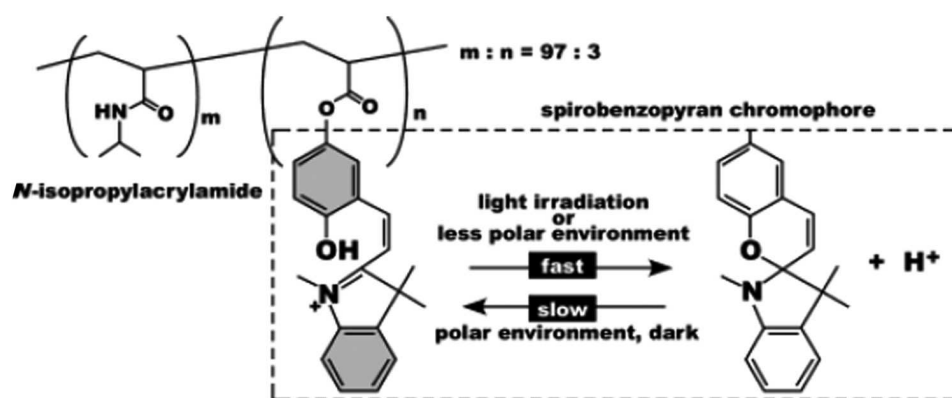


Figure 2-10. Chemical structure of poly(spiropyran-co-NIPAAm) (pSPNIPAAm) and characteristics of its components: pNIPAAm main chain and spiropyrans side chain. Source: Reprinted with permission from Sumaru *et al.* (2004). Copyright 2004 American Chemical Society. pNIPAAm: poly(*N*-isopropylacrylamide).

In a parallel publication Sumaru[35] investigated this system further. Solutions of pNIPAM-co-acrylated spiropyran were analysed at acidic, basic and neutral pH with respect to the temperature and light induced precipitation of the polymer. The following observations were reported:

- The protonated merocyanine (MC-H⁺) pNIPAM copolymer absorbs at 422 nm. The uncharged merocyanine copolymer absorbs strongly at 530 nm and weakly around 370nm.
- Without light irradiation the acidified pNIPAM solution becomes turbid around 32 °C however the turbidity increase is not significant due to the remaining protonated MC-H⁺ chromophores that stabilise the polymer

- With light irradiation at 422 nm (absorption band of MC-H⁺) the acidified polymer solution becomes turbid at 29 °C and increases with increasing temperature. Also the absorption intensity at 422 nm is decreasing as the merocyanine chromophore reverts to the spiropyran form
- A significant turbidity increase is also observed when the same sample is kept at 31.5 °C in the dark and then irradiated with 422 nm light
- Little precipitation is observed when the pNIPAM solutions are neutral or basic due to the fact that at these conditions the chromophore is mostly in the spiropyran (SP) form

These results suggest that the status of the SP \rightleftharpoons MC equilibrium in the copolymer chain, which is controlled by light irradiation, changes the hydrophobic-hydrophilic character of the whole polymer, leading to changes in the LCST. The system works best in acidic pH because under these conditions, the equilibrium predominantly favours the formation of MC. Based on this work of Sumaru, it seems that the LCST is lowered as the equilibrium shifts towards the closed-hydrophobic SP form. This implies that the hydrophilic merocyanine form raises the entire copolymer's LCST. However, it should be noted that the opposite effect has been reported by Ivanov *et al.*[36] In this case, a 10 °C downward shift of the LCST was reported when the sample was irradiated with UV light in deionised water, and the merocyanine absorption at 450 nm became apparent. However, Ivanov used a spiropyran molecule functionalised with a methacryloyl group through the indoline nitrogen linker, in contrast with Sumaru, who acrylated the spiropyran through the 6-hydroxybensopyran group.

Important claims in Sumaru's papers[37, 38, 40] are as follows:

- No protonation at the tertiary amine of spirobenzopyrans with electron-withdrawing substituents in the closed-ring form was detectable by NMR even at acidic conditions.[34]
- The open merocyanine form of the chromophore used by Sumaru has a $pK_a \approx 6-7$ and is not strong enough base to remove protons from water molecules[35]

Additionally, Krüger *et al.*[37] shows that the LCST can be shifted as much as by 20 °C in acrylamide copolymerised with monomers containing azobenzenes.[37] Here, a similar explanation for the phenomena seen by Sumaru[37, 38] is also suggested.

To optimise the actuation of spiropyran functionalised pNIPAM polymers one needs to consider not only changes happening at the chromophore modified units, but also the contraction and swelling processes throughout the entire pNIPAM polymer. It is well known that pNIPAM collapses from an expanded coil to a compact globule form when heated above ~ 32 °C and the opposite happens when cooled down. Wang[11] *et al* showed that there is a particle diameter-temperature hysteresis when pNIPAM is precipitated and left to reswell (Figure 2-11).

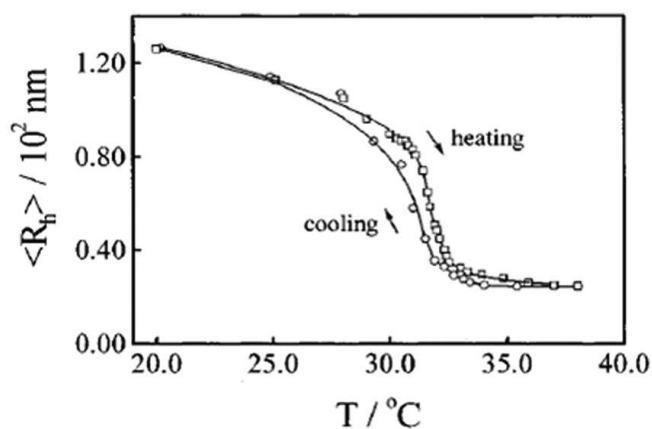


Figure 2-11. Temperature dependence of the average hydrodynamic radius (R_h) of the pNIPAAm chains in the coil-to-globule (heating) and the globule-to-coil (cooling) transitions, respectively. Source: Reprinted with permission from Wang (1998). Copyright 1998 American Chemical Society. pNIPAAm: poly(*N*-isopropylacrylamide).

The authors claim that the pNIPAM chains collapse above the LCST and form intrachain hydrogen bonds that make the resulting globule difficult to dissolve once the temperature decreases.[11] Moreover, according to Sun[12] *et al.*, during heating the backbone chains collapse first, the side isopropyl groups react next and then water is expelled last. On the other hand, during cooling the globule swells once water becomes again a sufficiently good solvent for the polymer chains and diffuses in between the collapsed pNIPAM chains. After the water has diffused into the polymer network the intrachain hydrogen bonds break and the side chains reswell first and then the backbone follows.[11, 12]

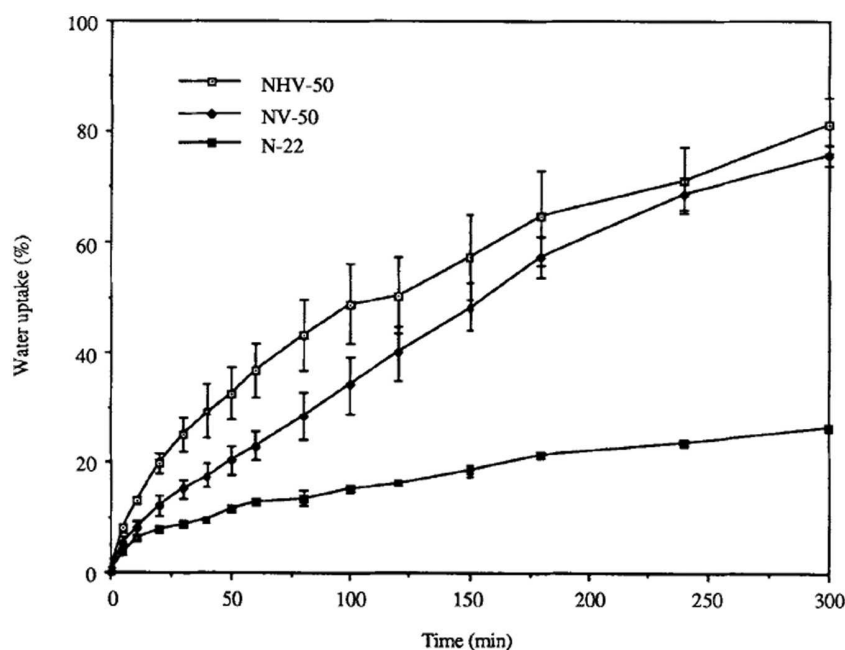


Figure 2-12. Reswelling kinetics of macroporous and conventional pNIPAAm hydrogels. NHV-50 cellulose modified macroporous hydrogel, NV-50 macroporous hydrogel and N 22 standard hydrogel. Source: Reprinted with permission from Wu *et al.* (1992). Copyright 2003 Wiley.

On a macroscopic scale, one way to increase the speed of reswelling of pNIPAM hydrogels is to modify the morphology of the bulk material and increase the polymer surface area in contact with water. An effective way of using the inherent LCST pNIPAM property to make macroporous hydrogels was developed by Wu *et al.* [41] In this work the NIPAM is polymerised and crosslinked above its LCST with and without hydroxypropyl cellulose. As a result NIPAM polymerised in its precipitated state and a porous network was formed in which swelling/deswelling ratio and rates were significantly higher than for the conventional hydrogel. The cellulose additive improved the gel performance even further (Figure 2-12).

Although all those approaches improve the characteristics of pNIPAM-spiropyran system little has been done to optimise the fundamental phenomenon at the very core of the actuation process. Satoh *et al.*[38] prepared spiropyran monomers with different electron donating and electron withdrawing groups and demonstrated that the spiropyran opening in HCl can be drastically improved by certain substituents on the pyran-benzene ring (Figure 2-13).

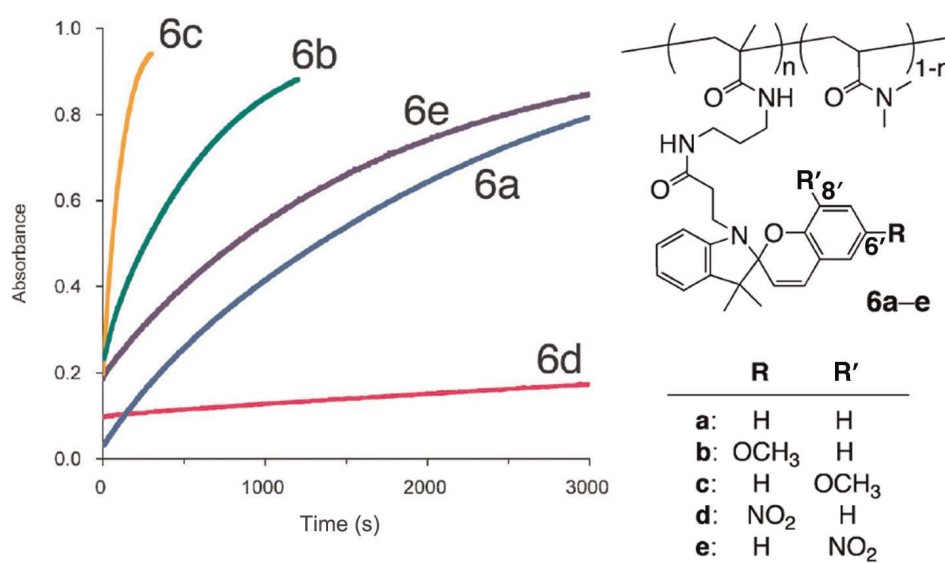


Figure 2-13. Left: Time course of the absorbance of the MC-H⁺ in polymers 6a–6e after stopping the light irradiation. The measurements were performed in 2 mM HCl at 25 °C. The values of the absorbance before the light irradiation were normalised to be 1.0 for comparison. Right: Substituents for different chromophore monomers prepared (a–e). Source: Reproduced from Satoh *et al.* (2011) by permission of the PCCP Owner Societies. MC-H⁺: protonated merocyanine.

With this approach it was demonstrated that pNIPAM-spiropyran hydrogels can collapse and reswell within 15 min.[39] However, the authors themselves admit that the “fastest” hydrogels did not return to the original size. This was ascribed to photo-induced decomposition of the polymer. As for other systems mentioned above, the LCST driven collapse of the gel is rather fast but the reswelling of the gel is comparatively slow and problematic.[28] This is because the actuation of the pNIPAM-spiropyran gel is a two-step process. For the shrinking the protonated merocyanine has to be first isomerised to the hydrophobic SP form. This increase in the hydrophobicity of the chain induces its collapse and water ejection.[28, 35] The reverse process is more difficult as after conversion of SP to the charged MC form, protonation occurs followed

by diffusion of water into the collapsed polymer globules before the chains can reorder and swell.[11, 12] A manifold with microvalves made from such material was demonstrated by Sagiura *et al* (Figure 2-14).[28] The maximum pressure the pSPNIPAAm gel microvalves could withstand was determined to be 30 ± 6.6 kPa. At pressures in excess of this, the gels deformed and leakage occurred.

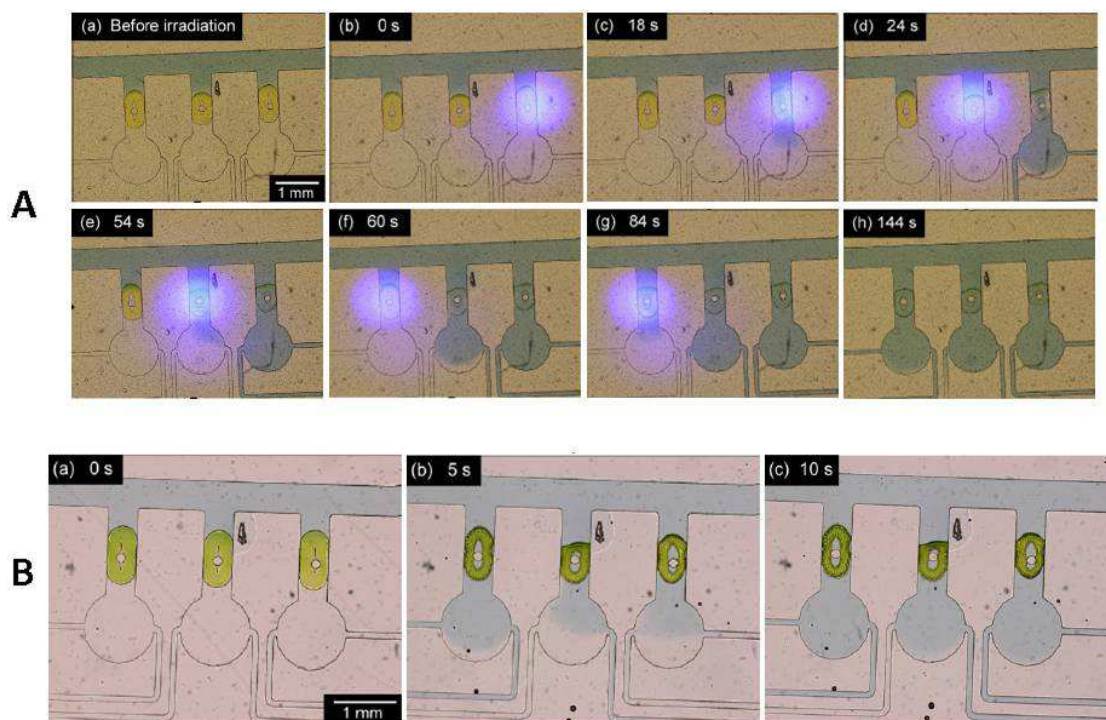


Figure 2-14. (a) Independent control of multiple poly(spiropyran-co-NIPAAm) (pSPNIPAAm) gel microvalves by means of local light irradiation: (i) a solution containing blue dye was introduced into the main microchannel; (ii) blue light was locally irradiated to the right-side poly(spiropyran-co-NIPAAm) (pSPNIPAAm) gel microvalve; (iii) the right-side microvalve was opened after 18 s of blue light irradiation; (iv) blue light was locally irradiated to the centre microvalve; (v) the centre microvalve was opened after 30 s of blue light irradiation; (vi) blue light was locally irradiated to the left-side microvalve; (vii) the left-side microvalve was opened after 24 s of blue light irradiation and (viii) after light irradiation, the chambers were filled with the blue dye solution (for interpretation of the references to colour in this figure legend, the reader is referred to the web version of the article). (b) Simultaneous control of multiple poly(spiropyran-co-NIPAAm) (pSPNIPAAm) gel microvalves by means of temperature change: (i) a solution containing blue dye was introduced into the main microchannel at 23 °C, (ii) temperature was raised by dipping the microchip into hot water. All of the microvalves were opened within 5 s after temperature rise to 46 °C and (iii) 10 s after temperature rise. Source: Reprinted with permission from Sugiura *et al.* (2007). Copyright 2007 Elsevier.

A similar approach was presented by Benito-Lopez *et al.*[30, 31]. However, in this case, an ionic liquid (IL) was incorporated within a poly(*N*-isopropylacrylamide) polymer matrix copolymerised with acrylated benzospiropyran. Using various IL components within the gels allows the kinetics of valve actuation to be controlled, and the IL mediates the rate of protonation/deprotonation and movement of counterions and solvent (water). Different ionogels were photo-polymerised in situ in the channels of a poly(methyl methacrylate) (PMMA) microfluidic platform. After immersion for 2 h in 0.1 mM HCl aqueous solution, in which the ionogel exhibits a rapid swelling effect due to protonation of the polymer backbone, the rate of

photo-induced shrinking due to dehydration of the ionogel was measured. The required light intensity is so low that low cost LEDs can be employed for successful valve actuation. Results showed that trihexyl-tetradecylphosphonium dicyanamide based ionogel produced the fastest valve-opening kinetics, opening 4s after light irradiation (Figure 2-15). Although it is possible to reuse the valves several times, the time to re-close the ionogel valve is relatively long (ca. 30 min) and requires re-immersion in an acidic solution.

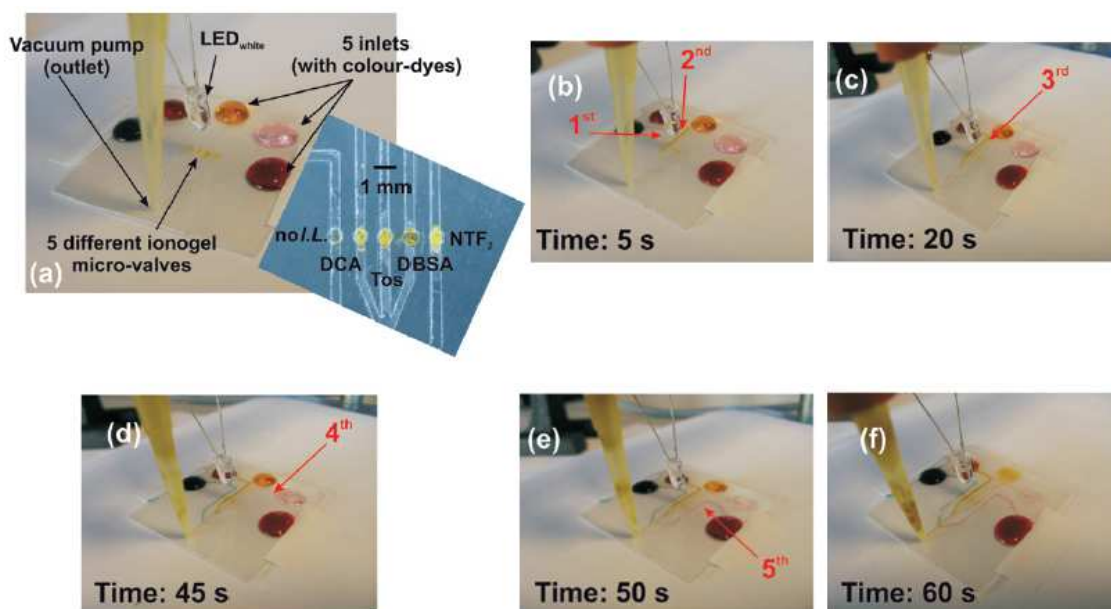


Figure 2-15. Performance of the ionogel microfluidic valves: (a) microvalves closed; the applied vacuum is unable to pull the dyes through the microchannels. (b) White light is applied for the time specified in each picture. (c) ‘no I.L.’ valve is first to actuate followed by ionogels incorporating dicyanamide [dca], (d) toluenesulfonate [tos], (e) dodecylbenzenesulphonate [dbsa], (f) bis(trifluoromethanesulfonyl)amide [NTf₂], all valves are open. Numbers and arrows indicate when the channel is filled with the dye because of microvalve actuation. Source: Reproduced from Benito-Lopez *et al.* (2010) by permission of The Royal Society of Chemistry. LED: Light Emitting Diode.

An innovative approach to microfluidics incorporating photoresponsive pSPNIMAAm hydrogels was described by Sugiura *et. al.*[29] The group demonstrated on-demand formation of microchannels with arbitrary pathways using micropatterned light irradiation of (initially planar) hydrogel sheets. After light irradiation through an appropriately designed mask, a microchannel between adjacent inlet/outlet ports spontaneously formed under the irradiated area, allowing for fluid flow between a designated input and output and the channels rapidly became filled with reagent within a few minutes of illumination (Figure 2-16). The effect was repeated for several channel configurations – straight, bent or serpentine. What is more, the authors demonstrated independent and parallel flow control in a polydimethylsiloxane (PDMS) microchannel network by micropatterned light irradiation of photoresponsive microvalves prepared from the same 200 μm thick hydrogel sheet. As a result of light irradiation, the gel in the irradiated area adjacent to the through-holes shrank, thus opening the valve within several minutes.

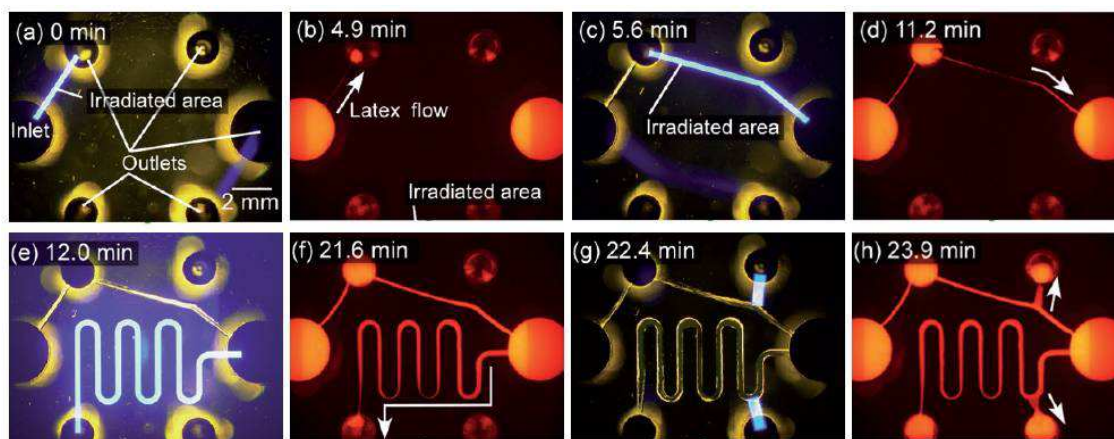


Figure 2-16. On-demand formation of microchannels with arbitrary pathways in the universal microfluidic system by micropatterned light irradiation. White arrows indicate the flow direction of a fluorescently labelled latex bead suspension. (a) Microchannel formation by micropatterned light irradiation of the poly(spiropyran-co-NIPAAm) (pSPNIPAAm) hydrogel sheet. (b) Latex bead suspension flow through the microchannel after irradiation. Flow of the coloured latex bead suspension from the inlet to the upperleft-side outlet is slightly visible. (c)–(h) Three consecutive sequences of micropatterned light irradiation and microchannel formation. Source: Reproduced from Sugiura *et al.* (2009) by permission of The Royal Society of Chemistry.

2.4.3 Azobenzene based polymeric actuators

Another interesting class of photoactuated materials is based on azobenzenes[40-44]. These molecules are in a *trans* configuration in the ground state but when irradiated with UV light they isomerise to the *cis* orientation.[40, 45] The structural reorganisation of the molecule and the attached chains can have a significant macroscopic effect on the host material.[40] This phenomenon was greatly enhanced by D. Broer's group by incorporation of azobenzenes in liquid crystal structures.[46, 47] When the azobenzene molecule isomerises to the *cis* form under UV light there is an increase in disorder resulting in shrinkage along the direction of the liquid crystal structure and expansion in the perpendicular direction. When the white light is used the molecules and the polymer return to the initial state.[47] This shows a reversible and quick photoactuation of the polymeric material (Figure 2-17).

The speed of actuation and strength of this material must be emphasised. The films reach 70 % of the maximum deformation within 7 seconds and take the same to return to the original shape while having over 1 GPa of elastic modulus. This material is therefore much suitable to generate mechanical work and displace fluids than considerably softer gels. Coupled with biomimetic approaches such as artificial cilia[46] these azobenzenes-ordered materials open new perspectives in microfluidic and lab-on-a-chip devices. The field of photomechanical actuators containing azobenzenes is covered in a review by Barrett *et al.*[40]

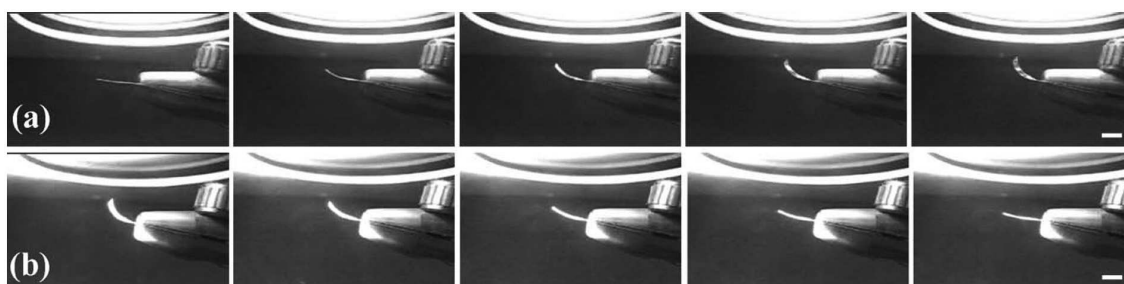


Figure 2-17. (a) Bending of films under UV light 0, 8, 16, 24 and 32 s of UV exposure, respectively. (b) Return of the film to the original shape under white light shown after 0, 4, 8, 12 and 20 s, respectively. The white bar corresponds to 5 mm in length. The UV intensity was roughly 10 mW/cm². Source: Reprinted with permission from Harris *et al.* (2005) by permission of The Royal Society of Chemistry. UV: Ultraviolet.

Table 2-1. Approximate ranges for the characteristics of microvalves.

Actuator type	Energy requirement	Applied Pressure (kPa)	Actuation time	Generated deflection or volume change	Measured flow ($\mu\text{l min}^{-1}$)	References
Pneumatic	0.04–0.5 W	20-230	<25 s	3.5 -150 μm	$3 \cdot 10^3 - 1 \cdot 10^6$	[48-50]
Magnetic gels	59.5 kA/m	-	<13 min	-	0.2 - 100	[2, 48]
Chemically responsive gels	None	-	12 s – 30 min	<200 μm	10-150	[10, 52, 53]
Thermoresponsive gels	0.2-0.4 W	-	1 - 9 s	<30 %	1 - 50	[22, 54]
Spiropyran based photoactive gels	1-20 mW/cm ²	3.4-69	30 s -1hr	<60 %	30 ± 6.6	[32, 34, 56]
Azobenzene based photoactive polymers	10mW/cm ²	-	<15 s	100 m^{-1} (curvature[45])	-	[45]

2.5 Conclusions

Table 2-1 summarises the features of the presented classes of actuators. There are many exciting developments happening in materials chemistry that one can only ‘touch the surface’ in a review paper of this type. The potential range of stimuli responsive materials is virtually unlimited, and this, coupled with new deposition techniques that offer unsurpassed control of feature offer a tremendously rich research landscape for science to explore. The potential benefits to society emerging from this research are truly enormous. Perhaps the great issue of biofouling will

finally be put to rest, opening up new opportunities in long-term implantable chem/bio-sensors that can monitor, report, and ultimately control the levels of key biomarkers. Similarly, reliable low cost sensors could open the way to environmental monitoring on a massive scale. Stimuli-responsive polymers could form the basis of new generations of biomimetic sensing based on polymer pumps and valves incorporated in microfluidic platforms much more reminiscent of our own circulation systems. The convergence of technologies that facilitate the control of micro/nano-structured surfaces coupled with these new materials is a powerful combination – materials chemistry now must be recognised as the core foundation underpinning these exciting possibilities.

Acknowledgements:

This work was performed as part of the EU Framework 7 project “ATWARM” (Marie Curie ITN, No. 238273)”. D. D. acknowledges funding from Science Foundation Ireland (SFI) under the CLARITY CSET award (Grant 07/CE/I1147).

2.6 References:

1. Kovacs, K. G., *Microfluidic devices. In Micromachined Transducers - Sourcebook.* WCB/McGraw-Hill: Boston, 1998.
2. Satarkar, N. S.; Zhang, W.; Eitel, R. E.; Hilt, J. Z., Magnetic hydrogel nanocomposites as remote controlled microfluidic valves. *Lab on a Chip* **2009**, *9*.
3. Ghosh, S.; Yang, C.; Cai, T.; Hu, Z. B.; Neogi, A., Oscillating magnetic field-actuated microvalves for micro- and nanofluidics. *Journal of Physics D-Applied Physics* **2009**, *42*.
4. Zhang, W.; Lin, S.; Wang, C.; Hu, J.; Li, C.; Zhuang, Z.; Zhou, Y.; Mathies, R. A.; Yang, C. J., PMMA/PDMS valves and pumps for disposable microfluidics. *Lab on a Chip* **2009**, *9*, 3088.
5. Go, J. S.; Shoji, S., A disposable, dead volume-free and leak-free in-plane PDMS microvalve. *Sensors and Actuators A: Physical* **2004**, *114*, 438-444.
6. Kaigala, G. V.; Hoang, V. N.; Backhouse, C. J., Electrically controlled microvalves to integrate microchip polymerase chain reaction and capillary electrophoresis. *Lab on a Chip* **2008**, *8*, 1071.
7. Selvaganapathy, P.; Carlen, E. T.; Mastrangelo, C. H., Electrothermally actuated inline microfluidic valve. *Sensors and Actuators A: Physical* **2003**, *104*, 275-282.
8. Garcia-Cordero, J. L.; Kurzbuch, D.; Benito-Lopez, F.; Diamond, D.; Lee, L. P.; Ricco, A. J., Optically addressable single-use microfluidic valves by laser printer lithography. *Lab on a Chip* **2010**, *10*, 2680-2687.

9. Moorthy, J.; Beebe, D. J., Peer Reviewed: Organic and Biomimetic Designs for Microfluidic Systems. *Analytical Chemistry* **2003**, *75*, 292 A-301 A.
10. Beebe, D. J.; Moore, J. S.; Bauer, J. M.; Yu, Q.; Liu, R. H.; Devadoss, C.; Jo, B.-H., Functional hydrogel structures for autonomous flow control inside microfluidic channels. *Nature* **2000**, *404*, 588-590.
11. Wang, X.; Qiu, X.; Wu, C., Comparison of the Coil-to-Globule and the Globule-to-Coil Transitions of a Single Poly(N-isopropylacrylamide) Homopolymer Chain in Water. *Macromolecules* **1998**, *31*, 2972-2976.
12. Sun, S.; Hu, J.; Tang, H.; Wu, P., Chain Collapse and Revival Thermodynamics of Poly(N-isopropylacrylamide) Hydrogel. *The Journal of Physical Chemistry B* **2010**, *114*, 9761-9770.
13. Welton, T., Room-Temperature Ionic Liquids. Solvents for Synthesis and Catalysis. *Chemical Reviews* **1999**, *99*, 2071-2084.
14. David J. Beebe, J. S. M., Qing Yu, Robin H. Liu, Mary L. Kraft, Byung-Ho Jo, and Chelladurai Devadoss, Microfluidic tectonics: A comprehensive construction platform for microfluidic systems. *Proceedings of National Academy of Sciences of the United States of America* **2000**, *97*, 13488-13493.
15. Cole, A. C.; Jensen, J. L.; Ntai, I.; Tran, K. L. T.; Weaver, K. J.; Forbes, D. C.; Davis, J. H., Novel Brønsted Acidic Ionic Liquids and Their Use as Dual Solvent–Catalysts. *Journal of the American Chemical Society* **2002**, *124*, 5962-5963.
16. Schild, H. G., Poly (n-isopropylacrylamide) - experiment, theory and application. . *Progress in Polymer Science* **1992**, *17*, 163-249.
17. Richter, A.; Kuckling, D.; Howitz, S.; Thomas, G.; Arndt, K. F., Electronically controllable microvalves based on smart hydrogels: magnitudes and potential applications. *Microelectromechanical Systems, Journal of* **2003**, *12*, 748-753.
18. Yu, C.; Mutlu, S.; Selvaganapathy, P.; Mastrangelo, C. H.; Svec, F.; Fréchet, J. M. J., Flow Control Valves for Analytical Microfluidic Chips without Mechanical Parts Based on Thermally Responsive Monolithic Polymers. *Analytical Chemistry* **2003**, *75*, 1958-1961.
19. Jiun-Min Wang, L.-J. Y., Electro-Hydro-Dynamic (EHD) Micropumps with Electrode Protection by Parylene and Gelatin. *Tamkang Journal of Science and Engineering* **2005**, *8*, 231-236.
20. Richter, A.; Klatt, S.; Paschew, G.; Klenke, C., Micropumps operated by swelling and shrinking of temperature-sensitive hydrogels. *Lab on a Chip* **2009**, *9*.
21. Gerlach, G.; Guenther, M.; Sorber, J.; Suchanek, G.; Arndt, K.-F.; Richter, A., Chemical and pH sensors based on the swelling behavior of hydrogels. *Sensors and Actuators B: Chemical* **2005**, *111–112*, 555-561.
22. Luo, Q.; Mutlu, S.; Gianchandani, Y. B.; Svec, F.; Fréchet, J. M. J., Monolithic valves for microfluidic chips based on thermoresponsive polymer gels. *Electrophoresis* **2003**, *24*, 3694-3702.
23. M.Irie, D. K., Photoresponsive polymers. 8. Reversible photo-stimulated dilation of polyacrylamide gels having triphenylmethane leuco derivatives. *Macromolecules* **1986**, *19*, 2476–2480.
24. Irie, M.; Hosoda, M., Photoresponsive polymers. Reversible solution viscosity change of poly(N,N-dimethylacrylamide) with pendant triphenylmethane leucohydroxide residues in methanol. *Die Makromolekulare Chemie, Rapid Communications* **1985**, *6*, 533-536.
25. M. Irie, A. M., K. Hayashi, Photoresponsive polymers. reversible solution viscosity change of poly (methyl methacrylate) having spiroben-zopyran side groups. *Macromolecules* **1979**, *12*, 1176–1180.

26. A. Menju, K. H., M. Irie, Photoresponsive polymers. 3. Reversible solution viscosity change of poly(methacrylic acid) having spirobenzopyran pendant groups in methano. *Macromolecules* **1981**, *14*, 755–758.
27. Lo, C.-W.; Zhu, D.; Jiang, H., An infrared-light responsive graphene-oxide incorporated poly(N-isopropylacrylamide) hydrogel nanocomposite. *Soft Matter* **2011**, *7*, 5604-5609.
28. Sugiura, S.; Sumaru, K.; Ohi, K.; Hiroki, K.; Takagi, T.; Kanamori, T., Photoresponsive polymer gel microvalves controlled by local light irradiation. *Sensors and Actuators A: Physical* **2007**, *140*, 176-184.
29. Sugiura, S.; Szilagyi, A.; Sumaru, K.; Hattori, K.; Takagi, T.; Filipcsei, G.; Zrinyi, M.; Kanamori, T., On-demand microfluidic control by micropatterned light irradiation of a photoresponsive hydrogel sheet. *Lab on a Chip* **2009**, *9*, 196-198.
30. Benito-Lopez, F.; Byrne, R.; Raduta, A. M.; Vrana, N. E.; McGuinness, G.; Diamond, D., Ionogel-based light-actuated valves for controlling liquid flow in micro-fluidic manifolds. *Lab on a Chip* **2010**, *10*, 195-201.
31. Byrne, R.; Ventura, C.; Lopez, F. B.; Walther, A.; Heise, A.; Diamond, D., Characterisation and analytical potential of a photo-responsive polymeric material based on spiropyran. *Biosensors and Bioelectronics* **2010**, *26*, 1392-1398.
32. Smets, G.; Braeken, J.; Irie, M., Photomechanical effects in photochromic systems. *Pure and Applied Chemistry* **1978**, *50*.
33. Irie, M.; Menju, A.; Hayashi, K., Photoresponsive Polymers. Reversible Solution Viscosity Change of Poly(methyl methacrylate) Having Spirobenzopyran Side Groups. *Macromolecules* **1979**, *12*, 1176-1180.
34. Sumaru, K.; Kameda, M.; Kanamori, T.; Shinbo, T., Reversible and Efficient Proton Dissociation of Spirobenzopyran-Functionalized Poly(N-isopropylacrylamide) in Aqueous Solution Triggered by Light Irradiation and Temporary Temperature Rise. *Macromolecules* **2004**, *37*, 7854-7856.
35. Sumaru, K.; Kameda, M.; Kanamori, T.; Shinbo, T., Characteristic Phase Transition of Aqueous Solution of Poly(N-isopropylacrylamide) Functionalized with Spirobenzopyran. *Macromolecules* **2004**, *37*, 4949-4955.
36. Ivanov, A. E.; Eremeev, N. L.; Wahlund, P. O.; Galaev, I. Y.; Mattiasson, B., Photosensitive copolymer of N-isopropylacrylamide and methacryloyl derivative of spirobenzopyran. *Polymer* **2002**, *43*, 3819-3823.
37. Kröger, R.; Menzel, H.; Hallensleben, M. L., Light controlled solubility change of polymers: Copolymers of N,N-dimethylacrylamide and 4-phenylazophenyl acrylate. *Macromolecular Chemistry and Physics* **1994**, *195*, 2291-2298.
38. Satoh, T.; Sumaru, K.; Takagi, T.; Takai, K.; Kanamori, T., Isomerization of spirobenzopyrans bearing electron-donating and electron-withdrawing groups in acidic aqueous solutions. *Physical Chemistry Chemical Physics* **2011**, *13*, 7322-7329.
39. Satoh, T.; Sumaru, K.; Takagi, T.; Kanamori, T., Fast-reversible light-driven hydrogels consisting of spirobenzopyran-functionalized poly(N-isopropylacrylamide). *Soft Matter* **2011**, *7*, 8030-8034.
40. Barrett, C. J.; Mamiya, J.-i.; Yager, K. G.; Ikeda, T., Photo-mechanical effects in azobenzene-containing soft materials. *Soft Matter* **2007**, *3*, 1249-1261.
41. Long, K. N.; Scott, T. F.; Jerry Qi, H.; Bowman, C. N.; Dunn, M. L., Photomechanics of light-activated polymers. *Journal of the Mechanics and Physics of Solids* **2009**, *57*, 1103-1121.
42. Lee, K. M.; Koerner, H.; Vaia, R. A.; Bunning, T. J.; White, T. J., Relationship between the Photomechanical Response and the Thermomechanical Properties of Azobenzene Liquid Crystalline Polymer Networks. *Macromolecules* **2010**, *43*, 8185-8190.

43. Wang, H.; Lee, K. M.; White, T. J.; Oates, W. S., trans–cis and trans–cis–trans Microstructure Evolution of Azobenzene Liquid-Crystal Polymer Networks. *Macromolecular Theory and Simulations* **2012**, *21*, 285-301.
44. Lee, K. M.; Tabiryan, N. V.; Bunning, T. J.; White, T. J., Photomechanical mechanism and structure-property considerations in the generation of photomechanical work in glassy, azobenzene liquid crystal polymer networks. *Journal of Materials Chemistry* **2012**, *22*, 691-698.
45. Harris, K. D.; Cuypers, R.; Scheibe, P.; van Oosten, C. L.; Bastiaansen, C. W. M.; Lub, J.; Broer, D. J., Large amplitude light-induced motion in high elastic modulus polymer actuators. *Journal of Materials Chemistry* **2005**, *15*, 5043-5048.
46. van Oosten, C. L.; Bastiaansen, C. W. M.; Broer, D. J., Printed artificial cilia from liquid-crystal network actuators modularly driven by light. *Nature Materials* **2009**, *8*, 677-682.
47. van Oosten, C. L.; Corbett, D.; Davies, D.; Warner, M.; Bastiaansen, C. W. M.; Broer, D. J., Bending Dynamics and Directionality Reversal in Liquid Crystal Network Photoactuators. *Macromolecules* **2008**, *41*, 8592-8596.
48. Santaneel, G.; Tong, C., Controlled actuation of alternating magnetic field-sensitive tunable hydrogels. *Journal of Physics D: Applied Physics* **2010**, *43*, 415504.

Chapter 3:

Mechanical properties and U.V. curing behaviour of poly(*N*-isopropylacrylamide) in phosphonium based ionic liquids.

Bartosz Ziółkowski^a, Zeliha Ates^b, Simon Gallagher^a, Robert Byrne^a, Andreas Heise^b, Kevin J Fraser^a and Dermot Diamond^{a*}

a) CLARITY Centre for Sensor Web Technologies, National Centre for Sensor Research, Dublin City University, Dublin 9, Ireland

b) School of Chemical Sciences, Dublin City University, Dublin 9, Ireland

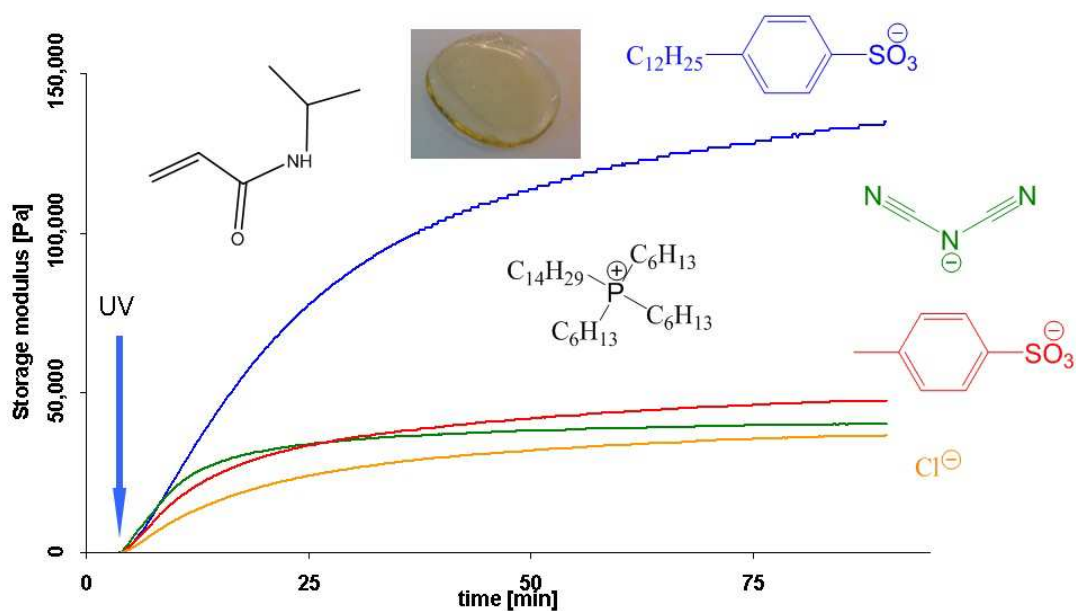
Published: *Macromolecular Chemistry and Physics*, **2013**. 214, 787-796.

DOI: 10.1002/macp.201200616

Abstract

N-isopropylacrylamide was photo-polymerised in a range of phosphonium based ionic liquids (ILs). The curing behaviour of polymer-IL solutions (linear pNIPAM) and ionogels (crosslinked pNIPAM) were studied using rheometry, differential scanning calorimetry and gel permeation chromatography. It was found that the IL not only influences the mechanical properties of the ionogel and the rate of polymerisation but also the lower critical solution temperature (LCST) of the resulting pNIPAM ionogels. Ionogels made in trihexyl-tetradecyl phosphonium dicyanamide show an order of magnitude smaller ratio of loss/storage moduli (mechanical $\tan\delta$) compared to that of trihexyl-tetradecyl phosphonium chloride while showing a twice higher UV polymerisation rate. These ionogels exhibit also different LCSTs with xP-Cl having the lowest (15.5 °C) and xPi-Tos displaying the highest at 32.2°C. Finally, temperature ramp rheology scans of the water swollen ionogels showed that upon the LCST transition the moduli of the polymer network increases and this increase is more rapid in the P-DCA and P-Tos than in the other formulations.

Keywords: ionic liquids; ionogels; NIPAM; viscoelastic properties



3.1 Introduction

Poly(*N*-isopropylacrylamide), (pNIPAM) gels are widely used in microfluidic applications as flow controllers and actuators,[1-5] drug delivery systems and bioassays.[6-10] A particularly attractive feature of pNIPAM is its lower critical solution temperature (LCST), which is typically in the range of 30-35 °C.[10, 11] Below this temperature the polymer chains are solvated by water molecules while above this temperature, the LCST the polymer chains collapse and precipitate. A gel made out of this material will therefore expel water and shrink above the LCST or swell and expand below this transition temperature due to water uptake.[12] However, the dependency of this behaviour on water uptake and release is its greatest disadvantage, as evaporation leads to loss of its mechanical properties. Consequently, actuators based on these hydrogels must be kept in an aqueous environment in order to maintain their physical integrity. Other solvents are therefore required to overcome this disadvantage. Ionic liquids (ILs) are currently attracting considerable attention as potentially benign solvents for many areas of chemistry, as well as various electrochemical devices[13-20], including rechargeable lithium cells,[21, 22] solar cells,[23-25] actuators[26-28] and double layer capacitors (DLCs).[29-31] This interest in ILs can be attributed to the many favourable properties such as low volatility, electrochemical, thermal stability, and high ionic conductivity - all of which can be tailored through careful choice of cation and anion.[32, 33] Ionic liquids based on tetraalkylphosphonium cations have been demonstrated to exhibit greater thermal stability than their tetraalkylammonium based counterparts[34] and a range of phosphonium salts are commercially available in large quantities.[35] Reports of the utility of ionic liquids prepared from phosphonium cations with anions such as hexafluorophosphate ($[\text{PF}_6]^-$), tetrafluoroborate ($[\text{BF}_4]^-$) and bis(trifluoromethanesulfonimide) ($[\text{NTf}_2]^-$) have appeared in the literature.[36] Currently for applications in materials science, there is growing interest in 'ionogels', i.e. polymers with ILs integrated such that they retain their specific properties within the polymer/gel environment. An excellent review by Bideau *et. al.*[37] discusses ionogels as a new class of hybrid materials, in which the properties of the IL are hybridized with those of various components, which may be organic (low molecular weight gelator[38], polymer[39]), inorganic (e.g. carbon nanotubes, silica)[40] or hybrid organic-inorganic (e.g. polymer and inorganic fillers).[41]

One particular and useful application that would benefit from the afore-mentioned advantages of both poly(NIPAM) and ILs is the area of microfluidic valves.[42] Conventional microfluidic pNIPAM hydrogels are susceptible to drying and the choice of solvent for their synthesis is limited.[10] On the other hand, ILs offer properties that can be tailored by changing the anion/cation combinations.[43] They also exhibit negligible vapour pressure at room temperature, and when used in NIPAM microfluidic valves, these qualities of ILs result in a

very robust system.[8] For example NIPAM easily dissolves in a range of phosphonium based ILs and their negligible vapour pressure keeps the reaction volume constant during polymerisation. At the same time a gel made with these rather hydrophobic ILs can still swell with water producing a functioning microfluidic structure in which the hydrophobic IL is retained, which allows the material to maintain its IL-mediated properties. Therefore, the pNIPAM- phosphonium IL system is a very attractive platform for microfluidic flow control and stimulus responsive materials.[8, 44]

We have published several papers on various phosphonium-based ILs, and their use in ionogels.[7, 8, 45-47] Some of these materials were used in microfluidic applications as valves and have been shown to open with white light irradiation when benzospiropyran (a photo-responsive molecule) is copolymerised as pendant group in the poly(*N*-isopropylacrylamide) backbone. The gel valves exhibited different response times depending on the IL used for their preparation, which was explained in terms of solvation of the benzospiropyran by the ILs and their polarity[8]. However, during further investigation it was noticed that the mechanical strength of the ionogels and their UV curing rates were noticeably different depending on the IL used. Ueki *et. al.*[48, 49] reported that ILs can drastically influence polymer sol-gel transitions and LCST behaviour. Polymerisation kinetics have also been reported to depend strongly on the IL used as a solvent for polymerisation.[50, 51] Moreover, it is known that the gel swelling time and therefore the valve operation speed is proportional to the mechanical modulus of the gel network and the friction of the network with the internal liquid.[52] Therefore, more insight into the polymerisation properties of NIPAM-phosphonium IL system and mechanical/actuation characteristics of the resulting ionogels would be highly valuable in order to fully understand the behaviour of these perspective soft polymer actuators.

This current study reports the differences in mechanical properties observed for pNIPAM polymers and gels prepared in a range of phosphonium based ILs together with the resulting differences in the LCST behaviour of the material. The majority of the ILs tested in this work correlate with the ones previously reported as light triggered ionogel valves[8]. The monomer-IL mixtures have been tested for mechanical moduli in real time during the UV-initiated polymerisation process. The resulting pNIPAM polymers have been analysed with gel permeation chromatography (GPC). The photo-polymerisation process has also been investigated with differential scanning calorimetry (DSC). The observed differences in polymerisation rate, its impact on the mechanical properties and LCST behaviour are discussed.

3.2 Experimental

3.2.1 Materials

N-isopropylacrylamide 98% (NIPAM), *N,N'*-methylenebisacrylamide 99% (MBIS) and dimethoxyphenylacetophenone 98% (DMPA) were obtained from Sigma Aldrich, Ireland and used as received. trihexyl-tetradecylphosphonium chloride ([P_{6,6,6,14}][Cl]), methyl-triisobutylphosphonium tosylate ([P_{1,4,4,4}][Tos]), Trihexyl-tetradecylphosphonium dicyanamide ([P_{6,6,6,14}][DCA]), trihexyl-tetradecylphosphonium toluenesulfonate ([P_{6,6,6,14}][Tos]) and trihexyl-tetradecylphosphonium dodecylbenzenesulphonate [P_{6,6,6,14}][dbsa] were supplied by Cytec® (Ontario Canada) and purified as described in Appendix A.

Table 3-1 Abbreviations and compositions of samples used in this study

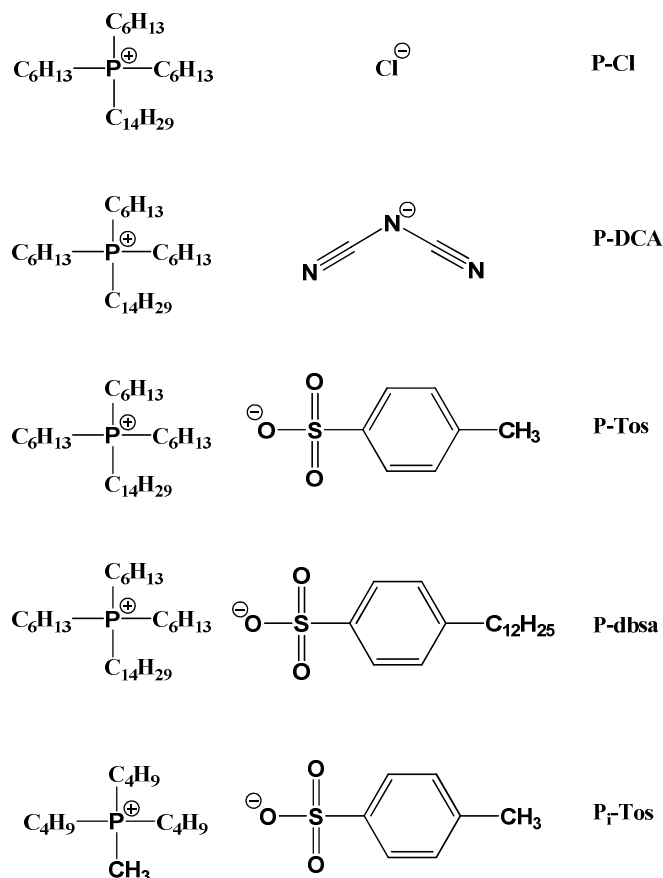
Sample abbreviation	IL (1.2 mL)	NIPAM [mmol]	MBIS [mmol]	DMPA [mmol]
P-Cl	[P _{6,6,6,14}][Cl]	3.53	-	0.07
xP-Cl	[P _{6,6,6,14}][Cl]	3.53	0.18	0.07
P-DCA	[P _{6,6,6,14}][DCA]	3.53	-	0.07
xP-DCA	[P _{6,6,6,14}][DCA]	3.53	0.18	0.07
P-NTf ₂	[P _{6,6,6,14}][NTf ₂]	3.53	-	0.07
P-Tos	[P _{6,6,6,14}][Tos]	3.53	-	0.07
xP-Tos	[P _{6,6,6,14}][Tos]	3.53	0.18	0.07
P _i -Tos	[P _{1,4,4,4}][Tos]	3.53	-	0.07
xP _i -Tos	[P _{1,4,4,4}][Tos]	3.53	0.18	0.07
P-dbsa	[P _{6,6,6,14}][dbsa]	3.53	-	0.07
xP-dbsa	[P _{6,6,6,14}][dbsa]	3.53	0.18	0.07

3.2.2 Sample preparation

pNIPAM ionogels were prepared by mixing 400 mg of NIPAM (3.53 mmol) with 5 mol % MBIS, 2 mol % DMPA and 1.2 mL of the IL (crosslinked samples). The MBIS is not added in the non-crosslinked samples. The mixture was heated to 50 °C and sonicated for 5 min until a transparent solution was observed. Found in Table 3-1 is a list of abbreviations and compositions of the mixtures studied. The chemical structures of the ILs used are shown in Scheme 3-1. xP-Cl, xP-DCA, xP-Tos, xP_i-Tos, xP-dbsa were also placed on Teflon moulds and polymerised for 60 min with a 30 Watt, 365 nm Blacklite UV lamp placed 20 mm from the mould. The moulds were 15 mm diameter circles 1 mm deep. The UV light intensity at the

mould surface was measured with a Lutron UV-340A UV probe and was 950 $\mu\text{W}/\text{cm}^2$.

For Gel Permeation Chromatography (GPC) measurements the non-crosslinked samples taken from the rheometry-UV-curing experiments were washed 2 times with diethyl ether and dried at room temperature overnight. Diethyl ether was found to be most suitable for the samples studied because it dissolves the IL present in the sample but precipitates the linear pNIPAM. However, the P₁-Tos sample had to be fully dissolved in acetone and then the polymer precipitated by adding diethyl ether as the [P_{1,4,4,4}][Tos] IL does not dissolve in diethyl ether.



Scheme 3-1 Structures of ILs and the corresponding abbreviations used in this study

3.2.3 Rheometry

3.2.3.1 UV-polymerisation

An Anton-Paar MCR301 rheometer equipped with a CP50 cone measuring tool was used to measure the evolution of mechanical properties during polymerisations. The rheometer also had a bottom glass plate transparent to UV light above 350 nm. The polymerisation mixture, (volume = 1.1 mL), was placed onto the bottom glass plate and pressed with the 50 mm cone measurement tool with a gap of 208 μm . A house-built array of 9 LEDs (XSL-365-5E, Roithner

Lasertechnik Austria) was placed 40 mm under the glass plate. The LEDs had an emission wavelength peak at 365 nm and an average optical output power of 4 mW each. The UV light intensity was measured with a Lutron UV-340A UV probe and was found to have a light intensity of 1100 $\mu\text{W}/\text{cm}^2$. This was measured at the top of the rheometer glass plate where the polymerisation happens. To monitor the curing and mechanical properties of ionogels in real time, rheometry measurements were taken over a course of ninety minutes. The UV light was switched on after three minutes twenty seconds (20th measurement point). The storage and loss moduli were analysed at 0.1 % strain and 1 Hz oscillation frequency and plotted versus time. Data points were collected every 10 seconds.

3.2.3.2 LCST transitions

The 15 mm ionogel circles polymerised in Teflon mould were immersed in deionised water and equilibrated for 7 days. The swollen ionogels were then analysed for changes in the modulus during a temperature step program. All the swollen ionogels were analysed in oscillation mode with a parallel plate PP15 tool 15 mm diameter at 0.05 % strain and frequency of 10 Hz. The data points were collected every second and the following temperature ramp was applied: 5 minutes at 25 °C, ramp to 45 °C (20 °C/min) and isotherm for 10 min, thereafter ramp to 25 °C (20 °C/min) and isotherm for 10 min. Because the water-swollen ionogels shrink during LCST transition, the instrument was set to adjust the gap according to 1N normal force on the sample. Therefore, the smaller peaks in moduli present on the plots are due to the instrument adjusting the pressing force on the sample.

3.2.4 Gel Permeation Chromatography (GPC):

GPC analysis using DMF (0.1 M LiBr) as eluent was done using two PSS GRAM analytical (300 and 100 Å, 10 l) columns on an Agilent 1200 series equipped with a Wyatt Optilab rEX refractive index detector thermostat at 40 °C and a Wyatt DAWN HELEOS-II multi angle light scattering (MALS) detector. Molecular weights and PDI were calculated from the MALS signal using the ASTRA software (Wyatt) and a dn/dc value of 0.0731 mL/g (PNIPAM) in DMF. Before analysis, samples were filtered through a 0.2 μm PTFE filter.

3.2.5 Thermal Analysis:

Temperature scans were carried out at a heating/cooling rate of 10 °C /min in the range of -80 – 110 °C using a TA Q200 series calorimeter. Thermal scans below room temperature were calibrated with the cyclohexane solid-solid transition and melting point at -87.0 °C and 6.5 °C respectively. Thermal scans above room temperature were calibrated using indium, tin and zinc with melting points at 156.6, 231.93 and 419.53 °C, respectively.

TGA analysis was conducted using a TA Q50 in a flowing dry nitrogen atmosphere (50 mL / min.) between 25 and 800 °C with a heating rate of 10 °C/min. Sample sizes ranged between 10-20 mg. The instrument was calibrated using the curie points of three reference materials, Alumel, iron and nickel. Platinum pans were used in these experiments.

3.2.6 Heat of Polymerisation

A Pyris 1 DSC was used to analyse the heat of polymerisation. This instrument was calibrated with indium with melting point at 156.6 °C. To directly analyse the polymerisation speed a DSC experiment method was adopted from Achilias et al.[53], the difference being a UV-light photoinitiated polymerisation with an open DSC pan setup was employed. The experiments were performed in isothermal mode at 25 °C. The sample pan and a reference pan were covered with an in-house-made chamber equipped with a holder for the same LED array as in the rheometry experiments. The design of the chamber can be found in Figure A1 and Figure A2 (Appendix A). The LEDs were placed 20 mm from the sample pan, giving a light intensity of ca. 2500 $\mu\text{W}/\text{cm}^2$ as measured with the Lutron UV-340A UV-light probe. (With the instrumental setup available it was not possible to match the UV-intensity used in the rheology experiments. However, the comparison between samples within the respective experimental design is still applicable. The pans were loaded with the mixture of monomer (~ 20 mg), IL and the photoinitiator. These mixtures were the same as used for the polymerisation of linear pNIPAM in ILs during rheometry. The UV light was switched on after two minutes and the heat flow data collected for 15 minutes. When switched on, the LED array had its own constant contribution to the heat release recorded by the instrument. For this reason the baseline was set at the thermogram plateau ($t = 15$ min) at which point the reaction heat release had already ceased but the LEDs were still on. By doing so, the heat contribution of the LEDs was excluded from the heat flow data. The results presented are an average of at least two scans.

3.2.6.1 LCST:

The xP-Cl, xP-DCA, xP-Tos, xP_i-Tos, xP-dbsa samples polymerised during rheometry experiments were collected and immersed in deionised water for 7 days. These water-swollen ionogels were dried with a tissue and cut into circles of 4 mm diameter (ca. 10 mg). These were placed on aluminium DSC pans and sealed. The LCST values for these samples were determined by thermal scans at 5 °C/min with the following temperature program: I. Hold at 10 °C for 2 min. II. Heat from 10 °C to 50 °C then cool from 50 °C to 10 °C. Cycle II was done twice and showed excellent reproducibility. The LCSTs were determined as the endothermic peak during heating and exothermic peak during cooling.

3.3 Results and Discussion

3.3.1 Linear pNIPAM

Crosslinked ionogel materials are difficult to study as polymeric systems mainly because they do not dissolve. Therefore, a simpler system was examined first. By analysing the linear polymerisation of NIPAM it was hoped to gain some insight to the effects of the studied ILs on the polymerisation rates and the mechanical properties of the polymers produced. It was assumed that any influence of the IL on the polymerisation of linear pNIPAM will be also present during the formation of ionogels.

The polymerisation of linear polymers / ionogels can be followed with mechanical modulus analysis and the reaction is considered finished when no change in mechanical properties is observed. For this reason the rheology UV-curing experiments were done first. In the UV-curing rheology experiment results shown in Figure 3-1 a linear polymer is formed as the monomers photopolymerise in the IL as a solvent. Therefore, as the polymer chains grow the viscosity of the respective IL- polymer mixture will increase and this will affect both the loss and storage moduli. It must be noted here that P-NTf₂ sample gave unusual 1 MPa of elastic modulus and 0.1 MPa of viscous modulus measured after 60 minutes of polymerisation. The resulting material was opaque, waxy and very brittle, possibly due to the polymer precipitation in this relatively hydrophobic [P_{6,6,6,14}][NTf₂] IL used for this sample. Due to this precipitation and poor mechanical durability the P-NTf₂ polymer was not selected for further studies. The viscous ILs in our study gave higher moduli for the respective polymer-IL solutions compared to the less viscous ILs. Therefore, we attempted to compensate for this by dividing the loss moduli data by the sample initial loss modulus (therefore all plots start at value 1). The resulting “relative viscous moduli” curves are shown in Figure 3-1.

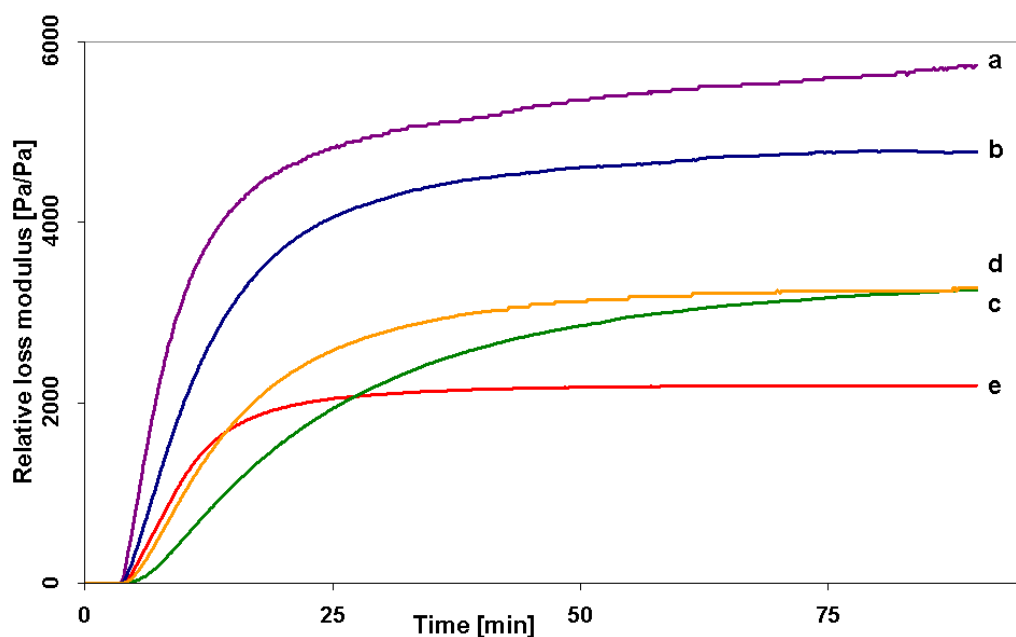


Figure 3-1. Relative viscous moduli curves during UV polymerisation of a) Pi-Tos, b) P-dbsa, c) P-Cl, d) P-Tos, e) P-DCA. For each curve, the data was normalised by dividing the initial loss modulus value into the series. The raw data plots can be found in Appendix A Figure A3.

It can be clearly seen that the slope of these curves varies depending on the IL used. Moreover, the time required for the mixtures moduli to plateau is different. This suggests that the rate of polymer forming is different depending on the IL present in the sample. The Pi-Tos curve shows the highest slope, followed by P-dbsa, P-DCA and P-Tos, with P-Cl having the lowest initial rate of increasing modulus. (The raw data plots can be found in the Appendix A Figure A3)

Table 3-2. Physiochemical properties of linear polymers:

Sample:	Maximum heat flow [W·mol ⁻¹ NIPAM]	Time to reaction peak [s]	Total heat released [kJ·mol ⁻¹ NIPAM]	Average molecular weight Mn [g·mol ⁻¹]	Polydispersity index (PDI)	IL viscosity 25°C [Pa·s]
Pi-Tos	1861	16.7	56.4	117 800	1.76	1.36 ^a
P-dbsa	1516	17.6	58.4	150 900	2.2	1.8 ^b
P-DCA	1315	20.7	60.9	130 600	1.6	0.256 ^b
P-Tos	960	21.0	53.4	111 300	1.42	0.96 ^a
P-Cl	530	24.8	45.0	62 650	1.56	1.955 ^b

^a) Values measured for this study with the rheometer. (Shear rate 100 [s⁻¹]); ^b) Values from reference[54]

It was hypothesized that if the mechanical moduli develop at different rates and stabilise after different times then after the same UV irradiation time the polymer chains must have different chainlengths. Table 3-2 shows the GPC analysis of pNIPAM samples polymerised for 90 min

during the rheology UV curing experiment (Figure 3-1). All of the samples tested have similar and rather high final molecular weight for the pNIPAM with the exception of P-Cl. Therefore, one can state that under equivalent irradiation conditions, the P-dbsa and P-DCA samples produce polymers of significantly higher molecular weight. Whereas with P-Cl, the final molecular weight is only approximately half that of P-dbsa.

Samples used in the UV curing rheology experiment (Figure 3-1) were also UV polymerised in the DSC to follow the evolved heat of polymerisation. The emitted heat per second is directly related to the amount of monomers reacting and therefore it can be regarded as the overall polymerisation kinetics comparison tool. Table 3-2 shows that the peak heat flow differs greatly between the tested samples and ranges from the highest for P₁-Tos, P-dbsa, P-DCA through P-Tos to P-Cl with the lowest heat peak, i.e.

$$P_1\text{-Tos} > P\text{-dbsa} > P\text{-DCA} > P\text{-Tos} > P\text{-Cl}$$

Due to the unknown molar heat of NIPAM polymerisation in the ILs used, the heat flow cannot be related to reaction rates or the degree of conversion of the sample. However, the average total heat released expressed per mole of NIPAM and the peak heat flows are given (Table 3-2). The results show that the peak reaction heat emission linked with the polymerisation speed can vary up to 3-fold depending on the IL chosen as a medium for NIPAM polymerisation. The time required for the polymerisation heat generation to cease is also different depending on the IL used (Figure A4). Found in Appendix A Table A1 are the glass transition (T_g) and decomposition temperatures (T_{dec}) of the samples listed in Table 3-1. The heat analysis and the rheology data suggests that, depending on the anion tested, polymerisation of NIPAM in these phosphonium-based ILs proceeds at different rates and therefore is finished at different times. Moreover the different ILs used produce polymer-IL solutions with different viscoelastic characteristics.

The inherently higher viscosities of these ILs could cause autoacceleration of the polymerisation reaction by lowering the termination rate.[50, 51, 55] However, from the heat of polymerisation data it is clear that viscosity is not the major rate controlling factor, as [P_{6,6,6,14}][dbsa] and [P_{6,6,6,14}][Cl] have similar viscosities (1.8 vs. 1.955 Pa·s, respectively) but the maximum NIPAM polymerisation heats generated in these IL systems are significantly different (1516 [W/mol] vs. 530 [W/mol] respectively).

Another parameter that has a significant influence on the polymerisation process is the polarity of the solvent, in our case, the IL. It has been reported that ILs can greatly speed up the polymerisation process and increase the final conversion of monomer due to their polar and coordinating nature.[50, 51, 56] It has been known for some time that the molar heat of polymerisation, and therefore the ease of polymerisation, depends on the monomer association

with the solvent medium.[57] Therefore the polymerisation kinetics of polar monomers like acrylamides may strongly depend on the polarity of the ionic liquid. However, the polarity of ILs is a complex subject of considerable research in its own right.[58] Recent work has shown that in comparison to other ILs, phosphonium-based ILs have relatively low polarity, which decreases even more with increasing alkyl chain length. Moreover, the anion basicity and size also influences the IL polarity.[58] Based on these factors, one can hypothesize that the higher polymerisation speed in $[P_{1,4,4,4}][Tos]$ compared to $[P_{6,6,6,14}][Tos]$ is due to the shorter alkyl chains of the $[P_{1,4,4,4}]$ cation, which results in higher overall solvent polarity. Furthermore, the $[P_{6,6,6,14}][DCA]$ IL has a small basic anion compared to the other ILs bearing the $[P_{6,6,6,14}]$ cation. This should increase the IL's polarity significantly, and is a plausible explanation for the relatively high total polymerisation heat of NIPAM in $[P_{6,6,6,14}][DCA]$ compared to eg. $[P_{6,6,6,14}][Cl]$ (Table 3-2). The polymerisation of pNIPAM in P-Cl proceeds at the slowest rate and produces the shortest chains, despite the apparently highly mobile and polar nature of the Cl⁻ ion. However previous studies suggest that the Cl⁻ anion is very strongly associated with the $[P_{6,6,6,14}]^+$ cation, to the extent that the local charge is greatly shielded from the external environment, producing a much more non-polar character than might be expected.[59, 60]

It is reasonable to expect that such variations in the curing behaviour must surely have significant implications when the crosslinker is subsequently added to the system to obtain ionogels.

3.3.2 Crosslinked polymers:

In our previous work[8] it was noticed that photoresponsive phosphonium based ionogels had different mechanical characteristics, depending on the anion used. To some extent, the data presented for the linear pNIPAM experiments so far can help interpret the results for the crosslinked ionogels. Gelling should be slower in the xP-Cl and xP-Tos ionogels as these ILs in the corresponding linear pNIPAM gave the shortest chains and lowest polymerisation heats (Table 3-2). When the crosslinker is present, the rise in elastic moduli is a direct indication of the polymeric network being formed. Therefore the storage modulus increase and time to reach a steady state provides an insight into the gelation kinetics.

During the rheology experiments with the crosslinked samples, after the UV light was switched on the storage modulus quickly overcame the loss modulus. The crossover of these two moduli can be taken as the gelpoint (Table 3-3) as from this moment the samples show more elastic than viscous behaviour. After ~90 min of UV-curing all samples except the xP-dbsa exhibit

similar elastic moduli (Figure 3-2). The modulus plateaus at 40 min for the xP-DCA. However, a steady state is not reached for other samples.

Table 3-3. Rheological and LCST properties of the ionogels:

Sample:	Time to moduli crossover [s]	G_0'' [Pa]	G'' [Pa]	G' [Pa]	Tan δ	IL viscosity 25°C [Pa·s]	LSCT during heating [°C]	LCST during cooling [°C]
P _i -Tos	6	3.06	52 000	65 170	0.80	1.36 ^a	32.2	31.9
P-dbsa	35	7.5	200 000	134 000	1.48	1.8 ^b	30.4	28.7
P-DCA	11	0.946	6 770	40 400	0.168	0.256 ^b	29.3	27.4
P-Tos	22	3.53	38 500	47 700	0.81	0.96 ^a	30.4	28.7
P-Cl	40	4.17	42 700	36 700	1.16	1.955 ^b	15.5	8.3

^{a)} Values measured for this study with the rheometer. (Shear rate 100 [s⁻¹]); ^{b)} Values from reference[54]; G_0'' - loss modulus before curing; G'' - loss modulus after 90 min of curing; G' - storage modulus after 90 min of curing; Tan δ - G''/G' after 90 min of curing

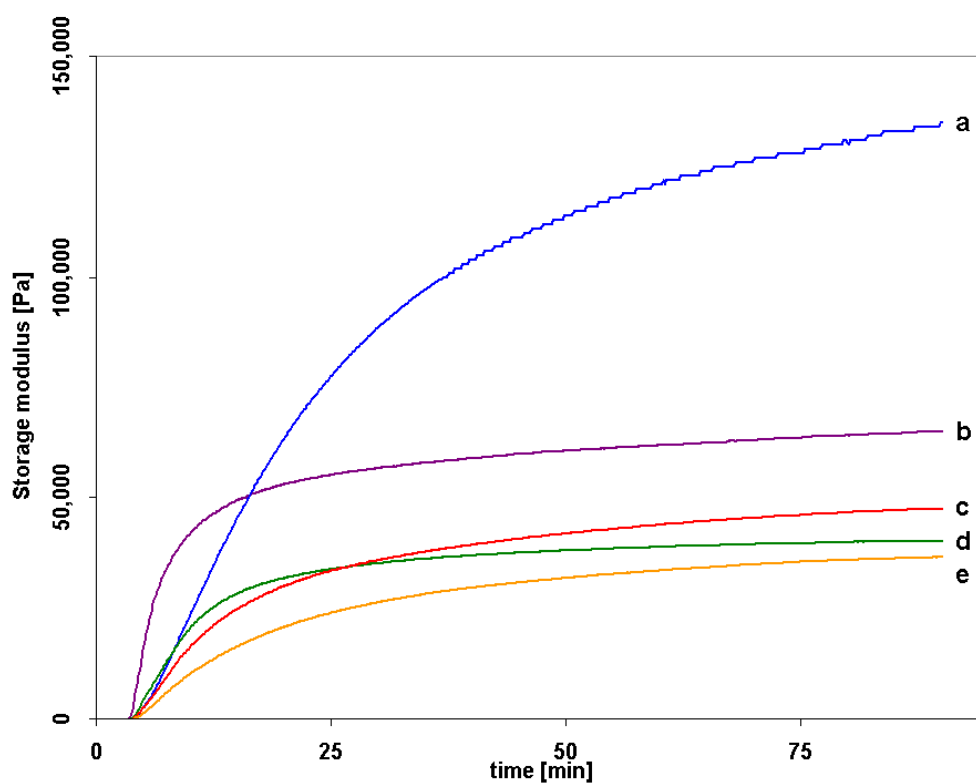


Figure 3-2. Storage moduli during UV polymerisation of a) xP-dbsa, b) xPi-Tos, c) xP-Tos, d) xP-DCA and e) xP-Cl. UV curing was initiated after 3 minutes 20 seconds.

For viscoelastic materials a typical parameter characterising the general mechanical properties is the ratio of the viscous (loss) to elastic (storage) moduli G''/G' ($\tan\delta$). In the case of linear pNIPAM-IL mixtures the number was not so meaningful as these systems formed liquid linear polymer solutions in ILs for which $\tan\delta$ is always higher than 1 (loss modulus higher than storage modulus). However, for the crosslinked systems this number directly tells how rubbery/tacky these ionogels are. The higher the $\tan\delta$ is, the “stickier” and “tackier” the material will be. Table 3-3 shows the key mechanical parameters for the crosslinked samples before and after polymerisation. As found in the linear polymer systems, the IL seems to have a significant impact on the viscoelasticity of the ionogels. The xP-dbsa and xP-Cl ionogels are the “tackiest”. The $\tan\delta$ values of xP-Tos and xP_i-Tos ionogels lie between the xP-dbsa and the xP-DCA ionogels, but have very similar $\tan\delta$ irrespective of the $[P_{6,6,6,14}]^+$ or $[P_{1,4,4,4}]^+$ cation. The xP-DCA ionogel exhibits the lowest $\tan\delta$ and is the most elastic and rubber-like of all the ionogels tested.

Taking into account the kinetics data from the linear pNIPAM experiments and the viscoelastic properties of the ionogel curing it is expected that the xP-DCA will gel more rapidly than other phosphonium samples tested. This ionogel forms quickly due to a high polymerisation speed and has a low $\tan\delta$ which makes it robust. The xP-dbsa produces a network with the highest storage modulus, but the high $\tan\delta$ value is consistent with the tackiness of the ionogel, which makes it difficult to handle. The xP-Tos and xP_i-Tos lie somewhere in between with regard to their strength, $\tan\delta$, and therefore their robustness. In terms of physical integrity, xP-Cl produces the weakest of all the ionogels. It is very tacky, and tears relatively easily, due to its relatively low storage modulus.

Bearing in mind the envisaged application of these materials as soft actuators in microfluidic platforms, a knowledge of viscoelastic properties is important not only because of its influence during fabrication, but also because it largely determines the robustness of the actuator and the actuation speed. Therefore, since pNIPAM is a thermo-responsive polymer, experiments were carried out to determine the LCST actuation behaviour of these ionogels.

DSC scans reveal that most of the water-swollen ionogels exhibit an LCST between 29 and 32 °C, with the exception of xP-Cl (Table 3-3). There is a slight asymmetry in the LCST between the DSC heating and cooling runs as has been reported for other pNIPAM polymers in the literature.[61, 62] The xP-DCA, xP-dbsa and xP-Tos ionogels have very similar LCST values at ca. 30 °C, whereas the xP-Cl ionogel has an unusually low transition temperature at 15.5 °C and the xP_i-Tos ionogel has a slightly higher LCST point at 32.2 °C. The relevant DSC thermograms can be found in the Appendix, Figure A5.

In addition to DSC scans, the LCST transitions were also analysed using rheometry. During the LCST transition while heating the water-swollen ionogels became stiffer. However, the rate of

stiffening and its magnitude was also found to vary depending on the ionic liquid contained in the ionogel. Figure 3-3 shows the storage modulus changes during a step temperature program from 25 °C to 45 °C and back. xP-DCA, xP-dbsa, xP-Tos ionogels increased their moduli as the temperature rose above the LCST and returned to their approximate starting moduli once the temperature had fallen back below the LCST. The biggest increase in modulus during the LCST transition (approx. 7-fold) was measured for the xP-DCA ionogel. In contrast, the xP-Cl ionogel showed no increase in modulus with increasing temperature, whereas a significant increase in the modulus was observed for the xP_i-Tos, with no subsequent relaxation (unlike the other ionogels) upon restoring the temperature to 25 °C. However, this latter sample returned to the original modulus when placed in water overnight.

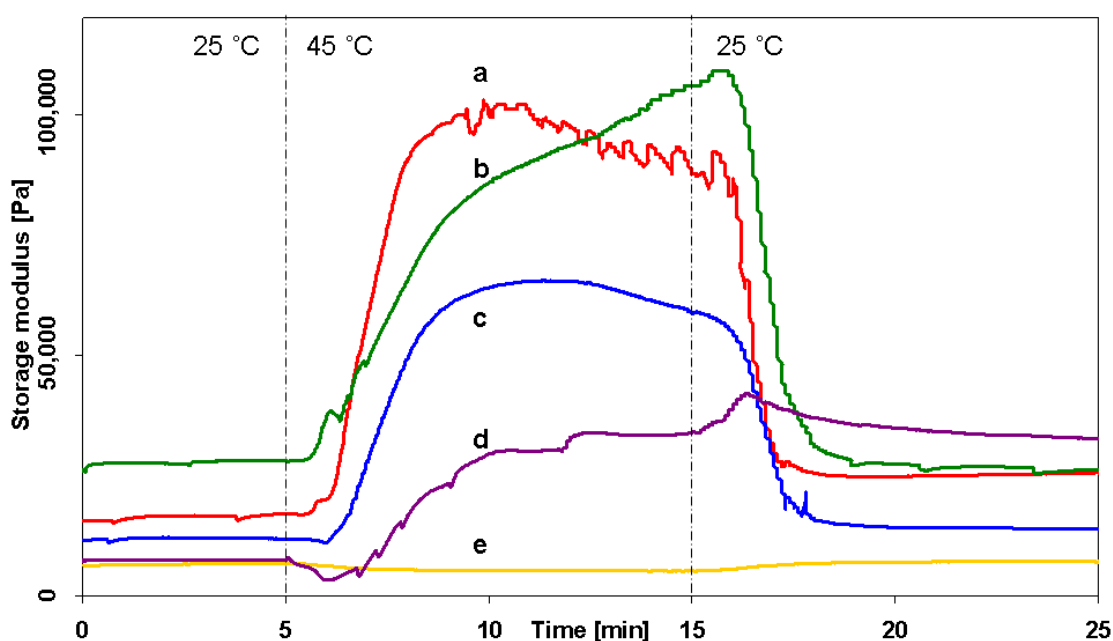


Figure 3-3. Plots of storage modulus versus time during a temperature step program. The temperature was raised from 25 °C to 45 °C starting at 5 min and was decreased at 15 min from 45 °C to 25 °C. a) xP-DCA, b) xP-Tos, c) xP-dbsa, d) xP_i-Tos, e) xP-Cl.

From the DSC data it is clear that, in contrast to the other samples studied, the xP-Cl sample was always above the LCST at room temperature. This observation explains why the xP-Cl sample did not show any modulus changes in the temperature ramp experiment: As the LCST of this ionogel was 15.5 °C, then under the experimental conditions used for the LCST rheology, the sample was always above its LCST, and no phase change occurred. Therefore, to investigate the xP-Cl sample a lower temperature window of 5 – 25 °C was used, the results of which can be seen in Figure A6 Appendix A. This experiment showed that the xP-Cl also increased its modulus reversibly during the LCST transition. However, the magnitude and rate of the modulus increase in xP-Cl is the smallest of all the samples tested.

In Figure 3-4 the modulus values were normalised by subtracting the initial modulus from each

point of the respective plot. From this it is easier to see that the rate of LCST transition induced modulus increase is different depending on the ionogel composition. The ionogels with higher elastic character (lower $\tan\delta$ of xP-DCA and xP-Tos) had a faster polymer network modulus response than the xP-dbsa which had a higher $\tan\delta$.

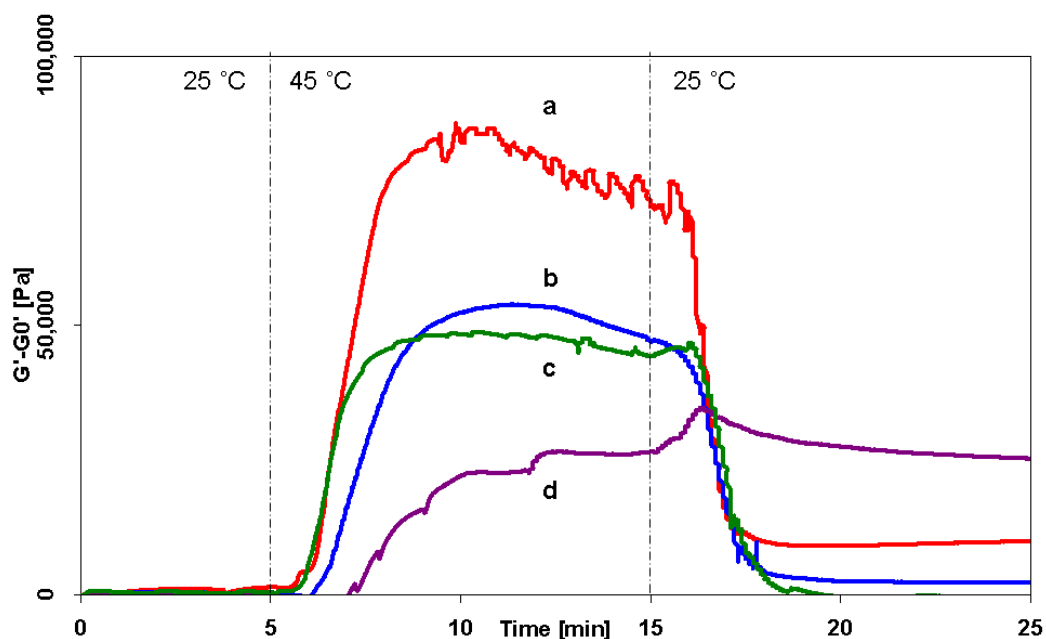


Figure 3-4. Plots of storage modulus versus time during a temperature step program for water swollen ionogels. The temperature was raised from 25 °C to 45 °C (20 °C/min) starting at $t = 5$ min and was decreased at $t = 15$ min from 45 °C to 25 °C (20 °C/min). a) xP-DCA, b) xP-dbsa, c) xP-Tos d) xP₁-Tos. The initial moduli value was subtracted from the respective plots.

The sharp peaks found in Figure 3-3 and Figure 3-4 are due to the instrument readjusting the normal force on the sample. As the sample shrunk and changed modulus the reaction force of the sample dropped and the instrument corrected for this (as described in the experimental section). The degree and frequency of this adjustment itself gives some insight into the sample behaviour under stress during the LCST transition. Noteworthy is the fact that the speed of gap shrinking was not correlated with the speed of modulus increase for the respective samples (eg. xP-DCA and xP-dbsa, Figure A7 Appendix A). Moreover, the thickness decrease for all samples never exceeded 10%. The small dimension change suggests that the ILs are not leaching under pressure. It is interesting to see that the LCST transitions of the polymer chains can be visualised with the rheometer by analysing the storage modulus increase and recovery. These results show that the mechanical and curing characteristics of the ionogels (arising from the different ILs used) also have an impact on their LCST triggered polymer network actuation speed. However, as mentioned previously, in these ionogels the volume change does not correlate with the modulus change. This conclusion is consistent with other studies that suggest the chain collapse/revival of pNIPAM and volume change (water uptake/release) are linked but not simultaneous processes.[62, 63] These are important findings with respect to strategies for systematically optimising formulations for generating stimulus-responsive structures (such as

microvalves for microfluidic systems) based on these ionogels.

3.4 Conclusion

In this study NIPAM monomer was polymerised in a series of commercially available phosphonium based ILs. The increase in viscoelastic moduli during UV-photopolymerisation was monitored using a rheometer for samples with and without a crosslinker (MBIS). This, combined with DSC and GPC analysis showed clear differences in the mechanical properties, polymer chain lengths, emitted polymerisation heat and the LCSTs of the resulting materials. It was demonstrated that changing between phosphonium based ILs changes not only the viscosity of the polymerisation medium, but also the NIPAM polymerisation speed (in some cases by a factor of 3) and the resulting ionogel mechanical viscoelastic properties. Rheometry shows that when these ionogels are swollen in water, they undergo a reversible modulus increase when the temperature is raised above the LCST. The rate of modulus change differs and appears to be correlated with the original ionogel $\tan\delta$ value. The ionogel based on xP-DCA showed a 7-fold increase in the storage modulus when heated above its LCST.

The most “mechanically robust” ionogel was obtained after 30 minutes of UV curing (1.1 mW/cm²) when [P_{6,6,6,14}][DCA] or [P_{1,4,4,4}][Tos] was used as the solvent/IL, and the “tackiest” ionogel was obtained with [P_{6,6,6,14}][dbsa] and [P_{6,6,6,14}][Cl] (still not fully cured after 90 minutes).

Therefore, bearing in mind the time required for curing of these ionogels, processability of the monomer-IL cocktail, the viscoelastic properties and the speed of the LCST actuation of the resulting material the [P_{6,6,6,14}][DCA] IL appears to be the optimum choice for the microfluidic applications mentioned.

Acknowledgements: This work was performed as part of the EU Framework 7 project “ATWARM” (Marie Curie ITN, No. 238273). K.J.F acknowledges the European Commission for financial support through a Marie Curie Actions International Re-integration Grant (IRG) (PIRG07-GA-2010-268365) and Irish Research Council for Science, Engineering and Technology. R. B. and D. D. acknowledge funding from Science Foundation Ireland (SFI) under the CLARITY CSET award (Grant 07/CE/I1147). The author would also like to thank Dylan Orpen, Damien Maher and Cormac Fay (Dublin City University) for engineering and assembly support, Garrett McGuinness (Dublin City University) and Steve Goodyer from Anton

Paar for mechanical testing consultation. All authors would like to thank Al Robertson of Cytec Industries (Ontario Canada) for providing phosphonium ILs.

Notes

Supplementary Information (Appendix A) available: Details regarding IL synthesis, purification and purity, experimental DSC setup, UV curing DSC kinetics data, rheology LCST scans.

3.5 References:

1. Dong, L.; Jiang, H., Autonomous microfluidics with stimuli-responsive hydrogels. *Soft Matter* **2007**, *3*.
2. Richter, A.; Klatt, S.; Paschew, G.; Klenke, C., Micropumps operated by swelling and shrinking of temperature-sensitive hydrogels. *Lab on a Chip* **2009**, *9*.
3. Sugiura, S.; Sumaru, K.; Ohi, K.; Hiroki, K.; Takagi, T.; Kanamori, T., Photoresponsive polymer gel microvalves controlled by local light irradiation. *Sensors and Actuators A: Physical* **2007**, *140*, 176-184.
4. Satarkar, N. S.; Zhang, W.; Eitel, R. E.; Hilt, J. Z., Magnetic hydrogel nanocomposites as remote controlled microfluidic valves. *Lab on a Chip* **2009**, *9*.
5. Satoh, T.; Sumaru, K.; Takagi, T.; Kanamori, T., Fast-reversible light-driven hydrogels consisting of spirobenzopyran-functionalized poly(N-isopropylacrylamide). *Soft Matter* **2011**, *7*, 8030-8034.
6. Guan, Y.; Zhang, Y., PNIPAM microgels for biomedical applications: from dispersed particles to 3D assemblies. *Soft Matter* **2011**, *7*, 6375-6384.
7. Byrne, R.; Ventura, C.; Lopez, F. B.; Walther, A.; Heise, A.; Diamond, D., Characterisation and analytical potential of a photo-responsive polymeric material based on spiropyran. *Biosensors and Bioelectronics* **2010**, *26*, 1392-1398.
8. Benito-Lopez, F.; Byrne, R.; Raduta, A. M.; Vrana, N. E.; McGuinness, G.; Diamond, D., Ionogel-based light-actuated valves for controlling liquid flow in micro-fluidic manifolds. *Lab on a Chip* **2010**, *10*, 195-201.
9. Liu, F.; Urban, M. W., Recent advances and challenges in designing stimuli-responsive polymers. *Progress in Polymer Science* **2010**, *35*, 3-23.
10. Schild, H. G., Poly (n-isopropylacrylamide) - experiment, theory and application. *Progress in Polymer Science* **1992**, *17*, 163-249.
11. Madsen, J.; Armes, S. P., (Meth)acrylic stimulus-responsive block copolymer hydrogels. *Soft Matter* **2012**, *8*, 592-605.
12. Alarcon, C. d. I. H.; Pennadam, S.; Alexander, C., Stimuli responsive polymers for biomedical applications. *Chemical Society Reviews* **2005**, *34*, 276-285.
13. Bansal, D.; Cassel, F.; Croce, F.; Hendrickson, M.; Plichta, E.; Salomon, M., Conductivities and Transport Properties of Gelled Electrolytes with and without an Ionic Liquid for Li and Li-Ion Batteries. *Journal of Physical Chemistry B* **2005**, *109*, 4492-4496.

14. Frackowiak, E.; Lota, G.; Pernak, J., Room-temperature phosphonium ionic liquids for supercapacitor application. *Applied Physics Letters* **2005**, *86*, 164104/164101-164104/164103.
15. Lee, J. S.; Bae, J. Y.; Lee, H.; Quan, N. D.; Kim, H. S.; Kim, H., Ionic liquids as electrolytes for Li ion batteries. *Journal of Industrial and Engineering Chemistry (Seoul, Republic of Korea)* **2004**, *10*, 1086-1089.
16. Lu, W.; Norris, I. D.; Mattes, B. R., Electrochemical Actuator Devices Based on Polyaniline Yarns and Ionic Liquid Electrolytes. *Australian Journal of Chemistry* **2005**, *58*, 263-269.
17. MacFarlane, D. R.; Forsyth, M., Plastic crystal electrolyte materials: new perspectives on solid state ionics. *Advanced Materials* **2001**, *13*, 957-966.
18. Marwanta, E.; Mizumo, T.; Nakamura, N.; Ohno, H., Improved ionic conductivity of nitrile rubber/ionic liquid composites. *Polymer* **2005**, *46*, 3795-3800.
19. Pernak, J.; Stefaniak, F.; Weglewski, J., Phosphonium acesulfamate based ionic liquids. *European Journal of Organic Chemistry* **2005**, 650-652.
20. Wassercheid, P.; Welton, T., *Ionic liquids in synthesis*. Wiley-VCH: 2003.
21. Webber, A.; Blomgren, G. E., *Ionic liquids for lithium ion and related batteries*. 2002; p 185-232.
22. Sakaebe, H.; Matsumoto, H., N-Methyl-N-propylpiperidinium bis(trifluoromethanesulfonyl)imide (PP13-TFSI) - novel electrolyte base for Li battery. *Electrochemistry Communications* **2003**, *5*, 594-598.
23. Papageorgiou, N.; Athanassov, Y.; Armand, M.; Bonhote, P.; Pettersson, H.; Azam, A.; Graetzel, M., The performance and stability of ambient temperature molten salts for solar cell applications. *Journal of the Electrochemical Society* **1996**, *143*, 3099-3108.
24. Wang, P.; Zakeeruddin, S. M.; Exnar, I.; Graetzel, M., High efficiency dye-sensitized nanocrystalline solar cells based on ionic liquid polymer gel electrolyte. *Chemical Communications (Cambridge, United Kingdom)* **2002**, 2972-2973.
25. Wang, P.; Zakeeruddin, S. M.; Graetzel, M.; Kantlehner, W.; Mezger, J.; Stoyanov, E. V.; Scherr, O., Novel room temperature ionic liquids of hexaalkyl substituted guanidinium salts for dye-sensitized solar cells. *Applied Physics A: Materials Science & Processing* **2004**, *A79*, 73-77.
26. Lu, W.; Fadeev, A. G.; Qi, B.; Smela, E.; Mattes, B. R.; Ding, J.; Spinks, G. M.; Mazurkiewicz, J.; Zhou, D.; Wallace, G. G.; MacFarlane, D. R.; Forsyth, S. A.; Forsyth, M., Use of ionic liquids for p-conjugated polymer electrochemical devices. *Science (Washington, DC, United States)* **2002**, *297*, 983-987.
27. Ding, J.; Zhou, D.; Spinks, G.; Wallace, G.; Forsyth, S.; Forsyth, M.; MacFarlane, D., Use of Ionic Liquids as Electrolytes in Electromechanical Actuator Systems Based on Inherently Conducting Polymers. *Chemistry of Materials* **2003**, *15*, 2392-2398.
28. Zhou, D.; Spinks, G. M.; Wallace, G. G.; Tiyaiboonthaiya, C.; MacFarlane, D. R.; Forsyth, M.; Sun, J., Solid state actuators based on polypyrrole and polymer-in-ionic liquid electrolytes. *Electrochimica Acta* **2003**, *48*, 2355-2359.
29. Nanjundiah, C.; McDevitt, S. F.; Koch, V. R., Differential capacitance measurements in solvent-free ionic liquids at Hg and C interfaces. *Journal of the Electrochemical Society* **1997**, *144*, 3392-3397.
30. McEwen, A. B.; McDevitt, S. F.; Koch, V. R., Nonaqueous electrolytes for electrochemical capacitors: imidazolium cations and inorganic fluorides with organic carbonates. *Journal of the Electrochemical Society* **1997**, *144*, L84-L86.

31. McEwen, A. B.; Ngo, E. L.; LeCompte, K.; Goldman, J. L., Electrochemical properties of imidazolium salt electrolytes for electrochemical capacitor applications. *Journal of the Electrochemical Society* **1999**, *146*, 1687-1695.
32. Wasserscheid, P.; Keim, W., Ionic liquids - new "solutions" for transition metal catalysis. *Angewandte Chemie, International Edition* **2000**, *39*, 3772-3789.
33. Welton, T., Room-Temperature Ionic Liquids. Solvents for Synthesis and Catalysis. *Chemical Reviews (Washington, D. C.)* **1999**, *99*, 2071-2083.
34. Wooster, T. J.; Johanson, K. M.; Fraser, K. J.; MacFarlane, D. R.; Scott, J. L., Thermal degradation of cyano containing ionic liquids. *Green Chemistry* **2006**, *8*, 691-696.
35. Bradaric, C. J.; Downard, A.; Kennedy, C.; Robertson, A. J.; Zhou, Y., Industrial preparation of phosphonium ionic liquids. *Green Chemistry* **2003**, *5*, 143-152.
36. Ramnial, T.; Ino, D. D.; Clyburne, J. A. C., Phosphonium ionic liquids as reaction media for strong bases. *Chemical Communications (Cambridge, United Kingdom)* **2005**, 325-327.
37. Le Bideau, J.; Viau, L.; Vioux, A., Ionogels, ionic liquid based hybrid materials. *Chemical Society Reviews* **2011**.
38. Mohmeyer, N.; Kuang, D.; Wang, P.; Schmidt, H.-W.; Zakeeruddin, S. M.; Gratzel, M., An efficient organogelator for ionic liquids to prepare stable quasi-solid-state dye-sensitized solar cells. *Journal of Materials Chemistry* **2006**, *16*, 2978-2983.
39. Susan, M. A. B. H.; Kaneko, T.; Noda, A.; Watanabe, M., Ion Gels Prepared by in Situ Radical Polymerization of Vinyl Monomers in an Ionic Liquid and Their Characterization as Polymer Electrolytes. *Journal of the American Chemical Society* **2005**, *127*, 4976-4983.
40. Viau, L.; Tourne-Peteilh, C.; Devoisselle, J.-M.; Vioux, A., Ionogels as drug delivery system: one-step sol-gel synthesis using imidazolium ibuprofenate ionic liquid. *Chemical Communications* **2010**, *46*, 228-230.
41. Gayet, F.; Viau, L.; Leroux, F.; Mabilhe, F. d. r.; Monge, S.; Robin, J.-J.; Vioux, A., Unique Combination of Mechanical Strength, Thermal Stability, and High Ion Conduction in PMMA–Silica Nanocomposites Containing High Loadings of Ionic Liquid. *Chemistry of Materials* **2009**, *21*, 5575-5577.
42. Au, A. K.; Lai, H.; Utela, B. R.; Folch, A., Microvalves and Micropumps for BioMEMS. *Micromachines* **2011**, *2*, 179-220.
43. Fraser, K. J.; MacFarlane, D. R., Phosphonium-Based Ionic Liquids: An Overview. *Australian Journal of Chemistry* **2009**, *62*, 309-321.
44. Byrne, R.; Benito-Lopez, F.; Diamond, D., Materials science and the sensor revolution. *Materials Today* **2010**, *13*, 9-16.
45. Kavanagh, A.; Byrne, R.; Diamond, D.; Radu, A., A two-component polymeric optode membrane based on a multifunctional ionic liquid. *Analyst* **2011**, *136*, 348-353.
46. Kavanagh, A.; Hilder, M.; Clark, N.; Radu, A.; Diamond, D., Wireless radio frequency detection of greatly simplified polymeric membranes based on a multifunctional ionic liquid. *Electrochimica Acta* **2011**, *56*, 8947-8953.
47. Kavanagh, A.; Copperwhite, R.; Oubaha, M.; Owens, J.; McDonagh, C.; Diamond, D.; Byrne, R., Photo-patternable hybrid ionogels for electrochromic applications. *Journal of Materials Chemistry* **2011**, *21*, 8687-8693.
48. Ueki, T.; Watanabe, M., Lower Critical Solution Temperature Behavior of Linear Polymers in Ionic Liquids and the Corresponding Volume Phase Transition of Polymer Gels. *Langmuir* **2006**, *23*, 988-990.
49. Ueki, T.; Watanabe, M., Macromolecules in Ionic Liquids: Progress, Challenges, and Opportunities. *Macromolecules* **2008**, *41*, 3739-3749.

50. Kubisa, P., Ionic liquids as solvents for polymerization processes—Progress and challenges. *Progress in Polymer Science* **2009**, *34*, 1333-1347.
51. Andrzejewska, E.; Podgorska-Golubska, M.; Stepniak, I.; Andrzejewski, M., Photoinitiated polymerization in ionic liquids: Kinetics and viscosity effects. *Polymer* **2009**, *50*, 2040-2047.
52. Irie, M.; Kunwatchakun, D., Photoresponsive polymers. 8. Reversible photostimulated dilation of polyacrylamide gels having triphenylmethane leuco derivatives. *Macromolecules* **1986**, *19*, 2476-2480.
53. Achilias, D. S.; Sideridou, I. D., Kinetics of the Benzoyl Peroxide/Amine Initiated Free-Radical Polymerization of Dental Dimethacrylate Monomers: Experimental Studies and Mathematical Modeling for TEGDMA and Bis-EMA. *Macromolecules* **2004**, *37*, 4254-4265.
54. Fraser, K. J.; Izgorodina, E. I.; Forsyth, M.; Scott, J. L.; MacFarlane, D. R., Liquids intermediate between "molecular" and "ionic" liquids: Liquid Ion Pairs? *Chemical Communications* **2007**, 3817-3819.
55. Andrzejewska, E., Photopolymerization kinetics of multifunctional monomers. *Progress in Polymer Science* **2001**, *26*, 605-665.
56. Carmichael, A. J.; Haddleton, D. M.; Bon, S. A. F.; Seddon, K. R., Copper(I) mediated living radical polymerisation in an ionic liquid. *Chemical Communications* **2000**, 1237-1238.
57. Joshi, R. M., Influence of association on the heats of polymerization. *Journal of Polymer Science* **1962**, *60*, S56-S59.
58. Ab Rani, M. A.; Brant, A.; Crowhurst, L.; Dolan, A.; Lui, M.; Hassan, N. H.; Hallett, J. P.; Hunt, P. A.; Niedermeyer, H.; Perez-Arlandis, J. M.; Schrems, M.; Welton, T.; Wilding, R., Understanding the polarity of ionic liquids. *Physical Chemistry Chemical Physics* **2011**, *13*, 16831-16840.
59. Thompson, D.; Coleman, S.; Diamond, D.; Byrne, R., Electronic structure calculations and physicochemical experiments quantify the competitive liquid ion association and probe stabilisation effects for nitrobenzospiropyran in phosphonium-based ionic liquids. *Physical Chemistry Chemical Physics* **2011**, *13*, 6156-6168.
60. MacFarlane, D. R.; Forsyth, M.; Izgorodina, E. I.; Abbott, A. P.; Annat, G.; Fraser, K., On the concept of ionicity in ionic liquids. *Physical Chemistry Chemical Physics* **2009**, *11*.
61. Wang, X.; Qiu, X.; Wu, C., Comparison of the Coil-to-Globule and the Globule-to-Coil Transitions of a Single Poly(N-isopropylacrylamide) Homopolymer Chain in Water. *Macromolecules* **1998**, *31*, 2972-2976.
62. Sun, S.; Hu, J.; Tang, H.; Wu, P., Chain Collapse and Revival Thermodynamics of Poly(N-isopropylacrylamide) Hydrogel. *The Journal of Physical Chemistry B* **2010**, *114*, 9761-9770.
63. Wang, Z.; Wu, P., Spectral Insights into Gelation Microdynamics of PNIPAM in an Ionic Liquid. *The Journal of Physical Chemistry B* **2011**, *115*, 10604-10614.

Chapter 4:

Magnetic ionogels (MagIGs) based on iron oxide nanoparticles, poly(N-isopropylacrylamide), and the ionic liquid trihexyl-tetradecyl phosphonium dicyanamide

Bartosz Ziółkowski,^a Katrin Bleek,^b Brendan Twamley,^c Kevin J. Fraser,^a Robert Byrne,^a Dermot Diamond,^{a,*} and Andreas Taubert^{b,*}

a) CLARITY Centre for Sensor Web Technologies, National Centre for Sensor Research, Dublin City University, Dublin 9, Ireland

b) Institute of Chemistry, University of Potsdam, Karl-Liebknecht-Str. 24-25, Building 26, D-14476 Potsdam, Germany. E-mail: ataubert@uni-potsdam.de; Tel: +49 (0)331 977 5773.

c) School of Chemical Sciences, Dublin City University, Dublin 9, Ireland

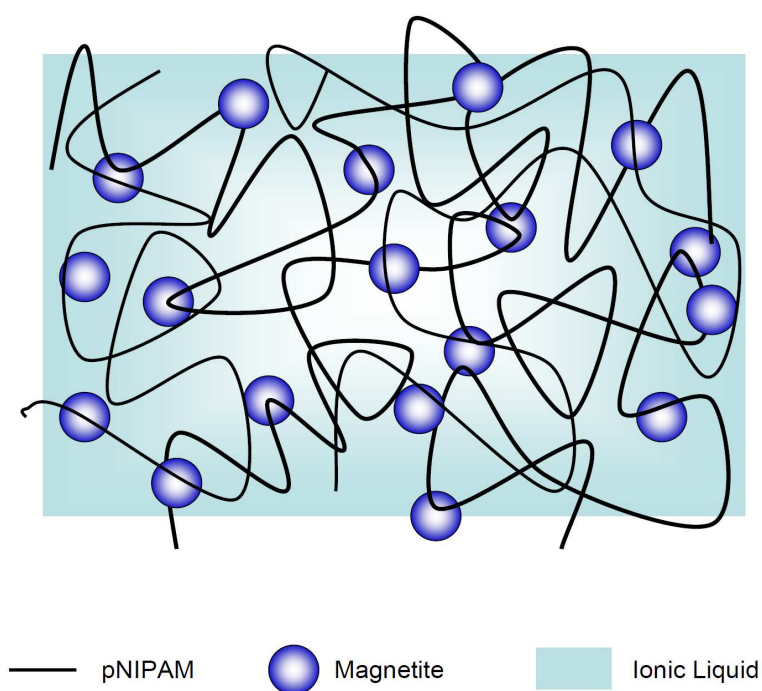
Published: *European Journal of Inorganic Chemistry*, **2012**(32), 5245-5251.

DOI: 10.1002/ejic.201200597

Abstract

Magnetic ionogels (MIGs) were prepared from organosilane-coated iron oxide nanoparticles, N-isopropylacrylamide, and the ionic liquid trihexyl-tetradecyl phosphonium dicyanamide. The ionogels prepared with the silane-modified nanoparticles are more homogeneous than ionogels prepared with non-modified magnetite particles. The silane-modified particles are immobilized in the ionogel and are resistant towards nanoparticle leaching. The modified particles also render the ionogels mechanically more stable than the ionogels synthesized with non-modified nanoparticles. The ionogels respond to external permanent magnets and are therefore prototypes of a new soft magnetic actuator.

Key words: Magnetic nanoparticles, iron oxide, ionic liquids, ionogels, pNIPAM



4.1 Introduction

Gels have tremendous application potential in materials science,[1, 2] sensors,[3] actuators,[4, 5] and stimulus responsive materials.[6-8] Historically research has focused on organo- or hydrogels but the recent past has seen a surge of publications on ionogels, that is, gels based on ionic liquids (ILs) instead of molecular solvents.[9-11] ILs consist entirely of ions and have useful properties like electric and ionic conductivity, rather high thermal stability, and a low vapor pressure.[12, 13] Finally, the number of potential anion-cation combinations available reputedly equates to one trillion (10^{12}) different ILs,[14] theoretically providing access to a very large number of different IL properties useful for both academia and industry.[15]

ILs have been explored as components in functional hybrid materials termed ionogels. Depending on the nature of the ionogel network the ionogels can be inorganic (mostly silica-based) [9, 11, 16-19] or organic.[20-23] The properties of an organic ionogel arise from both the polymeric network stabilizing the ionogel and the functionalities of the contained IL.[12, 21, 24, 25] Among others, ionogels resist drying and cracking due to the very low vapor pressure of the contained IL.[26] Ionogels therefore provide a clear advantage in terms of evaporation resistance and long term stability for application, for example as soft actuators, where other gels lose their solvent by evaporation and therefore crack and fail.[23, 27]

Polymer gels are useful for incorporating stimulus responsive entities.[6, 7, 28] Stimulus-responsive gels can be actuated by external stimuli like changes of temperature,[7] pH,[29, 30] light,[31, 32] and electric[33] or magnetic fields.[34-36] Stimulus-responsive gels (often termed smart materials) have therefore been studied for drug delivery,[3, 28] sensing,[37] and microfluidics.[38-41] Magnetic soft materials are particularly attractive for actuation because of their remote, non-invasive triggering.[39, 42-46]

In an attempt to combine magnetic actuation and the advantages of ILs, magneto-responsive ionogels have been prepared from iron-based, paramagnetic ILs.[47, 48] However, the magnetic susceptibility of these materials and therefore their response to a magnetic field is fairly low at ~ 1 emu/g.[48] The response of magnetic nanoparticles (instead of a magnetic IL) to a magnetic field is much higher by virtue of their much higher magnetic susceptibility of ~ 60 emu/g.[49] Magnetic nanoparticles would therefore be interesting ionogel components, similar to magnetic hydrogels.[35, 40, 50, 51] There is thus an interest in the development of ionogels combining the general advantages of ILs with the advantages of magnetic gels. Such materials could be used in soft actuation under conditions where other gel types such as hydrogels or organogels fail, for example because the water or organic solvent evaporate.

The current report therefore describes a new approach towards magnetic ionogels (MIGs) that can be actuated with a commercial permanent magnet. The ionogels were synthesized via the

copolymerization of silane-modified iron oxide nanoparticles with N-isopropylacrylamide (one of the most popular polymers for responsive gels[7, 36, 50, 52-57]) and the hydrophobic IL trihexyl-tetradecyl phosphonium dicyanamide ([P_{6,6,6,14}][DCA]). The approach is based on the recognition that iron oxide nanoparticles can be modified with allyltrimethoxysilane (ATMS) or 3-mercaptopropyl trimethoxysilane (MPTMS). These coated particles can be (co)polymerized[49] or used for chain transfer during copolymerization with NIPAM.[52] The choice of the IL is dictated by the fact that the trihexyl-tetradecyl phosphonium cation is hydrophobic and should therefore not leach out from the ionogel in aqueous environments,[12] enabling an application of the corresponding ionogel, for example, in diagnostics in aqueous media. Moreover, the dicyanamide anion provides the IL with one of the lowest viscosities and lowest melting points compared to ILs based on other anions such as chloride, bromide, tetrafluoroborate, methylsulfate, and others.[12] Low viscosities and low melting points are convenient for dissolving the ionogel components and processing. Lastly, preliminary experiments in our laboratory have shown that the [P_{6,6,6,14}][DCA] IL imparts ionogels with optimal mechanical and curing properties in comparison with other IL anions such as chloride, tosylate, dodecylbenzylsulphate.

4.2 Experimental

4.2.1 Materials

N-isopropylacrylamide (NIPAM, 98 %), *N,N'*-methylenebisacrylamide (MBIS, 99 %), benzoyl peroxide (BPO, 75 %), (3-mercaptopropyl)trimethoxysilane (MPTMS, 95 %), allyltrimethoxysilane (ATMS, 98%), iron(III) chloride hexahydrate (>98 %), iron(II) chloride tetrahydrate (99 %), tetramethylammonium hydroxide (TMAOH, 25 wt% in H₂O), and ammonium hydroxide (28 - 30 % in H₂O) were obtained from Sigma Aldrich (Ireland) and used as received unless stated otherwise. Ethanol (96 %) and Acetone (99.8 %) were obtained from Sigma Aldrich Germany. Buffer solutions (pH 7, phosphate and pH 4, citric acid/sodium hydroxide/sodium chloride) were obtained from neoLab Migge.

Trihexyl-tetradecylphosphonium dicyanamide [P_{6,6,6,14}][DCA] was kindly donated by Cytec Industries and purified as described previously:[53] 20 mL of the IL was decolorized by redissolution in 30 mL of acetone followed by treatment with activated charcoal (Darco-G60, Aldrich) at 40 °C overnight. Carbon was removed by filtration through alumina (acidic, Brockmann I, Aldrich) and the solvent removed under vacuum at 40 °C for 48 hrs at 0.1 Torr.

^1H NMR δ_{H} (400 MHz; CDCl_3): 2.0-2.3 (8 H, m, CH_2), 1.4-1.5 (16 H, m, CH_2), 1.2-1.3 (32 H, m, CH_2), 0.79-0.85 (12 H, m, CH_3) ppm. ES-MS: ES^+ m/z 483 [$\text{P}_{6,6,6,14}$] $^+$ ES^- m/z 66 [dca].

The permanent magnets were NdFeB cylinders (Magnet-Disc S16x15Ni-N35, 16 mm diameter x 15 mm height) from magnetmonster.de/HKCM Engineering e.k.

4.2.2 Fe_3O_4 synthesis

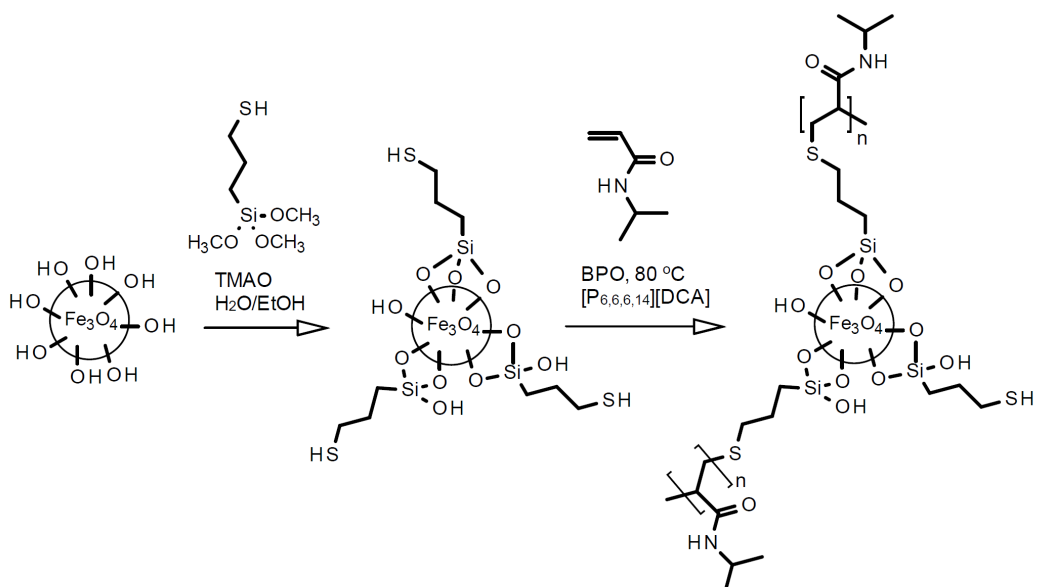
Magnetic particles were prepared according to Massart.[54] $\text{FeCl}_3 \cdot 6\text{H}_2\text{O}$ (0.008 moles) were mixed with $\text{FeCl}_2 \cdot 4\text{H}_2\text{O}$ (0.004 moles) in 30 mL of deionised water. The mixture was mechanically stirred at 600 rpm with nitrogen purge. Next, 7 mL of 30 % aqueous ammonia were rapidly injected. The solution turned black immediately but was kept stirring for 15 minutes. The particles were collected with a magnet and washed three times with deionised water. To the wet and clean particles 500 μL of an aqueous 2.79 M tetramethylammonium hydroxide (TMAOH) solution was added. After shaking the mixture formed a stable ferrofluid (~ 0.9 g Fe_3O_4 /8 mL water) that was used for further functionalisation.

4.2.3 Silane coating of the Fe_3O_4 nanoparticles

The ferrofluid described above was dispersed in a mixture of 125 mL of deionised water and 35 mL of ethanol. This dispersion was purged with nitrogen and sonicated for 5 minutes in an Erlenmeyer flask. During the last minute of sonication 200 μL of MPTMS or 150 μL of ATMS were added, respectively, with vigorous stirring. The flask was sealed with parafilm and left with magnetic stirring for 3 days. The particles were subsequently precipitated by adding 2 mL of a pH 7 buffer per 1 mL of the reaction mixture. The precipitate was collected with a magnet and redispersed in 2 mL of acetone. The samples will, in the remainder of the text, be referred to as 0- Fe_3O_4 (unmodified nanoparticles), M- Fe_3O_4 (modified with MPTMS), and A- Fe_3O_4 (modified with ATMS), respectively. The dispersions of the nanoparticles in [$\text{P}_{6,6,6,14}$][DCA] were prepared as follows. 1 mL of a particle dispersion in acetone (0- Fe_3O_4 , M- Fe_3O_4 , or A- Fe_3O_4) was mixed with 2 g of [$\text{P}_{6,6,6,14}$][DCA]. After sonication, the acetone was removed by rotary evaporation. The resulting IL-based ferrofluids were dried overnight (room temperature, 20 mBar) yielding dispersions with a particle concentration of ~ 20 wt%.

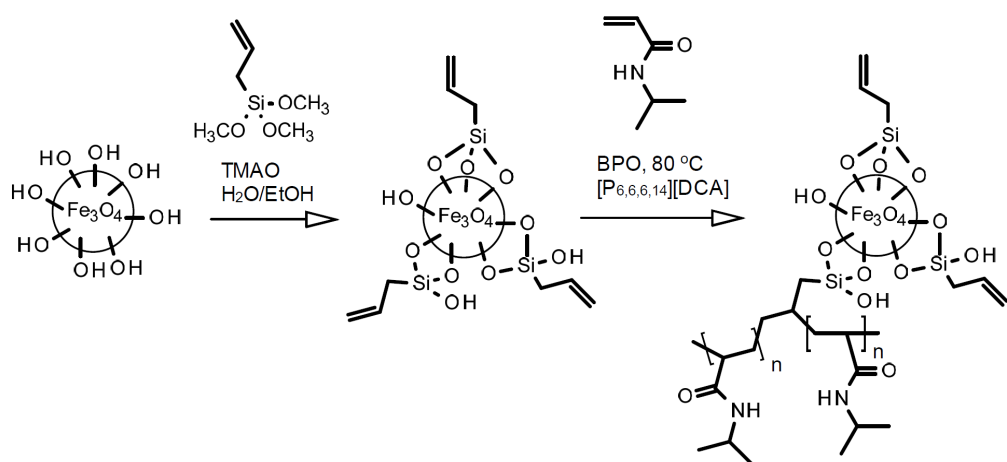
4.2.4 Preparation of magnetic pNIPAM ionogels

pNIPAM gels were prepared (Scheme 4-1 and Scheme 4-2) by mixing NIPAM (500 mg, 0.0044 mol) with 1 mol% of MBIS, 2 mol% BPO and 1.2 mL of the IL/particle dispersion. The mixture was heated to 50 °C and sonicated for 5 min until the solids dissolved and the solution was homogenous. This mixture was poured into a preheated Teflon mould with circular pits (diameter = 15 mm, depth = 1 mm) which was heated by placing flat on a laboratory hotplate. The thermostat was set to measure the temperature at the top surface of the mould.



Scheme 4-1. Preparation of M-ionogels.

The polymerization was done for 15 hours at ca. 80 °C at ambient atmosphere. The ionogels prepared with 0-Fe₃O₄, M-Fe₃O₄, or A-Fe₃O₄ particles will be called 0-, A-, and M-ionogels, respectively.



Scheme 4-2. Preparation of A-ionogels.

4.2.5 FT-IR spectroscopy

IR spectra were recorded on a Thermo Nicolet FT-IR Nexus 470 in ATR mode with a resolution of 2 cm^{-1} . The particle/acetone dispersions were placed on the ATR ZnSe crystal and the solvent was evaporated. Each spectrum is an average of 30 scans.

4.2.6 Dynamic light scattering (DLS)

The particles were dispersed in water or acetone and the dispersions were diluted with water until transparent. The DLS intensity distribution and polydispersity index (PDI) was analyzed with a Malvern High Precision Particle Sizer using PMMA disposable cuvettes. Dilutions were adjusted so that the measured scattering intensity was between 200 and 700 counts/sec. The hydrodynamic radii are averages of 2 experiments each consisting of 13 scans of 10 sec/scan. Data were analyzed with the Malvern Zetasizer software package.

4.2.7 Electron Microscopy

Transmission electron microscopy (TEM) was done on a Philips CM10 with tungsten filament operated at 80 kV. The nanoparticles were dispersed in acetone. A drop of the suspension was deposited on a carbon-coated copper grid, blotted with filter paper, and dried in air for 30 min before microscopy. Scanning electron microscopy (SEM) was done on a Hitachi S3400n operated at 20 kV. EDX spectra were obtained at 20 kV using an EDAX X-ray detector. Prior to measurements, all samples were sputter-coated with a 10 nm carbon layer.

4.2.8 Mechanical testing

After polymerization the samples were immersed in acetone to extract the IL, followed by soaking in water. Rheology was done on an Anton-Paar MCR301 with PP15 15 mm parallel plates. Storage and loss moduli were recorded during a frequency sweep from 100 to 0.01 Hz at 0.1 % strain.

4.3 Results

Functionalisation of the particles with the silanes is confirmed by IR spectroscopy (Figure 1A). Bands at 3650 - 2960 and 1643 cm^{-1} can be assigned to residual water. A- Fe_3O_4 particles show further bands at 1631 (C=C stretch), 1421 (CH_2 deformation), 1392 and 903 (deformations of $=\text{CH}_2$ but also SiOH) and 934 cm^{-1} (C-C stretch).[55] These signals can all be assigned to the allyltrimethoxysilane coating. M- Fe_3O_4 particles show bands at 1411 (CH_2 deformation), 1341 and 1300 (CH deformation), 1237 (CH_2 twist), a shoulder at 1117 (Si-O-Si asymmetric stretch), and a weak shoulder at 937 cm^{-1} that can be assigned to uncondensed Si-OH.[56] These bands arise from the mercaptopropyltrimethoxysilane coating. Moreover, the samples show strong bands at 1000, 1052 (Si-O-Si asymmetric stretch), 587 and 572 cm^{-1} (M- Fe_3O_4 and A- Fe_3O_4 symmetric Si-O-Si stretch, respectively. This signal overlaps with Fe-O symmetric stretch signals).[57] The presence of Si-O-Si bonds clearly shows that the silanes have condensed on the nanoparticle surface, leading to an organically modified silica shell on the iron oxide cores.

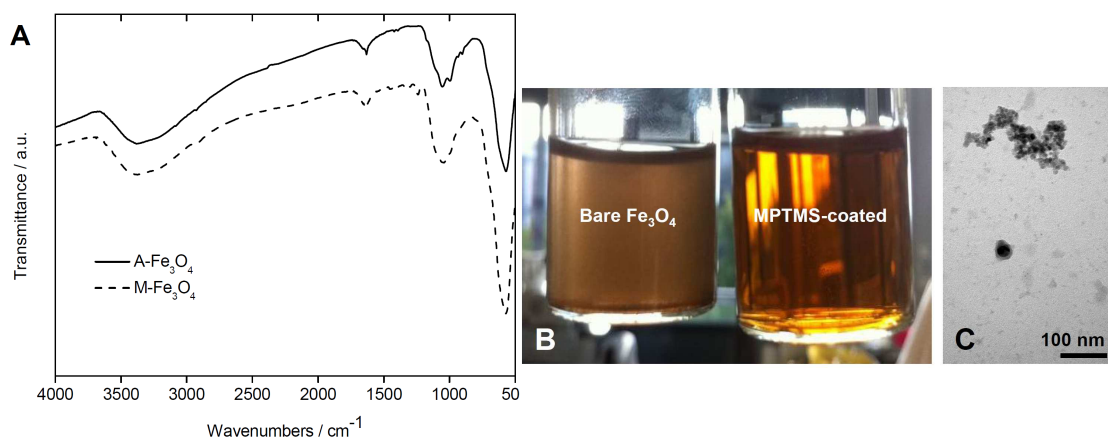


Figure 4-1. (A) IR spectra of functionalized nanoparticles, (B) photograph of nanoparticle dispersions in acetone (identical concentrations, see experimental for details), and (C) representative TEM image of MPTMS-coated nanoparticles (M- Fe_3O_4).

Table 4-1 and Figure 4-1A show further data of the iron oxide nanoparticles. Only with the functionalized nanoparticles, homogeneous and transparent dispersion can be obtained in acetone (Figure 4-1B). In spite of the transparency of the dispersions obtained with the functionalized particles, transmission electron microscopy (TEM, Figure 4-1C) shows that the coated particles are not present as individual nanoparticles but as polydisperse agglomerates with mean diameters between ca. 160 - 190 nm. This is further confirmed by dynamic light scattering (DLS), which finds hydrodynamic radii of 160 to 190 nm as well. In summary, DLS, TEM, and IR spectroscopy show that the particles, although not present as single particles, have been successfully modified with silane/organosilica coatings rendering them stable in acetone.

Table 4-1. DLS data of bare and functionalized nanoparticles in acetone.

Sample	0-Fe ₃ O ₄	M-Fe ₃ O ₄	A-Fe ₃ O ₄
Hydrodynamic radius / nm	--- ^{a)}	162	188
Polydispersity index (PDI)	--- ^{a)}	0.167	0.177

a) The samples based on 0-Fe₃O₄ could not be measured due to sedimentation and very high turbidity (Figure 4-1A). However, DLS measurements in water (instead of acetone) show a hydrodynamic radius of 46 nm and a PDI of 0.153, indicating that the samples are relatively uniform, but cannot easily be dispersed in acetone.

For preparation of the ionogels, the particles were dispersed in acetone (Figure 4-1A) and the IL was added (see experimental part for details). After acetone removal, the nanoparticle/IL dispersions are viscous brown to black, homogeneous, but non-transparent dispersions. The stability of the dispersions in the IL is difficult to assess due to high viscosity of the IL (slower sedimentation) and high particle concentrations. Phase separation was not observed during processing but the 0-Fe₃O₄/IL dispersion separates when placed on a magnet. Upon addition of the monomer/nanoparticle/IL mixture to the preheated mould, the mixture containing the A- and M-Fe₃O₄ nanoparticles thickens within 5 minutes. The final MIGs (A- and M-ionogel) are dark brown solids that can easily be removed from the mould. The ionogels made with bare nanoparticles (0-ionogel) are much softer and easily fold and wrinkle (Figure 4-2).

**Figure 4-2. MIGs after removal from the moulds. Diameter is 15 mm.**

The homogeneity and dark brown color of the ionogels clearly shows that all nanoparticle types are compatible with the hydrophobic IL and the polymer matrix. Scanning electron microscopy (SEM) however shows that the ionogels made with the coated particles are much more homogeneous than ionogels made from 0-Fe₃O₄, Figure 4-3. The ionogels based on the bare nanoparticles contain many aggregates as can be inferred from the large number of bright speckles in the SEM images, Figure 4-3A. In contrast, the ionogels based on the silane-coated nanoparticles show a rather smooth surface and exhibit much less particle aggregates or clusters, Figure 4-3B.

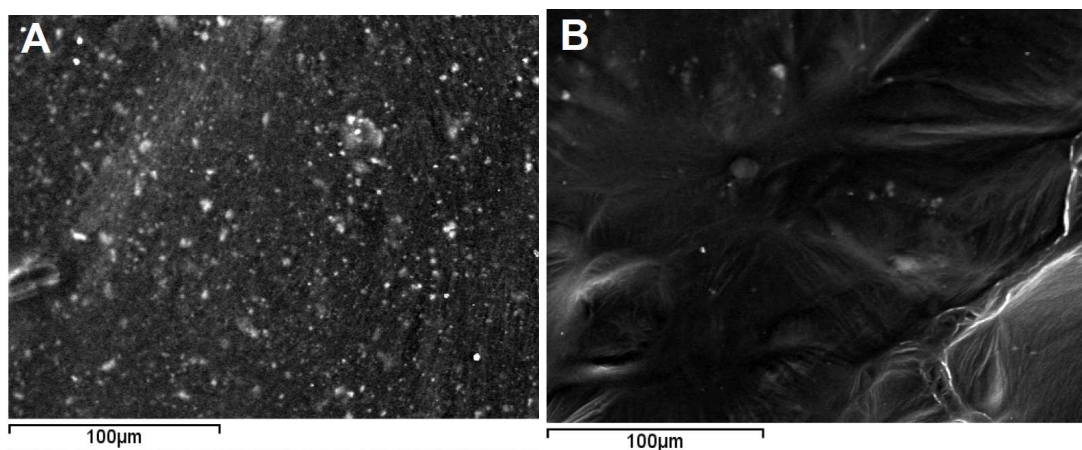


Figure 4-3. SEM images of (A) 0-ionogel and (B) A-ionogel surfaces. The light spots are backscattered electrons from inorganic (iron oxide) components.

Table 4-2. EDX analysis of ionogels (wt%).

Element	C	O	Si	P	Cl	S	Fe	Total
0-ionogel								
Mean	76.80 ± 9.20	13.59 ± 6.50	-	4.45 ± 0.90	0.13 ± 0.01	-	5.01 ± 4.10	100.0
A-ionogel								
Mean	75.57 ± 4.40	7.85 ± 2.90	0.24 ± 0.03	4.71 ± 0.06	0.13 ± 0.04	-	11.50 ± 1.50	100.0
M-ionogel								
Mean	70.64 ± 1.41	11.11 ±2.05	0.26 ± 0.01	4.48 ± 0.28	-	0.31 ± 0.01	13.13 ± 0.41	100.0

Table 4-3. Typical EDX Fe/P mass ratios vs. selected regions of the samples.

Location on sample	0-ionogel	A-ionogel	M-ionogel
1	0.28	2.83	3.00
2	0.97	2.36	2.82
3	3.44	2.14	3.00

SEM is further supported by energy dispersive X-ray spectroscopy (EDXS), which finds phosphorus and iron signals in the case of the 0-ionogels and additional silicon signals in the A- and M- ionogels. The homogeneity of the samples prepared with the silanised nanoparticles is further confirmed by EDXS spot or selected area analysis (Table 4-2). The 0-ionogels show large variations in the Fe/P ratios (that is, the concentration of the phosphonium IL and the iron oxide nanoparticles is locally very different, Table 4-3). This is not the case for the A- and M-

ionogels. Here we always observe very uniform Fe/P ratios indicating that the iron oxide nanoparticles or small aggregates are evenly distributed in the phosphonium IL.

Figure 4-4 shows that the ionogels strongly respond to external magnetic fields. For example, if an ionogel is immersed in water, it will float freely until a strong magnet comes close to it. Due to the flexibility of the ionogels, they can adapt to the geometric constraints such as limited space close to the magnet. In the current case the ionogels lie flat at the bottom of the vial until released by removing the magnet upon which they adopt their initial shape. This demonstrates that the material can be used as externally triggered soft actuator.

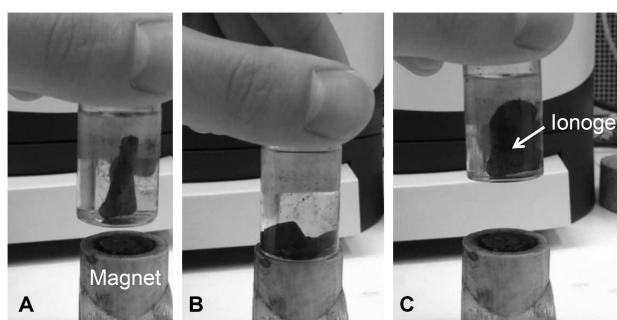


Figure 4-4. Behavior of the magnetic A-ionogel in a nonuniform magnetic field. (A) Ionogel far away from the magnet, (B) close to the magnet, and (C) after increasing the magnet-ionogel distance again.

To determine whether or not the surface modification of the nanoparticles has an influence on the stability of the ionogels (that is, on the nanoparticle/polymer hybrid matrix) we have removed the IL by a washing process in acetone and water. The acetone used for the washing process was clear in the case of the modified iron oxide nanoparticles. This indicates that the silane modification indeed leads to a covalent crosslinking with the pNIPAM chains. In contrast, samples prepared with 0-Fe₃O₄ show some coloration of the acetone used for washing, indicating a poor contact between the polymer and the nanoparticles.

This is consistent with the macroscopic appearance of the extracted polymer/nanoparticle matrices. The matrix of the 0-ionogel is weak and easily breaks and crumbles, again indicating a poor connection between the pNIPAM and the iron oxide nanoparticles. The A- and M-ionogels appear mechanically more robust. This is further confirmed by rheology on the same samples, Figure 4-5. Frequency sweeps show that the gels made with the silanised particles have a higher storage modulus across all measured frequencies. In the 0.1 – 10 Hz range these polymer/nanoparticle matrices are roughly 10 times stiffer than those based on the non-modified particles. This clearly indicates that the coating of the particles allows a more crosslinked polymeric network to be formed.

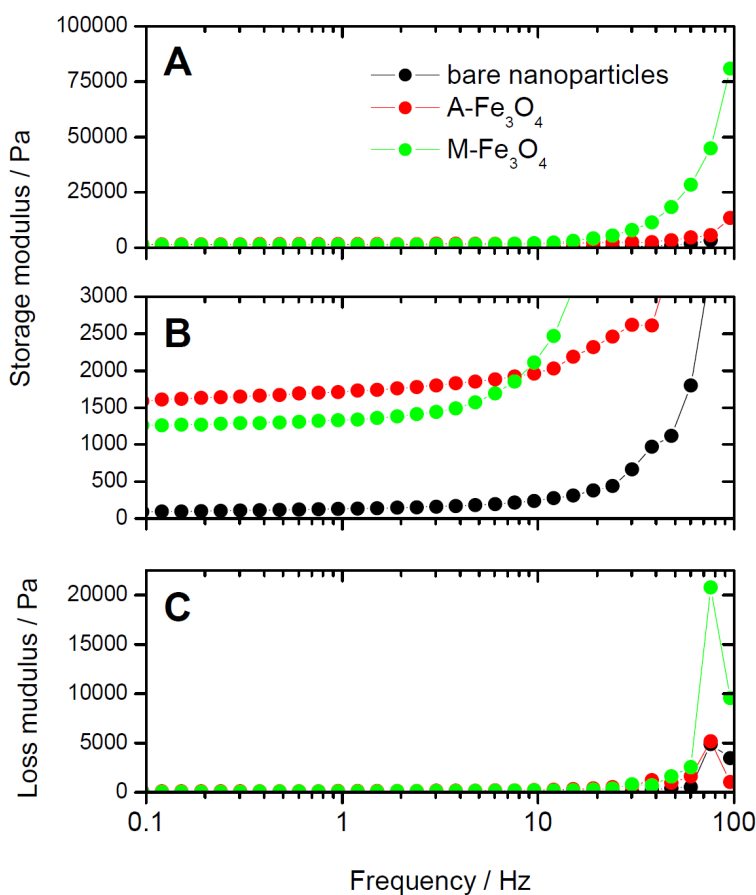


Figure 4-5. (A, B) Storage modulus-frequency sweeps and (C) loss modulus-frequency sweeps of MIGs after extraction of the IL. Panel (B) is a magnified view of panel (A) in the low storage modulus region.

4.4 Discussion

MIGs could, for reasons outlined in the introduction, be interesting materials for a wide range of applications. However, all examples in the literature so far[47, 48] exhibit a poor response to external magnets. This causes problems with their applicability. Mechanically robust ionogels with a large magnetic susceptibility and a correspondingly strong response to external magnetic fields are therefore needed.

The current study clearly shows that magnetite nanoparticles coated with a functional silane, (3-trimethoxysilyl)propylmethacrylate or 3-mercaptopropyl trimethoxysilane, are both efficient crosslinks and valuable magnetic components for the synthesis of robust MIGs, Figure 4-4 and Figure 4-5. A key parameter in the ionogel synthesis is the dispersion on the nanoparticles (or at least reasonably small nanoparticle aggregates, Figure 4-1 and Table 1) in a suitable solvent (here acetone) to yield a homogeneous reaction mixture to prepare the ionogels. Uncoated nanoparticles are difficult to process and already precipitate before ionogel synthesis (Figure 4-1A) yielding soft and heterogeneous ionogels (Figure 4-2 and Figure 4-3,

Table 4-2 and Table 4-3).

In contrast, the silane coatings are beneficial for the dispersion and immobilization of the nanoparticles both in the reaction mixture (IL, monomer, and nanoparticles) and the final ionogels. In spite of this, the particles are not present as single particles and, possibly, the ionogels could further be improved by using a more localized and softer silanisation process. TMAOH stabilizes the bare particles during the silanisation but it is a strong base which causes rapid condensation of the alkoxysilanes. Arguably, this is one of the reasons for the formation of the nanoparticle aggregates observed in TEM and DLS. A solution to this problem could involve a silanisation catalyst that is directly immobilized on the surface of each individual particle, similar to an approach Graf *et al.* where single silver nanoparticles have been coated by immobilizing a peptide on the nanoparticle surface which catalyzes alkoxysilane hydrolysis.[58] In the current case, this would lead to individually coated magnetic particles and an even more homogeneous distribution of the nanoparticles in the ionogel.

The main reason for the improved homogeneity and mechanical stability of the ionogels based on the modified nanoparticles is certainly that the nanoparticle surface is actively participating in the polymerization process. The bare 0-Fe₃O₄ nanoparticles have no possibility of forming covalent bonds with the growing polymer chain. Consistent with literature[49, 58] the silane coating of the A- and M-Fe₃O₄ enables a covalent bonding between the particles and the polymer leading to crosslinked networks (Scheme 4-1 and Scheme 4-2) with improved mechanical properties. The effective crosslinking of particles with the polymer network is evidenced by a 10 fold increase in the elastic modulus (Figure 4-5). The current approach is therefore suitable for the synthesis of MIGs and demonstrates that the choice of the nanoparticles, the reaction parameters such as solvents, and especially the surface coating of the magnetic nanoparticles are key parameters to control if a homogeneous and functional MIG is to be obtained.

4.5 Conclusions

Magnetite nanoparticles are suitable building blocks for a new class of responsive materials, magnetic ionogels (MIGs). MIGs are emerging materials for a wide range of applications and the materials and processes described here should therefore pave the way towards new multifunctional soft materials based on ionic liquids such as soft, magnetically triggered actuators. Of particular importance is the observation that the surface chemistry of the magnetic nanoparticles governs the macroscopic properties of the ionogels.

Acknowledgements. We thank Cytec Industries for donation of the IL. B.Z. and A.T. acknowledge funding from a DFG (German Research Council) Research Intensification grant (TA571/9-1). The authors also acknowledge funding from the EU Framework 7 project “ATWARM” (Marie Curie ITN, No. 238273)”. K.J.F acknowledges the European Commission for financial support through a Marie Curie Actions International Re-integration Grant (IRG, PIRG07-GA-2010-268365) and the Irish Research Council for Science, Engineering and Technology. R. B. and D. D. acknowledge funding from Science Foundation Ireland (SFI) under the CLARITY CSET award (Grant 07/CE/I1147). Further funding from the Max Planck Institute of Colloids and Interfaces, the University of Potsdam, and the DFG (TA571/3-1) is also acknowledged.

4.6 References

1. Messing, R.; Schmidt, A. M., Perspectives for the mechanical manipulation of hybrid hydrogels. *Polymer Chemistry* **2011**, *2*, 18-32.
2. Motornov, M.; Roiter, Y.; Tokarev, I.; Minko, S., Stimuli-responsive nanoparticles, nanogels and capsules for integrated multifunctional intelligent systems. *Progress in Polymer Science* **2010**, *35*, 174-211.
3. Pasparakis, G.; Vamvakaki, M., Multiresponsive polymers: nano-sized assemblies, stimuli-sensitive gels and smart surfaces. *Polymer Chemistry* **2011**, *2*, 1234-1248.
4. Suzuki, H., Stimulus-responsive Gels: Promising Materials for the Construction of Micro Actuators and Sensors. *Journal of Intelligent Material Systems and Structures* **2006**, *17*, 1091-1097.
5. Maeda, S.; Hara, Y.; Yoshida, R.; Hashimoto, S., Active Polymer Gel Actuators. *International Journal of Molecular Sciences* **2010**, *11*, 52-66.
6. Liu, F.; Urban, M. W., Recent advances and challenges in designing stimuli-responsive polymers. *Progress in Polymer Science* **2010**, *35*, 3-23.
7. Ahn, S.-k.; Kasi, R. M.; Kim, S.-C.; Sharma, N.; Zhou, Y., Stimuli-responsive polymer gels. *Soft Matter* **2008**, *4*, 1151-1157.
8. Imran, A. B.; Seki, T.; Takeoka, Y., Recent advances in hydrogels in terms of fast stimuli responsiveness and superior mechanical performance. *Polymer Journal* **2010**, *42*, 839-851.
9. Néouze, M.-A.; Bideau, J. L.; Gaveau, P.; Bellayer, S.; Vioux, A., Ionogels, New Materials Arising from the Confinement of Ionic Liquids within Silica-Derived Networks. *Chemistry of Materials* **2006**, *18*, 3931-3936.
10. Vioux, A.; Viau, L.; Volland, S.; Le Bideau, J., Use of ionic liquids in sol-gel; ionogels and applications. *Comptes Rendus de l'Academie des Sciences Serie IIc:Chemie* **2009**, *13*, 242-255.
11. Le Bideau, J.; Viau, L.; Vioux, A., Ionogels, ionic liquid based hybrid materials. *Chemical Society Reviews* **2011**.

12. Fraser, K. J.; MacFarlane, D. R., Phosphonium-Based Ionic Liquids: An Overview. *Australian Journal of Chemistry* **2009**, *62*, 309-321.
13. Welton, T., Room-Temperature Ionic Liquids. Solvents for Synthesis and Catalysis. *Chemical Reviews* **1999**, *99*, 2071-2084.
14. Rogers, R. D.; Seddon, K. R., *Ionic Liquids as Green Solvents: Progress and Prospects*. American Chemical Society: 2003; Vol. 125, p 15684.
15. Plechkova, N. V.; Seddon, K. R., Applications of ionic liquids in the chemical industry. *Chemical Society Reviews* **2008**, *37*, 123-150.
16. Adams, C. J.; Bradley, A. E.; Seddon, K. R., *Rapid Communication*: The Synthesis of Mesoporous Materials Using Novel Ionic Liquid Templates in Water. *Australian Journal of Chemistry* **2001**, *54*, 679-681.
17. Zhou, Y.; Schattka, J. H.; Antonietti, M., Room-Temperature Ionic Liquids as Template to Monolithic Mesoporous Silica with Wormlike Pores via a Sol–Gel Nanocasting Technique. *Nano Letters* **2004**, *4*, 477-481.
18. Neouze, M.-A.; Bideau, J. L.; Leroux, F.; Vioux, A., A route to heat resistant solid membranes with performances of liquid electrolytes. *Chemical Communications* **2005**, 1082-1084.
19. Li, D.; Shi, F.; Guo, S.; Deng, Y., One-pot synthesis of silica gel confined functional ionic liquids: effective catalysts for deoxygenation under mild conditions. *Tetrahedron Letters* **2004**, *45*, 265-268.
20. Lodge, T. P., A Unique Platform for Materials Design. *Science* **2008**, *321*, 50-51.
21. Susan, M. A. B. H.; Kaneko, T.; Noda, A.; Watanabe, M., Ion Gels Prepared by in Situ Radical Polymerization of Vinyl Monomers in an Ionic Liquid and Their Characterization as Polymer Electrolytes. *Journal of the American Chemical Society* **2005**, *127*, 4976-4983.
22. Rao, M.; Geng, X.; Liao, Y.; Hu, S.; Li, W., Preparation and performance of gel polymer electrolyte based on electrospun polymer membrane and ionic liquid for lithium ion battery. *Journal of Membrane Science* **2012**, *399–400*, 37-42.
23. Ueki, T.; Watanabe, M., Macromolecules in Ionic Liquids: Progress, Challenges, and Opportunities. *Macromolecules* **2008**, *41*, 3739-3749.
24. Pernak, J.; Goc, I.; Mirska, I., Anti-microbial activities of protic ionic liquids with lactate anion. *Green Chemistry* **2004**, *6*, 323-329.
25. Kavanagh, A.; Byrne, R.; Diamond, D.; Fraser, K. J., Stimuli Responsive Ionogels for Sensing Applications—An Overview. *Membranes* **2012**, *2*, 16-39.
26. Dai, S.; Ju, Y. H.; Gao, H. J.; Lin, J. S.; Pennycook, S. J.; Barnes, C. E., Preparation of silica aerogel using ionic liquids as solvents. *Chemical Communications* **2000**, 243-244.
27. Benito-Lopez, F.; Byrne, R.; Raduta, A. M.; Vrana, N. E.; McGuinness, G.; Diamond, D., Ionogel-based light-actuated valves for controlling liquid flow in micro-fluidic manifolds. *Lab on a Chip* **2010**, *10*, 195-201.
28. Alarcon, C. d. I. H.; Pennadam, S.; Alexander, C., Stimuli responsive polymers for biomedical applications. *Chemical Society Reviews* **2005**, *34*, 276-285.
29. Philippova, O. E.; Hourdet, D.; Audebert, R.; Khokhlov, A. R., pH-Responsive Gels of Hydrophobically Modified Poly(acrylic acid). *Macromolecules* **1997**, *30*, 8278-8285.
30. Beebe, D. J.; Moore, J. S.; Bauer, J. M.; Yu, Q.; Liu, R. H.; Devadoss, C.; Jo, B.-H., Functional hydrogel structures for autonomous flow control inside microfluidic channels. *Nature* **2000**, *404*, 588-590.

31. Techawanitchai, P.; Ebara, M.; Idota, N.; Asoh, T.-A.; Kikuchi, A.; Aoyagi, T., Photo-switchable control of pH-responsive actuators via pH jump reaction. *Soft Matter* **2012**, *8*.
32. Satoh, T.; Sumaru, K.; Takagi, T.; Kanamori, T., Fast-reversible light-driven hydrogels consisting of spirobenzopyran-functionalized poly(N-isopropylacrylamide). *Soft Matter* **2011**, *7*, 8030-8034.
33. O'Grady, M. L.; Kuo, P.-I.; Parker, K. K., Optimization of Electroactive Hydrogel Actuators. *ACS Applied Materials & Interfaces* **2009**, *2*, 343-346.
34. Satarkar, N. S.; Zhang, W.; Eitel, R. E.; Hilt, J. Z., Magnetic hydrogel nanocomposites as remote controlled microfluidic valves. *Lab on a Chip* **2009**, *9*, 1773-1779.
35. Fuhrer, R.; Athanassiou, E. K.; Luechinger, N. A.; Stark, W. J., Crosslinking Metal Nanoparticles into the Polymer Backbone of Hydrogels Enables Preparation of Soft, Magnetic Field-Driven Actuators with Muscle-Like Flexibility. *Small* **2009**, *5*, 383-388.
36. Ghosh, S.; Yang, C.; Cai, T.; Hu, Z. B.; Neogi, A., Oscillating magnetic field-actuated microvalves for micro- and nanofluidics. *Journal of Physics D-Applied Physics* **2009**, *42*.
37. Byrne, R.; Benito-Lopez, F.; Diamond, D., Materials science and the sensor revolution. *Materials Today* **2010**, *13*, 9-16.
38. Agarwal, A. K.; Dong, L.; Beebe, D. J.; Jiang, H., Autonomously-triggered microfluidic cooling using thermo-responsive hydrogels. *Lab on a Chip* **2007**, *7*, 310-315.
39. Fahrni, F.; Prins, M. W. J.; van Ijzendoorn, L. J., Micro-fluidic actuation using magnetic artificial cilia. *Lab on a Chip* **2009**, *9*, 3413-3421.
40. Hou, C.; Zhang, Q.; Wang, H.; Li, Y., Functionalization of PNIPAAm microgels using magnetic graphene and their application in microreactors as switch materials. *Journal of Materials Chemistry* **2011**, *21*, 10512-10517.
41. Ramírez-García, S.; Baeza, M.; O'Toole, M.; Wu, Y.; Lalor, J.; Wallace, G. G.; Diamond, D., Towards the development of a fully integrated polymeric microfluidic platform for environmental analysis. *Talanta* **2008**, *77*, 463-467.
42. le Digabel, J.; Biais, N.; Fresnais, J.; Berret, J.-F.; Hersen, P.; Ladoux, B., Magnetic micropillars as a tool to govern substrate deformations. *Lab on a Chip* **2011**, *11*, 2630-2636.
43. Khaderi, S. N.; Craus, C. B.; Hussong, J.; Schorr, N.; Belardi, J.; Westerweel, J.; Prucker, O.; Ruhe, J.; den Toonder, J. M. J.; Onck, P. R., Magnetically-actuated artificial cilia for microfluidic propulsion. *Lab on a Chip* **2011**.
44. Ganguly, R.; Puri, I. K., Microfluidic transport in magnetic MEMS and bioMEMS. *Wiley Interdisciplinary Reviews-Nanomedicine and Nanobiotechnology* **2010**, *2*, 382-399.
45. Hatch, A.; Kamholz, A. E.; Holman, G.; Yager, P.; Bohringer, K. F., A ferrofluidic magnetic micropump. *Journal of Microelectromechanical Systems* **2001**, *10*, 215-221.
46. Zrinyi, M., Chapter 11 Magnetic Polymeric Gels as Intelligent Artificial Muscles ntelligent Materials. In *The Royal Society of Chemistry*: 2007; pp 282-300.
47. Xie, Z.-L.; Jelacic, A.; Wang, F.-P.; Rabu, P.; Friedrich, A.; Beuermann, S.; Taubert, A., Transparent, flexible, and paramagnetic ionogels based on PMMA and the iron-based ionic liquid 1-butyl-3-methylimidazolium tetrachloroferrate(iii) [Bmim][FeCl₄]. *Journal of Materials Chemistry* **2010**, *20*, 9543-9549.
48. Dobbelin, M.; Jovanovski, V.; Llarena, I.; Claros Marfil, L. J.; Cabanero, G.; Rodriguez, J.; Mecerreyes, D., Synthesis of paramagnetic polymers using ionic liquid chemistry. *Polymer Chemistry* **2011**, *2*, 1275-1278.

49. Xia, H.; Wang, J. A.; Tian, Y.; Chen, Q. D.; Du, X. B.; Zhang, Y. L.; He, Y.; Sun, H. B., Ferrofluids for Fabrication of Remotely Controllable Micro-Nanomachines by Two-Photon Polymerization. *Advanced Materials* **2010**, *22*, 3204.
50. Caykara, T.; Yoruk, D.; Demirci, S., Preparation and Characterization of Poly(N-tert-butylacrylamide-co-acrylamide) Ferrogel. *Journal of Applied Polymer Science* **2009**, *112*, 800-804.
51. Krekhova, M.; Lang, T.; Richter, R.; Schmalz, H., Thermoreversible Hydroferrogels with Tunable Mechanical Properties Utilizing Block Copolymer Mesophases As Template. *Langmuir* **2010**, *26*, 19181-19190.
52. Wang, S.; Zhou, Y.; Guan, W.; Ding, B., One-step copolymerization modified magnetic nanoparticles via surface chain transfer free radical polymerization. *Applied Surface Science* **2008**, *254*, 5170-5174.
53. Fraser, K. J.; Izgorodina, E. I.; Forsyth, M.; Scott, J. L.; MacFarlane, D. R., Liquids intermediate between "molecular" and "ionic" liquids: Liquid Ion Pairs? *Chemical Communications* **2007**, 3817-3819.
54. Massart, R., Preparation of aqueous magnetic liquids in alkaline and acidic media. . *Ieee Transactions on Magnetism* **1981**, *17*, 1247-1248.
55. Li, Y.-S.; Vecchio, N. E.; Wang, Y.; McNutt, C., Vibrational spectra of metals treated with allyltrimethoxysilane sol-gel and self-assembled monolayer of allyltrimethoxysilane. *Spectrochimica Acta Part A: Molecular and Biomolecular Spectroscopy* **2007**, *67*, 598-603.
56. Thompson, W. R.; Cai, M.; Ho, M.; Pemberton, J. E., Hydrolysis and Condensation of Self-Assembled Monolayers of (3-Mercaptopropyl)trimethoxysilane on Ag and Au Surfaces. *Langmuir* **1997**, *13*, 2291-2302.
57. Kahani, S. A.; Jafari, M., A new method for preparation of magnetite from iron oxyhydroxide or iron oxide and ferrous salt in aqueous solution. *Journal of Magnetism and Magnetic Materials* **2009**, *321*, 1951-1954.
58. Graf, P.; Manton, A.; Haase, A.; Thünemann, A. F.; Mašić, A.; Meier, W.; Luch, A.; Taubert, A., Silicification of Peptide-Coated Silver Nanoparticles—A Biomimetic Soft Chemistry Approach toward Chiral Hybrid Core-Shell Materials. *ACS Nano* **2011**, *5*, 820-833.

Chapter 5:

Self-protonating spiropyran-*co*-NIPAM-*co*-acrylic acid hydrogel photoactuators

Bartosz Ziółkowski,^a Larisa Florea,^a Jannick Theobald,^a Fernando Benito-Lopez^b and Dermot Diamond*^a

a) CLARITY Centre for Sensor Web Technologies, National Centre for Sensor Research, Dublin City University, Dublin 9, Ireland

b) CIC microGUNE, Arrasate-Mondragón, Spain

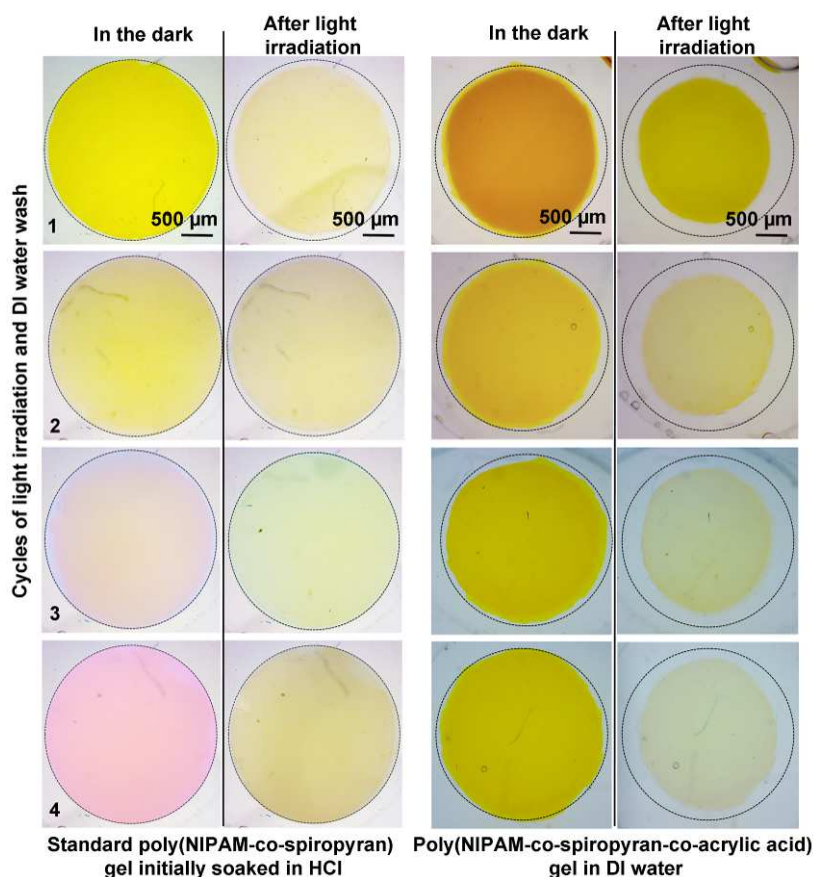
Published: Soft Matter **2013**, 9, 8754-8760.

DOI: 10.1039/C3SM51386F

Abstract

Up to now, photoresponsive hydrogels and ionogels based on poly(*N*-isopropylacrylamide) copolymerised with pendant spiropyran groups require exposure to external acidic solution (usually millimolar HCl) to generate the swollen gel prior to photo-triggered contraction. This serious functional limitation has been solved by copolymerising acrylic acid into the gel matrix, to provide an internal source of protons. Due to the relative pK_a values of acrylic acid and the spiropyran and merocyanine isomers, the protonation and deprotonation occurs internally within the gel and there is no need for an external source of protons. Furthermore, the shrinking-expansion cycles of these gels in deionised water are repeatable, as protonation throughout the gel does not rely on movement of protons from an external acidic solution into the bulk gel. In contrast to previous formulations, these gels do not show degradation of their photo-induced shrinking ability after multiple washings in deionised water and repeated switching over a 2 month period.

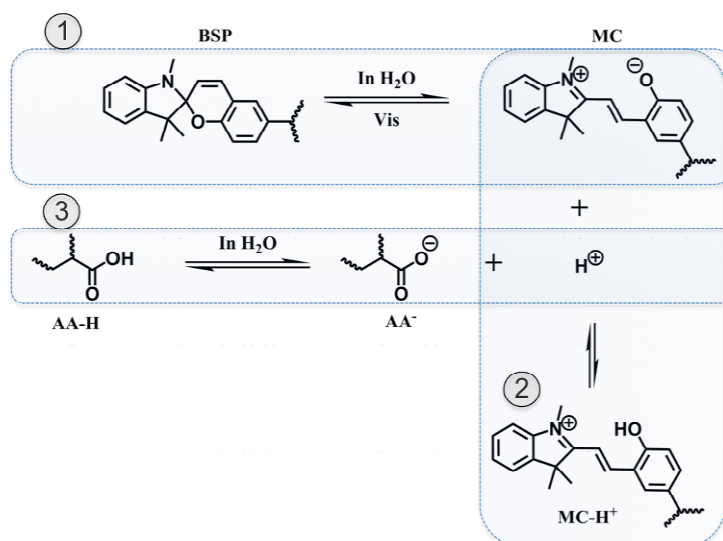
Keywords: Photoresponsive gel, spiropyran, polymer actuator, NIPAM, acrylic acid, hydrogel, spiropyran



5.1 Introduction

Stimulus responsive gels are receiving increasingly intensive attention due to the autonomous manner in which they respond to changes in their local environment.[1] Consequently, they are often referred to as “smart materials” because they can perform functions without the need for any human input. Examples include materials that respond to temperature,[2] pH,[3] light,[4] and magnetic[5] and electric[6] fields. In recent years, interest has been growing in the use of *N*-isopropylacrylamide (NIPAM) as a base material for producing photoresponsive gels.[7-11] In general, these gels consist of two stimulus responsive entities. First, is the poly(NIPAM) gel which shrinks when heated above the lower critical solution temperature (LCST).[2, 12, 13] Second is spiropyran (BSP, Scheme 5-1), a molecular photo-switch which, in a polar environment, spontaneously opens to the charged merocyanine isomer (MC, Scheme 5-1: step 1). This process can be reversed by illumination of the MC isomer with white light. The conversion of BSP to MC is reinforced in acidic media, through the formation of the protonated merocyanine (MC-H⁺, Scheme 5-1: step 2). Illumination of MC-H⁺ with visible light causes regeneration of the SP form, with consequent release of a proton[14, 15] (Scheme 5-1).

When a poly(NIPAM) gel incorporating spiropyran in the polymer backbone is exposed to millimolar aqueous HCl, the benzospiropyran (BSP) molecules spontaneously open to the positively charged protonated merocyanine (MC-H⁺), accompanied by a yellowing of the gel due to absorbance by MC-H⁺ in the visible spectrum centred between 400 - 500 nm.[15] When this gel is irradiated with white light, the same photoreversible process happens, with MC-H⁺ spontaneously switching back to the colourless BSP form, releasing a proton in the process.[4, 10] As a consequence the gel becomes more hydrophobic and shrinks through expulsion of water.[4]



Scheme 5-1. Photochromism and acidochromism of benzospiropyran derivatives

A potentially important application of this actuation behaviour is the generation of photoswitchable valves[4] and on-demand patterned channels for microfluidic systems[9]. In the case of valves, typically the acidified swollen gel containing MC-H⁺ blocks the channel until it is exposed to white light, whereupon shrinking of the gel is induced, and the channel opens.[4] For the generation of photo-patterned channels, a planar sheet of photoresponsive gel is placed under a microfluidic chip inlet/outlet system having no channels. Irradiation with light through a mask triggers shrinking only along the exposed lines resulting in formation of channels between pre-formed external fluid inlets and outlets.[9]

In these valve systems the shrinking times of the gels are usually relatively fast (from several seconds up to several minutes)[4, 7] However, the reswelling time and consequently valve closing time is much slower, up to several hours, which is not ideal for fast fluid handling and valve operations[4, 7]. Satoh *et al.* recently reported gels with improved actuation behaviour, through control of the spiropyran opening and closing kinetics.[10, 15] This was demonstrated by attaching different electron donating/withdrawing substituents to the spiropyran molecule and then copolymerising it with *N, N*-dimethylacrylamide. The resulting derivatives showed (in most cases) improved protonation rates compared to non-functionalised spiropyran.[15] The best performing modified spiropyran molecules were then incorporated into poly(NIPAM) gels and these showed different speeds of reversible gel shrinking.[10] The “fastest” gel was shown to fully contract within 10 min and re-swell back to ~95% of the original size within 10 min. However, when comparing results between groups, it should be noted that these gels were in the form of 300 µm diameter rods, as the dimensional scale of the entity obviously has a significant impact on the overall diffusion kinetics of water into and/out of the gel.

Improvements in the physical robustness of the photoswitchable gels were also reported by using ionogels in place of the original spiropyran/poly(NIPAM) hydrogels.[16] There are two advantages arising from this approach. Firstly, the tendency of conventional hydrogels to crack and flake when stored in air does not occur, due to the low vapour pressure of ionic liquids and their ability to plasticise the gel polymer structure.[17] Secondly, the spiropyran isomerisation kinetics (and consequently the ionogel actuation kinetics) can be strongly influenced by the ionic liquid used to form the ionogel. [16, 18]

Despite the enormous potential of these photoresponsive actuators, they have not as yet been broadly exploited in microfluidic devices due to significant performance limitations arising from:

1. The need to expose the gel to a strongly acidic solution (typically pH 3 HCl) in order to generate the photoresponsive MC-H⁺ species

2. The rather slow recovery of contracted gels to the swollen form after use (can take many minutes or even hours).

Together, these constraints have a significant negative impact on the range of practical applications of these actuators, essentially limiting their use to “single shot” disposable microfluidics, and to chemistries that will not be affected by the release of protons into the external solution during shrinkage of the gel. In this work, we address these issues by incorporating acrylic acid (AA) co-monomer into the structure of the poly(NIPAM)-*co*-spiropyran hydrogels, to act as an internalised proton donor/acceptor. We report the light induced shrinking behaviour of the gels for different amounts and ratios of AA to BSP in poly(NIPAM) and suggest gel composition range within which these actuation characteristics are optimal.

5.2 Experimental

5.2.1 Materials

N-isopropylacrylamide 98% (NIPAM), Acrylic Acid 99% (AA) (180-200 ppm MEHQ as inhibitor), *N,N'*-methylenebisacrylamide 99% (MBIS), Phenylbis(2,4,6-trimethylbenzoyl) phosphine oxide 97% (PBPO) were obtained from Sigma Aldrich, Ireland and used as received. Trimethyl-6-hydroxyspiro-(2H-1-benzopyran-2,2'-indoline) 99% was obtained from Acros Organics and acrylated as described in the Appendix B.

5.2.2 Gel preparation

For the hydrogel synthesis, typically 200 mg (1 mol equivalent) of NIPAM was mixed with 3 mol % equivalent of MBIS and the given amount of AA and spiropyran acrylate (BSP). These compounds were then dissolved in 500 μ L of 1,4-dioxane/water mixture (4:1 vol:vol). To this mixture 1 mol % equiv. of the photo-initiator (PBPO) was added. This mixture was poured onto a PDMS mould containing circular pits with various sizes, covered with a glass microscope slide and polymerised for 30 min under white light. The white light source used was a Dolan-Jenner-Industries Fiber-Lite LMI LED lamp with an intensity of 780 lumens projected through

two gooseneck waveguides placed at a distance of 10 cm from the mould. The polymerised gels were allowed to swell in deionised water that was changed twice with 4 h intervals between each change. After 24 h the swollen and equilibrated gels were cut into 3 mm discs using a manual puncher. All measurements were performed on gels produced according to this protocol.

White light induced polymerisation of the spiropyran-modified polymer using PBPO initiator is the preferred approach rather than the more usual UV-photopolymerisation. This is because white light irradiation ensures the BSP is present predominantly in the colourless spiropyran form, minimising any co-absorbance of the incident light by the merocyanine isomer. Experiments conducted in our laboratory with other spiropyran acrylates (particularly the commonly used -NO₂ derivative[11]) show that under UV irradiation, BSP converts to MC, which absorbs strongly in the visible region and inhibits the polymerisation process.

5.2.3 Gel shrinking measurements

To quantify the degree of shrinking, we estimate the percent decrease in the diameter of a 3 mm gel disc relative to the greatest possible degree of shrinkage, which is defined as the difference in diameter of a gel disc in its most swollen state (d_{\max}) and the diameter of the same gel disc in its most contracted (dried) state (d_{\min}), according to expression (5.1), below;

$$D\% = \left[1 - \left[\frac{(d_{\max} - d_x)}{(d_{\max} - d_{\min})} \right] \right] \times 100\% \quad (5.1)$$

where $D\%$ is the relative percent swelling of the disc diameter, d_x = measured diameter; d_{\max} = diameter of the fully swollen gel; d_{\min} = diameter of the fully contracted gel (dried at room temperature for 3 days). The dried gels had diameters between 64-67 % of the fully swollen gel. Therefore, the relative percent of swelling that is used expresses dimension changes taking place between fully swollen gel (d_{\max} = 100 % relative swelling) and the maximally shrunken, dried state (d_{\min} = 0 % relative swelling). Therefore from here onwards, unless stated otherwise, % swelling/shrinking refers to the relative % as defined above. Further details are given in the Appendix B, Figure B1.

For white light stimulated shrinking measurements, the 3mm hydrogel discs were placed in a 5 mm wide and 2mm deep PDMS circular recess filled with water and covered with a second PDMS 2 mm thick slide. The imaging was performed using an Aigo GE-5 microscope with a 60x objective lens and the accompanying software. The light was provided by a Dolan-Jenner-

Industrie Fiber-Lite LMI at maximum power (780 lumens) through two waveguide goosenecks fixed at a distance of 10 cm from the samples.

5.2.4 UV-Vis Spectroscopy

UV-Vis spectroscopy was used to study the absorbance behaviour of the spiropyran hydrogels under different illumination conditions. The absorbance spectra were recorded in reflectance mode using a fibre-optic light guide connected to a Miniature Fiber Optic Spectrometer (USB4000 – Ocean Optics Inc.) and a specially designed probe holder (see Appendix B Figure B2 for the setup details). The light source was a LS-1 tungsten halogen lamp (white light) obtained from Ocean Optics Inc. Data from the spectrometer was processed using Spectrasuite software provided by Ocean Optics Inc. For clarity, the absorbance spectra were smoothed using Origin software with a Savitzky–Golay algorithm on a total of 3648 data points per spectrum, and an averaging window of 50 data points.

5.3 Results and discussion

Table 5-1. Composition and molar ratios of reactants used to produce photoresponsive poly(NIPAM) gels.

Gel code	AA [mol %]	BSP- acrylate [mol%]	Cross- linker [mol %]	Initiator [mol%]	NIPAM [mmol]	Solvent [μ L]
0-0	0	0	3	1	1.77	500
0-1	0	1	3	1	1.77	500
1-1	1	1	3	1	1.77	500
2-1	2	1	3	1	1.77	500
2-2	2	2	3	1	1.77	500
5-1	5	1	3	1	1.77	500
5-2	5	2	3	1	1.77	500
5-3	5	3	3	1	1.77	500

Table 5-1 shows the compositions of the hydrogels tested. The AA content was varied along with that of BSP-acrylate to determine the ratio that provides optimal actuation behaviour, in terms of extent and rate of photo-induced shrinking. The gels have been named according to the

convention “gel[amount of AA mol%]-[amount of BSP-A mol%]” eg. gel 2-1 has 2 mol% AA and 1 mol% BSP-acrylate, all relative to NIPAM.

The initial experiments on light induced shrinking were performed using the 0-1 gels (Table 5-1), which did not contain AA. These gels, when placed in DI water and in darkness, swell naturally and turn red (Figure 5-1a) upon swelling indicating spontaneous conversion of BSP to the unprotonated MC form (Scheme 5-1, step 1), confirmed by the absorbance band centred around 560 nm.

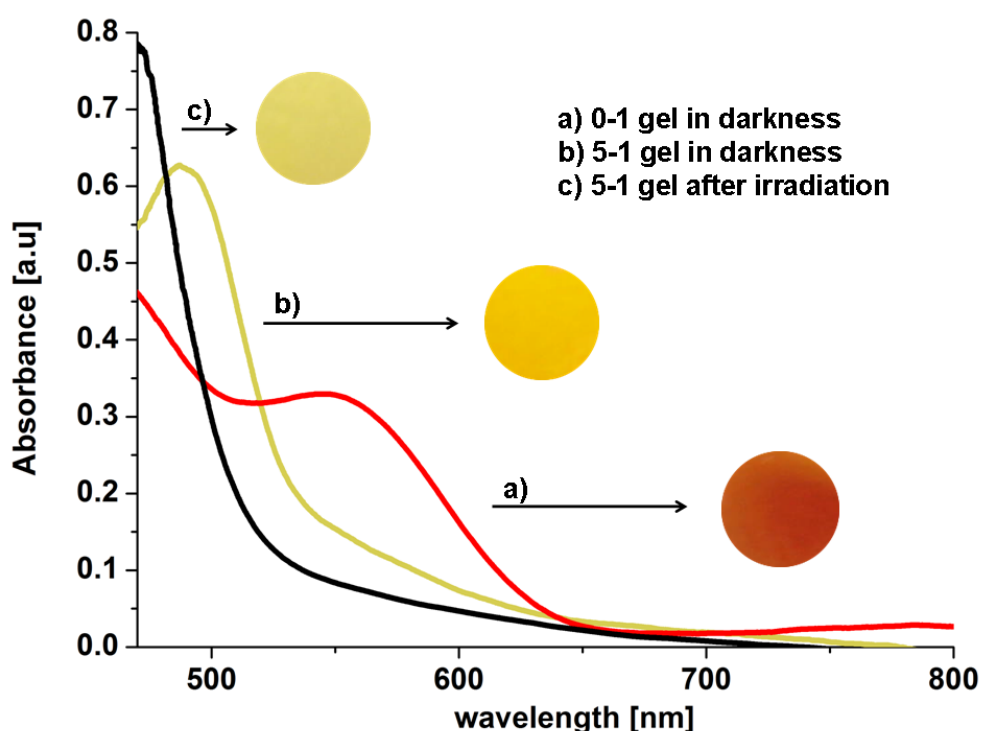


Figure 5-1. UV-Vis spectra and associated colours of 1% BSP-A gels. a) 0% AA, 1% BSP gel in DI water in darkness, b) 5% AA, 1% BSP gel in DI water in darkness, c) 5% AA, 1% BSP gel in water after irradiation with white light for 20 min.

When acrylic acid is incorporated into the gel (eg. gel 5-1) the samples also swell in darkness in deionised water, but adopt a yellow colouration after several minutes (Figure 5-1b) due to an absorbance band centred around 480 nm, which is characteristic for the protonated MC-H⁺ form of the spiropyran. All these gels, when in the MC or MC-H⁺ form, become decolourised under white light due to isomerisation back to the BSP form, as confirmed by the disappearance of bands at 560 and 480 nm, respectively. Figure 5-1 shows this happening for gel 5-1, which spontaneously adopts the MC-H⁺ form in the absence of light (Figure 5-1b), and reverts to the BSP form when irradiated with white light (Figure 5-1c).

Interestingly, under white light the MC isomer present in gel 0-1 reverts to the initial BSP form, but minimal shrinking is induced, similar to the blank poly(NIPAM) discs that do not contain any BSP (Figure 5-2). However, samples from the same batch (gel 0-1) pre-soaked in 1mM HCl exhibit a yellow colour characteristic of the protonated MC form (MC-H^+), and shrink considerably (down to 80 % relative swelling) under white light as previously reported for such systems.[4, 10, 16] This suggests that the shrinking of these gels is induced more by the combined deprotonation of MC-H^+ and conversion to BSP, rather than the conversion of MC to BSP on its own (i.e. deprotonation of MC-H^+ is inherent to the shrinking mechanism).

A small but discernable shrinkage of the poly(NIPAM) blank gel under white light irradiation (Gel 0-0, Figure 5-2 and Figure 5-4) occurs because the light source used to actuate the gels, although a 'cold' LED source, induces a small degree of heating of the gel and surrounding water due to absorption of incandescent radiation. In fact, the temperature rose from the initial 18°C to 22°C during the 20 min period of measurement. Therefore, because poly(NIPAM) gels are thermoresponsive and have been shown to shrink slightly even at temperatures several degrees below the actual LCST[12, 13, 19] a slight temperature induced shrinkage in the blank poly(NIPAM) gels occurs.

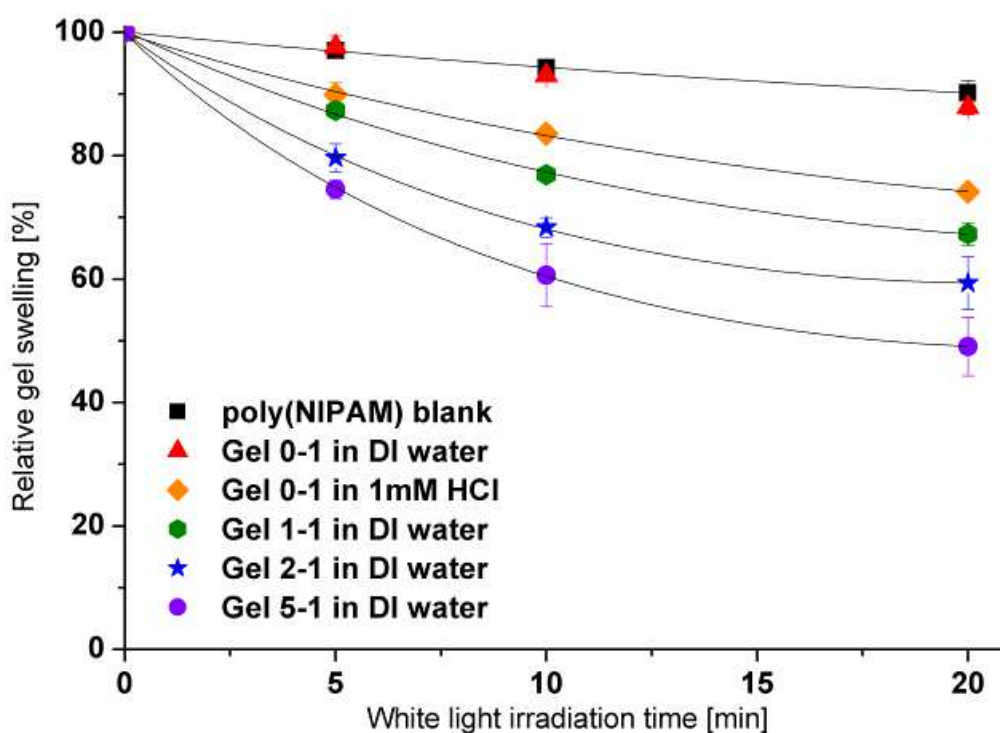


Figure 5-2. Shrinking of gels containing 1% spiropyran and varying amounts of acrylic acid. Error bars are standard deviations, note that in some cases they are obscured by the marker. (n=6)

5.3.1 Influence of AA content on gels with 1 % BSP

Figure 5-2 shows the results of photoinduced shrinking experiments performed on gels containing 1% BSP and 0 to 5% AA. The first observation is that the gels incorporating AA function remarkably well without the need for prior soaking in HCl. When placed in DI water and in darkness, a yellow colouration of the AA-modified gels can be observed after 5-10 minutes, indicating spontaneous formation of MC-H⁺ and, by implication, an equivalent number of deprotonated -COO⁻ groups. A schematic of this equilibrium within the gel is shown in Figure 5-3. Moreover, the shrinking of the 1-1 gel is both faster and greater in extent than for the equivalent non-AA modified 0-1 gel pre-equilibrated in HCl (30% versus 20%, respectively, Figure 5-2). Gel 5-1 shrinks most, reaching 50% relative swelling after 20 min of irradiation with white light.

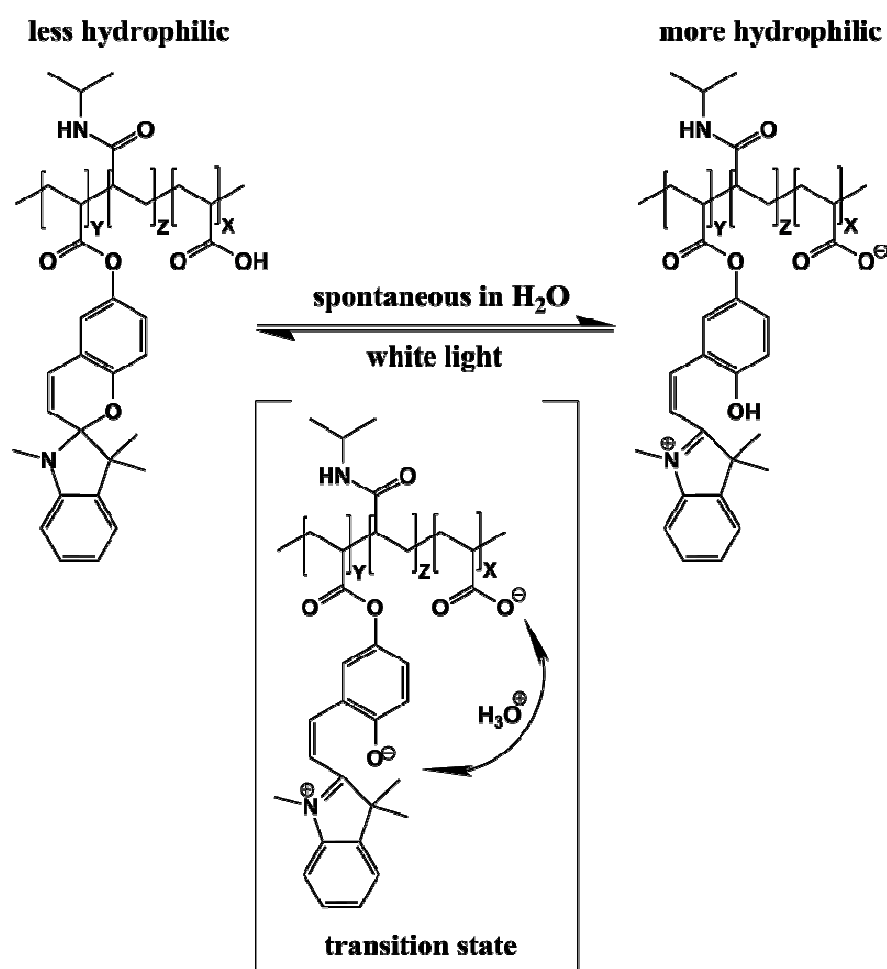


Figure 5-3. Schematic representation of the proton exchange taking place in the gels between the acrylic acid and the spiropyran together with the effect of light irradiation; Y:Z:X refer to the mol% of BSP, poly(NIPAM), and acrylic acid in the formulation (see Table 5-1).

Poly(acrylic acid) polymers are themselves pH responsive, and gels made from this polymer have been shown to swell when the acid is deprotonated to the acrylate anion, and shrink when reprotonated to the uncharged form.[20] During the light-induced deprotonation of the MC-H⁺

protons are liberated (sometimes referred to as a pH jump reaction).[14] and these re-protonate the acrylic acid groups and increase the extent of shrinkage (Figure 5-2). These results show that the incorporation of AA into these gels simplifies the actuator operation by removing the need to use an external HCl bathing solution to prime the gel prior to photo-induced shrinking.

5.3.2 Influence of BSP content on gels

Intuitively it might be assumed that increasing the BSP-acrylate content in the gel formulation will increase the rate and extent of the photo-induced actuation effect. However, the results in Figure 5-4 suggest that there is an optimum BSP content of ca. 1-2 mol % (gels 5-1 and 5-2) which in both cases produces ~50 % relative shrinking. However, increasing the BSP content in the polymer to 3 % (gel 5-3) reduces the relative shrinking extent to ~20 %.

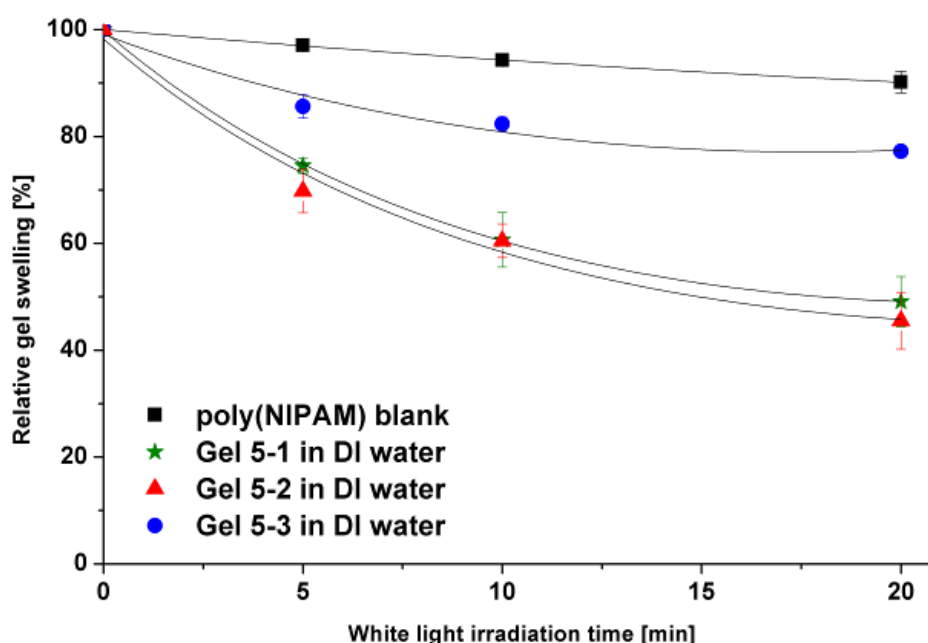


Figure 5-4. Shrinking of gels containing varying amounts of spiropyran. Best fit (black) are for eye guidance. Error bars are standard deviations, note that in some cases they are obscured by the marker. (n=6)

Another optimisation aspect of these gels is the reswelling rates. When the gels (Table 5-1) had adopted their steady-state contracted form under white light irradiation, they, were kept for 1 hour in the dark and their diameters measured again. The resulting data (Table 5-2) shows that all gels with 1% BSP ie. 1-1, 2-1, 5-1 shrink more with increasing amount of AA and reswell to ~100% after one hour storage in darkness.

Table 5-2. Swelling values [relative %] and standard deviations (s) for gels in Table 5-1 after 20 min under white light and after 1h in the dark (n=4)

Gel	20 min (Vis. light)	60 min (in darkness)
0-0	87.85 ± 1.18%	97.44 ± 1.60%
1-1	67.33 ± 1.85%	100.45 ± 0.64%
2-1	59.37 ± 4.26%	96.48 ± 1.34%
5-1	49.10 ± 4.73%	97.35 ± 1.93%
2-2	61.31 ± 5.20%	83.69 ± 1.27%
5-2	45.50 ± 5.33%	82.69 ± 3.33%
5-3	77.22 ± 1.12%	76.44 ± 1.46%

When the BSP content is increased to 2 mol% the extent of shrinkage also increases with increasing amount of AA (gels 2-2 and 5-2). However, these formulations do not re-swelling fully within the one-hour period, reaching only ~83% relative swelling. For formulation 5-3, the extent of shrinkage is reduced relative to gel 5-2, and it re-swells only to ~76 % within one hour. This suggests that there is an optimum concentration of BSP in the polymer for both light-induced shrinking and the re-swelling kinetics. This can be explained by the fact that BSP, regardless of the isomerisation state, is a rather hydrophobic molecule, and at higher concentrations in the gel, it reduces the overall hydrophilicity, making it a less attractive environment for water uptake, and hence the actuation effect is impaired.

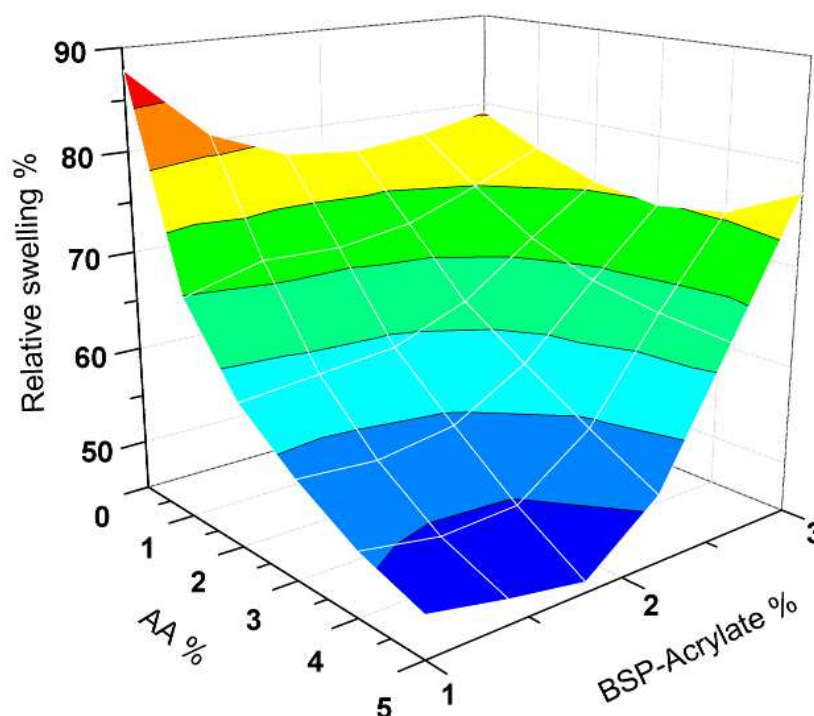


Figure 5-5. Extent of relative swelling upon white light irradiation for 20 min as a function of gel composition. AA% – acrylic acid content; BSP-Acrylate% – spiropyran content; both expressed as molar % relative to NIPAM.

The extent of photo-induced shrinking of the gels versus their composition can be seen in Figure 5-5. This shows that the shrinking extent is maximised for gels with AA % \geq ca.3 %, and for BSP-acrylate % in the range 1-2% (all mol% relative to NIPAM). In order to ensure maximum protonation of the MC isomer, a molar excess of AA will be required. From Figure 5-5, the maximum actuation effect coincides with the blue plateau region, and this in turn depends on the population of protons migrating between the MC and AA sites (Figure 5-3).

Assuming 100 % conversion of monomers during polymerisation of the gels, and given the pK_a of AA[21] to be 4.2, the local pH within the gels will be ca. 2.8 for gel 1-1, and ca. 2.5 for gel 5-1. Therefore, it is reasonable to expect the local pH of gels containing 1 - 5 % AA to be ca. pH 3, which coincides with the acidic conditions reported previously to swell non-AA containing gels.[4, 7, 9, 10, 16] Therefore, in order to provide effective photoactuation without affecting the overall gel hydrophilicity unduly, and to ensure there is a reasonable molar excess of AA over BSP groups, we selected 1 % BSP-acrylate and 5%AA (Gel 5-1) for further study.

5.3.3 Gel photoactuation stability studies

A critical property of these gel photo-actuators is their stability over a series of actuation cycles. In DI water, Gel 5-1 contracted to about 75% relative swelling within 5 min of white light irradiation and subsequently re-swelled back to around 90% within 20 min in darkness. This process was repeated 4 times using the same sample and was found to be reproducible over a series of actuation cycles (Figure 5-6).

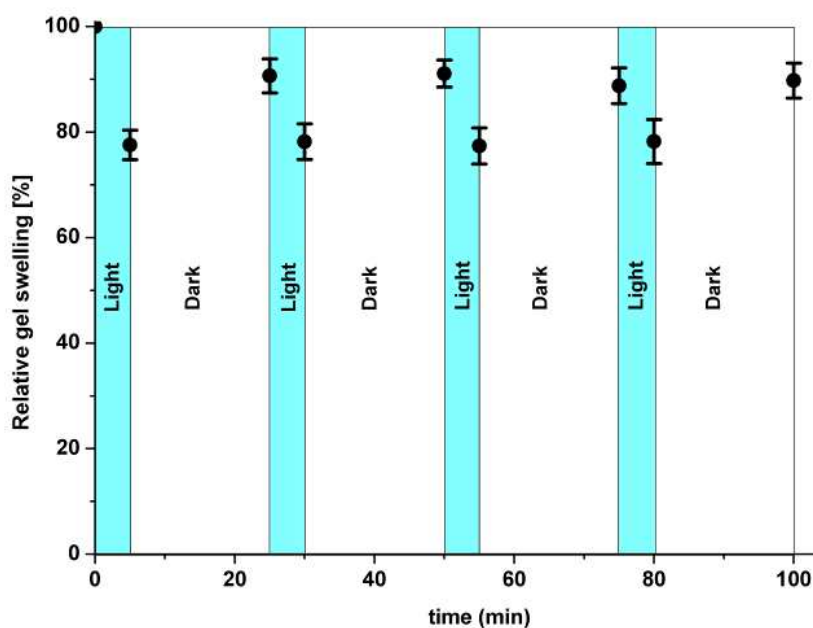


Figure 5-6. Alternating light (5 min) and dark (20 min) cycles for the 5-1 gel. in DI water (n=3)

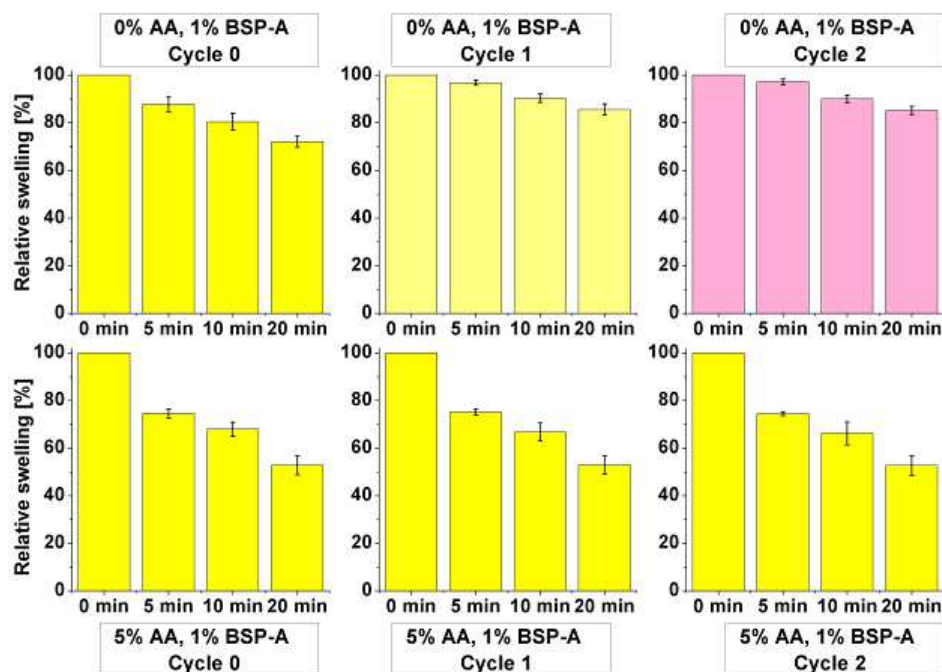


Figure 5-7. Light induced shrinking of 0-1 (top) and 5-1 (bottom) gels after 2 repeat cycles of drying and reswelling in DI water. Gel 0-1 was initially protonated by pre-soaking in 1mM HCl for 2 h, whereas Gel 5-1 was pre-soaked in DI water. The X-axis indicates minutes under white light irradiation. Error bars are standard deviations for 3 samples.

The photoresponsiveness and the self-protonating stability were also tested versus drying cycles. Three fully swollen gel 5-1 samples were contracted under white light, dried for 48 hours at room temperature, re-swelled in DI water, and their photo-induced shrinking measured again. This drying/reswelling cycle was then repeated twice and impressive reproducibility of the photo-shrinking behaviour was evident (Figure 5-7). In contrast, gel 0-1, after initially swelling in 1mM HCl, showed drastically impaired actuation behaviour after one drying/reswelling cycle in DI water, and had effectively lost its photo-actuation ability after the second cycle (Figure 5-7). This result confirms that, in contrast to the standard gels, the AA-modified gels do not need to be exposed to HCl to induce reswelling after photo-induced contraction, and can be repeatedly recycled through contraction/expansion in DI water.

The effect of washing with water on the gel actuation behaviour was also examined. The Gel 5-1 samples were fully swollen in DI water, shrunk with white light and then kept in fresh DI water for 24 hours in the dark. Then the light induced shrinking was measured again, and the procedure repeated 4 times. Similar measurements were performed on the Gel 0-1 samples which were initially pre-soaked in 1 mM HCl to induce MC protonation. The photos in Figure 5-8 show that Gel 5-1 can undergo light induced shrinkage even after re-swelling 3 times in fresh DI water (i.e. no exposure to HCl). In contrast, Gel 0-1 loses its photoresponsive character after two washes. Simultaneously, Gel 0-1 adopts an increasingly reddish colour (left column, Figure 5-8A), indicative of a tendency to preferentially form the unprotonated MC isomer rather

than MC-H^+ , due to the loss of protons from the gel during washing. The behaviour of Gel 5-1 is strikingly different, as it retains the yellow colour of the protonated MC-H^+ form in the swollen state (left column, Figure 5-8B). After 4 wash cycles, the pH of the external bathing water of equilibrated gels was 5.8 for both 5-1 and 0-1 gels, which was equivalent to the pH of the fresh DI water. This, coupled with the theoretical pH values within the gel discussed earlier, suggests that AA modification of the gels creates a pH buffering effect within the gel.

5.3.4 Mechanism of gel protonation/deprotonation

The MC-H^+ copolymer used in this study has been reported to have a pK_a value in the range of 6 – 7[22]. On the other hand, closed form of a BSP molecule has been reported to have pK_a of 2.3.[23]. Considering these values with respect to acrylic acid, ($\text{pK}_a = 4.2$), when these functionalities are co-immobilised within a gel, in the absence of light, acrylic acid will spontaneously protonate MC to MC-H^+ (Scheme 5-1, steps 2 and 3), driving the conversion of BSP to MC in the process (step 1). Hence, the gel will become populated with equal numbers of MC-H^+ and -COO^- ions, considerably increasing the gel hydrophilicity in the process, and triggering gel swelling due to water ingress. Conversely, when MC-H^+ is converted to the BSP (very weak base) form under white light, the protons released migrate back to the acrylate anions in the polymer, as they are now the strongest base present (Scheme 5-1 step 3). Protonation of the acrylate -COO^- anions and simultaneous formation of uncharged BSP induces a much more hydrophobic gel character, and water is expelled. Therefore, during swelling and contraction cycles, protons migrate between these sites, as shown in Figure 5-3. Furthermore, this proton exchange is internalised within the gel, with no requirement for an external proton source (i.e. pH 3 HCl bathing solution). In addition, the shorter (internalised) diffusional pathways for bulk proton transfer within the AA-modified gels produces a more efficient system in terms of the overall actuation behaviour, rather than depending on proton transfer from an external acidified bathing solution. Finally, the operational pH range of the gel actuation effect is dramatically extended.

In the AA-modified polymers, the protons preferentially reside on the MC groups when they are present (in the dark) and preferentially on the -COO^- groups in the absence of MC (i.e. when MC is converted to BSP under white light irradiation), as proposed in Figure 5-3. As long as there is no stronger base competing for the free protons, the charge neutrality rule ensures the population of protons in the gel is essentially conserved. However, this does mean that the mechanism will breakdown at $\text{pH} > \text{ca. } 7.0$, due to the increasing presence of competing OH^- ions.

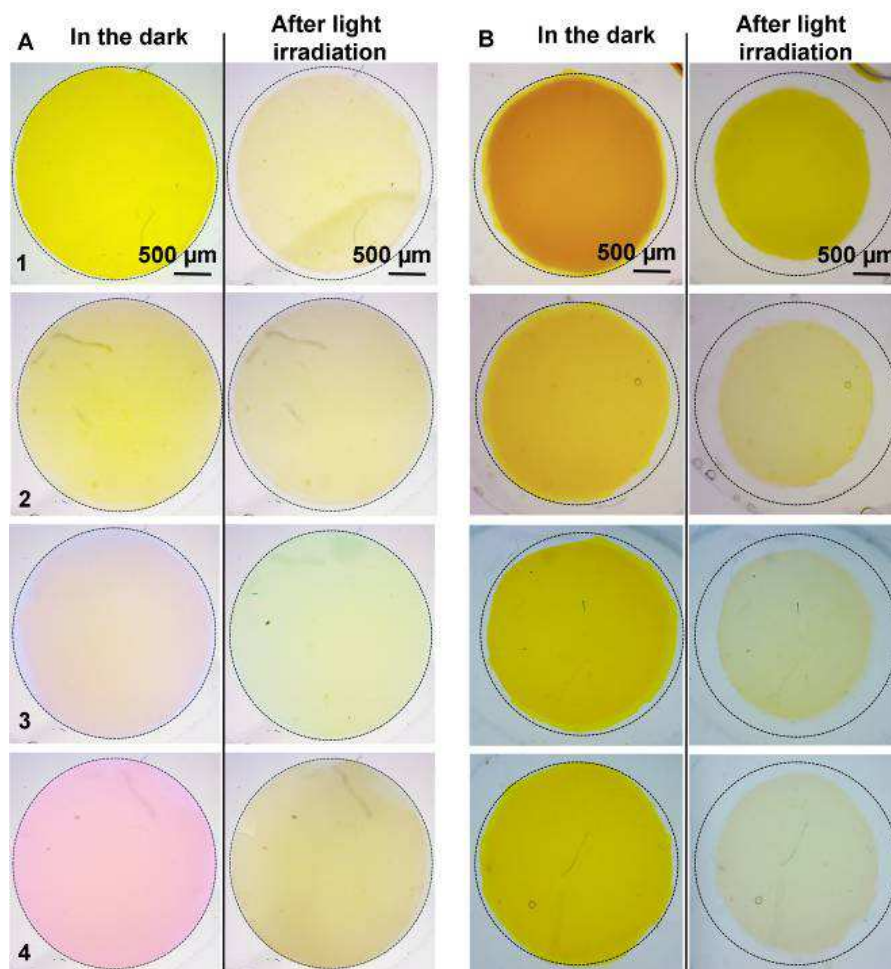


Figure 5-8. Light induced shrinking and re-swelling (in the dark) cycles for A: Gel 0-1 0% AA, 1% BSP-A (left) and B: Gel 5-1 5% AA, 1% BSP-A (right). For each re-swelling cycle fresh DI water was used in all cases. Cycles are numbered 1-4.

During this study some of the samples were kept in 20 ml vials filled with DI water for over 2 months. Even though the water was changed 5 times during this time, the randomly selected 5-1 and 2-2 gel samples were found to retain their photo-induced shrinking ability. For example: the extent of shrinking for gel 5-1 decreased by only 2 % absolute shrinking (20 % initially vs. 18% after 2 months). This demonstrates that these formulations are much more stable compared to the standard NIPAM-*co*-BSP-A gels. These improvements will greatly broaden the potential scope for applications of these materials as, up to now, they have required repeated exposure to acidic conditions (at least pH 3) to induce re-swelling and the photoactuation property. For example, the ability to repeatedly photoactuate these AA-modified gels in DI water up to about pH7 will open up multiple applications in the clinical and environmental areas, and should dramatically simplify the design of microfluidic systems incorporating these actuators for control of liquid movement.[24]

5.4 Conclusions

Copolymerising acrylic acid into the pNIPAM gels along with acrylated spiropyran provides an effective way to mediate the proton exchange that underpins the swelling/contraction mechanism of these gel actuators. In the dark, the gels spontaneously swell due to water ingress accompanying the formation of protonated MC-H⁺ by proton transfer from AA groups to MC. The rate and extent of photo-induced shrinking is enhanced compared to known spiropyran modified gels that do not contain AA groups, and have to be primed by exposing to pH 3 HCl to induce swelling. Furthermore, these new gels exhibit reproducible light-induced shrinking even after several drying/reswelling/washing cycles, and two months storage in DI water. This level of robustness has not been achieved for such gel actuators before, and should dramatically broaden their applicability, for example in areas like photo-controlled valving in microfluidics.

Acknowledgements

This work was performed as part of the EU Framework 7 project “ATWARM” (Marie Curie ITN, No. 238273)”. Support under Science Foundation Ireland under the CLARITY initiative, grant 07/CE/I1147 is also kindly acknowledged.

Notes

Supplementary Information (Appendix B) available: BSP-A synthesis, relative swelling calculation example and UV-Vis spectrometry setup.

5.5 References

1. Byrne, R.; Benito-Lopez, F.; Diamond, D., Materials science and the sensor revolution. *Materials Today* **2010**, *13*, 9-16.
2. Schild, H. G., Poly (n-isopropylacrylamide) - experiment, theory and application. . *Progress in Polymer Science* **1992**, *17*, 163-249.
3. Beebe, D. J.; Moore, J. S.; Bauer, J. M.; Yu, Q.; Liu, R. H.; Devadoss, C.; Jo, B.-H., Functional hydrogel structures for autonomous flow control inside microfluidic channels. *Nature* **2000**, *404*, 588-590.

4. Sugiura, S.; Sumaru, K.; Ohi, K.; Hiroki, K.; Takagi, T.; Kanamori, T., Photoresponsive polymer gel microvalves controlled by local light irradiation. *Sensors and Actuators A: Physical* **2007**, *140*, 176-184.
5. Satarkar, N. S.; Zhang, W.; Eitel, R. E.; Hilt, J. Z., Magnetic hydrogel nanocomposites as remote controlled microfluidic valves. *Lab on a Chip* **2009**, *9*, 1773-1779.
6. O'Grady, M. L.; Kuo, P.-I.; Parker, K. K., Optimization of Electroactive Hydrogel Actuators. *ACS Applied Materials & Interfaces* **2009**, *2*, 343-346.
7. Sumaru, K.; Ohi, K.; Takagi, T.; Kanamori, T.; Shinbo, T., Photoresponsive Properties of Poly(N-isopropylacrylamide) Hydrogel Partly Modified with Spirobenzopyran. *Langmuir* **2006**, *22*, 4353-4356.
8. Szilágyi, A.; Sumaru, K.; Sugiura, S.; Takagi, T.; Shinbo, T.; Zrínyi, M.; Kanamori, T., Rewritable Microrelief Formation on Photoresponsive Hydrogel Layers. *Chemistry of Materials* **2007**, *19*, 2730-2732.
9. Sugiura, S.; Szilagy, A.; Sumaru, K.; Hattori, K.; Takagi, T.; Filipcsei, G.; Zrinyi, M.; Kanamori, T., On-demand microfluidic control by micropatterned light irradiation of a photoresponsive hydrogel sheet. *Lab on a Chip* **2009**, *9*, 196-198.
10. Satoh, T.; Sumaru, K.; Takagi, T.; Kanamori, T., Fast-reversible light-driven hydrogels consisting of spirobenzopyran-functionalized poly(N-isopropylacrylamide). *Soft Matter* **2011**, *7*, 8030-8034.
11. Florea, L.; Diamond, D.; Benito-Lopez, F., Photo-Responsive Polymeric Structures Based on Spiropyran. *Macromolecular Materials and Engineering* **2012**, *297*, 1148-1159.
12. Wu, C.; Zhou, S., Volume Phase Transition of Swollen Gels: Discontinuous or Continuous? *Macromolecules* **1997**, *30*, 574-576.
13. Wu, X. S.; Hoffman, A. S.; Yager, P., Synthesis and characterization of thermally reversible macroporous poly(N-isopropylacrylamide) hydrogels. *Journal of Polymer Science Part A: Polymer Chemistry* **1992**, *30*, 2121-2129.
14. Sumaru, K.; Kameda, M.; Kanamori, T.; Shinbo, T., Reversible and Efficient Proton Dissociation of Spirobenzopyran-Functionalized Poly(N-isopropylacrylamide) in Aqueous Solution Triggered by Light Irradiation and Temporary Temperature Rise. *Macromolecules* **2004**, *37*, 7854-7856.
15. Satoh, T.; Sumaru, K.; Takagi, T.; Takai, K.; Kanamori, T., Isomerization of spirobenzopyrans bearing electron-donating and electron-withdrawing groups in acidic aqueous solutions. *Physical Chemistry Chemical Physics* **2011**, *13*, 7322-7329.
16. Benito-Lopez, F.; Byrne, R.; Raduta, A. M.; Vrana, N. E.; McGuinness, G.; Diamond, D., Ionogel-based light-actuated valves for controlling liquid flow in micro-fluidic manifolds. *Lab on a Chip* **2010**, *10*, 195-201.
17. Ziółkowski, B.; Ates, Z.; Gallagher, S.; Byrne, R.; Heise, A.; Fraser, K. J.; Diamond, D., Mechanical Properties and UV Curing Behavior of Poly(N-Isopropylacrylamide) in Phosphonium-Based Ionic Liquids. *Macromolecular Chemistry and Physics* **2013**, *214*, 787-796.
18. Byrne, R.; Coleman, S.; Gallagher, S.; Diamond, D., Designer molecular probes for phosphonium ionic liquids. *Physical Chemistry Chemical Physics* **2010**, *12*, 1895-1904.
19. Zhang, X.-Z.; Yang, Y.-Y.; Chung, T.-S.; Ma, K.-X., Preparation and Characterization of Fast Response Macroporous Poly(N-isopropylacrylamide) Hydrogels. *Langmuir* **2001**, *17*, 6094-6099.
20. Philippova, O. E.; Hourdet, D.; Audebert, R.; Khokhlov, A. R., pH-Responsive Gels of Hydrophobically Modified Poly(acrylic acid). *Macromolecules* **1997**, *30*, 8278-8285.

21. Echeverria, C.; Peppas, N. A.; Mijangos, C., Novel strategy for the determination of UCST-like microgels network structure: effect on swelling behavior and rheology. *Soft Matter* **2012**, *8*, 337-346.
22. Sumaru, K.; Kameda, M.; Kanamori, T.; Shinbo, T., Characteristic Phase Transition of Aqueous Solution of Poly(N-isopropylacrylamide) Functionalized with Spirobenzopyran. *Macromolecules* **2004**, *37*, 4949-4955.
23. Mistlberger, G.; Crespo, G. A.; Xie, X.; Bakker, E., Photodynamic ion sensor systems with spiropyran: photoactivated acidity changes in plasticized poly(vinyl chloride). *Chemical Communications* **2012**, *48*, 5662-5664.
24. Cleary, J.; Maher, D.; Slater, C.; Diamond, D. In *In situ monitoring of environmental water quality using an autonomous microfluidic sensor*, Sensors Applications Symposium (SAS), 2010 IEEE, 23-25 Feb. 2010, 2010; 2010; pp 36-40.

Chapter 6:

Porous and self-protonating spiropyran-based NIPAM gels with fast reswelling kinetics

Bartosz Ziółkowski,^a Larisa Florea,^a Jannick Theobald,^a Fernando Benito-Lopez^b and Dermot Diamond*^a

a) CLARITY Centre for Sensor Web Technologies, National Centre for Sensor Research, Dublin City University, Dublin 9, Ireland

b) CIC microGUNE, Arrasate-Mondragón, Spain

6.1 Introduction

Photoresponsive gels based on N-isopropylacrylamide and spiropyran have been investigated in recent years.[1-5] These gels actuate on the following principle. A spiropyran-acrylate photoswitch molecule is incorporated into an *N*-isopropylacrylamide thermoresponsive hydrogel. The photoswitch can exist in two isomer forms, the hydrophobic, closed spiropyran (BSP) and the more hydrophilic open merocyanine form (MC) that can also become protonated (MC-H⁺). When such gels are placed in a millimolar HCl solution, the photoswitch spontaneously switches from BSP to MC-H⁺, the gel swells and becomes yellow. When this gel is irradiated with light of the wavelength of the absorption of the protonated MC-H⁺ (eg. white LED light) the MC-H⁺ reverts back to the more hydrophobic and colourless BSP form. As a consequence the hydrophilicity of the material changes and the gel shrinks.

Applications of this material were demonstrated as microfluidic light-actuated valves[2] or on-demand photo-patterned microfluidic channels.[3] However, the materials employed in these studies suffered from several drawbacks. First, the gel needs to be immersed in HCl to be photoresponsive. Second, after the contraction step the gel needs to be reswollen in HCl if it is to be shrunk again. These limit the application practically to only one-shot devices[5]. Lastly, the shrinking and reswelling speeds are still rather slow for satisfactory performance.

Improvements in the gel reswelling kinetics reported previously by the modification of substituents on the photoswitch molecule[6] but the authors pointed out that the gels composed of the fastest photoswitch molecules were not stable.[4] This was attributed to the reactive methoxy groups – the same groups that gave the molecule the fastest opening kinetics.

In our recent paper we have demonstrated that the severely limiting HCl soaking step can be avoided by copolymerisation of acrylic acid into these gel structures.[7] It was shown that these gels self-protonate in deionised water and can be actuated repeatedly even after being washed many times with water or dried and reswollen. However, the reswelling speeds for the 3mm gel disks were still around 60 minutes.

In this work we attempt to improve the reswelling performance of the gels by inducing porosity into the poly(NIPAM) gels. It has been demonstrated that poly(NIPAM) gels shrink and reswell significantly faster if they are porous[8-10] Therefore, we have used poly(ethylene glycol) of two molecular weights as a pore forming agent and combined it with our previously reported

spiropyran-NIPAM-acrylic acid gels to produce porous, photoresponsive and self protonating soft hydrogel actuators. The porosity is analysed with Scanning Electron Microscopy, the photo-induced size shrinking and reswelling of the gels is measured together with the UV-Vis spectra of the reswelling gels. The properties of the materials and their impact on the actuation properties are discussed.

6.2 Experimental

6.2.1 Materials

N-isopropylacrylamide 98% (NIPAM), acrylic acid 99% (AA) (180-200 ppm MEHQ as inhibitor), *N,N'*-methylenebisacrylamide 99% (MBIS), phenylbis(2,4,6 trimethyl benzoyl) phosphine oxide 97% (PBPO), poly(ethylene glycol) Mw = 2000 g/mol and Mw = 20 000 g/mol were obtained from Sigma Aldrich, Ireland and used as received. Trimethyl-6-hydroxyspiro-(2H-1-benzopyran-2,2'indoline) 99% was obtained from Acros Organics and acrylated as described previously.[7]

6.2.2 Gel preparation

For the hydrogel synthesis, typically 200 mg (1 mol equiv.) of NIPAM was mixed with 3 mol% equiv. of MBIS and the given amount of AA and spiropyran acrylate (BSP). These compounds were then dissolved in 500 μ L of 1,4-dioxane/water mixture (4:1 vol:vol) in which a given amount of PEG was previously dissolved.. To this mixture 1 mol % equiv. of the photo-initiator (PBPO) was added. The full sample compositions can be found in Table 6-1. This mixture was poured onto a PDMS mould containing circular pits with various sizes, covered with a glass microscope slide and polymerised for 30 min under white light. The white light source used was a Dolan-Jenner-Industries Fiber-Lite LMI LED lamp with an intensity of 780 lumens projected through two gooseneck waveguides placed at a distance of 10 cm from the mould. The light intensity measured with a Multicomp LX-1309 light meter was ~30 kLux. The polymerised gels were allowed to swell in deionised water that was changed 3 times with 4 h intervals until no colouration of the supernatant could be observed. Removal of the PEG porogen was confirmed by Raman spectroscopy (Appendix C). After 24 h the swollen and equilibrated gels were cut

into 3 mm discs using a manual puncher. All measurements were performed on gels produced according to this protocol.

Table 6-1. Compositions of samples tested

		Blank gel	2k gel	20k gel
AA	[mol %]	5	5	5
BSP	[mol %]	1	1	1
MBIS	[mol %]	3	3	3
PBPO	[mol %]	1	1	1
NIPAM	[mg]	200	200	200
PEG 2k	[mg]	-	400	-
PEG 20k	[mg]	-	-	200
Solvent	[μ L]	500	500	500

6.2.3 Gel shrinking measurements

For white light irradiation and shrinking measurements the hydrogels were placed in a 5 mm wide and 2mm deep PDMS mould filled with water and covered with another PDMS 2mm thick slide. The imaging was done with an Aigo GE-5 microscope using a 60x objective lens and the accompanying software. The light was provided by a Dolan-Jenner-Industrie Fiber-Lite LMI at maximum power through two waveguide goosenecks placed 5 cm from the sample. The swelling ratio “d” was calculated using equation 6.1:

$$d = \frac{d_x}{d_0} \quad (6.1)$$

where, d_x – measured diameter; d_0 – is the diameter of a fully swollen gel

6.2.4 SEM

The hydrogel samples were first swollen in DI water, then frozen with liquid nitrogen and subsequently freeze-dried using a Labconco freeze-drier, model 7750060. The samples were kept for 24 hours at 0.035 mBar pressure and temperature of -40 °C.

The freeze-dried hydrogels were cut in half to reveal the cross section and imaged using scanning electron microscopy (SEM) performed on a Carl Zeiss EVOLS 15 system at an accelerating voltage between 14.64-17.78 V. Samples were placed onto silicon wafers and coated with 10 nm of gold layer prior to imaging. During the imaging process, the stage was tilted at an angle between 0–15° for better imaging of the cross section of the hydrogels.

6.2.5 Rheology

Rheology measurements on the DI water equilibrated samples were carried out with an Anton Paar MCR 301 rheometer using a PP15 parallel plate tool 15 mm diameter. The amplitude sweep tests were done at 1 Hz frequency and a normal force of 0.1 N. The frequency sweeps were done at 0.1 % strain from 100 Hz to 0.1 Hz and normal force of 0.1 N.

6.2.6 UV-Vis spectroscopy

UV–Vis spectroscopy was used to study the colours of the spiropyran hydrogels under different illumination conditions. The absorbance spectra were recorded in reflectance mode using a fibre-optic light guide connected to a Miniature Fiber Optic Spectrometer (USB4000 – Ocean Optics) and a specially designed probe holder (Schematics in the ESI). The light source was a LS-1 tungsten halogen lamp (white light) obtained from Ocean Optics, Inc. Data from the spectrometer was processed using Spectrasuite software provided by Ocean Optics Inc. For clarity, the absorbance spectra recorded were smoothed using Origin software using Savitzky–Golay algorithm.

6.3 Results and Discussion

6.3.1 Porous poly(NIPAM)-co-BSP-A-co-AA gels

When a PEG solution is used as a medium for polymerisation of NIPAM gel a porous network is formed because the PEG polymer chains are occupying space without taking part in the

polymerisation process. In comparison to the blank gels that are transparent at all times, the porous gels are partially transparent after polymerisation and turn completely opaque after equilibrating in water. This observation often constitutes the first indication of pores present in the gel. After the synthesis, the PEG porogen can be easily washed out from the gels by soaking in deionised water as confirmed by Raman spectroscopy in Figure C 1 (Appendix C).

After equilibration and washing with DI water some of the gels were freeze dried. The SEM images of cross sections of the freeze-dried gels can be seen in Figure 6-1. One can notice that even for the samples without the PEG porogen a pore-like structures are formed as previously shown by others.[9, 10] This is expected for freeze-dried samples as the sublimated water leaves empty spaces behind and allows imaging the gel as it is in its hydrated/swollen state. In our case, the size of features in the blank gel varies significantly with smaller pore-like features being in the range of $\sim 2 - 5 \mu\text{m}$ (Figure 6-1a). Photos of the 2k gel reveal much smaller pore features formed compared to the blank. Here the feature size is typically $< 2 \mu\text{m}$ Figure 6-1b. This might allow easier water passage in and out of the gel with respect to the non-porous gel due to a higher surface/volume ratio. Finally, the photos of 20k gels reveal the most homogenous and clear porous character of all the gels. Given the magnification of the photo in Figure 6-1c one can speculate that the pores are $< 1 \mu\text{m}$ in diameter.

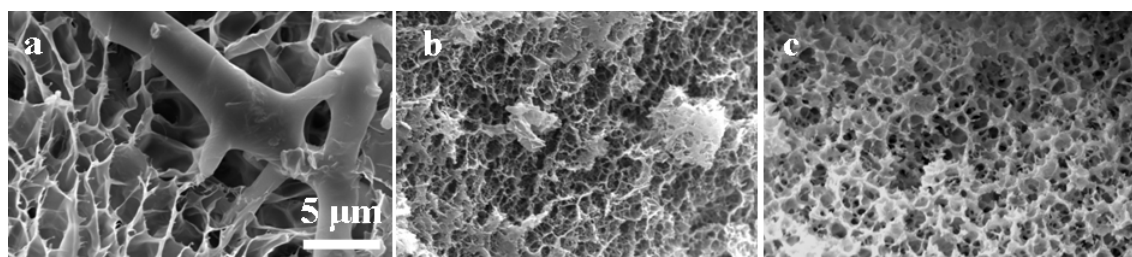


Figure 6-1. SEM images of freeze dried gels: a) gel with no porogen used; b) 2k gel; c) 20k gel

6.3.2 Mechanical stability of the gels

It is well known that porosity often lowers the mechanical stability of gels compared to their non-porous equivalents. In the case of the above gels the fact that the freshly polymerised porous gels swell more in DI water (30 % in diameter) than the blank gels (20 % in diameter) results in the decreased mechanical strength of the porous gels (Figure 6-2). Despite the lower modulus of the porous gels and smaller linear viscoelastic region (Figure 6-2a) compared to the blank, the porous gels still possess mechanical moduli within the typical range ($\sim 10^4$ Pa) reported for swollen hydrogels.[11]

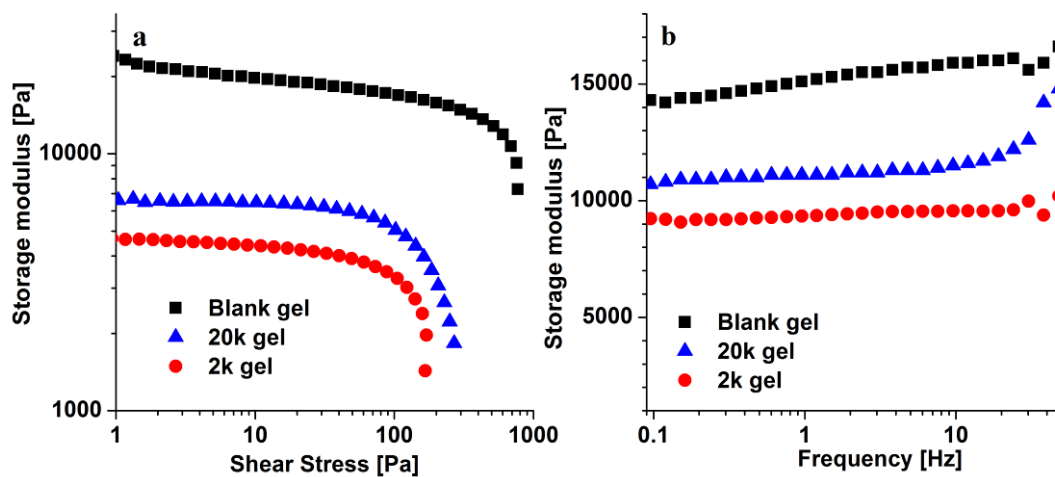


Figure 6-2. a) Storage modulus vs. shear stress of the gels during a strain amplitude sweep (frequency 1 Hz); b) Frequency sweep for the same gels (amplitude 0.1 %).

6.3.3 Light induced shrinking and reswelling of the gels

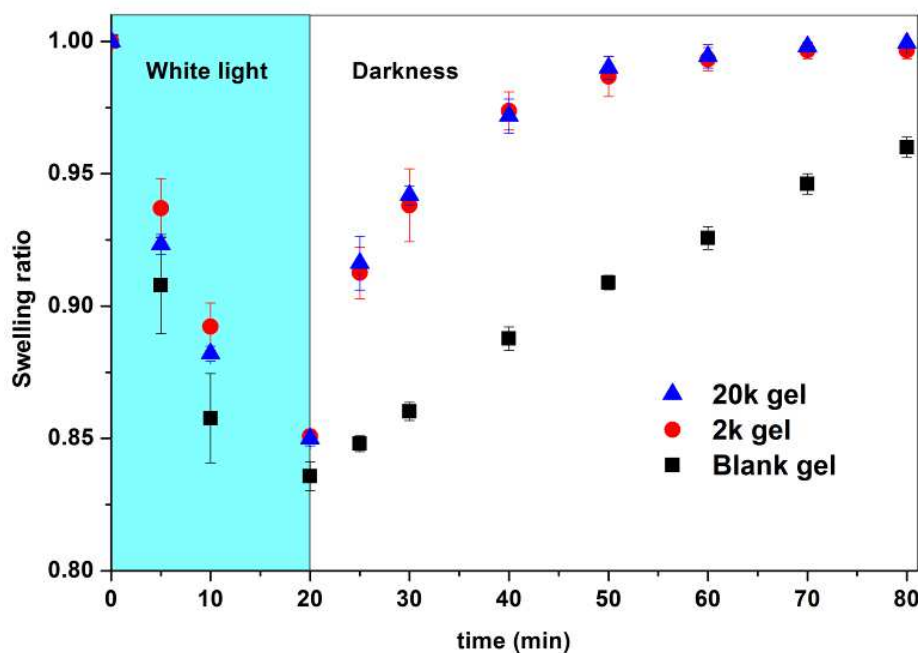


Figure 6-3. Light induced shrinking and reswelling in the dark for poly(NIPAM)-co-BSP-A-co-AA porous gels.

The light induced shrinking of these gels is a faster process than reswelling, as we have reported previously,[7] and appears to be slightly affected by the presence of pores (Figure 6-3). In fact, the volume decrease is smaller for the porous gels than for the blank gel. This can be explained by the fact that, as mentioned earlier, the porous gels swell more when placed in water after the polymerisation than the blank gels. In turn, this results in a lower overall concentration of BSP

in the gel/water. As reported previously, the BSP content has a significant effect on the speed and degree of shrinking of these gels.[7] Moreover, in the more swollen gels, a smaller mass of polymer has to expel a higher mass of water to reach the same shrinking ratio as the blank. On the other hand, significant differences between the blank and porous gels were observed during the reswelling part of the experiment (Figure 6-3). Note that the blank gels need more than an hour to re-swell to their initial state and the swelling ratio increase is almost linear with time. In contrast the porous gels reached 97% of the initial diameter within 20 minutes after the light has been switched off i.e., in the dark.

Surprisingly, the different molecular weight of pore forming PEGs used did not affect the reswelling speed between the porous gels. The UV-Vis spectroscopy measured on the same gels show that the kinetics of BSP opening and protonation is similar (Figure 6-4a) but seems to depend slightly on the initial swelling of the gels. After applying an exponential growth model

$$y = A \cdot e^{-k \cdot t} \quad (6.2)$$

where y – absorbance Figure 6-4a / swelling Figure 6-4b; A – preexponential factor; k – rate constant [s^{-1}]; t – time [s]

it was possible to determine the first order kinetic rate constants for both the reswelling and absorbance data. From these calculations one can conclude that the blank has the higher rate constant of $2.53 \times 10^{-3} [s^{-1}]$ while the porous gels have BSP reprotonation kinetic constants of $2.44 \times 10^{-3} [s^{-1}]$ and $1.25 \times 10^{-3} [s^{-1}]$ for the 20k and 2k gel respectively. On the other hand, the reswelling kinetics shown in Figure 6-4b reveal that the non-porous gel reswelling speed ($k \sim 2 \times 10^{-4} [s^{-1}]$) is an order of magnitude slower than the porous gels ($k \sim 1.6 \times 10^{-3} [s^{-1}]$). Given the fact that for the non-porous gels the protonation kinetics is an order of magnitude higher than the reswelling kinetics one can presume that in this case the reswelling is a diffusion limited process.

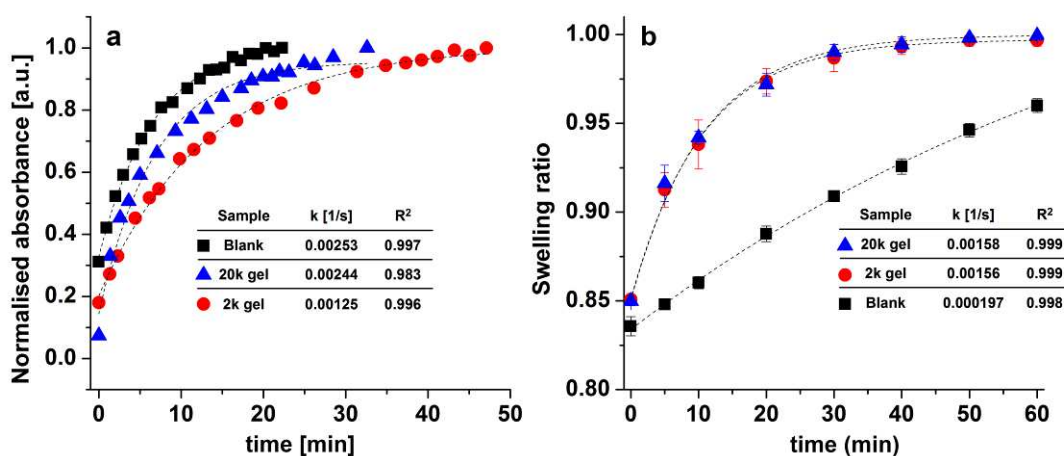


Figure 6-4. a) Normalised absorbance (at 480 nm) kinetic curves of the BSP re-protonation in DI water after 20 min white light irradiation; b) Reswelling of the gels during the re-protonation process in DI water after 20 min white light irradiation.

However for the porous gels, the reswelling kinetic constants values are much closer to the protonation rate values ($\sim 1-2.5 \times 10^{-3} \text{ [s}^{-1}\text{]}$). Bearing in mind the fact that the reswelling speed does not seem to depend on the pore size, it is speculated that in the case of the porous gels the reswelling is no longer diffusion limited but dependant on the rate constant of BSP \rightarrow MC-H⁺ reaction.

These results suggest that the presented material can function not only as a reversible photoactuator as demonstrated previously[7] but has a potential to be used as a fast “on/off” microfluidic soft actuator valve.

6.4 Conclusions

In standard spiropyran containing poly(NIPAM) photoresponsive gels the light induced shrinking is faster than the re-swelling (several minutes vs 1-2 hours). By using PEG porogens in our recently published acrylic acid modified spiropyran/NIPAM gels it was possible to produce porous photoresponsive gels that not only had reversible photoactuation property but also significantly faster reswelling kinetics (by a factor of 3) than the non-porous blank. The spiropyran opening kinetics measured along with the size swelling kinetics suggest that when pores are present in the gel the reswelling is no longer limited by water diffusion but by the spiropyran opening kinetics. These findings provide the basis for development of novel photoresponsive soft actuators for fast on/off microfluidic flow control.

Acknowledgements:

This work was performed as part of the EU Framework 7 project “ATWARM” (Marie Curie ITN, No. 238273)”. Support under Science Foundation Ireland under the CLARITY initiative, grant 07/CE/I1147 is also kindly acknowledged.

6.5 References:

1. Sumaru, K.; Ohi, K.; Takagi, T.; Kanamori, T.; Shinbo, T., Photoresponsive Properties of Poly(N-isopropylacrylamide) Hydrogel Partly Modified with Spirobenzopyran. *Langmuir* **2006**, *22*, 4353-4356.

2. Sugiura, S.; Sumaru, K.; Ohi, K.; Hiroki, K.; Takagi, T.; Kanamori, T., Photoresponsive polymer gel microvalves controlled by local light irradiation. *Sensors and Actuators A: Physical* **2007**, *140*, 176-184.
3. Sugiura, S.; Szilagy, A.; Sumaru, K.; Hattori, K.; Takagi, T.; Filipcsei, G.; Zrinyi, M.; Kanamori, T., On-demand microfluidic control by micropatterned light irradiation of a photoresponsive hydrogel sheet. *Lab on a Chip* **2009**, *9*, 196-198.
4. Satoh, T.; Sumaru, K.; Takagi, T.; Kanamori, T., Fast-reversible light-driven hydrogels consisting of spirobenzopyran-functionalized poly(N-isopropylacrylamide). *Soft Matter* **2011**, *7*, 8030-8034.
5. Benito-Lopez, F.; Byrne, R.; Raduta, A. M.; Vrana, N. E.; McGuinness, G.; Diamond, D., Ionogel-based light-actuated valves for controlling liquid flow in micro-fluidic manifolds. *Lab on a Chip* **2010**, *10*, 195-201.
6. Satoh, T.; Sumaru, K.; Takagi, T.; Takai, K.; Kanamori, T., Isomerization of spirobenzopyrans bearing electron-donating and electron-withdrawing groups in acidic aqueous solutions. *Physical Chemistry Chemical Physics* **2011**, *13*, 7322-7329.
7. Ziólkowski, B.; Florea, L.; Theobald, J.; Benito-Lopez, F.; Diamond, D., *Soft Matter* **2013**, *Accepted 10 June 2013*.
8. Wu, X. S.; Hoffman, A. S.; Yager, P., Synthesis and characterization of thermally reversible macroporous poly(N-isopropylacrylamide) hydrogels. *Journal of Polymer Science Part A: Polymer Chemistry* **1992**, *30*, 2121-2129.
9. Zhang, X.-Z.; Yang, Y.-Y.; Chung, T.-S.; Ma, K.-X., Preparation and Characterization of Fast Response Macroporous Poly(N-isopropylacrylamide) Hydrogels. *Langmuir* **2001**, *17*, 6094-6099.
10. Li, L.; Du, X.; Deng, J.; Yang, W., Synthesis of optically active macroporous poly(N-isopropylacrylamide) hydrogels with helical poly(N-propargylamide) for chiral recognition of amino acids. *Reactive and Functional Polymers* **2011**, *71*, 972-979.
11. Anseth, K. S.; Bowman, C. N.; Brannon-Peppas, L., Mechanical properties of hydrogels and their experimental determination. *Biomaterials* **1996**, *17*, 1647-1657.

Chapter 7:

Thermoresponsive poly ionic liquid gels

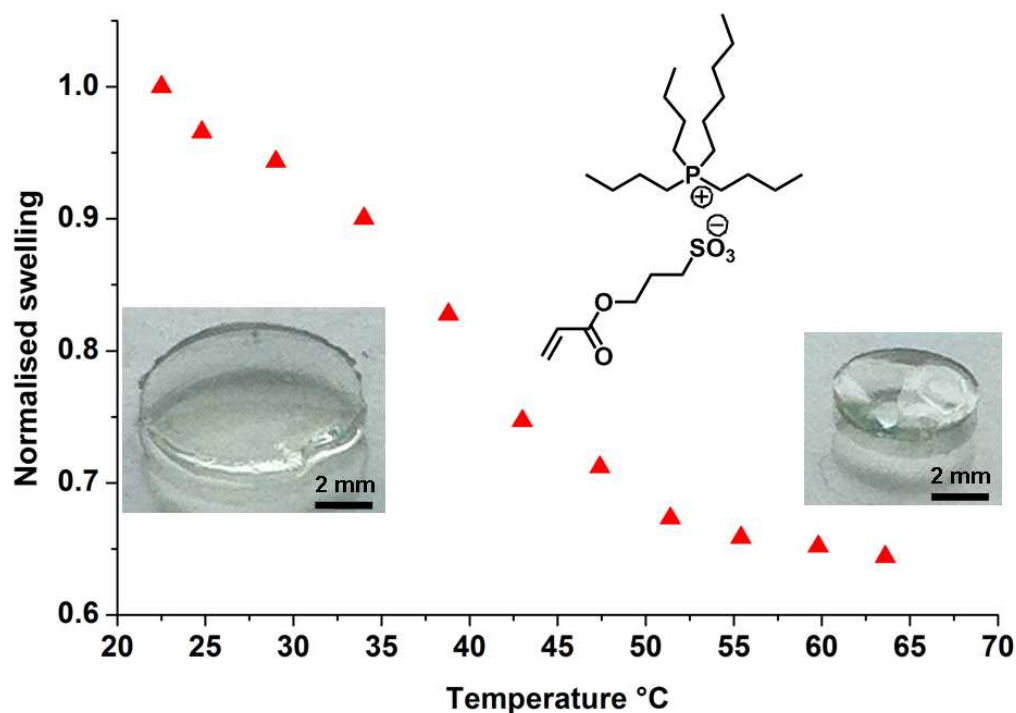
Bartosz Ziółkowski and Dermot Diamond*

Submitted to Chemical Communications 31 July 2013.

Abstract

So far all reports on the novel class of thermoresponsive poly ionic liquids (LCST polyILs) have been dealing with linear polymers. Therefore it has been proposed to synthesise covalently crosslinked hydrogels based on two monomeric LCST ILs to afford a material with properties similar to the well known thermoresponsive poly(N-isopropylacrylamide) hydrogels. Two monomeric LCST ILs: Tetrabutylphosphonium styrenesulfonate and tributyl-hexyl phosphonium 3-sulfopropylacrylate have been copolymerised with crosslinkers of varying length to afford the first ever thermoresponsive poly(ionic liquid)-based hydrogels. Surprisingly, only using longer chain crosslinkers resulted in stable hydrogels that would not crack during swelling. Thermal DSC analysis revealed that the crosslinking of the LCST ILs results in significant broadening (~ 40 °C) of the endothermic LCST peak compared to the linear polymer solutions (~ 10 °C). Consequently the volume phase transition actuation of the hydrogels also occurs over a broader temperature range (~ 40 °C). This behaviour has been attributed to the lack of freedom for the bulky ionic polymer chains in the crosslinked state and explains the ineffectiveness of the shorter crosslinkers.

Keywords: LCST, ionic liquid, hydrogel, thermoresponsive



7.1 Communication

Ionic liquids (ILs) – organic salts that exhibit melting points below ca. 100 °C are a widely known and continuously developing class of materials.[1] The main advantages of these materials include low vapour pressure and the possibility to tune the properties of the IL by alternating the structures of the constituent cations and anions. These features make them particularly useful for synthesis of ionogels[1] and stimuli responsive materials.[2]

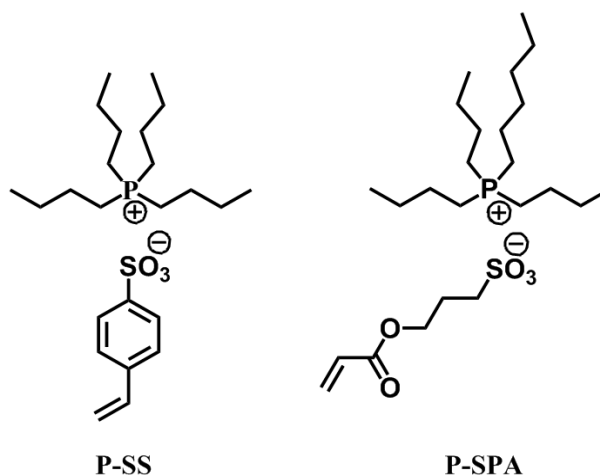
Gel materials (in which a crosslinked polymeric network is filled with an IL phase) combine the characteristics of the polymer with those of the IL, often resulting in new hybrid materials with interesting properties.[1-3] These include appearance of Lower Critical Solution Temperature (LCST) of the gel network that allows shrinkage of the gel when the temperature is raised above the LCST.[3] Also the ability to tune mechanical,[4] photoresponsive,[5] and magnetic[6] ionogel properties has been reported.

Moreover a subgroup of ILs wherein either the cation or anion is also a monomer and can be polymerised to form macromolecular ILs is also rapidly growing.[7] These monomeric and polymeric ILs have also attracted significant attention due to the possibility of having the properties of macromolecules and ILs integrated in one network. These include polyIL electrolytes and sorbents, and electroactive materials.[8]

Recently a new and fascinating class of thermo-responsive ILs has been reported.[9, 10] These ILs are miscible with water at room temperatures but when heated, they phase separate, much like thermoresponsive polymers such as *N*-isopropylacrylamide.[11] Such temperature-sensitive behaviour opens up new possibilities for using these ILs as functional fluids e.g. for reversible protein extraction.[10, 12] Interestingly, out of many different cation/anion combinations, the majority of the thermo-responsive ILs reported are based on variations of phosphonium cations, such as tetrabutyl or tributyl-hexyl phosphonium [10, 12, 13] The most common anions employed to make LCST ILs thus far have been derivatives of benzenesulfonic acid. A particularly interesting development was to use 4-styrene sulfonate as an anion[14]. This combination of cation and anion produced a monomeric IL that displayed LCST behaviour.[14] This IL was then polymerised to form the first ever thermo responsive poly IL. This polyIL when dissolved in water precipitated when heated above the LCST and re-dissolved when cooled below the LCST. Consequently, other monomeric ILs based on sulfopropylmethacrylate anion and tributyl-hexyl phosphonium cation [13] or C3-C6 sulfoalkyl anion and tributyl-4-vinylbenzyl phosphonium cation[15] have been reported.

A common property of these LCST polymeric ILs is that their LCST depends on the concentration of the polyIL in water.[13, 15, 16] This phenomenon allows easy tuning of the LCST of these materials. As the concentration of the IL in water increases the LCST decreases. Moreover, addition of salts such as KBr[16] or phosphate buffer[13] can alter the LCST higher

or lower, respectively, behaviour that is attributed to the salt's cosmotropicity.[13] The LCST of these materials can also be tuned using the standard route which involves copolymerisation of the responsive monomer with a hydrophobic comonomer. For example, when tetrabutylphosphonium 4-vinylsulfonate was copolymerised with 30% tributylhexylphosphonium 4-vinylsulfonate, the LCST was shown to decrease from 60 to 40 °C (at the same polymer concentration).[14] This thermoresponsive behaviour make these ILs and poly(ILs) very promising candidates for a new group of stimulus responsive polyionic materials such as, for example, reversible graphene solution stabilisers.[16]



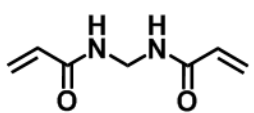
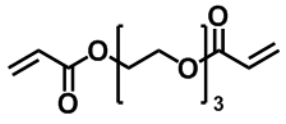
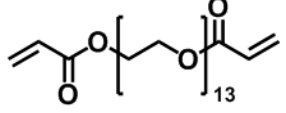
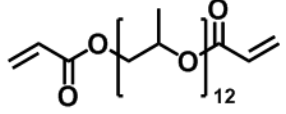
Scheme 7-1. Structures and abbreviations of the monomeric ILs used in this study

Therefore, it has been proposed that these thermoresponsive monomeric ILs can be polymerised into a hydrogel to form thermoresponsive poly IL hydrogels. Ideally these materials should behave similarly to the well known thermoresponsive poly(*N*-isopropylacrylamide) (NIPAAm) hydrogels, but with modification of properties due to the presence of the IL component. These materials could open new approaches to the production of polyIL-based stimulus responsive gels, with potential applications as, for example, microfluidic flow controllers and actuators, controlled absorb, release and delivery materials etc.

The following work investigates the preparation and the thermal and actuation properties of crosslinked thermoresponsive polyILs using two monomeric LCST ILs. We have synthesised the known tetrabutylphosphonium styrenesulfonate (P-SS)[14] and the new tributylhexyl phosphonium 3-sulfopropylacrylate (P-SPA) (Scheme 7-1) with the aim of photopolymerising these monomers with various crosslinkers such as *N,N'*-methylenebisacrylamide (MBAAm), poly(ethylene glycol) diacrylate Mn = 256 (PEG256), poly(ethylene glycol) diacrylate Mn = 700 (PEG700) and poly(propylene glycol) diacrylate Mn = 800 (PEG800) to form thermoresponsive gels. Since these monomeric ILs are liquid at room temperature and, like most ILs, have high solvating ability, they are miscible with organic initiators and crosslinkers, allowing easy handling of the mixtures, via moulding and subsequent photopolymerisation.

Initial gels were prepared with P-SS and 5 mol% of MBAAm as the crosslinker (details of IL and gel synthesis found in Appendix D). These gels when placed in DI water at room temperature swelled enormously (more than ~400 % in diameter) in less than 2 hours and the material disintegrated in the process (Figure D1a). The same swelling behaviour occurred with 10% MBAAm. Therefore, 5% PEG256 was used as another type of crosslinker but yielded same excessive swelling and cracking as occurred with MBAAm.

Table 7-1. Monomeric ILs and crosslinkers used to produce hydrogels with their respective appearances after swelling for 4 hours in DI water at room temperature.

	P-SS	P-SPA
	Cracks, no stable shape, excessive swelling	Cracks, no stable shape, excessive swelling
	Cracks, no stable shape	Cracks, no stable shape
	Stable, transparent gel	Stable, transparent gel
	Stable, transparent gel (up to 9 %mol)	Stable, transparent gel (up to 9 %mol)

From our experience with standard poly(NIPAAm) hydrogels, generally speaking at 10 mol% MBAAm and PEG256 crosslinker, the material is very tightly crosslinked and can swell in water not more than 20 % in diameter. Bearing this in mind it was suspected that, in the case of our monomeric ILs, the crosslinking was not efficient. Conversion of vinyl groups during polymerisation was confirmed by the disappearance of characteristic vinyl bands at $\sim 1630\text{ cm}^{-1}$ in Figures D2 and D3 Appendix D. Given this, it was hypothesised that steric hindrance might have been responsible for the ineffective crosslinking. Therefore, longer chain crosslinkers were used. When both P-SS and P-SPA were crosslinked with 5 % of PPO800 and the gel placed in DI water observable swelling occurred but stopped after 60 minutes reaching $\sim 146\%$ of the initial diameter. These gels were quite stiff in their hydrated forms but did not crack during swelling and were relatively easy to handle (Figure D1b). Similar behaviour was observed when PEG700 was used with P-SS and P-SPA. A summary of the outcomes of these experiments can be found in Table 7-1. It must be noted that PPO800 is hydrophobic in nature and immiscible with water. It is miscible in the monomeric IL but above 9 mol% of this crosslinker the resulting gel becomes opaque during the swelling process. Thermal analysis was performed on the water-swollen gels to determine their LCST behaviour. DSC scans were conducted on the poly(IL) gels to observe the LCST endothermic peak during heating.

As previously mentioned, polyILs have been reported to manifest concentration dependant LCST behaviour.[13, 15] Therefore, it was hypothesised that the LCST of the gel could be controlled via the amount of crosslinker used. This was based on the phenomenon that the crosslinker amount in polymers (among other factors) dictates the maximum swelling of the network and therefore the polymer concentration in the solvent swollen gel. It was assumed that in our case, higher crosslinker concentrations should produce a lower LCST for the water swollen gel. Consequently, the P-SS monomeric IL was polymerised with 3 different concentrations of crosslinker. It was found that gels prepared with 5 % PPO800 displayed the highest LCST (52.6 °C) compared to 7 and 8% PPO800 (46.1 and 42.9 °C) respectively (Table 7-2). The swelling of these gels (in diameter and weight) is also lower for the higher crosslinker content which further confirms previous assumptions.

Table 7-2 Crosslinker content used for the P-SS gels and the resulting gel swelling and LCST characteristics

PPO 800 content [mol %]	Swollen gel polymer concentration [wt %]	Swelling [% initial diam.]	Gel DSC LCST peak [°C]
5	26	46	52.6
7	32	39	46.1
8	34	34	42.9

What is striking about the DSC results of the crosslinked gels (Appendix D, Figure D4) is the broadness of the LCST peaks (~40 °C). When P-SPA gel (5 % PPO800) is compared to a linear poly(P-SPA) solution in water (1:1 by weight, Figure 7-1) one can see that the LCST of the linear polymer solution is much sharper (10 °C) and that the LCST DSC peak becomes broad once the polyIL is crosslinked.

These broad DSC peak distributions can be caused by a broad chain length distribution and crosslinking inhomogenities due to the free radical polymerisation used to make these gels. Based on the general knowledge that RAFT polymerisation allows more even chain length distribution[17] and reports that RAFT agents used to make poly(NIPAM) gels improve their LCST behaviour[18, 19] we added 2-(Dodecylthiocarbonothioylthio)-2-methylpropionic acid as a RAFT agent (monomer: RAFT ratio 50:1) to the P-SPA 5 mol% PPO800 system. The resulting gels had the same broad DSC thermal characteristics as the gel without the RAFT agent (Figure D5).

Therefore, in light of these results, this broadening of the LCST peak after crosslinking the polyIL is suspected to be caused by the decreased level of freedom the bulky polyIL has in the

gel. This DSC thermal response broadening after crosslinking also manifests itself in the temperature induced volume transition of the gels.

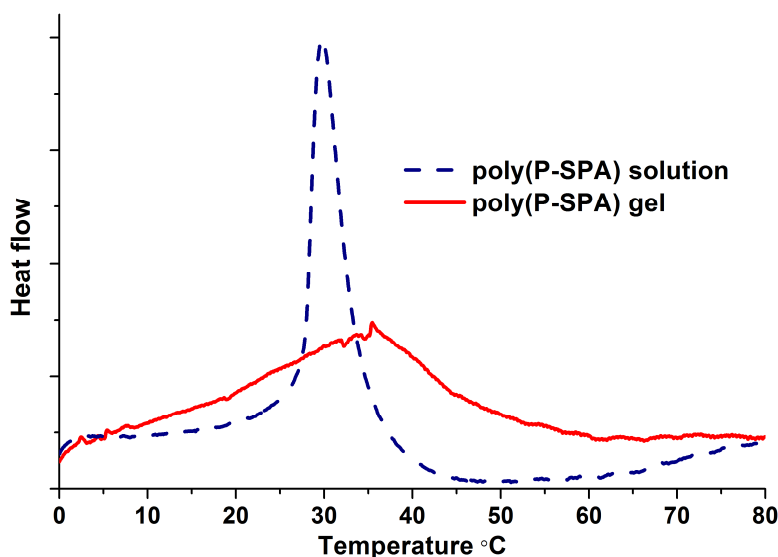


Figure 7-1. DSC scans of P-SPA gel crosslinked with 5 mol% PPO 800 and P-SPA linear polymer solution in DI water 1:1 weight %.

Figure 7-2 shows the temperature induced shrinking behaviour of two gels with the highest swelling (and presumably highest shrinking degree): P-SPA and P-SS both crosslinked with 5 % of PPO800 diacrylate. When these gels are subjected to heating, they do not shrink as is typical with thermoresponsive gels eg. poly(*N*-isopropylacrylamide). This means that the shrinking behaviour does not take place suddenly at one particular temperature. Rather, these polyIL gels shrink gradually over ~40 °C as the temperature increases (Figure 7-2). At the same crosslinker concentration, the P-SPA gel appears to be slightly more hydrophobic than P-SS, which results in the former shrinking to a greater extent at lower temperatures.

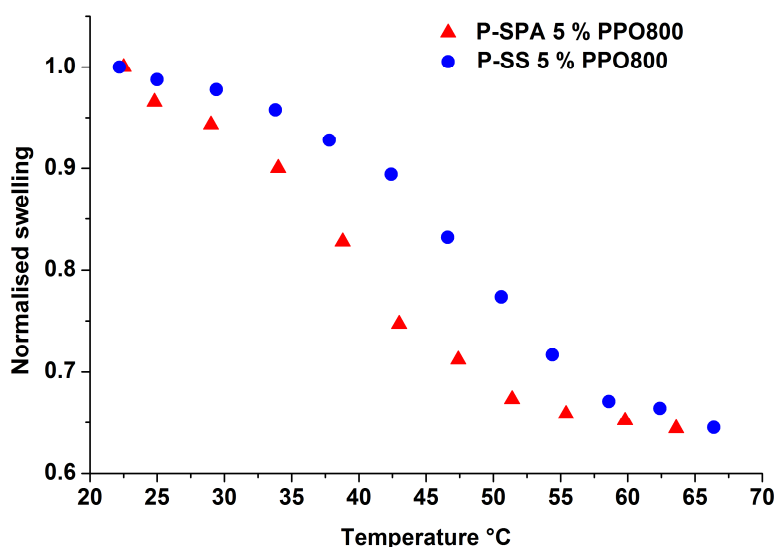


Figure 7-2. Temperature induced shrinking profiles of P-SS and P-SPA both crosslinked with 5 mol % of PPO800.

This unusual thermal shrinking behaviour could have interesting applications in scenarios that demand a continuous change in the material volume over a temperature range, rather than an abrupt phase change. For example, in microfluidics, these gels may have potential as temperature controlled flow regulators, since their volume can be varied over a temperature range in order to control the extent by which flow in a microfluidic channel is impeded

To conclude, a new and fascinating family of thermoresponsive monomeric ILs have been used to synthesise first ever thermoresponsive polyIL hydrogels. These monomeric ILs have been photopolymerised with crosslinkers of varying length to show that only long chain crosslinkers allow the material to swell in water without cracking and disintegrating. The LCST of these gels decreases with increasing gel crosslinker concentration, which is in accordance with previously reported LCST concentration dependence of these materials. However, the thermal behaviour of these materials did not mirror the similar linear systems reported. Instead, the crosslinked polyILs display a significant broadening of the temperature range over which the LCST behaviour occurs. Consequently, the gels shrink over a wide temperature range compared to typical thermoresponsive polymeric gels. This is attributed to the lack of freedom that the bulky and highly charged polymer backbone experiences in the crosslinked hydrogel state.

Acknowledgements:

The authors thank Dr Kevin J. Fraser for helpful consultations and discussions. This work was performed as part of the EU Framework 7 project “ATWARM” (Marie Curie ITN, No. 238273). D. D. acknowledges funding from Science Foundation Ireland (SFI) under the CLARITY CSET award (Grant 07/CE/I1147).

^aCLARITY, The Centre for Sensor Web Technologies, National Centre for Sensor Research, School of Chemical Sciences, Dublin City University, Glasnevin, Dublin 9, Ireland. E-mail: dermot.diamond@dcu.ie; Tel: +35317005405

7.2 References:

1. Le Bideau, J.; Viau, L.; Vioux, A., Ionogels, ionic liquid based hybrid materials. *Chemical Society Reviews* **2011**, *40*, 907-925.
2. Kavanagh, A.; Byrne, R.; Diamond, D.; Fraser, K. J., Stimuli Responsive Ionogels for Sensing Applications—An Overview. *Membranes* **2012**, *2*, 16-39.
3. Ueki, T.; Watanabe, M., Macromolecules in Ionic Liquids: Progress, Challenges, and Opportunities. *Macromolecules* **2008**, *41*, 3739-3749.

4. Ziólkowski, B.; Ates, Z.; Gallagher, S.; Byrne, R.; Heise, A.; Fraser, K. J.; Diamond, D., Mechanical Properties and UV Curing Behavior of Poly(N-Isopropylacrylamide) in Phosphonium-Based Ionic Liquids. *Macromolecular Chemistry and Physics* **2013**, *214*, 787-796.
5. Benito-Lopez, F.; Byrne, R.; Raduta, A. M.; Vrana, N. E.; McGuinness, G.; Diamond, D., Ionogel-based light-actuated valves for controlling liquid flow in micro-fluidic manifolds. *Lab on a Chip* **2010**, *10*, 195-201.
6. Ziólkowski, B.; Bleek, K.; Twamley, B.; Fraser, K. J.; Byrne, R.; Diamond, D.; Taubert, A., Magnetic Ionogels (MagIGs) Based on Iron Oxide Nanoparticles, Poly(N-isopropylacrylamide), and the Ionic Liquid Trihexyl(tetradecyl)phosphonium Dicyanamide. *European Journal of Inorganic Chemistry* **2012**, *2012*, 5245-5251.
7. Yuan, J.; Mecerreyes, D.; Antonietti, M., Poly(ionic liquid)s: An update. *Progress in Polymer Science* **2013**, *38*, 1009-1036.
8. Green, O.; Grubjesic, S.; Lee, S.; Firestone, M. A., The Design of Polymeric Ionic Liquids for the Preparation of Functional Materials. *Polymer Reviews* **2009**, *49*, 339-360.
9. Fukaya, Y.; Sekikawa, K.; Murata, K.; Nakamura, N.; Ohno, H., Miscibility and phase behavior of water-dicarboxylic acid type ionic liquid mixed systems. *Chemical Communications* **2007**, 3089-3091.
10. Kohno, Y.; Ohno, H., Ionic liquid/water mixtures: from hostility to conciliation. *Chemical Communications* **2012**, *48*, 7119-7130.
11. Schild, H. G., Poly (n-isopropylacrylamide) - experiment, theory and application. . *Progress in Polymer Science* **1992**, *17*, 163-249.
12. Kohno, Y.; Ohno, H., Temperature-responsive ionic liquid/water interfaces: relation between hydrophilicity of ions and dynamic phase change. *Physical Chemistry Chemical Physics* **2012**, *14*, 5063-5070.
13. Kohno, Y.; Deguchi, Y.; Ohno, H., Ionic liquid-derived charged polymers to show highly thermoresponsive LCST-type transition with water at desired temperatures. *Chemical Communications* **2012**, *48*, 11883-11885.
14. Kohno, Y.; Ohno, H., Key Factors to Prepare Polyelectrolytes Showing Temperature-Sensitive Lower Critical Solution Temperature-type Phase Transitions in Water. *Australian Journal of Chemistry* **2011**, *65*, 91-94.
15. Men, Y.; Schlaad, H.; Yuan, J., Cationic Poly(ionic liquid) with Tunable Lower Critical Solution Temperature-Type Phase Transition. *ACS Macro Letters* **2013**, *2*, 456-459.
16. Men, Y.; Li, X.-H.; Antonietti, M.; Yuan, J., Poly(tetrabutylphosphonium 4-styrenesulfonate): a poly(ionic liquid) stabilizer for graphene being multi-responsive. *Polymer Chemistry* **2012**, *3*, 871-873.
17. Lowe, A. B.; McCormick, C. L., Reversible addition-fragmentation chain transfer (RAFT) radical polymerization and the synthesis of water-soluble (co)polymers under homogeneous conditions in organic and aqueous media. *Progress in Polymer Science* **2007**, *32*, 283-351.
18. Liu, Q.; Li, S.; Zhang, P.; Lan, Y.; Lu, M., Facile preparation of PNIPAM gel with improved deswelling kinetics by using 1-dodecanethiol as chain transfer agent. *Journal of Polymer Research* **2007**, *14*, 397-400.
19. Liu, Q.; Zhang, P.; Qing, A.; Lan, Y.; Lu, M., Poly(N-isopropylacrylamide) hydrogels with improved shrinking kinetics by RAFT polymerization. *Polymer* **2006**, *47*, 2330-2336.

Chapter 8:

Thesis summary and future outlook

8.1 Thesis summary

This thesis presented research undertaken in selected key areas of the fascinating field of stimulus responsive materials. Given the vast application possibilities of these materials the presented investigations were mainly focused on the properties that could allow implementation of said material in microfluidic systems as valves. Chapter 1 presented a general introduction into different classes of stimulus responsive materials, their advantages and disadvantages focusing on thermo, electric, light and magnetic responsive materials. A more detailed look at photoresponsive materials together with potential areas for improvement was presented in Chapter 2. In addition, different microfluidic valving solutions including magnetic and photoresponsive valves were also discussed in Chapter 2.

Due to the increased interest in making stimuli responsive materials in the presence of ionic liquids, Chapter 3 investigated one of the most popular polymers used to produce stimulus responsive gels in this environment. Key fundamental aspects of N-isopropylacrylamide in a range of phosphonium ILs were investigated in this chapter. It has been demonstrated that the anion of the hydrophobic $[P_{6,6,6,14}]^+$ cation can have a significant effect on the polymerisation kinetics, LCST and viscoelastic properties of the resulting ionogel. Ionogels made with $[P_{6,6,6,14}][DCA]$ were shown to have most elastic mechanical properties. Moreover, it was shown that the $[P_{1,4,4,4}][Tos]$ allowed the NIPAM to polymerise 3 times faster than in $[P_{6,6,6,14}][Cl]$. The $[P_{6,6,6,14}][Cl]$ IL was also been shown to decrease the poly(NIPAM)'s LCST from the standard ~ 30 °C to 15 °C. Even more interestingly $[P_{6,6,6,14}][DCA]$ ionogels swollen in water exhibited stiffening (7-fold modulus increase) when heated over their LCST (29 °C), but with minimal shrinking. These findings not only show that materials with unexpected properties can be made by combining known polymers with known ILs, and this allows the resulting ionogel properties to be tuned depending on the desired application.

In Chapter 4, knowledge from Chapter 3 was utilised to synthesise a magnetic ionogel. NIPAM and $[P_{6,6,6,14}][DCA]$ were chosen as they had been shown (Chapter 3) to give the ionogels the best elastic properties. Magnetic stimulus is non-invasive and therefore attractive for microfluidic valving as the valve could be operated from outside of the manifold with minimum impact on the fluidics. To prevent leaching the magnetic particles providing the magnetic susceptibility were coated with allyl and mercapto groups to allow the particles to be copolymerised into the ionogel structure. Due to the crosslinked magnetic particles, these ionogels showed improved mechanical properties and high dispersion homogeneity compared to the uncoated particles. Fast bending and actuation was achieved for these ionogels in water by using a permanent magnet, although electromagnets could be used to either actuate the gel by a gradient field or induce heating and shrinking through an oscillating magnetic field.

Magnetic stimuli are non-invasive and offer a unique new level of stimulus apart from the standard thermal or electric. However, generating magnetic stimulus can require considerable amounts of energy if electromagnets are used. On the other hand powerful neodymium permanent magnets cannot be switched off. Since electromagnetic radiation in the form of light can be generated using considerably smaller amounts of energy (eg. 1 V LED diodes) photoresponsive gels were investigated in this thesis. Recent reports on spiropyran in poly(NIPAM) gels showed that these materials shrink after applying white light stimulus but they have to be immersed in millimolar HCl for the actuation to take place. This serious limitation was solved in Chapter 5 by incorporating an internal source of acid in the gel in the form of copolymerised acrylic acid. These modified gels were shown to swell and protonate in DI water. Since the protons reside either on the photochrome molecule or on the acrylic acid the reprotonation is spontaneous and allows the gels to be actuated by light repeatedly as demonstrated. Washing with DI water and storing the gels for 2 months did not reduce the material's self-protonating ability and the performance. This improvement now allows this material to be used as a microfluidic reversible valve for applications that require pH in the range of 2 - 7.

Despite the satisfactory reversible photoactuation behaviour of the gels in Chapter 5 they still required about an hour to reswell. Therefore, in Chapter 6 the speed of reswelling was investigated and improved. By incorporation of PEG porogen in the monomer mixture prior polymerisation the resulting gels exhibited a highly porous structure. This morphology was demonstrated to significantly improve the reswelling speed of the self-protonating spiropyran photoresponsive gels due to the reduced average diffusion pathways related to the increased surface area/volume ratio. The kinetic constant of reswelling was increased by an order of magnitude compared to the non-porous gels ($\sim 0.0015 \text{ [s}^{-1}]$ for porous, $\sim 0.0002 \text{ [s}^{-1}]$ non-porous) and the data presented suggested that the reswelling kinetics in the porous gels was no longer limited by water diffusion but by the spiropyran isomerisation kinetics. Therefore, it can be speculated that these formulations have been optimised to their limits. Without altering the speed of spiropyran isomerisation or decreasing the feature size it will be difficult to achieve faster polymer actuation.

Research to find "faster" spiropyran molecules for these gels has been undertaken already [1, 2] but the molecules synthesised, though faster, were regarded as unstable. For this reason investigation for a new material as a replacement for the poly(NIPAM) backbone was investigated in Chapter 7. The recent discoveries of LCST ionic liquids quickly led to the synthesis of polymeric ionic liquids with LCST behaviour. Chapter 7 investigated if these materials can be crosslinked to form hydrogels similar to poly(NIPAM) hydrogels. It was demonstrated that in contrast to the linear polyILs that exhibit the typical sharp LCST behaviour, these crosslinked gels had a very broad LCST DSC peak. This results in the gels shrinking gradually as the temperature is increased. This unexpected behaviour was attributed to

the bulky and highly charged structure of the mer-units in the polymer chains. When spiropyran was incorporated into the polyIL gel structure a negligible photochromic effect with white light was observed. There were two explanations suggested for this: lack of isomerisation mobility of the spiropyran due to the bulky nature of the polymer chains or IL interactions with the spiropyran stabilising it in the open form. The first explanation might be supported by the fact that short chain crosslinkers (MBIS, PEG256) were ineffective and only longer chain crosslinkers (PEG700, PPO800) could crosslink these monomeric ILs into gels.

8.2 Future outlook

Having brought improvements to the properties of the materials presented there are still areas where further enhancements can be made. The following paragraphs discuss some potential routes for further investigations of the materials presented so far, as well as some more ambitious ideas based on recent discoveries in materials science.

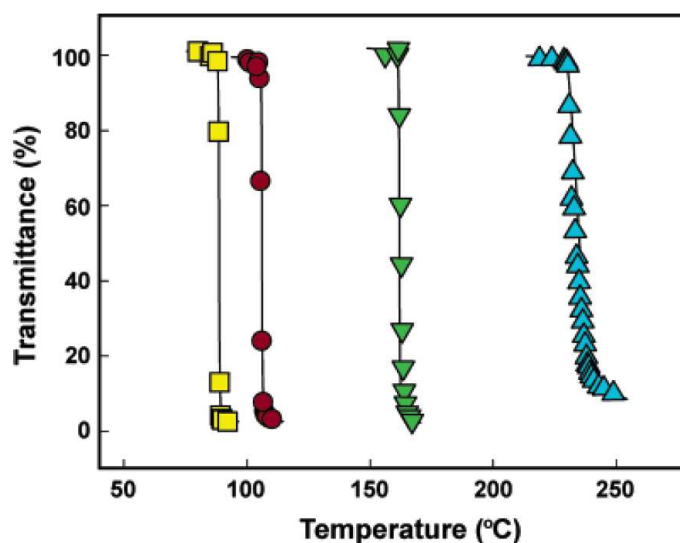


Figure 8-1. Temperature dependence of transmittance at 500 nm for a PBzMA solution in $[C_n\text{mim}][\text{NTf}_2]$. (yellow square): $[C_1\text{mim}][\text{NTf}_2]$; (red circle): $[C_2\text{mim}][\text{NTf}_2]$; (green inverted triangle): $[C_4\text{mim}][\text{NTf}_2]$; (blue triangle): $[C_6\text{mim}][\text{NTf}_2]$. $[C_n\text{mim}]$ represents the 1-alkyl-3-methylimidazolium cation.[3]

Considering the NIPAM-based ionogels, experiments in our laboratory have shown that the polymerisation of NIPAM proceeds generally faster in imidazolium ionic liquids and gives even higher distortions of the LCST behaviour. Therefore, one could carry out a parallel study where same anions as in Chapter 3 are used but an imidazolium cation is chosen instead of the phosphonium. This way a broader understanding of the interactions between NIPAM, ILs and the system's LCST can be obtained. Polymers normally not exhibiting LCST can exhibit such

behaviour in the presence of ionic liquids.[4] Therefore, different ILs could be used not only to tune the poly(NIPAM)'s LCST but also to induce LCST behaviour in polymers. Figure 8-1 shows that a poly(benzylmethacrylate) exhibits LCST behaviour in an imidazolium IL and this LCST is dependant on the length of the alkyl chain on the IL molecule. Shifts in the LCST can also be realised by a standard route of copolymerising monomers of different lypophilicity (Figure 8-2). All this is possible without the presence of water, making these systems IL-only with all the benefits of the IL low vapour volatility, thermal stability etc.

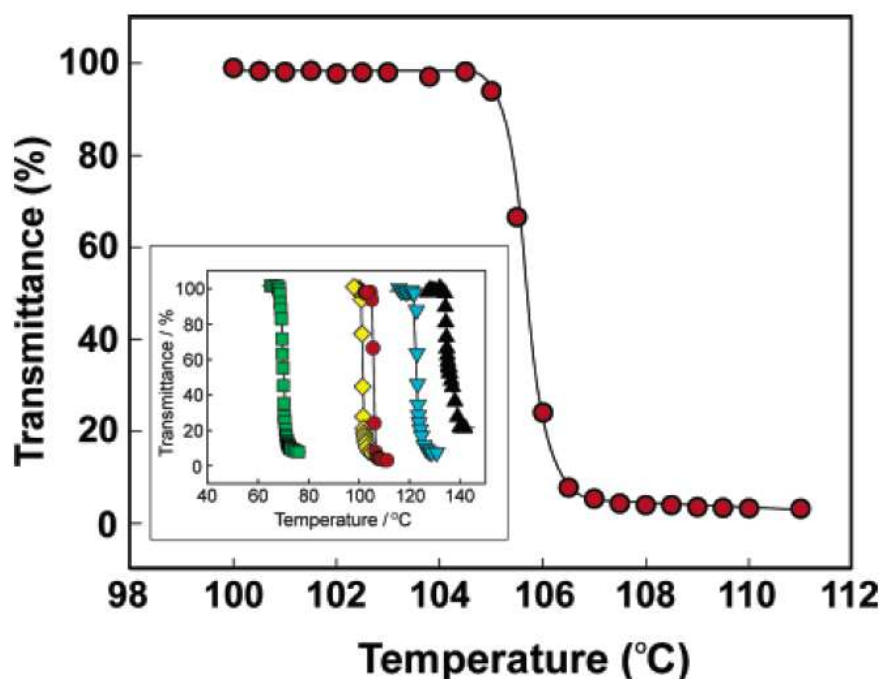


Figure 8-2. Temperature dependence of transmittance at 500 nm for a PBzMA solution in [C₂mim][NTf₂]. The transmittance of 100% indicates that the solution is a single-phase one (transparent), while that of 0% indicates that it is phase-separated (turbid). Inset shows the comparison of the turbidity measurements for BzMA copolymers with St or MMA. (red circle): PBzMA homopolymer, (M_n) 28 300 g/mol, (M_w/M_n) 2.76; (yellow diamond): P(BzMA-co-St) (1.6 mol %) (M_n) 19 100 g/mol, (M_w/M_n) 2.34; (green square): P(BzMA-co-St) (8.7 mol %), (M_n) 13 100 g/mol, (M_w/M_n) 1.88; (blue inverted triangle): P(BzMA-co-MMA) (5.1 mol %), (M_n) 21 600 g/mol, (M_w/M_n) 2.22; (black triangle): P(BzMA-co-MMA) (10 mol %), (M_n) 21 500 g/mol, (M_w/M_n) 2.15).[3]

The photoresponsive gels demonstrated in Chapter 5 and Chapter 6 have been optimised to some extent, but still possess limitations. Protonation of the spiropyran-NIPAM system will always depend on the pK_a of the open merocyanine and the surrounding availability of protons. One cannot alter the electronic structure of the molecule to induce faster isomerisation without compromising the stability.[2] Given this, it is reasonable to look for alternative derivatives of spiropyran or other molecules that have faster isomerisation kinetics. As the pK_a of the spiropyran/merocyanine currently limits these systems to pH < 7 one could also speculate to utilise alternative photoswitch systems where the change of hydrophilicity is not accompanied by pH changes. Azobenzenes might provide a solution to this problem.

A recently published photoresponsive ionogel briefly discussed in Chapter 1 is based on a poly(benzylmethacrylate) copolymerised with 3 mol% azobenzeneacrylate.[5] This gel exhibits shrinking under visible light irradiation and swelling under UV light irradiation at 83 °C (Figure 8-3). This behaviour is believed to be possible due to the interactions of the azobenzene, the benzene pendant rings on the polymer chains and the presence of the hydrophobic imidazolium Ntf₂ ionic liquid. This demonstrates that polymers that normally do not possess LCST can exhibit such behaviour when combined with ILs. Bearing in mind the almost unlimited combinations of cations and anions one can speculate that almost any polymer can be made into an ionogel that will exhibit a desired LCST or USCT (upper solution critical temperature) behaviour. This area of research is gaining increased attention due to the exciting possibilities to engineer the properties of ionogels for non-volatile and robust actuator applications and beyond.[3] Although azobenzene has been tested in the LCST ionogel system it would be very interesting if similar only-IL-containing light responsive ionogels with spiropyran could be synthesised. Having an ionogel with a tuneable actuation temperature or light responsiveness but filled with a non-volatile IL presents great advantages over the current actuator gels. It must be noted here that the photoresponsive spiropyran based ionogels reported so far [6] would still require to be soaked in aqueous HCl. Therefore, they are not pure ionogels.

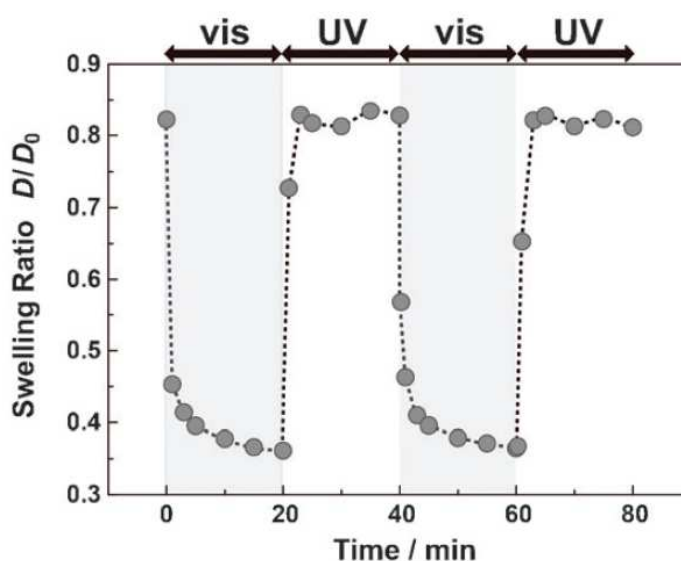


Figure 8-3. Light induced swelling and shrinking of a poly(benzylacrylate)-co-poly(azobenzeneacrylate) ionogel in 1-ethyl-3-methylimidazolium bis(trifluoromethane sulfonyl)amide ([C₂mim][NTf₂]) at 83 °C.

Similarly, azobenzene acrylate copolymer gel systems have certain limitations. For example, experiments in our laboratory have shown that the presence of azobenzene comonomer in the polymerisation mixture inhibits the polymerisation. Using linear polymerisation of NIPAM or *N,N*-dimethylacrylamide with azobenzene acrylate, conversions only up to ~60 % and ~40 % can be achieved when using 5 and 7 mol% of azobenzene comonomer, respectively. This is in

line with previous reports showing that azobenzenes can inhibit polymerisation.[7] Moreover, azobenzenes absorb strongly in the same range as most UV and Vis photoinitiators (350 - 450 nm) rendering photopolymerisation, so useful in microfluidic gel actuator system, impossible.

Therefore, it is suggested that azobenzenes may be more suited as thin film liquid crystal actuators. In such an arrangement, they have been shown to bend reversibly within several seconds.[8] This thin film crystal actuator approach operates on a bimetallic strip principle (Figure 8-4) and allows generation of forces higher than human muscles and in this respect they are significantly superior to the hydrogel approach. [9]

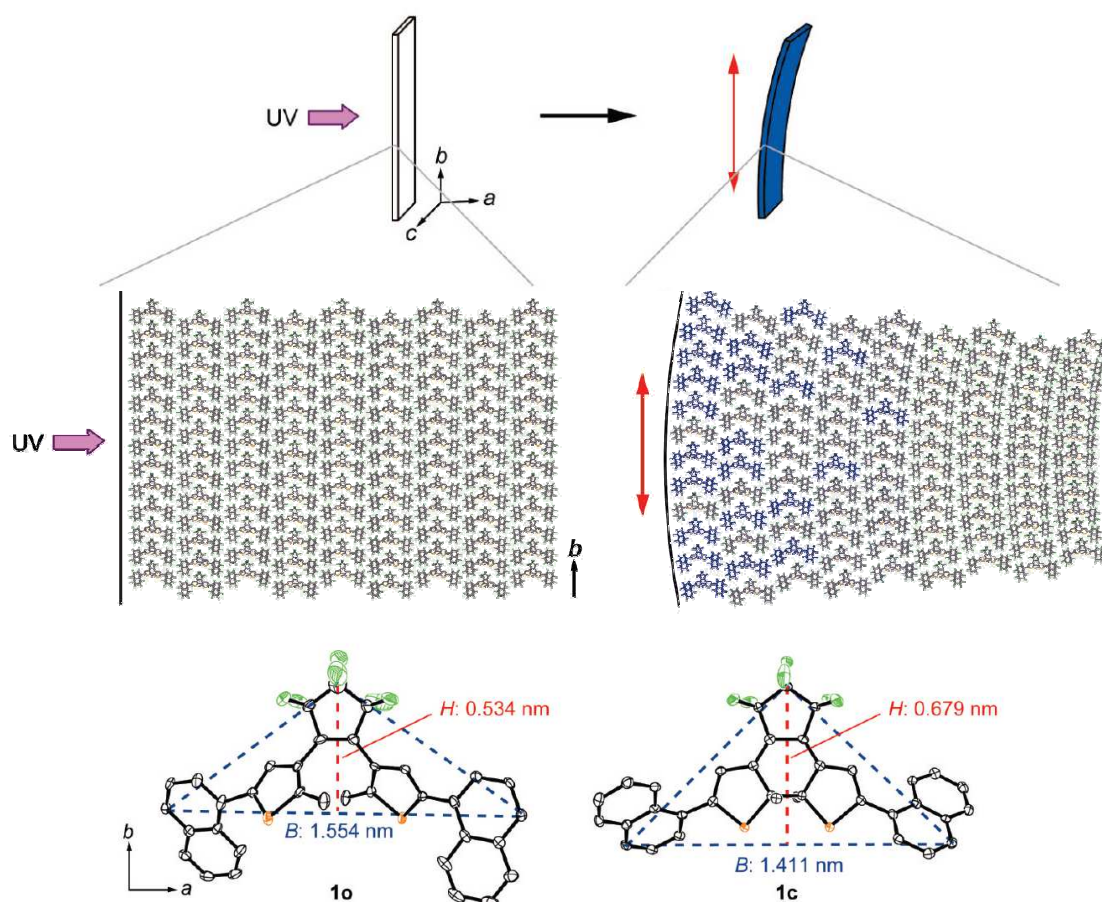


Figure 8-4. Illustration of the working principle of a diarylethene cocrystal that converts light into mechanical work. [9]

Another very interesting field where actuators are developing is the magnetic materials area. However, magnetic responsive materials are not very popular in the field of sensors and fluidics due to the high power consumption of electromagnets. Therefore, new concepts must arise to utilise the high magnetic forces provided by cheap and strong permanent magnets. One futuristic idea is to use a spin crossover phenomenon[10] as an external stimulus to switch the material between magnetic and non-magnetic states. This way a material present in a magnetic field of a permanent magnet would only be attracted (or repelled) by the magnet if the magnetism of the material is switched on. The possibility to switch magnetism on and off has

been demonstrated even with light. [11] Therefore one can speculate that an actuator can be constructed where the material incorporating the magnetic spin crossover particles is constantly within a field of a permanent magnet but it becomes magnetic only under light irradiation and consequently affected by the magnet (Figure 8-5). Theoretically such system would require relatively low power to support the light source, possibly an LED, as the permanent magnet does not require any power input to operate.

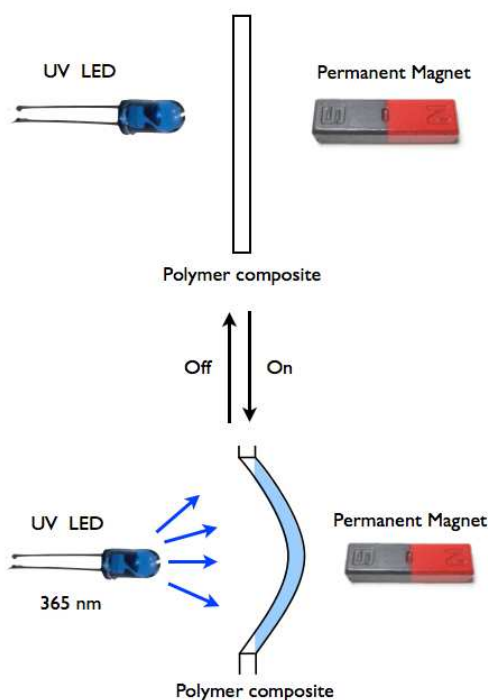


Figure 8-5. The principle of operation of an photo-magnetic actuator based on a material exhibiting a photo-induced magnetic spin crossover.

Lastly, one should consider extensive research in the field on LCST polyILs discussed in Chapter 7. As presented, initial tests have been carried out to mimic the spiropyran-NIPAM system using a polyIL that exhibits LCST much like poly(NIPAM) gels. The LCST ILs offer higher tunability of the LCST than poly(NIPAM) and therefore could be the basis of a next generation of photoresponsive gels. However, obtaining a photoresponsive actuator based on the LCST polyILs and spiropyran is not straightforward. The author has investigated LCST polyILs based on the monomers in Figure 8-6.

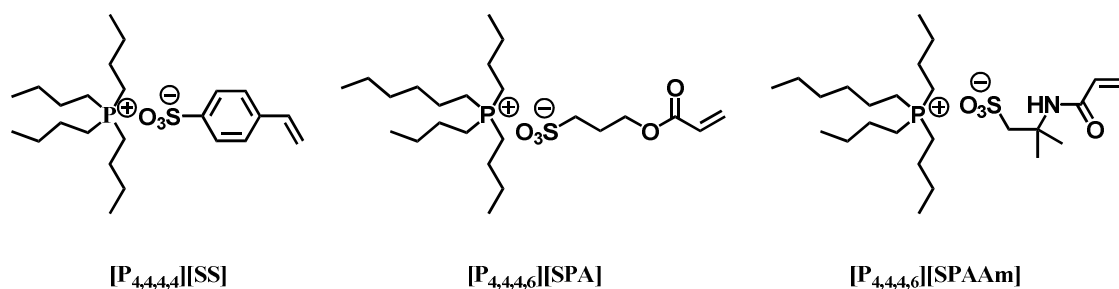


Figure 8-6. Structures of monomeric ILs that exhibit LCST studied in our laboratory.

Incorporation of spiropyran into these gels did not pose a problem and reversible photochromism was observed (Figure 8-7). What is surprising is that when the copolymer is dissolved in water the spiropyran comonomer undergoes spontaneous protonation without the addition of acid. It has been speculated that the IL polymer might be acidic in nature as the pH of the pure polyIL in water was 4.8. Moreover, the polyIL environment has shown to enhance the kinetics of spiropyran deprotonation compared to poly(NIPAM) systems (Table 8-1). No LCST shift has been observed when the spiropyran is isomerised. This applies to both linear polymers and gels. The gels decolourise but no light induced shrinking was observed. However, it must be noted that gels based on both $[P_{4,4,4,4}][SS]$ and $[P_{4,4,4,6}][SPA]$ decolourised slightly but the ones based on $[P_{4,4,4,6}][SPAAM]$ turned opaque upon decolourisation and the whole process happened much faster than in the case of the other gels. Moreover, it would seem that the polymerisation of $[P_{4,4,4,6}][SPAAM]$ is slow and yields polymers of low molecular weight. This is based on the observation that very little polymer is left after the linear polymer purification precipitation step and that similar observations were made for the NIPAM-azobenzene polymers discussed above.

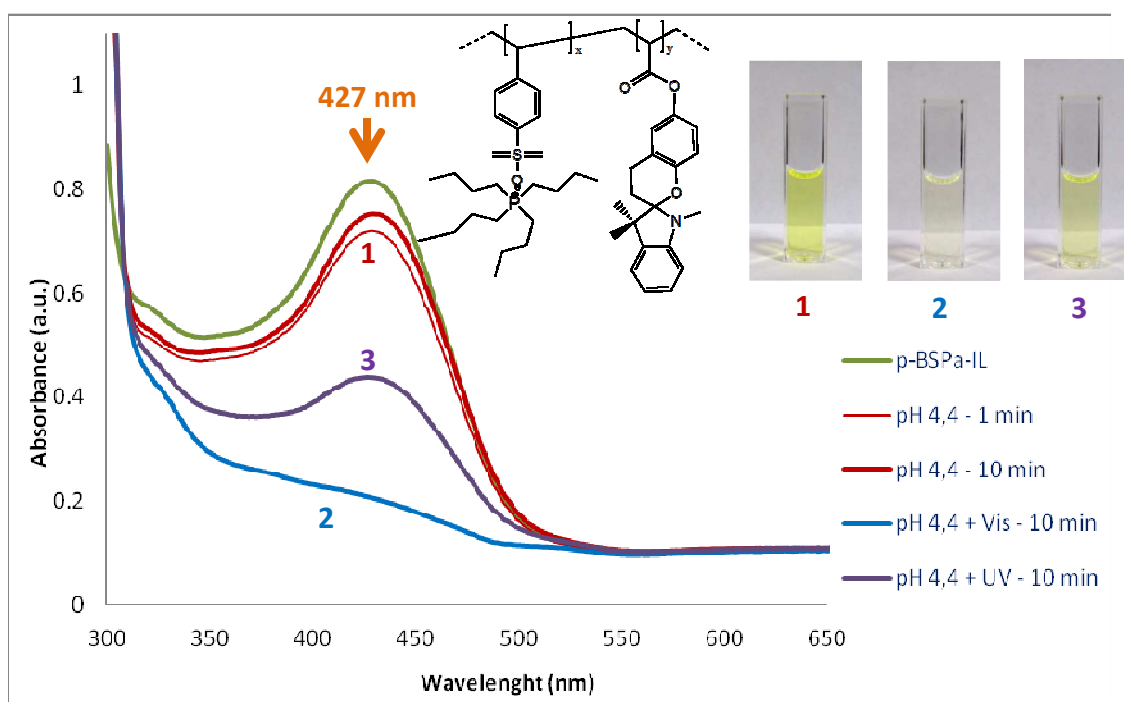


Figure 8-7. Photochromism of spiropyran copolymer with $[P_{4,4,4,4}][SS]$. Work carried out by an ENSIACET internship student Stephane Louisia.

Table 8-1. Protonation and deprotonation kinetic constants for Poly(NIPAM)-*co*-BSP and Poly([P_{4,4,4,4}][SS])-*co*-BSP linear polymers in DI water. Work carried out by an ENSIACET internship student Stephane Louisia.

	Protonation	Deprotonation (white light)
	k [s ⁻¹]	
Poly(NIPAM)- <i>co</i> -BSP	7.28×10^{-4}	8.59×10^{-3}
Poly([P _{4,4,4,4}][SS])- <i>co</i> -BSP	4.04×10^{-4}	1.18×10^{-2}

Faced with such challenges in synthesising a LCST polyIL photoresponsive gel, it is proposed to use the reliable poly(NIPAM)-*co*-BSP gel system and interpenetrate it with a polyIL network. This interpenetrating network gel (IPN) approach presents several benefits. First, the ionic liquid would be permanently immobilised in the gel and will not leach out. Secondly, as the photoresponsive character is given by the first poly(NIPAM) network the polyIL network does not necessarily need to have the LCST property. The IL cation/anions can also be varied, depending on the desired effect on the gel properties. This effect could include tuning the LCST of poly(NIPAM) or affecting the equilibrium and kinetics of spiropyran isomerisation. Not to mention tuning the overall hydrophilicity/hydrophobicity of the IPN gel. Lastly, interpenetrating networks are well known for having superior mechanical properties compared to standard gel networks.[12]

Investigations into the reasons for which the LCST of crosslinked poly IL gels is so broad should also be undertaken. The assumption that our photopolymerisation of the pIL gels produces an inhomogeneous structure and uneven polymer chains has been dis-proven by using RAFT agents to control the polymerisation process. The RAFT chain transfer agent (2-(Dodecylthiocarbonothioylthio)-2-methylpropionic acid) did not affect the broad distribution of the DSC peak of the polyIL gels from Chapter 7. Therefore, more ambitious approach would be to prepare sliding ring (SR) crosslinked polyIL gels.[13-15] This advanced polymer chemistry technique produces crosslinks that are not fixed to one point in the chain. Such polymer networks would allow the release of any molecular stress and therefore mimic a linear polymer solution system.

Many new concepts in material science arise every day. The miniaturisation of sensors and microfluidic platforms constantly drives the development of stimulus responsive materials for both sensing and actuating. In this chapter, only a few ideas for possible further exploration were presented. As time passes, many of these concepts will become redundant, for example, as disruptive discoveries arise that change our approach to materials synthesis. However, the author believes that this work has introduced some exciting knowledge into the field of stimulus responsive materials and I hope that it will assist and inspire new research investigations based on these fascinating materials.

8.3 References:

1. Satoh, T.; Sumaru, K.; Takagi, T.; Takai, K.; Kanamori, T., Isomerization of spirobenzopyrans bearing electron-donating and electron-withdrawing groups in acidic aqueous solutions. *Physical Chemistry Chemical Physics* **2011**, *13*, 7322-7329.
2. Satoh, T.; Sumaru, K.; Takagi, T.; Kanamori, T., Fast-reversible light-driven hydrogels consisting of spirobenzopyran-functionalized poly(N-isopropylacrylamide). *Soft Matter* **2011**, *7*, 8030-8034.
3. Ueki, T.; Watanabe, M., Lower Critical Solution Temperature Behavior of Linear Polymers in Ionic Liquids and the Corresponding Volume Phase Transition of Polymer Gels. *Langmuir* **2006**, *23*, 988-990.
4. Ueki, T.; Watanabe, M., Macromolecules in Ionic Liquids: Progress, Challenges, and Opportunities. *Macromolecules* **2008**, *41*, 3739-3749.
5. Ueki, T.; Yamaguchi, A.; Watanabe, M., Unlocking of interlocked heteropolymer gel by light: photoinduced volume phase transition in an ionic liquid from a metastable state to an equilibrium phase. *Chemical Communications* **2012**, *48*, 5133-5135.
6. Benito-Lopez, F.; Byrne, R.; Raduta, A. M.; Vrana, N. E.; McGuinness, G.; Diamond, D., Ionogel-based light-actuated valves for controlling liquid flow in micro-fluidic manifolds. *Lab on a Chip* **2010**, *10*, 195-201.
7. Luo, C.; Zuo, F.; Ding, X.; Zheng, Z.; Cheng, X.; Peng, Y., Light-triggered reversible solubility of α -cyclodextrin and azobenzene moiety complexes in PDMAA-co-PAPA via molecular recognition. *Journal of Applied Polymer Science* **2008**, *107*, 2118-2125.
8. Harris, K. D.; Cuypers, R.; Scheibe, P.; van Oosten, C. L.; Bastiaansen, C. W. M.; Lub, J.; Broer, D. J., Large amplitude light-induced motion in high elastic modulus polymer actuators. *Journal of Materials Chemistry* **2005**, *15*, 5043-5048.
9. Morimoto, M.; Irie, M., A Diarylethene Cocrystal that Converts Light into Mechanical Work. *Journal of the American Chemical Society* **2010**, *132*, 14172-14178.
10. Renz, F., Physical and chemical induced spin crossover. *Journal of Physics: Conference Series* **2010**, *217*, 012022.
11. Garcia, Y.; Ksenofontov, V.; Lapouyade, R.; Naik, A. D.; Robert, F.; Gütllich, P., Synthesis and magnetic properties of an iron 1,2-bis(thienyl) perfluorocyclopentene photochromic coordination compound. *Optical Materials* **2011**, *33*, 942-948.
12. Muniz, E. C.; Geuskens, G., Polyacrylamide hydrogels and semi-interpenetrating networks (IPNs) with poly(N-isopropylacrylamide): Mechanical properties by measure of compressive elastic modulus. *Journal of Materials Science: Materials in Medicine* **2001**, *12*, 879-881.
13. Tan, S.; Blencowe, A.; Ladewig, K.; Qiao, G. G., A novel one-pot approach towards dynamically cross-linked hydrogels. *Soft Matter* **2013**, *9*, 5239-5250.
14. Ito, K., Novel Cross-Linking Concept of Polymer Network: Synthesis, Structure, and Properties of Slide-Ring Gels with Freely Movable Junctions. *Polymer Journal* **2007**, *39*, 489-499.
15. Fleury, G.; Schlatter, G.; Brochon, C.; Travelet, C.; Lapp, A.; Lindner, P.; Hadziioannou, G., Topological Polymer Networks with Sliding Cross-Link Points: The "Sliding Gels". Relationship between Their Molecular Structure and the Viscoelastic as Well as the Swelling Properties. *Macromolecules* **2007**, *40*, 535-543.

Appendix A:

Mechanical properties and U.V. curing behaviour of Poly(N-isopropylacrylamide) in phosphonium based ionic liquids.

Electronic Supplementary Information (Chapter 3)

A.1 Purification of ionic liquids.

Tetradecyl(trihexyl)phosphonium chloride [P_{6,6,6,14}][Cl]

Purchased from Cytec Industries. 20 ml of the ionic liquid was decolorized by redissolution in 30 mL of acetone followed by treatment with activated charcoal (Darco-G60, Aldrich) at 40 °C overnight. Carbon was removed by filtration through alumina (acidic, Brockmann I, Aldrich) and the solvent removed under vacuum at 40 °C for 48hrs at 0.1 Torr.

¹H NMR δ_H(400 MHz; CDCl₃): 2.0-2.3 (8H, m, CH₂), 1.4-1.5 (16H, m, CH₂), 1.2-1.3 (32H, m, CH₂), 0.79-0.85 (12H, m, CH₃) ppm.

ES-MS: ES⁺ m/z 483 [P_{6,6,6,14}]⁺ ES⁻ m/z, 554, [P_{6,6,6,14}]⁺ 2.[Cl]⁻.

Tetradecyl(trihexyl)phosphonium dicyanamide [P_{6,6,6,14}][dca]

Purchased from Cytec Industries; purified according to the procedure for [P_{6,6,6,14}][Cl].

¹H NMR δ_H(400 MHz; CDCl₃): 2.0-2.3 (8H, m, CH₂), 1.4-1.5 (16H, m, CH₂), 1.2-1.3 (32H, m, CH₂), 0.79-0.85 (12H, m, CH₃) ppm.

ES-MS: ES⁺ m/z 483 [P_{6,6,6,14}]⁺ ES⁻ m/z 66 [dca]⁻.

Tetradecyl(trihexyl)phosphonium bis(trifluoromethylsulfonyl)amide [P_{6,6,6,14}][NTf₂]

Purchased from Cytec Industries; purified according to the procedure for [P_{6,6,6,14}][Cl].

¹H NMR δ_H(400 MHz; CDCl₃): 2.0-2.3 (8H, m, CH₂), 1.4-1.5 (16H, m, CH₂), 1.2-1.3 (32H, m, CH₂), 0.79-0.85 (12H, m, CH₃) ppm.

ES-MS: ES⁺ m/z 483 [P_{6,6,6,14}]⁺ ES⁻ m/z 279 [NTf₂]⁻.

Tetradecyl(trihexyl)phosphonium dodecylbenzenesulfonate [P_{6,6,6,14}][dbsa]

Purchased from Cytec Industries; purified according to the procedure for [P_{6,6,6,14}][Cl].

¹H NMR δ_H(400 MHz; CDCl₃): 7.8 (H, s, CH), 7.44 - 7.40 (2H, m, CH), 2.0-2.3 (7H, m, CH₂), 1.4 -1.8 (24H, m, CH₂), 1.16-1.3 (48, m, CH₂), 0.69-0.87 (15H, m, CH₃) ppm.

ES-MS: ES⁺ m/z 483 [P_{6,6,6,14}]⁺ ES⁻ m/z 325 [dbsa]⁻.

Tetrabutyl(methyl)phosphonium tosylate [P_{1,4,4,4}][tos]

Purchased from Cytec Industries; purified according to the procedure for [P_{6,6,6,14}][Cl].

¹H NMR δ_H(400 MHz; CDCl₃): 3.64 – 3.75 (6H, m, CH₂), 2.24 – 2.33 (6H, m, CH₂), 2.01 – 2.07 (6H, m, CH₂), 1.06 – 1.18 (12H, m, CH₃) ppm.

ES-MS: ES⁺ m/z 217 [P_{1,4,4,4}]⁺ ES⁻ m/z 171 [Tos]⁻.

Synthesis of Tetradecyl(trihexyl)phosphonium tosylate[P_{6,6,6,14}][tos]

Tetradecyl(trihexyl)phosphonium chloride (13.5 g, 26 mmol) was added to 50 mL of anhydrous acetone. Solid sodium tosylate (5.50 g, 28 mmol) was then added, giving a suspension which was stirred at 25 °C for 6 hrs. Precipitated sodium chloride was removed by filtration and the solvent removed under vacuum, yielding a yellowish viscous liquid. The ionic liquid was decolorized by redissolution in 30 mL of acetone followed by treatment with activated charcoal (Darco-G60, Aldrich) at 40 °C overnight. The carbon was removed by filtration through alumina (acidic, Brockmann I, Aldrich) and the solvent removed under vacuum to yield tetradecyl(trihexyl)phosphonium tosylate. [P_{6,6,6,14}][tos] as a colourless liquid (11.9 g, 89% yield).

¹H NMR δ_H (300 MHz; CDCl₃): 7.97 (2H, d, CH₂), 7.27 (2H, d, CH₂), 2.45 (3H, s, CH₃), 2.0-2.3 (8H, m, CH₂), 1.4-1.5 (16H, m, CH₂), 1.2-1.3 (32H, m, CH₂), 0.79-0.85 (12H, m, CH₃) ppm.

ES-MS: ES⁺ m/z 483 [P_{6,6,6,14}]⁺ ES⁻ m/z 171 [Tos]⁻.

A.2 Heat of polymerisation: DSC chamber setup.



Figure A 1. The sample chamber and LED array holder printed with a 3D printer. Design by B.Z.

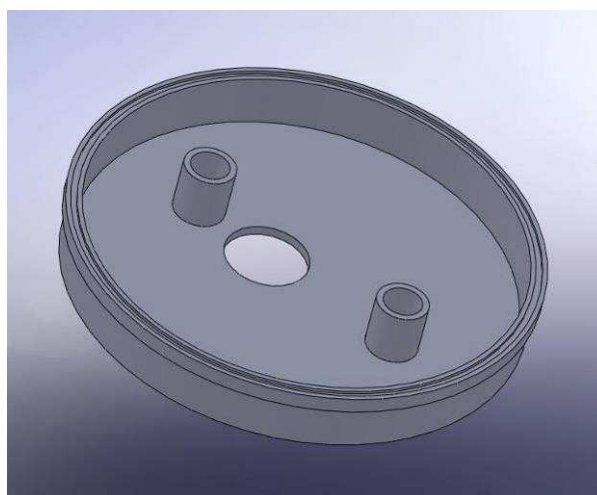


Figure A 2. In house 3D design of the chamber. The carving on the edge was filled with an O-ring for minimising heat noise. Design by B.Z.

A.3 UV curing rheology

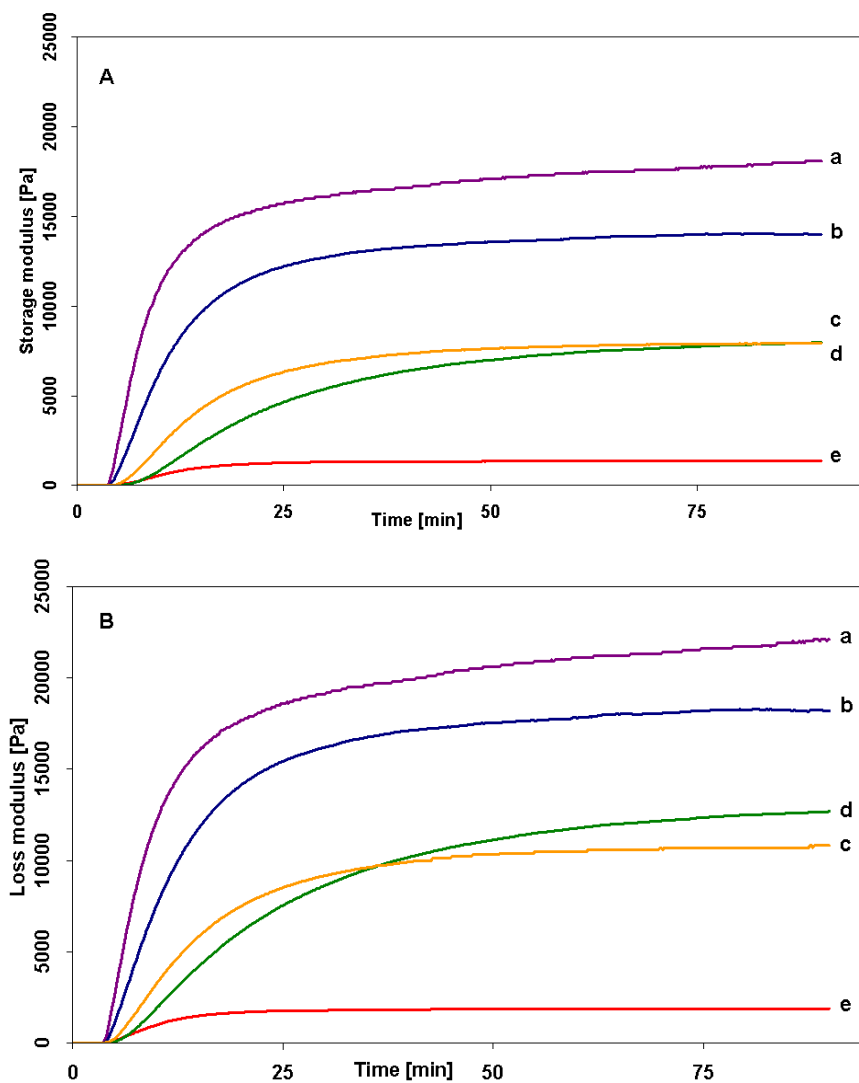


Figure A 3. Storage (A) and loss (B) moduli during UV polymerisation of a) Pi-Tos, b) P-dbsa, c) P-Tos, d) P-Cl, e) P-DCA.

A.4 Thermal Analysis of Poly(*N*-isopropylacrylamide) polymers.

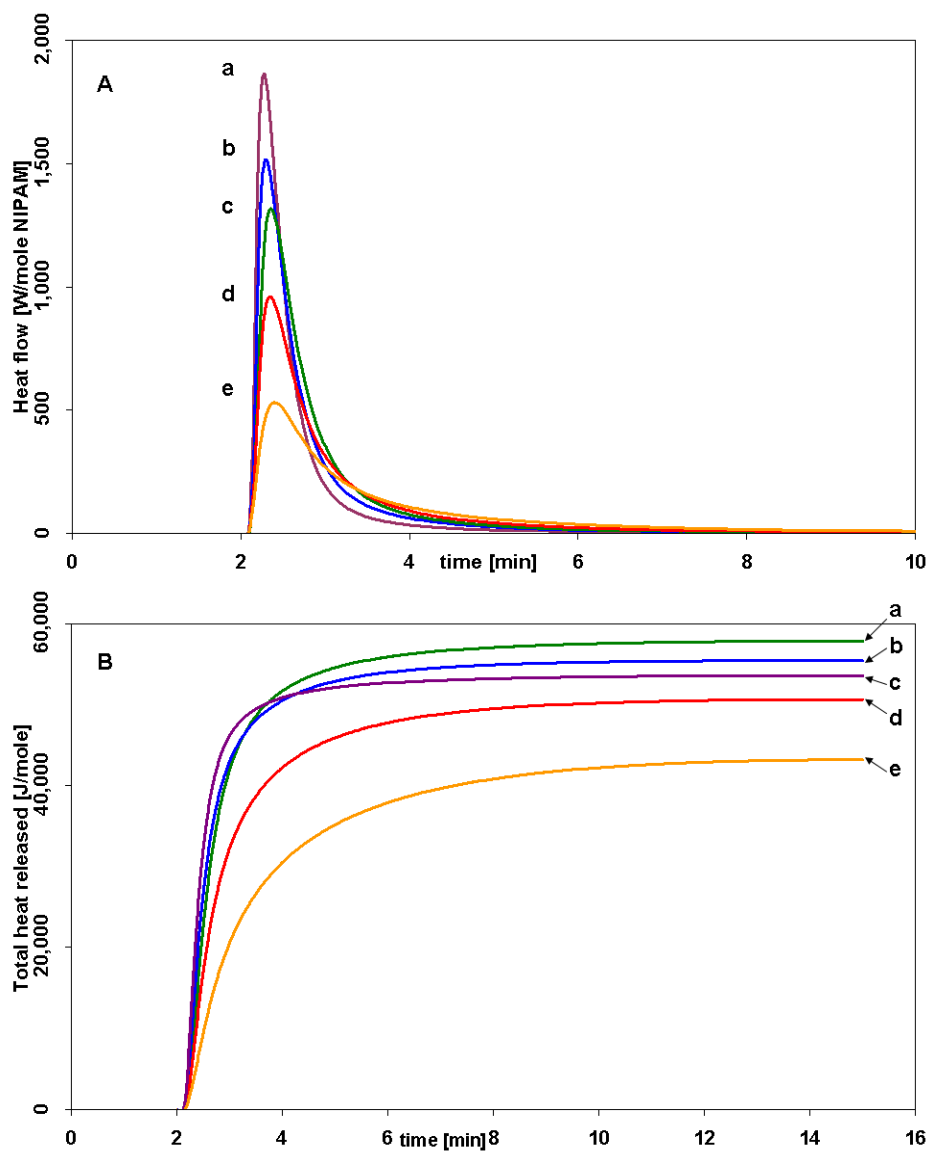


Figure A 4. A: DSC heat flow curves for the UV-initiated polymerisation of linear pNIPAM in a) P₁-Tos, b) P-dbsa, c) P-DCA, d) P-Tos and e) P-Cl. The heat flow is expressed in Watts per mole of NIPAM monomer; B: Integrated DSC heat flows for a) P-DCA, b) P-dbsa, c) P₁-Tos, d) P-Tos and e) P-Cl. The total heat released is expressed in Joules per mole of NIPAM monomer. The UV LEDs were switched on after 2 minutes.

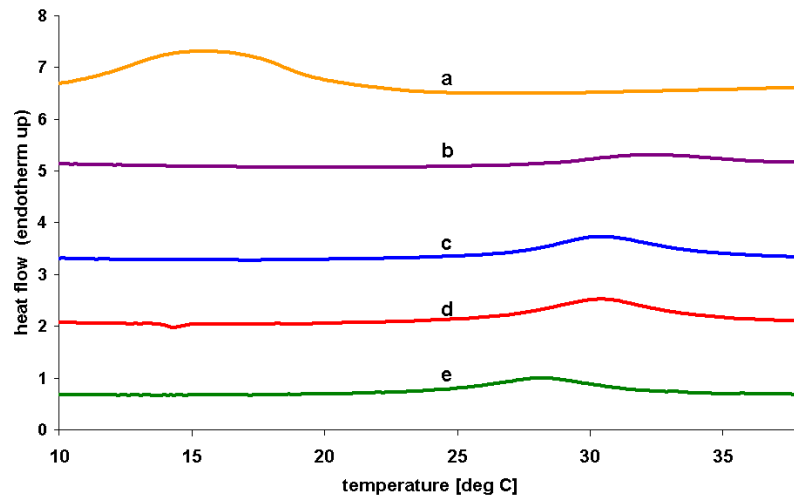


Figure A 5. DCS scans showing the LCST temperature for the water-swollen ionogels: a) xP-Cl, b) xP₁-Tos, c) xP-dbsa, d) xP-Tos, e) xP-DCA.

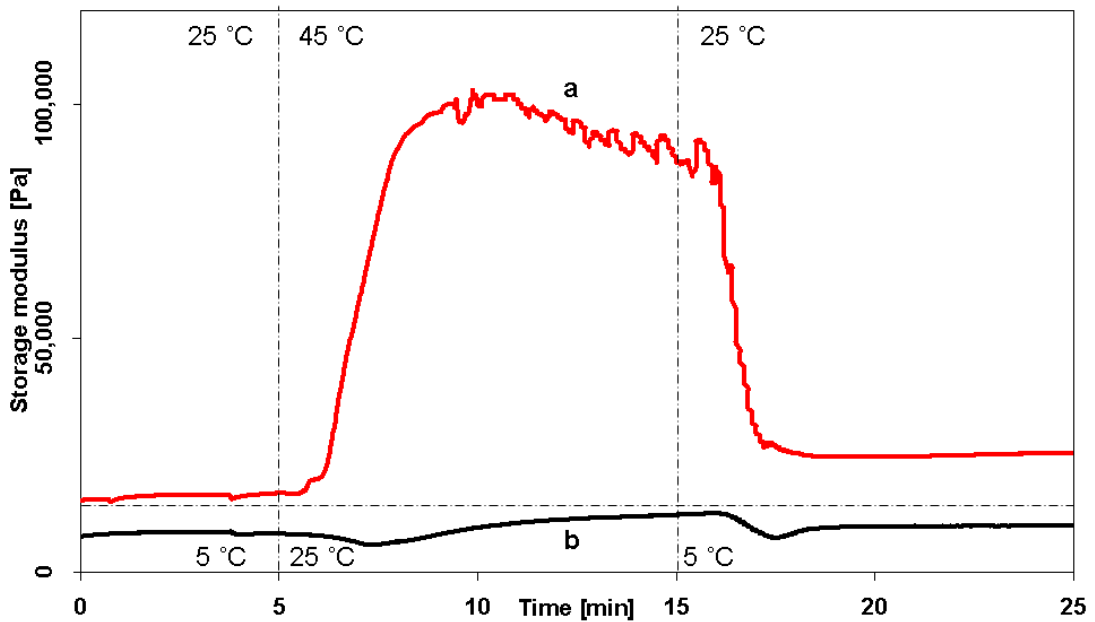


Figure A 6. Plots of storage modulus versus time during a temperature step program for water swollen ionogels. a) xP-DCA: the temperature was raised from 25 °C to 45 °C (20 °C/min) starting at $t = 5$ min and was decreased at $t = 15$ min from 45 °C to 25 °C (20 °C/min); b) xP-Cl: the temperature was raised from 5 °C to 25 °C (20 °C/min) starting at $t = 5$ min and was decreased at $t = 15$ min from 25 °C to 5 °C (20 °C/min).

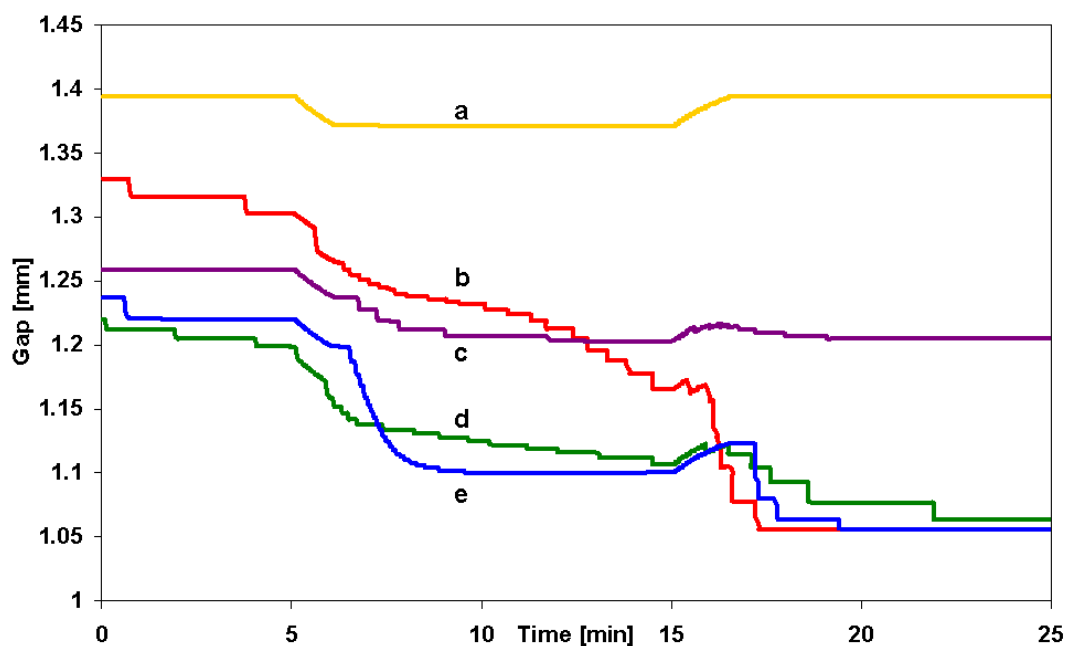


Figure A 7. The sample gap during the experiments from Figure 4 and 5. a) xP-Cl, b) xP-DCA, c) xP_i-Tos, d) xP-Tos, e) xP-dbsa.

Table A 1. Thermal data of cross linked and non crosslinked phosphonium based samples. T_g represents the glass transition temperature and T_{dec} is the decomposition temperature (onset) of the polymers.

Sample	T_g (°C)	T_{dec} (°C)
P-NTf ₂	-58.65	430
P-dbsa	-	421
P-Tos	-59.40	421
P-DCA	-59.52	370
P-Cl	-58.38	361
xP-NTf ₂	-	-
xP-Tos	-60.28	425
xP-dbsa	-	408
xP-DCA	-58.43	374
xP-Cl	-58.61	370

Appendix B:

Self-protonating spiropyran-*co*-NIPAM-*co*-acrylic acid hydrogels as reversible photoactuators

Electronic Supplementary Information (Chapter 5)

B.1 Synthesis of BSP-acrylate

Acrylation of trimethyl-6-hydroxyspiro-(2H-1-benzopyran-2,2'indoline) (abb. BSP-OH) was done as follows. 500 mg of BSP-OH was dissolved in 20 mL of anhydrous dichloromethane in a 100 mL round bottom flask. The flask was placed in an ethanol bath to which liquid nitrogen was poured until bubbling stopped. To such cooled mixture under magnetic stirring, 0.6 mL of triethylamide was added followed by 0.2 mL of acryloyl chloride added dropwise. The reaction was allowed to stir for 48 hours during which the mixture warmed up to room temperature as the ethanol evaporated. The reaction mixture was washed with a saturated solution of NaHCO₃ and deionised water several times to remove the byproducts. The coloured water phase was also washed with dichloromethane. The combined organic phases were evaporated on a rotary evaporator with an addition of column silica powder. The BSP-acrylate was purified by column chromatography using ethyl acetate/hexane 1:8 mixture as the mobile phase. After evaporation of the solvent and vacuum drying (0.1 mBar), 400 mg of white powder was obtained. Yield 67 %

B.2 Gel shrinking measurements

Since the cut gel samples are never ideal circles several diameters were measured before the light irradiation. Then as the gel shrunk the ratio in shrinking separately for every diameter was expressed in percent. The standard deviations were then calculated between the shrinking ratios for the given time interval. A calculation of the relative swelling percent example for the 0-0 blank poly(NIPAM) gel is given below.

The ratio of the diameter of the dried gel and fully swollen gel is:

$$\frac{d_{\min}}{d_{\max}} = 0.66$$

The measured shrinking of 3 dimensions of the gel versus the light irradiation in μm is given:

	0 min	5 min	10 min	20 min
Diameter 1	3876	3845	3794	3721
Diameter 2	3526	3484	3464	3433
Diameter 3	3879	3802	3818	3770

For every diameter the swelling ratios are calculated for each time interval and expressed in %:

	0 min	5 min	10 min	20 min
Diameter 1	100.0%	98.8%	98.2%	97.4%
Diameter 2	100.0%	99.2%	97.9%	96.0%
Diameter 3	100.0%	98.0%	98.4%	97.2%

Then for every given time interval the average swelling percent is calculated along with the standard deviation:

	0 min	5 min	10 min	20 min
Average swelling	100.0%	98.7%	98.2%	96.9%
Standard deviation	-	0.5%	0.2%	0.6%

After applying the following formula $D = \left[1 - \left[\frac{(d_{\max} - d_x)}{(d_{\max} - d_{\min})} \right] \right] \cdot 100\%$ we obtain the following relative swelling values.

	0 min	5 min	10 min	20 min
Average swelling	100%	98.03%	97.27%	95.30%
Standard deviation	-	0.76%	0.30%	0.91%

The standard deviations were multiplied by $\frac{1}{\frac{d_{\min}}{d_{\max}}} = \frac{1}{0.66} = 1.5151$

Therefore, the relative swelling percent we use expresses the change in dimensions between the fully swollen state and the dried dehydrated state. See

Figure B 1 below:

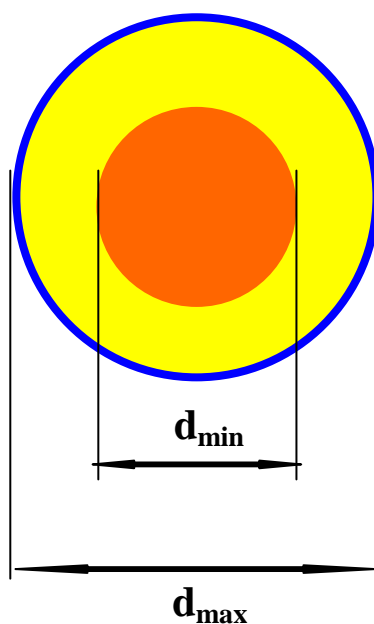


Figure B 1: Graphical representation of the relative percent of swelling used. Blue represents the fully swollen diameter d_{\max} (100 % relative swelling); orange represents the diameter of the dried gel d_{\min} (0 % relative swelling); yellow colour is the actuator operating range.

B.3 UV-Vis Spectroscopy

Changes in the absorbance spectra of the spiropyran hydrogels under different illumination conditions were recorded in reflectance mode using two fiber-optic light guides connected to a Miniature Fiber Optic Spectrometer (USB4000 - Ocean Optics) and aligned using an in-house made holder (Figure B 2). The in-house-designed holder was fabricated using a 3D printer (Dimension SST 768) in black acrylonitrile butadiene styrene co-polymer (ABS) plastic in order to minimise interferences from ambient light. The two parts of the holder (one to be placed underneath the hydrogel, the other one on top (Figure B 2A) were designed using ProEngineer CAD/CAM software package and fixed together to ensure no interferences from ambient light (Figure B 2B).

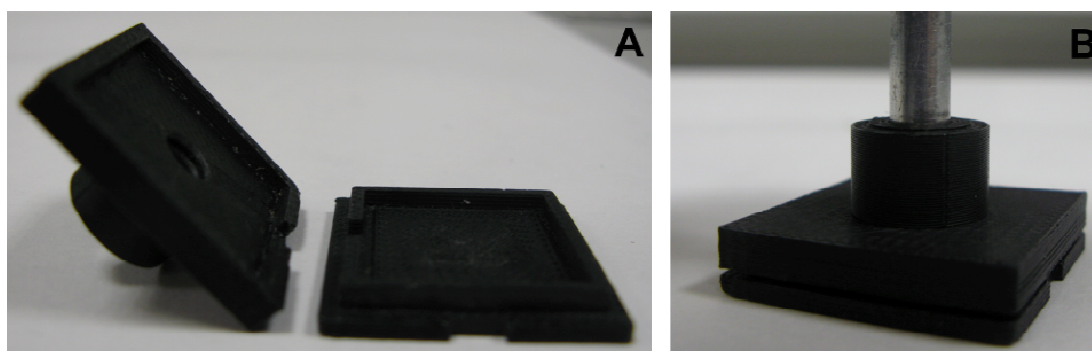


Figure B 2. In house designed holder used for absorbance measurements of the spiropyran hydrogels.

The light source was a LS-1 tungsten halogen lamp (white light) obtained from Ocean Optics, Inc. Data from the spectrometer was processed using Spectrasuite software provided by Ocean Optics Inc. For clarity, the absorbance spectra recorded were smoothed using Origin software using Savitzky–Golay algorithm.

Appendix C:

Porous and self-protonating spiropyran-based NIPAM gels with fast reswelling kinetics

Electronic Supplementary Information (Chapter 6)

C.1 Raman spectroscopy of porous gels

The removal of PEG 2000 porogen with 3 water washes was confirmed by Raman spectroscopy (Figure C 1). The PEG peaks at 280, 364, 537, 582, 861(C-O-C symmetric stretch), 1233, 1484 cm^{-1} all disappear when the porous gel is washed with DI water.

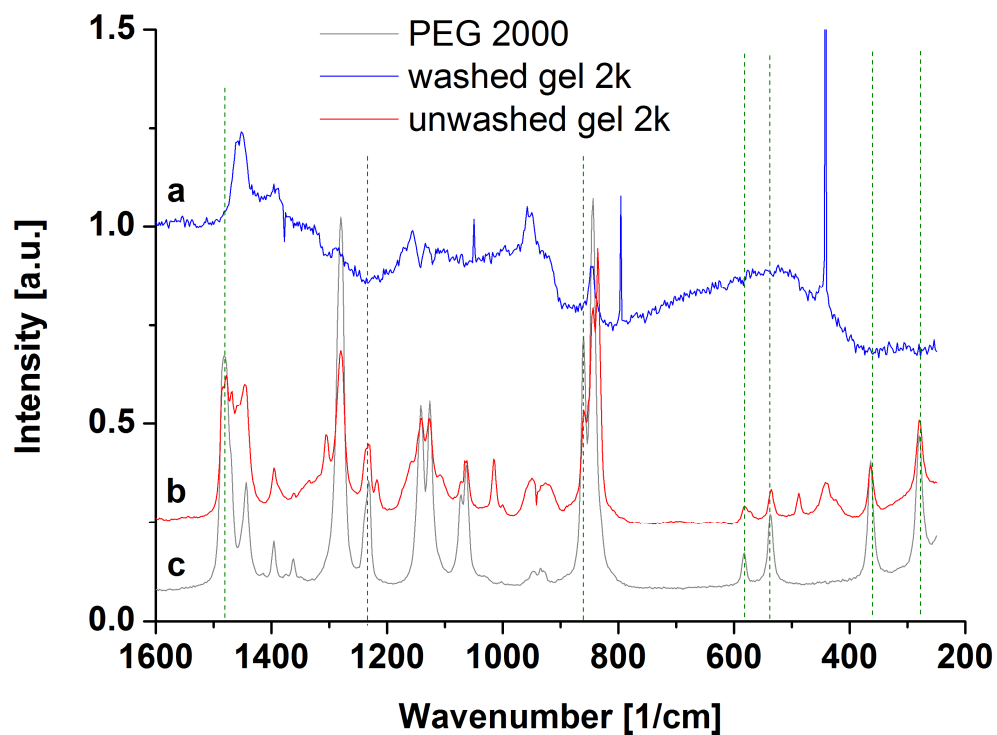


Figure C 1. Raman spectra of a) gel 2k swollen and washed with DI water; b) gel 2k right after polymerisation and before swelling and washing; c) PEG2000 polymer

Appendix D:

Thermoresponsive poly ionic liquid gels

Electronic Supplementary Information (Chapter 7)

D.1 Materials

Tetrabutylphosphonium chloride ($[P_{4,4,4,4}][Cl]$) (Cyphos 443W) and tributyl-hexyl phosphonium chloride ($[P_{4,4,4,6}][Cl]$) were supplied by Cytec® (Ontario Canada) and used as received. Potassium 3-sulfopropylacrylate (SPA), sodium 4-vinylbenzenesulfonate (SS), poly(propylene glycol) diacrylate Mn 800 (PPO800), poly(ethylene glycol) diacrylate Mn 256 (PEG256) and 700 (PEG700), *N,N'*-methylenebisacrylamide (MBIS), 2-hydroxy-2-methylpropiophenone (HMPP) were all obtained from Sigma-Aldrich and used as received.

D.2 Synthesis of $[P_{4,4,4,4}][4\text{-styrenesulfonate}]$ (P-SS) and $[P_{4,4,4,6}][3\text{-sulfopropylacrylate}]$ (P-SPA)

7 g of phosphonium chloride was mixed with 10 g of water and 1.2 molar equivalents of the anion salt ($[Na][4\text{-styrenesulfonate}]$ for $[P_{4,4,4,4}][Cl]$ or $[K][3\text{-sulfopropylacrylate}]$ for $[P_{4,4,4,6}][Cl]$). The mixture was stirred at room temperature for 48 hours. The IL was extracted from the water phase by dichloromethane (DCM), the DCM phase was reduced by a rotary evaporator and the residual liquid was dried at high vacuum 0.1 mBar for 24 hours at room temperature. A final product yield of 97% was obtained. The obtained ILs were stored at 5 °C. Tetrabutylphosphonium 4-vinylsulfonate will be referred to as P-SS and the tributyl-hexyl phosphonium 3-sulfopropylacrylate will be referred to as P-SPA.

P-SS 1H NMR, δ_H (400 MHz, $CDCl_3$): 0.82-0.85 (t, 12H, CH_3), 1.33-1.38 (m, 16H, CH_2), 2.07-2.74 (m, 8H, CH_2), 5.16-5.19 (d, 1H, CH), 5.65-5.69 (d, 1H, CH), 6.58-6.65 (q, 1H, CH), 7.27-7.29 (d, 2H, CH), 7.74-7.76 (d, 2H, CH) ppm.

P-SPA 1H NMR, δ_H (400 MHz, $CDCl_3$): 0.75-0.79 (t, 3H, CH_3), 0.84-0.88 (t, 9H, CH_3), 1.19-1.22 (m, 4H, CH_2), 1.38-1.44 (m, 16H, CH_2), 2.07-2.14 (m, 2H, CH_2), 2.15-2.24 (m, 8H, CH_2), 2.75-2.79 (m, 2H, CH_2), 4.13-4.17 (t, 2H, CH_2), 5.68-5.71 (dd, 1H, CH), 5.93-6.00 (q, 1H, CH), 6.23-6.28 (dd, 1H, CH) ppm

D.3 Gel preparation

The monomeric IL (200 mg) was mixed with the desired amount (mol %) of crosslinker (MBIS, PEG 256, PEG700, PPO800) and 1 mol% photoinitiator HMPP. The mixture was stirred and poured into a PDMS mould containing 1 mm deep circular pits of diameters 5 and 10 mm. The gels were polymerised for 30 min in a UV curing chamber that produced 365 nm UV light intensity of 3.5 mW/cm². After the polymerisation the gels were placed for 1 hour in DI water for swelling. All analysis was done on the swollen gels.

D.4 Analytical Techniques

D.4.1 NMR spectroscopy

The NMR spectra were collected on a Bruker 400 MHz spectrometer at 25 °C. Samples were dissolved in deuterated chloroform. The spectra were analysed using Bruker TopSpin software.

D.4.2 Raman spectroscopy

Raman spectroscopy was performed using a Perkin Elmer® Raman Station 400F. Measurements were taken from 800 to 3200 cm⁻¹ at 20 scans with 2 cm⁻¹. The samples were placed directly on a microscope slide covered with aluminium foil.

D.4.3 DSC

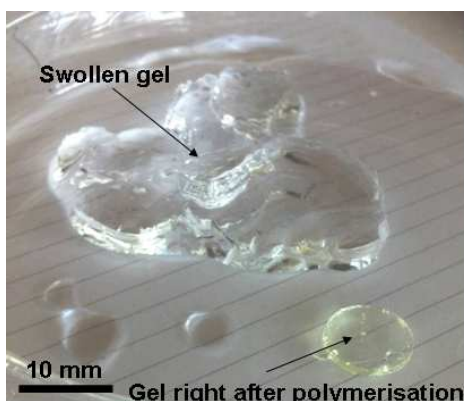
A Pyris 1 DSC was used to analyse the heat generated by the gels during the LCST transition. Thermal scans below room temperature were calibrated with the cyclohexane solid-solid transition and melting point at -87.0 °C and 6.5 °C, respectively. Thermal scans above room temperature were calibrated using indium, tin and zinc with melting points at 156.6, 231.93 and 419.53 °C, respectively. The water-swollen gels were placed on a tissue to remove excess DI water and cut into pieces ca. 10 mg. These were placed on aluminium DSC pans and sealed. The LCST values for these samples were determined by thermal scans at 10 °C/min with the following temperature program: Heat from 0 °C to 90 °C then cool from 90 °C to 0 °C. The LCSTs were determined as the endothermic peak during heating.

D.4.4 Temperature ramp microscopy.

The swollen gels were cut into squares roughly 3 mm in size. The imaging was performed using an Aigo GE-5 microscope with a 60x objective lens and the accompanying software. The gels were placed on an aluminium plate resting on a Anton Paar MCR 301 Rheometer peltier holder. The plate was filled with DI water and covered with a glass plate to avoid evaporation of water. The glass plate was also in contact with the filling water to avoid condensation. Temperature was controlled through the rheometer software and was ramped up from 20 °C to 70 °C by 5 °C steps. Each step the temperature around the sample was checked with a Fluke 62 Mini IR thermometer and gel size measurements were taken once the temperature stabilised.

D.5 Swelling behaviour of of P-SS and P-SPA gels

a



b

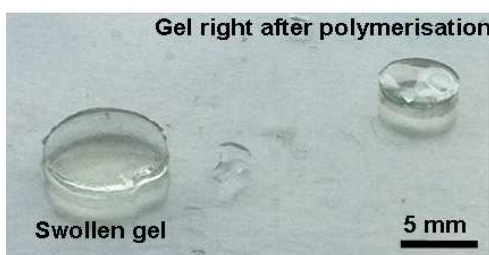


Figure D1. a) P-SS gel with 10% MBAAm right after polymerisation and after 2 hours of swelling in DI water at room temperature; b) P-SPA gel with 5 mol% PPO800 immediately after polymerisation and after swelling in DI water at room temperature.

D.6 Raman spectroscopy

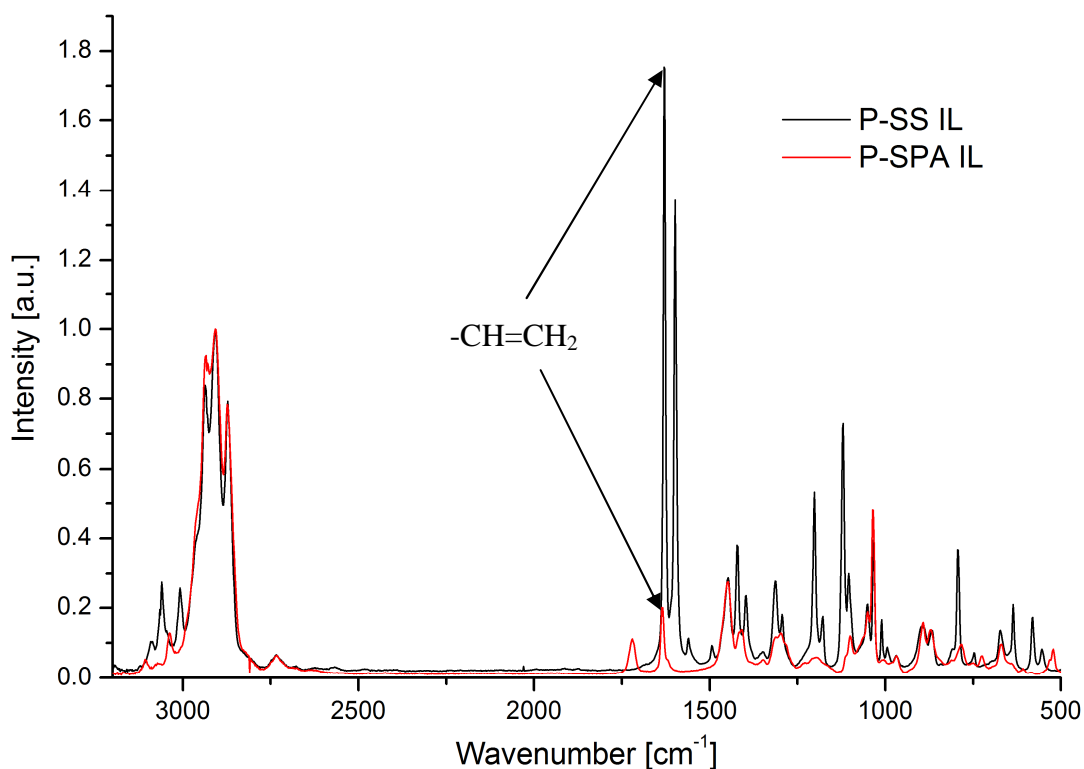


Figure D2. Raman spectra of P-SS and P-SPA monomeric ionic liquids. The 1630 cm⁻¹ bands marked with the arrow represent the polymerisable vinyl C=C bond.

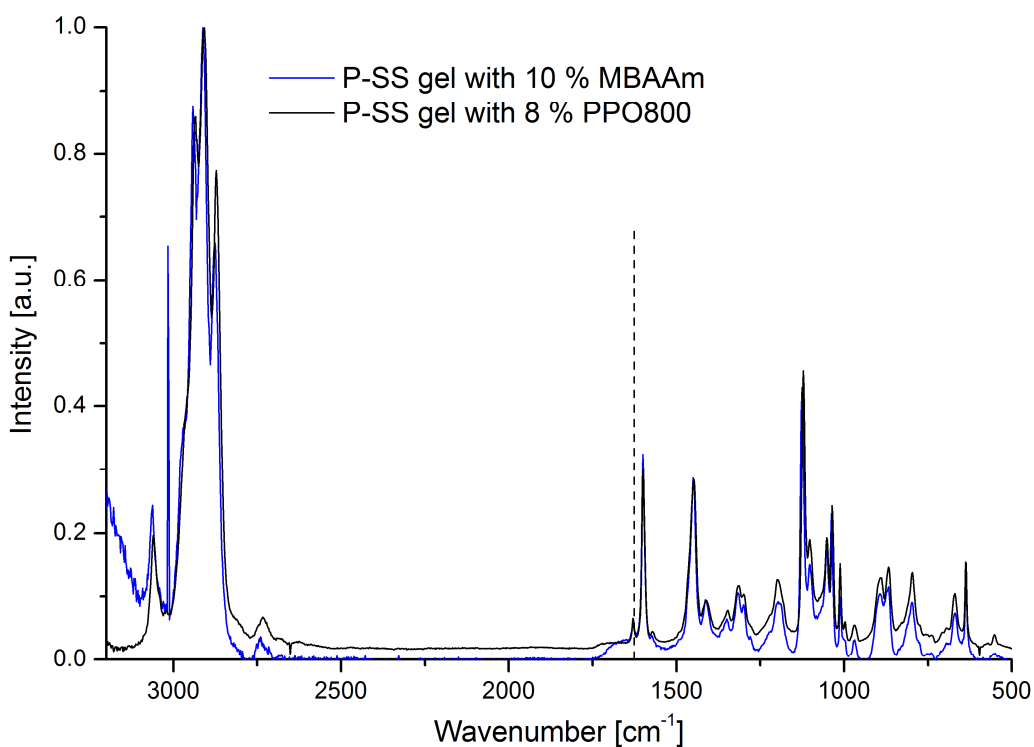


Figure D3. Raman spectra of two gels: P-SS with 10 % MBAAm and P-SS with 8 % PPO800. The dashed line indicates 1630 cm⁻¹ where the polymerisation active C=C band appears in the monomers.

D.7 DSC characterisation

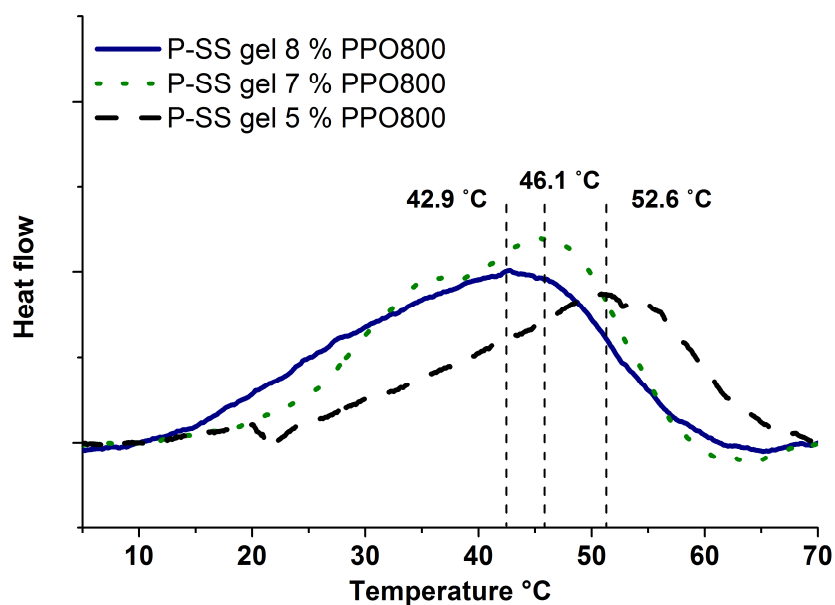


Figure D4. DSC scans of water swollen P-SS gels made with different amounts of PPO800 crosslinker.

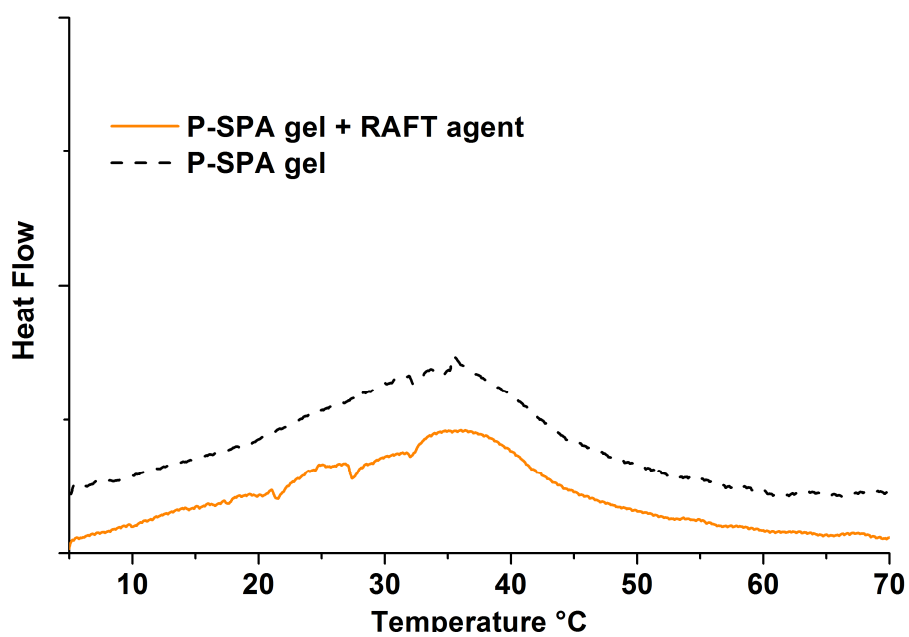


Figure D5. DSC scans of water swollen P-SPA gels made with 5 mol% PPO800 crosslinker. RAFT agent was used in 50:1 monomer-RAFT agent ratio.